Alternative splicing of large- conductance calcium- and voltage- activated potassium (BK) channels

Stephen Hsiao- Feng Macdonald, BSc., MSc.
(University of Edinburgh)

Presented for the Degree of Doctor of Philosophy

The University of Edinburgh

August 2005

Declaration

I hereby declare that composition of this thesis and work described herein has been carried out solely by me, except where otherwise explicitly stated, at the Centre for Integrative Physiology, at the University of Edinburgh. No part of this thesis has been submitted for any other degree or qualification.

Stephen Hsiao-Feng Macdonald

August 2005

Acknowledgements

First and foremost, to Professor Mike Shipston, without whom this entire endeavour would not exist, and I cannot thank enough for this opportunity. Special thanks to Lijun Tian, Hannah Florance, Heather McClafferty, Lorraine Coghill and Helene Widmer, for much assistance and patient instruction in the lab, Lie Chen for design of the Δe23 splice variant Taqman assay and Jean- Marc Huibant for aid in molecular biology. Many thanks also to Jenny Greaves, Rory Duncan, Rolly Wiegand and Linda Wilson for advice, molecular tools and assistance with fluorescence confocal microscopy. Also thanks to Heather Findlay, Eliane Chirnside, Mel Johnson, Derek Robertson, Karen Smillie, Angela McDonald, Mark Hillen, Iain Rowe, Gareth Evans, Colin Rickman, Helen Falconer, Harpreet Singh, David Apps, Andrew Hall, Mike Ludwig and Pete Bush for help, advice and random lab bits and pieces that I scrounged from them. Special mention to all the other MBG and CIP members who have encouraged and supported me over the past few years.

Also, thanks to all my family for their support: me old mum, Yvonne Macdonald, my sister Shan, my grandfather James Macdonald, my great-aunt Janet Macdonald and my father, Jimmy Ho.

Lastly, big-ups to members of EU Shotokan for their support and enthusiasm.

Dedicated to the memory of my grandmother, Susan Macdonald.

Abstract

Large conductance calcium- and voltage- activated potassium (BK) channels perform critical and diverse roles including regulation of action potential repolarisation and hyperpolarisation, potassium secretion and neurotransmitter release. Extensive pre-mRNA splicing from the single gene encoding the pore- forming α-subunit provides a mechanism to generate functional diversity of BK channels. Inclusion of different alternatively spliced exons may modify functional properties of BK channels; however the functional role and tissue distribution of different splice variants is largely unknown. The aim of this thesis was to test the hypotheses that: i) alternative splicing may control subcellular localisation of BK channel α-subunits and ii) splice variants are differentially expressed in tissues, using the murine BK channel as the model system. To address whether alternative splice variants may be trafficked specifically to different subcellular compartments, epitope- tagged BK channel splice variants were expressed in mammalian epithelial and endocrine cells. STREX and ZERO variants, in contrast to splice variant Δe23 that is C-terminally truncated, efficiently trafficked to the plasma membrane. Furthermore, splice variants can heteromultimerise in vivo. To investigate tissue specific distribution of splice variants, fluorogenic real time quantitative PCR assays were developed for five known BK channel alternative splice variants- ZERO, e20 (IYF), e21(STREX), e22, and Δe23 at site C2 of splicing, and used to profile: i) the expression of these splice variants across various tissues in the adult mouse; ii) changes in ZERO and STREX variant expression in the mouse central nervous system during development and iii) STREX variant splicing in steroid responsive tissues of the stress axis. Splice variant expression patterns were distinct in different tissues with, for example, STREX

expressed most highly in endocrine tissues and e22 in embryonic tissue. STREX variant expression was significantly reduced in the CNS across the period from embryo day 13 to postnatal day 35, possibly reflecting changes in cell excitability as development progresses and activity- dependent patterning of the CNS is completed. No significant changes in STREX expression were seen under various stress paradigms in adult mice. These data suggest that alternative pre-mRNA splicing is an important determinant of subcellular localisation and that tissues dynamically express a unique complement of BK channel splice variants to serve their physiological demand.

Abbreviations

$A_{260/280}$	absorbance at 260/ 280nm
A	adenine
ACTH	adrenocorticotrophic hormone
bp	base- pair(s)
BK channel	large- conductance Ca^{2+} and voltage- activated K^+ channel
C	cytosine
cDNA	complementary DNA
°C	degree(s) Celsius
CNS	central nervous system
CORT	corticosterone
DEPC	diethyl pyrocarbonate
DMEM	Dulbecco's modified Eagle's medium
DNA	deoxyribonucleic acid
dNTP	2'-deoxynucleoside 5'- triphosphate
dsDNA	double-stranded DNA
EDTA	ethylenediaminetetraacetate
EGFP	enhanced green fluorescent protein
FAM	6- carboxyfluorescein
FCS	foetal calf serum
fg	femtogramme(s)
FRET	fluorescence resonance energy transfer
g	gramme(s)
G	guanine
HA	haemagglutinin
HBSS	Hank's balanced salt solution
HcRed	*Heteractis crispa* far-red fluorescent protein
HPA	hypothalamic- pituitary- adrenocortical axis
h	hour(s)
kb	kilobase-pair(s)
l	litre(s)
LB	Luria-Bertrani
LTP	long- term potentiation
LTD	long- term depression
µg	microgramme(s)
µl	microlitre(s)
µM	micromolar
ml	millilitre(s)
min	minute(s)
M	molar
mRNA	messenger RNA
ng	nanogramme(s)
nm	nanometre(s)
nM	nanomolar
OD	optical density
PFA	paraformaldehyde
PBS	phosphate buffered saline

PCR	polymerase chain reaction
pHcRed-N1	expression vector for HcRed fluorescent protein
RNA	ribonucleic acid
RNase	ribonuclease
RNasin	RNase inhibitor
rpm	revolutions per minute
RT	reverse transcription
s	second(s)
SDS	sodium dodecyl sulphate
T	thymine
TAMRA	6- carboxytetramethylrhodamine
TBE	tris-borate-EDTA
T_m	melting temperature
UV	ultra violet
U	unit(s)
w/v	weight per volume
v/v	volume per volume
x *g*	x gravitational force

List of figures:

Chapter One: Large- conductance calcium- and voltage- activated potassium (BK) channels

Chapter Two: Materials and methods

Chapter Three: Expression of fluorescent protein- labelled BK channel alternative splice variants in mammalian cells

Chapter Four: Quantitation of BK channel alternative splice variant expression

Chapter Five: Regulation of BK channel alternative splicing during mouse CNS development

Chapter Six: Effect of HPA axis manipulation on BK channel alternative splicing

List of tables:

Chapter Four: Quantitation of BK channel alternative splice variant expression

Contents

Chapter Two: Materials and methods

Chapter Three: Expression of fluorescent protein- labelled BK channel alternative splice variants in mammalian cells

Chapter One:

Large- conductance calcium- and voltage-activated potassium (BK) channels

1-1 Overview

Calcium-activated potassium channels are almost ubiquitously expressed throughout tissues of multicellular organisms (Toro *et al.*, 1998, Sah, 1996), and can be divided into three broad groups (Small, Intermediate and Big conductance, abbreviated SK, IK and BK respectively) according to primary sequence, single-channel conductance, calcium- and voltage- dependence and pharmacology. Large conductance calcium- and voltage- activated potassium channels, hereafter referred to as BK channels, are expressed in most tissues including neurons (Wanner *et al.*, 1999), smooth muscle (Wellman and Nelson, 2003) and epithelia (Kwon and Guggino, 2004) where they perform critical diverse physiological roles such as repolarisation and hyperpolarisation of membrane potential following action potentials, regulation of vascular tone and potassium secretion.

The BK channel is characterised by a large single channel conductance of ~250pS in symmetrical potassium (Vergara *et al.*, 1998) and is activated by intracellular calcium and membrane depolarisation (McManus, 1991, Marty, 1981). Following membrane depolarisation or a rise in intracellular calcium, BK channels open, resulting in potassium efflux, causing hyperpolarisation of the membrane potential (Toro *et al.*, 1998), and enabling tight control of processes such as calcium influx through voltage- gated calcium channels. By coupling intracellular signalling with membrane potential in this manner, BK channels are a powerful modulator of cell excitability in response to a variety of stimuli. Due to reliance of numerous physiological and pathological processes on intracellular signalling in this manner, and the diverse functional phenotypes of BK channel that exist (Orio *et al.*, 2002,

Tian *et al.*, 2001a, b, Shipston *et al.*, 1999), the BK channel is a target for research into mechanisms by which regulated ion channel expression maintains homeostasis, and the deleterious effects of disregulated channel function.

1-2 Key structural features of the BK channel

1-2-1 Pore- forming α-subunit

BK channels are members of the voltage-gated potassium channel family; the pore-forming α subunits, which are the minimal molecular requirement for assembly of functional channels, can be separated into two distinct parts: a 'core' region, which contains a characteristic S1-S6 transmembrane domain structure homologous to this group (Wang *et al.*, 2003), as well as a 'tail' region which comprises the large intracellular C-terminus, that accounts for two thirds of the protein (Toro *et al.*, 1998) (fig. 1-1).

The intracellular cytoplasmic N- terminus of voltage- gated potassium channels is required for assembly of channel tetramers (Strang *et al.*, 2001), and in addition this region is required for modulatory associations with voltage- gated potassium channel interacting proteins (KvChIPs) (Bähring *et al.*, 2001). In contrast, although much of the transmembrane structure of the BK channel is homologous to that of the voltage-gated potassium channel superfamily, a property unique to the BK channel is that the N-terminus, due to an additional S0 transmembrane segment, is extracellular. Studies using epitope- tagged constructs showed that the N-terminus is accessible for immunolabelling in nonpermeabilised cells, demonstrating that it is exoplasmic (Meera *et al.*, 1997). In the BK channel, the N-terminal region is specifically

Figure 1-1
Key structural features of the BK channel

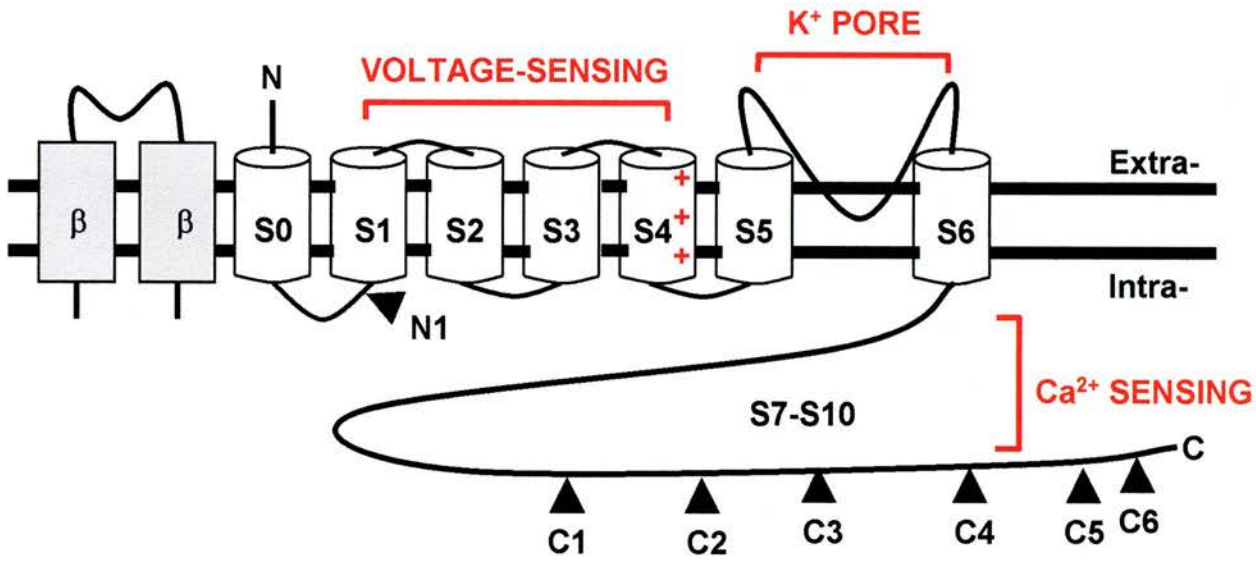

Figure 1-1 Key structural features of the BK channel

Showing transmembrane topology of BK channel, with extracellular N-terminus, 7 transmembrane segments (S0-S6), intracellular C-terminus (S7-S10), voltage and calcium- sensing regions, pore- forming region, sites of alternative splicing (N1, C1-C6) and optional β-subunit (not to scale).

required for interaction with accessory β-subunits. Studies of chimeric proteins revealed that whilst the Drosophila BK channel does not interact with the mammalian BK β-subunit, replacing the S0 region with that of the human BK channel then enables such regulation (Wallner *et al.*, 1996).

The S4 transmembrane segment of the BK channel contains regularly spaced, basic residues that are conserved among voltage- gated potassium channels, such a region being characteristic of the intrinsic voltage- sensing apparatus in this channel type (Diaz *et al.*, 1998). Arginine residues at positions 207, 210 and 213, as well as glutamate 219 are implicated as parts of the voltage- sensing apparatus, and gating charge of the channel was found to be significantly altered by mutation of these residues, the degree of this change being determined by $[Ca^{2+}]_i$ in the case of the R207 mutant (Cui *et al.*, 2000).

The P-loop, located between transmembrane segments S5 and S6, forms the selectivity filter of the channel pore, and is conserved across voltage gated potassium channel families (MacKinnon, 2003). This conserved region, when assembled in a tetramer of four α-subunits, forms the functional pore, most likely with the S5 transmembrane segments on the outside, and the S6 segments as the inside face, lining the ion permeation pathway (Jiang *et al.*, 2001). This structure is also homologous to the pore- forming region in sodium, calcium and glutamate channels (Zhorov and Tikhonov, 2004), however use of quarternary ammonium blocking studies has revealed that in spite of similarities in assembly and structure with other potassium channels, BK channels have a faster rate of blocking and unblocking (Li

and Aldrich, 2004). Whilst the underlying biophysical properties that determine the high conductance that is characteristic of the BK channel are unclear, these results suggest that a larger cavity and inner pore at least partially contribute to this. Additionally, in tetramers of BK channel α-subunits, conserved negative residues at positions 321 and 324 form a ring of negative charge at the entrance of the inner vestibule of the channel. This has the effect of concentrating K^+ ions in the inner vestibule, consequently doubling the outward conductance of the channel (Brelidze *et al.*, 2003).

In the absence of calcium, strong depolarisation alone can cause BK channel opening, whilst the presence of calcium causes an increase in voltage sensitivity, with more negative voltages required for activation. Several sites within the intracellular C-terminal tail of the BK channel are implicated in calcium sensing (Cox, 2005, Xia *et al.*, 2002, Schreiber and Salkoff, 1997). The existence of a 'calcium bowl' and also a separate calcium- sensing region led to the hypothesis that there exist both calcium- dependent and calcium- independent modes of channel regulation (Schreiber *et al.*, 1999) where the cytoplasmic tail region inhibits voltage-dependent gating of the channel, and this inhibition is removed in the presence of calcium. However, it is also possible that other sites within the BK channel are able to regulate channel activation in a calcium-dependent manner, as truncated BK channels lacking the intracellular C-terminus have been reported as having calcium sensitivity similar to that of the wild- type channel (Piskorowski and Aldrich, 2002).

The large, intracellular C-terminus of the BK channel has also been shown to be required for efficient cell surface expression. Studies on BK channel variants cloned from rabbit kidney indicated that whilst the full- length channel, which is highly homologous to the channel in other species, was able to traffic efficiently to the cell surface, a channel with a unique, truncated C-terminus localised cytoplasmically, presumably in the ER and Golgi (Wang *et al.*, 2003). However, although this truncated channel was not able to reach the cell surface, the truncation did not affect homomultimerisation of the α-subunits, therefore it is likely that several distinct regions exist for determining expression of functional channel tetramers at the plasma membrane, and that mechanisms which facilitate assembly operate independently of membrane trafficking. Additionally, the full-length channel was not able to rescue correct membrane trafficking of the truncated variant, and although the latter did not exert a fully dominant- negative influence on cell surface expression of the former, less full- length channel reached the membrane, either due to some degree of multimerisation with the truncated α-subunits, or competition for expression machinery.

Whilst other voltage- gated ion channels show a variety of isoforms, arising from multiple genes, the BK channel pore- forming α-subunit is encoded by only a single gene, KCNMA1, and sequence is highly conserved across mammalian species, with > 97% amino acid identity (whilst that of the β-subunit is around 82-85% (Toro *et al.*, 1998)). Nevertheless, several functional variants of the BK channel have been observed, since properties of the channel can be significantly modulated by a variety of factors, such as assembly with four accessory β-subunits (Orio *et al.*, 2002),

metabolic and posttranslational regulation (Schubert and Nelson, 2001) and extensive pre- mRNA splicing of the α-subunit (Shipston, 2001). Consequently, altered calcium and voltage sensitivities (Xie and McCobb, 1998), shifts in regulation by protein kinases (Tian *et al.*, 2001b) and significant changes in subcellular localisation of the α-subunit (Zarei *et al.*, 2001) are all possible. As a result of this diversity, control of membrane potential and cellular excitability by BK channels can be tightly regulated.

1-2-1-1 BK channel pre-mRNA alternative splicing

Processing of primary transcripts to remove the non-coding intronic sequences, and selection of exons for inclusion to generate mature mRNA is known as pre-mRNA splicing, and represents a means of generating diversity among products of a single gene (fig. 1-2). This process is reliant on multiple protein-protein, protein-DNA and protein-RNA interactions, frequently occurs cotranscriptionally, although this coupling is not obligatory (Kornblihtt *et al.*, 2004), and takes place in the multiprotein complex known as the spliceosome, which is formed of up to 300 proteins and 5 RNAs (Jurica and Moore, 2003). Whilst already subject to multiple levels of control regarding splicing occurrence and efficiency (Fong *et al.*, 2003), additional interactions also exist that only occur during specific states, such as depolarisation, that can specifically regulate the inclusion or exclusion of certain exons.

As a result of alternative splicing of the BK channel, cell excitability can be dynamically regulated in response to steroid hormone stimulation (Mahmoud and

Figure 1-2
Overview of pre-mRNA alternative splicing

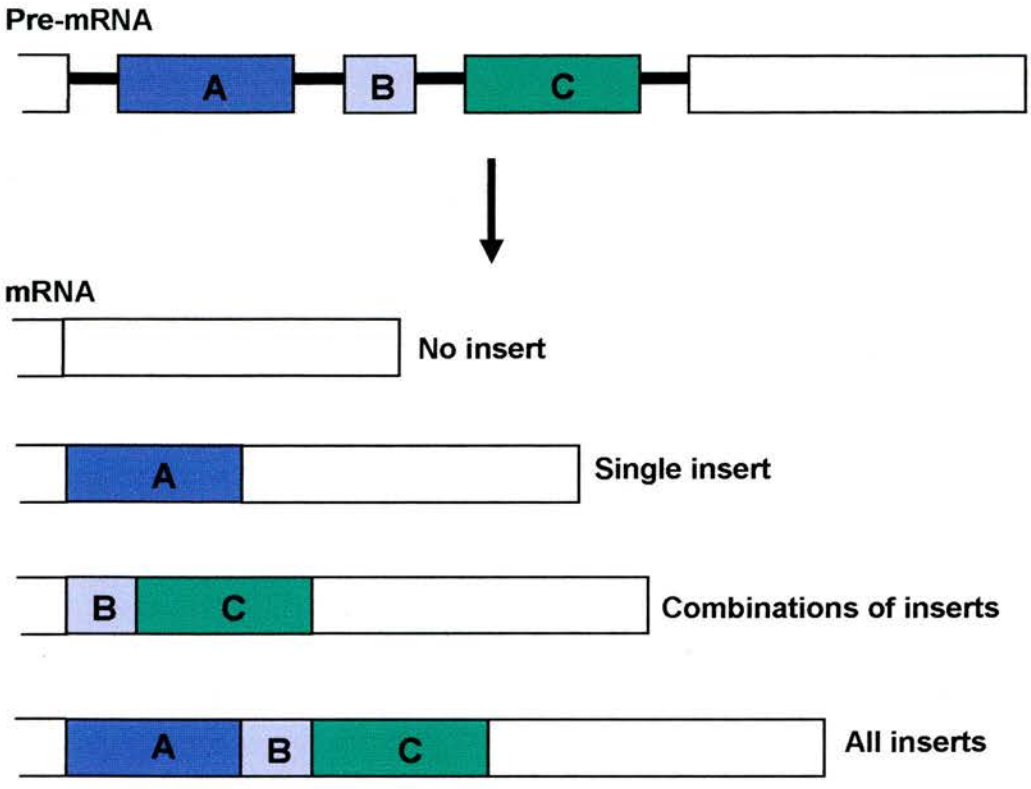

Figure 1-2 Overview of pre-mRNA alternative splicing
Showing possible fates of pre-mRNA during splicing. Alternative exons, A (blue), B (purple) and C (green) may be excluded from mature mRNA, included singly or in combination, or all included to form several products, increasing diversity of proteins encoded by a single gene.

McCobb, 2004) or as an activity- dependent feedback mechanism (Xie and Black, 2001). Within the intracellular C-terminus of the mammalian BK channel, there exist six major sites of alternative splicing, and another splice site is located between the S0 and S1 transmembrane domains (fig. 1-1) (reviewed in Shipston, 2001). Regulation of BK channel alternative splicing in adults can have significant effects on channel responses to calcium, voltage, phosphorylation and glucocorticoids (Tian *et al,* 2001a, b, Hanaoka *et al.*, 1999, Saito *et al.*, 1997). Furthermore, behavioural manipulations have shown that alternative splicing in this manner can be dynamically regulated in adult mammals, enabling the fine- tuning of cellular excitability, for example in adrenal chromaffin cells, to favour passive coping responses by downregulation of sympathoadrenal function following long- term behavioural stress (McCobb *et al.*, 2003). The alternative splicing of BK channels can therefore be seen as a mechanism for adjusting cellular excitability in response to physiological requirements.

1-2-2 Regulatory β-subunits

The N-terminal S0 transmembrane domain is required for modulation of BK channel activity by association with auxiliary β-subunits, and this interaction has been shown to be a significant regulator of channel function, with expression of particular β-subunit splice variants being limited to specific tissues (Jiang *et al.*, 1999). For example, downregulation of the β_1 subunit, exclusively expressed in smooth muscle, causes elevated blood pressure in rats (Amberg *et al.*, 2003). Complementing this, the occurrence of a gain-of-function mutation of the β_1 subunit in humans was found to be protective against diastolic hypertension (Fernandez-Fernandez *et al*, 2004),

increasing the evidence that suggests a role for this particular β-subunit in control of vascular resistance (Nelson and Bonev, 2004).

Certain variants of the β_2 and β_3 subunits are known to confer increased inactivation on the BK channel (Lingle *et al.*, 2001), mediated by the N-terminus of the β-subunit. Channels assembled with the β_3 subunit variant have a rapid, partial inactivation phenotype, and are expressed at a slightly higher level in human patients suffering from epilepsy (Hu *et al.*, 2003), again suggesting that alteration of BK channel function by disregulated expression of channel components can have significant pathological consequences. The β_4 BK channel β-subunit has been shown to confer lowered sensitivity to the BK- specific and potassium channel- specific pore blockers, iberiotoxin (IbTx) and charybdotoxin (CTx) (Meera *et al.*, 2000). This effect was dependent on the large extracellular loop of the β_4 subunit, which when transplanted onto the transmembrane regions of the β_1 subunit conferred IbTx and CTx insensitivity indistinguishable from that of the wild type β_4 subunit. Reduced toxin association in this manner by β-subunit assembly with BK channels may be the molecular basis by which toxin- insensitive channels are formed, for example in rat supraoptic magnocellular neurons (Dopico *et al.*, 1999) where BK channels of varying toxin sensitivities were found to differ in subcellular localisation, with CTx-sensitive channels being expressed on the cell body, whilst CTx- insensitive channels were observed at the nerve terminals. The distinct subcellular localisation of differentially- regulated BK channels in this manner indicates significant regulation of membrane trafficking, and it may therefore be the case that certain alternative splice variants are expressed at a particular region on the cell surface.

In contrast to the digital mode of regulation seen for BK channel tetramers composed of different alternative splice variant α-subunits (Tian *et al.*, 2003), regulation of channels resulting from assembly with β-subunits is more varied; functional channels may be assembled with up to four β-subunits, and the contribution of such is directly proportional to the number of β-subunits per channel (Wang *et al.*, 2002). The contribution of α-subunit alternative splicing to channel regulation in this manner is also of significance, since splice inserts can be incorporated into the channel at a site proximal to the N-terminus (Zarei *et al.*, 2001). By addition of sites favouring association with β-subunits, possibly specifying a particular β-subunit variant, alternative splicing at the BK channel N-terminus might provide further means of increasing functional diversity, separate from changing the intrinsic properties of the α-subunit. The presence of the STREX alternative splice exon has been shown to influence interactions of BK channels with β-subunits, dependent on the α-subunit sequence at the N-terminus. In this case, increased calcium sensitivity conferred by the β_1 subunit was only possible for STREX- containing channels with a truncated N-terminus, encoded by the third potential initiator methionine of the *Slo* gene (Erxleben *et al.*, 2002). This suggests that alternative splicing can also reciprocally affect assembly of functional channels with β-subunits that in turn potentiate shifts in channel gating.

1-3 Regulation of BK channels

1-3-1 Expression

Variable expression of BK channel subunits provides a means of generating functional variety amongst native BK channel populations. For example, in the

mechanosensory hair cells of the auditory sensory epithelium, responsible for translating acoustic stimulation into neuronal signalling, BK channel activity acts as a negative feedback mechanism in response to depolarisation- induced calcium entry. Channel expression then determines the resonant frequency of the hair cells in a graded manner along the tonotopic axis of the cochlea (Fettiplace and Fuchs, 1999). However, whilst in some species such as the chicken, it appears that extensive alternative splicing is the mechanism by which hair cell frequency tuning is achieved (Duncan and Fuchs, 2003), this is not the case in others such as the rat (Langer *et al.*, 2003).

During late pregnancy in rats, mice and humans (Chanrachakul *et al.*, 2004, Eghbali *et al.*, 2003), altered BK channel expression occurs in the myometrium, with the net effect of reducing the number of functional BK channels at the surface of the myocytes. This may represent a means of increasing uterine contractility, by reducing the regulatory influence of BK channels in order to facilitate parturition, and indicates a further means by which variable expression of BK channels can assist normal physiological functions.

1-3-2 Alternative splicing

A large number of studies have focussed on one of the most common alternative splice variants of the BK channel, which contains the 59 amino acid insert known as the 'stress axis- regulated exon' (STREX). Inclusion of the STREX exon is influenced by perturbations of the hypothalamic- pituitary- adrenal (HPA) axis, where the ratio of STREX to ZERO BK channel alternative splice variant transcripts

could be reduced following ablation of HPA axis activity by removal of the pituitary (hypophysectomy) (Xie and McCobb, 1998). Inclusion of the STREX exon in BK channel α-subunits confers increased sensitivity to calcium (Saito *et al.*, 1997) as well as a reversal of channel response to PKA phosphorylation - STREX channels are inhibited by PKA whereas those lacking STREX are activated (Tian *et al.*, 2001b). In addition, BK channels containing the STREX insert can be modulated by glucocorticoid- induced proteins, through serine/ threonine protein phosphatase activity. Since the ZERO BK channel cannot be modulated in this manner, this suggests that the STREX insert is sufficient to confer sensitivity to a glucocorticoid-induced signalling pathway (Tian *et al.*, 2001a).

Another means by which alternative splicing can regulate channel function is by influencing trafficking to the plasma membrane. Control of surface expression of the BK channel is critical to processes such as pregnancy, although there exist inter-species differences in the mechanisms that effect such changes. For example, during late pregnancy, diminished surface clustering of BK channels is observed in both rat and mouse myometrium. However, in the former this is attributable to reduced channel expression (Song *et al.*, 1999), whereas in the latter an increase in expression paradoxically accompanies a reduction in surface clustering (Eghbali *et al.*, 2003).

Whilst highlighting varying mechanisms by which different species regulate cell excitability by expression of BK channel populations, the paradigm of diminished surface trafficking in the mouse myometrium in late pregnancy could also represent a further means of control by alternative splicing, as it may be the case that expression

of a BK channel alternative splice variant, which is dominant- negative for cell surface expression, could cause retention of other α-subunits upon multimerising with them. Consistent with this notion, the BK channel alternative splice variant, SV1 has been shown to exhibit dominant- negative properties for cell surface expression (Zarei *et al.*, 2001), by inclusion of an endoplasmic reticulum retention/ retrieval motif, CVLF (Zarei *et al.*, 2004). This effect was also independent of the location of the CVLF motif in the channel sequence, therefore whilst the originally-observed occurrence of this motif was located between the S0 and S1 transmembrane segments of the channel, it may be the case that hitherto undiscovered alternative splice variants might also include this sequence within the intracellular C-terminus. The presence of such a motif may also be accompanied by additional sequences that increase tetramer stability (Jones *et al.*, 2004); during physiologically significant changes in excitability of uterine smooth muscle cells, such as those observed in late pregnancy, sex hormone signalling may upregulate expression of splice variants with a phenotype that is dominant- negative for surface expression, to reduce BK channel presence at the membrane, thus preparing the uterine smooth muscle for increased contractility.

Control of cell excitability by BK channel activity is contributed to by genomic and non- genomic responses. Alternative splice variants can be differentially regulated; changing expression of a specific subset of the BK channel population, such as the glucocorticoid- regulated STREX channels, represents one means by which a diversity of responses can be gained from products of a single gene. However, the mechanisms by which splicing decisions are made are unclear. While the factors that

promote STREX inclusion are unknown, in GH_3 rat pituitary cells depolarisation induces a repression of STREX BK channel transcripts (Xie and Black, 2001). This has been shown to require Ca^{2+}/ calmodulin- dependent protein kinase IV (CaMK IV) activity, in addition to a pyrimidine- rich repressor (D56) element within the STREX exon itself and a CaMK IV- responsive RNA element (CaRRE) within the intronic sequence upstream of STREX. Since reducing STREX expression will reduce the open probability of BK channels, and subsequently responsiveness of the BK population as a whole, significant effects on cell excitability can be controlled by this regulation.

In this manner, the depolarisation- induced STREX repression may be a form of negative feedback regulation, acting to maintain homeostasis during periods of chronic activity. It may therefore be of significance in regulation of lasting changes in cell responsiveness, for example in the cerebellum and hippocampus during motor and spatial learning. Additionally, this may be the mechanism by which STREX expression is reduced in adrenal chromaffin cells following chronic stress. Initially, acute stress of this nature might be expected to cause a temporary upregulation of STREX expression in the chromaffin cells, enabling heightened release of adrenal steroids, but with chronic stimulation, a reduction in STREX expression might be required to facilitate adaptation and coping, as well as reducing secretory activity to prevent damage arising from the allostatic load of chronic glucocorticoid release (McEwen, 2001).

1-3-3 Multimerisation

Functional BK channels are formed from tetramers of pore- forming α-subunits. Such assembly is dependent on presence of association domains (ADs). In the BK channel, several experimental approaches identified a protein domain, BK-T1, which acts as an AD (Quirk and Reinhart, 2001). Located downstream of the pore- forming region, in the hydrophilic linker region, L6, between hydrophobic segments S6 and S7. This region has been shown to self- associate to form tetramers, and is the only hydrophilic region of the channel that is able to do so. However, this may not be fully descriptive of assembly of functional channels. Structural analysis of a K^+ channel from *E.coli* showed it to contain a domain that regulates conductance of potassium, RCK, which is common to many prokaryotic K^+ channels (Jiang *et al.*, 2001). This structural feature was also found in BK channels, overlapping the BK-T1- containing L6 region. In spite of low sequence identity, conserved residues in the prokaryotic RCK sequence are also conserved in that of the eukaryotic BK channel. Dimerisation of RCK domains is significant in correct expression of *E.coli* K^+ channels, as well as BK channels in *Xenopus* oocytes, and is mediated by conserved hydrophobic residues on the outside face of the fourth α-helix of the domain. Assembly of functional channels may be dependent on hydrophobic interaction between residues from the RCK domain to form dimers, then other residues outside the RCK region stabilise the interaction between dimers to form tetramers.

The functional relevance of alternative splicing and tetramerisation of BK channel α-subunits raises an important issue of the composition of channel multimers at the membrane level; for example, are functional BK channels only composed of a single

splice variant (homotetramers), resulting in a strictly delimited set of functional properties, or is heterotetramerisation between differentially spliced α-subunits possible, enabling a much wider range of responses from the channel population? Since the tetramerisation domain of the BK channel is conserved between BK channel alternative splice variants, it is likely to be the case that heterotetramers can form *in vivo* (Quirk and Reinhart, 2001). However, there is also the possibility that alternative splicing can be a mechanism to prevent surface expression (Zarei *et al.*, 2004) therefore it is probable that heteromeric combinations containing certain alternative splice variants simply do not reach the membrane.

Using a site- directed mutagenesis approach to generate BK channel α-subunits that were insensitive to TEA, then expressing these with wild- type α-subunits, it has been shown that phosphorylation- induced activation and inhibition of BK channels containing alternatively spliced α-subunits is essentially digital (Tian *et al.*, 2004). For the ZERO splice variant, homomeric channels follow an 'all or nothing' rule regarding activation by PKA via phosphorylation of the conserved S899 PKA consensus site, where all four subunits within the tetramer required phosphorylation for activation. However, inhibition of channels containing the STREX splice variant only required a single STREX- containing α-subunit to be phosphorylated at the $S4_{STREX}$ PKA consensus site to decrease channel activity. It is clear therefore that even in homomeric assemblies of α-subunits, distinct modes of regulation arise as a result of alternative splicing. When ZERO and STREX α-subunits were assembled into heterotetramers, it was found that the inhibitory effect of the $S4_{STREX}$ PKA consensus site was only significant if the S899 sites on all four subunits were

dephosphorylated. In channel heterotetramers, activation was still facilitated by phosphorylation of all four S899 sites, regardless of the presence of one or more intact $S4_{STREX}$ site. It can therefore be seen that there is a strong possibility that heteromeric assembly of alternatively spliced BK channel α-subunits occurs *in vivo*, but that a hierarchy exists to determine the functional phenotype. Although regulation in response to PKA was effected in an essentially digital manner for ZERO and STREX channels, it may be the case that specific phosphorylation of either S899 or $S4_{STREX}$ sites within a channel heterotetramer can occur, leading to context- specific regulation.

Since the leucine zipper motif has been shown to be a requirement for assembly of other ion channel types (Zhong *et al.*, 2003), it may also be involved in BK channel tetramer assembly. Although the C-terminal "LZ1" domain in the BK channel was shown to be required for protein kinase A regulation, it may be the case that other leucine zipper sites within the C-terminus facilitate tetramerisation. Although the BK-T1/ RCK region is suggested as the primary site of interaction between α-subunits, the presence of leucine zipper motifs may help stabilise this interaction. Differential folding of certain BK channel α-subunit alternative splice variants may hide or expose the LZ motifs, and novel splice variants might even include additional LZ repeats, thereby engendering increased affinity for other α-subunits. Heightened subunit- subunit interaction in this manner may serve to make certain combinations of α-subunits more energetically stable than others, thereby acting as a means of preferential inclusion into functional channels.

1-3-4 Post-translational regulation

Phosphorylation by protein kinases such as cAMP- dependent protein kinase (PKA), protein kinase C (PKC) and cGMP-dependent protein kinase (PKG) is an important means of post-translational BK channel regulation, and is significant in modulation of BK channel calcium- and voltage- sensitivities during changes in Ca^{2+} concentration and membrane depolarisation (Schubert and Nelson, 2001). Several sites within the BK channel allow functional modulation of channel properties. Regulation of BK channel function via phosphorylation by endogenous cAMP-dependent protein kinase (PKA) has been shown to require a leucine zipper motif (LZ) (Tian *et al.*, 2003), which is known to be significant in ion channel assembly (Jones *et al.*, 2004) and also the interaction of protein kinases with other ion channel types (Hulme *et al.*, 2002). The stereotypical LZ domain consists of a seven residue (heptad) repeat, with hydrophobic residues at the first and fourth positions, and is critical for PKA phosphorylation, as it mediates anchoring of the kinase to several types of ion channel by A Kinase-Anchoring proteins (AKAPs). In the BK channel, a highly conserved, non- canonical LZ motif exists downstream of the RCK domain, at residues 513-548 in the intracellular C-terminal tail, and is required for the PKA-mediated regulation (Tian *et al.*, 2001b) of ZERO and STREX BK channel alternative splice variants in a manner that is independent of AKAPs (Tian *et al.*, 2003). A second putative LZ motif is located at residues 816-843, and it is thought that in the C-terminus of the BK channel there exist at least two additional sites containing LZ- like heptad repeats (Tian *et al.*, 2003). Other modes of interaction also exist, that facilitate functional regulation of the BK channel by PKA. For example, formation of a macromolecular complex containing BK channels, L-type

calcium channels and β2 adrenergic receptors enables β adrenergic regulation of BK channel function. This interaction requires association of the β2 adrenergic receptor with the BK channel and AKAP79, facilitating cAMP- dependent phosphorylation of the BK channel by anchored PKA (Liu *et al.*, 2004).

Protein kinases regulate BK channel activity in many tissues (Zhang *et al.*, 2004, Schubert and Nelson, 2001) and variable responses to the same kinase, PKA for example, can be elicited by alternative splicing of the BK α-subunit. Kinase or phosphatase activity likely forms a context- dependent means of selective activation or inhibition of a specific subset of the channel population (Widmer *et al.*, 2003). Evidence also exists for differential regulation by other cyclic nucleotide- dependent protein kinases, (Barman *et al.*, 2004, Barman *et al.*, 2003), with functional cross-activation between the signalling pathways- for example, in pulmonary smooth muscle, PKC- induced relaxation is achieved by opening of BK channels via cyclic GMP- dependent kinase. As well as the conserved phosphorylation sites in the BK channel, additional sites may be added by alternative splicing (Tian *et al.*, 2001b), therefore it is evident that multiple modes of regulation can exist, and as for other aspects of channel function, such as tetrameric assembly, there may be a hierarchy regarding which subunits control the phenotype of the whole channel.

Additionally, there exist other, physiologically significant forms of post- translational regulation of BK channel activity, such as redox regulation (Tang *et al.*, 2001). Methionine and cysteine oxidation have been shown to act in an opposing manner to regulate BK channel opening, and therefore may be of significance in mediating

effects of reactive oxygen species on cell excitability (Tang *et al.*, 2001). Evidence also exists for modulation of BK channel function by hypoxia, where hemoxygenase-2 has been shown to act as a sensor for acute reductions in oxygen, causing downregulation of BK channel activity (Williams *et al.*, 2004), and this mechanism may be of physiological significance in respiratory control.

1-4 Physiology of BK channels

1-4-1 Distribution

The BK channel is distributed in invertebrates (Becker *et al.* 1995) and vertebrates, throughout a wide range of tissues, such as brain (Wanner *et al.*, 1999), smooth muscle (McCobb *et al.*, 1995), epithelia (Lam *et al.*, 2004) and gonads (Gong *et al.*, 2002, Kunz *et al.*, 2002). Coordinated expression of alternative splice variants of the BK channel, and/ or assembly with β-subunits likely provides a range of responses commensurate with functional requirement that is unique to the electrical properties of cells or tissues. Consistent with the notion that membrane proteins seldom function as discrete units, BK channels are frequently found to colocalise with intracellular calcium channels (ICCs) and voltage- dependent calcium channels (VDCCs) (Grunnet and Kaufmann, 2004). Such colocalisation gives the channels ready access to intracellular free calcium (Wellman and Nelson, 2003, Marrion and Tavalin, 1998), which is a requirement for activation under physiological conditions. It is also thought to enable their contribution to the regulation of intracellular calcium, for example by acting as a feedback mechanism following depolarisation-induced calcium entry.

Differential localisation of the BK channel has been observed in neurons of the rat brain (Knaus *et al.*, 1996), and continuing studies indicate an increasingly diverse range of subcellular distributions of the BK channel. For example, it has been shown that in epithelial cells, expression of the BK channel is delimited to the apical surface when the cells are grown in a monolayer (Bravo- Zehnder *et al.*, 2000). Whilst several transmembrane proteins are preferentially expressed at the apical surface of polarised cells as a result of glycosylation at specific residues (Vagin *et al.*, 2004, Potter *et al.*, 2004), deletion of the only such site in the BK channel showed that trafficking is independent of this pathway. Instead it has been suggested that apical trafficking might be determined by assembly of the BK channel with lipid rafts (Lam *et al.*, 2004, Bravo-Zehnder *et al.*, 2000). Since trafficking of BK channels to specific subcellular regions is significant in regulation of cell excitability (Hu *et al.*, 2001) and altered surface trafficking has been observed for BK channels incorporating certain alternatively- spliced exons (Zarei *et al.*, 2004), there is also the possibility that other BK channel alternative splice variants are subject to regulated cell surface expression. Whilst the CVLF motif in the SV1 splice insert was discovered to cause retention/ retrieval of the BK channel to the endoplasmic reticulum (Zarei *et al.*, 2004), it may be the case that similar motifs may influence BK channel trafficking to distinct cell regions, such as axons or synapses, with functional consequences arising from this regulated localisation.

1-4-2 Functional role of the BK channel

1-4-2-1 Neurons

BK channels are expressed in a variety of neurons (Gong *et al.*, 2001, Safronov and Vogel, 1998), and have been shown to colocalise with voltage- dependent calcium channels (VDCC) (Grunnet and Kaufmann, 2004, Marrion and Tavalin, 1998). Following membrane depolarisation, and subsequent increase in intracellular calcium due to VDCC activation, BK channel activation facilitates repolarisation and hyperpolarisation of the membrane potential, thereby also acting as a regulator of VDCC function. By responding to depolarisation- induced calcium entry in this manner (Gribkoff *et al.*, 2001), BK channels may act presynaptically as significant modulators of transmitter release (Raffaelli *et al.*, 2004, Lim *et al.*, 1998, Robitaille *et al.*, 1993). BK channels also contribute to shaping of action potentials (Miranda *et al.*, 2003) and action potential frequency (Hu *et al.*, 2001) suggesting a further role in changing cell firing patterns.

It is clear that the contribution of regulated BK channel expression to neuronal excitability facilitates normal brain function; mutation of the BK channel α-subunit has been shown to cause generalised epilepsy and paroxysmal dyskinesia, by causing increased cell excitability as a result of a three- to fivefold increase in calcium sensitivity of the BK channel (Du *et al.*, 2005). Futhermore, mutant mice lacking BK channel expression exhibit various signs of cerebellar learning deficiency, and has been suggested that regulation of Purkinje neuron excitability by BK channels is critical to correct cerebellar function and development (Sausbier *et al.*, 2004).

1-4-2-2 Development of the central nervous system

Since dynamic regulation of the BK channel has been observed in adults, and as a result can have significant effects on cell excitability, it is intuitive to speculate that channel expression may also change during development, particularly during the profound changes in excitability that occur as the CNS matures. Studies to date focusing on primary neurons in the spinal cord of the frog, *Xenopus laevis*, have been used as a model for investigating changes in expression of several ion channel types during embryogenesis (Spitzer and Ribera, 1998), and subsequent effects on cell and systems function.

During *Xenopus* embryogenesis, the main contributors to the outward voltage- gated potassium current in spinal cord neurons are delayed rectifier channels. However as development continues and the larval stage is reached, these are replaced by BK channels, over the period from stage 37/38 – 42 (Sun and Dale, 1998). Changes in the expression of high- voltage activated (HVA) calcium channels accompany this shift, with channels of the P/Q type gradually being expressed to partially replace the embryonic HVA calcium channels, until stage 42 where almost all of the spinal cord neurons possess a P/Q type current (Jiminez-Gonzalez *et al.*, 2003). This period corresponds with onset of burst firing in the spinal cord neurons, and it is likely that these shifts in channel expression are a major contributor to the repetitive firing and burst termination during this activity. In addition to the upregulation of total BK channel during development, the question of alternative splicing also arises. Since certain of the known alternative splice variants enhance the sensitivity of the channel to intracellular calcium, for example, these might be predicted to occur in systems

where repetitive firing occurs. This has been shown to be the case in *Xenopus*, where the STREX BK channel homolog, xSlo59, becomes upregulated during embryogenesis at the onset of developmentally- regulated changes in action potentials in the spinal neurons (Kukuljan *et al.*, 2003). Such changes in the expression of BK channel variants may enable specific tuning of the frequency of calcium transients in neurons (Kraft *et al.*, 2003, Komuro and Rakic, 1996), where the rates of migration during development are dependent on regulated calcium oscillations of distinct amplitudes and frequencies. Since BK channels are modulators of intracellular calcium concentration, adjusting BK channel properties by alternative splicing could provide a molecular switch that determines correct termination of neuronal migration in this manner. Investigation of expression of BK channel alternative splice variants in the central nervous system may therefore provide insight into the developmental stages at which such regulated changes in channel expression, and subsequently neuronal excitability, occur.

1-4-2-3 Smooth muscle

In vascular smooth muscle, BK channels are major contributors to negative feedback regulation of contractility (Herrera *et al.*, 2005). Following depolarisation and contraction- induced elevations of intracellular calcium, BK channels activate to repolarise the membrane potential. Posttranslational regulation of the BK channel enables generation of a range of responses to stimuli (Schubert and Nelson, 2001), and in addition to this, assembly of channel α-subunit tetramers with the smooth-muscle- specific β1 subunit (Jiang *et al.*, 1999, Knaus *et al.*, 1994) facilitates changes

in channel phenotype that are necessary for correct regulation of arterial pressure (Nelson and Bonev, 2004).

Evidence also supports a role for BK channel activity in other physiological processes where smooth muscle contractility is of significance. For example, in late pregnant rats and mice, diminished surface expression of BK channels in the myometrium has been observed (Eghbali *et al.*, 2003). In rats, a reduction in BK channel expression occurs, whilst in mice channel expression increases, but with reduced surface trafficking. In humans, the level of BK channel expression in the myometrium falls by approximately 50% after the onset of labour (Chanrachakul *et al.*, 2004). In spite of the inter- species differences in the manner in which it is achieved (Benkusky *et al.*, 2000, Wang *et al.*, 1998), it is likely that during late pregnancy, the reduction in surface BK channels in myocytes represents a mechanism for increasing myometrial contractility, thus facilitating parturition.

1-4-2-4 Endocrine cells

The BK channel is also of significance in the regulation of endocrine function. For example, in adrenal chromaffin cells, BK channel expression may be significant in tuning of cell excitability, subsequently influencing release of adrenal steroids (Lovell and McCobb, 2001). Chronic stress has been demonstrated to be a means of inducing robust, depression- like changes at behavioural and molecular levels in animal models (Rosenbrock *et al.*, 2005, Herman and Cullinan, 1997), and the major effector of such changes is the hypothalamic- pituitary- adrenocortical (HPA) axis. Following stress, increased secretion of corticotrophin releasing hormone (CRH) by

the paraventricular nucleus of the hypothalamus causes release of adrenocorticotropic hormone (ACTH) from the anterior pituitary. ACTH signalling from the pituitary then causes upregulated release of adrenal steroids- most significantly cortisol in humans, and corticosterone in rodents. Adrenal responsiveness is therefore critical to correct control of secretion, as it determines the capacity of the animal to adapt to stressful stimuli (al'Absi and Arnett, 2000). The BK channel has been shown to be a key regulator of excitability in the secretory cells of the adrenal gland (Lovell *et al.*, 2004, Nagayama *et al.*, 1998). Since both glucocorticoids as well as sex steroids can influence expression of BK alternative splice variants (Song *et al.*, 1999, Xie and McCobb, 1998), investigation into BK alternative splicing in the tissues of the HPA axis, as well as other steroid- responsive tissues will increase understanding of the role of regulated expression in control of secretory activity during stress as well as normal diurnal rhythm.

Control of cell excitability by BK channel activity occurs not only in the adrenal gland (Lingle *et al.*, 1996) but also at the pituitary (Miranda *et al.*, 2003, Shipston *et al.*, 1999) and hypothalamic (Dopico *et al.*, 1999) levels, where they are implicated in feedback control of depolarisation- induced secretion. The variability in BK channel gating that arises from alternative splicing of α-subunits is therefore of significance during the study of the stress response (Lovell *et al.*, 2004), particularly with regard to adaptation following long- term chronic stress (McCobb *et al.*, 2003). Effects of circulating glucocorticoids may be amplified or reduced according to the relative proportions of glucocorticoid- sensitive, or insensitive BK channel alternative splice variants expressed in target tissues, therefore the regulation of such

expression is likely to be significant in maintaining homeostasis during chronic elevation of HPA axis activity.

Manipulation of pituitary ACTH release has been shown to control the STREX splicing decision in the adrenal chromaffin cells (Lovell and McCobb, 2001), where the BK channel is a significant modulator of excitability, with subsequent effects on catecholamine release. Removal of the pituitary (hypophysectomy) causes a reduction in the proportion of adrenal BK channel transcripts containing the STREX exon, reversible by administration of ACTH (Xie and McCobb, 1998). This type of regulated alternative splicing has also been observed *in vivo*, in response to chronic subordination stress in tree shrews (McCobb *et al.*, 2003), leading to the suggestion that adrenal steroid release is tailored by changing BK channel expression. In this case, chronic social defeat in tree shrews led to a downregulation of STREX expression in the adrenal, the subsequent reduction in cell excitability favouring lower rates of adrenal secretion. As a result of this, animals might tend towards passive coping behaviours as opposed to proactive aggressive strategies. Additionally, sex differences were observed, with female tree shrews also displaying reduced adrenal STREX expression compared to both control and stressed male subjects. Such sex differences were not observed in rats (Mahmoud and McCobb, 2004), indicating that there are clear species differences in sexually dimorphic expression of BK channels. However, in both tree shrews and rats, decreased STREX expression in the pituitary correlated with lowered testosterone, suggesting male gonadal influence on HPA axis activity.

Since there is significant and complex functional crosstalk between the HPA and hypothalamic- pituitary- gonadal (HPG) axes (Viau, 2002) it is also possible that female steroids may be significant in regulation of STREX expression. The BK channel is critical to steroidogenesis in ovarian endocrine cells, where ablation of BK activity by iberiotoxin significantly reduced progesterone secretion (Kunz *et al.*, 2002). Since progesterone has a feedback effect on its own production, as well as that of oxytocin and prostaglandins (Schams and Berisha, 2002), it may be the case that tuning of BK channel activity by alternative splicing or differential channel assembly, and resultant expression of subsets of differentially regulated splice variants, is involved in regulating the cyclic nature of ovarian secretion, as well as endocrine effects of female steroids on homeostasis (Duncan, 2005, Dimitropoulou *et al.*, 2005). Additionally, the glucocorticoid- induced inhibition of female steroid secretion observed following stress (Kalantaridou *et al.*, 2004) might be mediated by altered BK channel splicing.

1-4-2-5 Epithelia

BK channels fulfil a variety of physiological roles in epithelial cells. Localised channel expression, for example at the apical surface of epithelia (Bravo-Zehnder *et al.*, 2000) may be of significance in active potassium secretion during normal homeostatic processes (Joiner *et al.*, 2003), and it has been shown that increased dietary K^+ intake causes upregulated BK channel expression at the apical surface of cells in rat distal colon (Butterfield *et al.*, 1997). In addition to regulating secretion in this manner, BK channels may also be of significance in other processes, such as cell volume regulation. Cell swelling, induced by perturbations in extracellular ion

concentration, has been shown to cause activation of BK channels in retinal pigment epithelial cells (Sheu *et al.*, 2004), and there is also evidence for BK- channel mediated oxygen sensing in alveolar epithelia (Jovanovic *et al.*, 2003), possibly contributing to fluid clearance from the lung.

1-4-2-6 Innate immunity

An additional role for BK channel activity has been discovered in the innate immune system, where the channel is expressed in the cell membrane as well as membranes of cytoplasmic granules from neutrophils and eosinophils (Ahluwalia *et al.*, 2004). Whilst the canonical view of microbicidal activity in the innate immune system is that bacteria are destroyed by activity of reactive oxygen species, a new role has been suggested for generation of a hypertonic, K^+- rich environment in the phagocytic vacuole by BK channel- mediated potassium release (Ahluwalia *et al.*, 2004), thereby inducing release of proteases from intracellular granules (Reeves *et al.*, 2002) that are responsible for the bactericidal activity.

1-4-3 BK channel roles in pathophysiological states

Since regulated BK channel expression is implicated in homeostasis, development and immune function, and the expression of a range of alternative splice variants with differing functional phenotypes may contribute to this, it is inevitable that perturbation of BK channel function can also contribute to certain pathological states (Du *et al.*, 2005, Weaver *et al.*, 2004, Meredith *et al.*, 2004). The role of BK channels in disease is therefore of significance, as pharmacological manipulation of these channels may be of therapeutic benefit.

Coordinated BK channel activity contributes to correct maintenance of blood pressure by regulating arterial diameter (Wellman and Nelson, 2003, Standen and Quayle, 1998). The increased intracellular Ca^{2+} that accompanies contraction of vascular smooth muscle cells leads to elevation of Ca^{2+} in the sarcoplasmic reticulum, and subsequent local release of Ca^{2+} as 'calcium sparks' from the sarcoplasmic reticulum through ryanodine- sensitive calcium release channels (ryanodine receptors) causes activation of BK channels (Wellman and Nelson, 2003), thereby enabling feedback regulation of cell excitability during smooth muscle contraction. Loss of this coupling of calcium sparks to BK channel activity may be an underlying cause of disregulated vascular contraction in hypertension, and has been shown to be due to decreased expression of the BK channel β_1-subunit (Amberg *et al.*, 2003). Control of the molecular composition of BK channels can therefore be seen to be of significance in homeostasis.

Regulated BK channel activity may also be significant in developmental processes. BK -/- knockout mice, which do not express BK channel α-subunits, show several symptoms of cerebellar learning deficiency, such as ataxia and inability to develop conditioned eye- blink responses to stimuli (Sausbier *et al.*, 2004). Since the cerebellum in knockout mice was morphologically similar to that of the wild type, it might be inferred that although BK channel α-subunit expression may not necessarily be required for gross morphological formation of the cerebellum, it is critical for correct cerebellar function and motor learning.

Another role of the BK channel is in control of potassium secretion (Woda *et al.*, 2001). In the kidney, baseline K^+ secretion is primarily through SK channels, whilst BK channels mediate flow- dependent K+ secretion. Disruption of correctly controlled BK channel expression may lead to inappropriate or excessive loss of potassium, therefore tight regulation of expression must be maintained to enable correct homeostasis. In patients with end- stage renal disease (ESRD), the potassium permeability in the colon is increased up to three times that of normal individuals (Mathialahan *et al.*, 2005), attributable to increased expression of BK channels in the surface colonocytes, as well as crypt cells, where they are absent in non- ESRD individuals, and the increased potassium loss is sufficient to be physiologically significant.

Since dysregulation of BK channel expression is a facilitator of pathological conditions, there is increasing evidence that certain splice variants of the channel are markers for disease. For example, the splice variant glioma BK (gBK) has been shown to be highly expressed in glioma cells, encoding a BK channel containing a 34aa insert at splice site C2 that enhances channel sensitivity to intracellular calcium concentration (Liu *et al.*, 2002). Although gBK is also expressed in normal cortical tissues, its expression is upregulated in glioma cells. Additionally, expression of BK channels has also been shown to be positively correlated with tumour malignancy grades, therefore this novel splice variant may be a facilitator of tumorigenesis.

Coordinated calcium signalling is a prerequisite for normal neuronal migration (Komuro and Rakic, 1996), and this process is also dependent on potassium channel

activity (Schwab *et al.*, 1999). In order to correctly complete migration, motility of neurons must be terminated once their destination is reached, and this is achieved by ablation of calcium transients (Kumada and Komuro, 2004). Since activation of BK channels influences intracellular calcium concentration (Wu, 2003), it is likely that they are involved in the tuning of such transients. Distinct frequencies of calcium oscillations were observed in migrating granule cells in cerebellar slices, therefore it may be the case that variable expression of BK channels is a means of increasing cell responsiveness, enabling coordinated control of both timing and magnitude of calcium signals, in a manner that is permissive to migration. Since gBK is expressed in non- neoplastic neurons, but was upregulated in glioma cells, and heightened BK channel expression is correlated with increasing tumour malignancy, it is possible that overexpression of this splice variant facilitates the correct pattern of calcium transients that enable migration of the tumour. However, during this process coordinated BK channel activity is still required, as the application of BK channel openers has been found to inhibit glioma migration (Bordey *et al.*, 2000). This might suggest that migration is terminated by an upregulation of BK channel activity. BK channels in normal glial cells may be sensitive to signalling factors released by target tissues, which may cause BK channel activation, thus facilitating termination of migration. It has been suggested that gBK is the only BK channel splice variant that is present in glioma cells (Liu *et al.*, 2002), and it may be the case that gBK channels are insensitive to the regulatory signals that normally limit neural cell mobility, thereby enabling inappropriate migration of the glioma.

Mutation of the BK channel α-subunit, resulting in altered activation properties, has also been shown to be of pathophysiological significance. In the case of generalised epilepsy and paroxysmal dyskinesia, a single A-G base mutation causes the aspartic acid residue at position 434, within the regulator of conductance of K^+ (RCK) domain of the channel to be changed to glycine. This has the effect of increasing BK channel calcium sensitivity three- to fivefold, thus causing disregulation of cell excitability, resulting in epilepsy and dyskinesia (Du *et al.*, 2005).

Whilst alteration of BK channel populations may be permissive for pathological states, coordinated channel activity may also have a protective role during certain conditions. For example, during ischemia following stroke or trauma, excessive levels of excitatory neurotransmitters are released (Babot *et al.*, 2005, Boris-Moller and Weiloch, 1998), leading to excitotoxic neuronal death resulting from excessive calcium influx (reviewed in Kristián and Siesjö, 1998), and this is pathologically significant in several neurological diseases. Since BK channels can activate as an 'emergency brake' to limit increases in intracellular calcium, it has been suggested that they might be part of an endogenous mechanism which enables neuroprotection during ischemic injury, evidenced by the fact that in organotypic cerebrocortical and hippocampal slice cultures, blockade of BK channel activity caused increased cell death following oxygen deprivation (Katsuki *et al.*, 2005, Rundén-Pran *et al.*, 2002). It is also possible that BK channel- mediated neuroprotection is enhanced presynaptically by hyperpolarising the cells to limit excessive excitatory neurotransmitter release. It may be the case that BK channel alternative splice

variants such as STREX, which have heightened calcium sensitivity, facilitate stronger neuroprotection during oxygen deprivation.

1-5 Aims and objectives of thesis

1-5-1 Issues to be addressed

Alternative splicing of the BK channel α-subunit is significant in the modulation of BK channel function during a number of physiological processes, however critical questions arise regarding this regulation. Firstly, although distinct patterns of subcellular distribution of BK channels have been observed (Knaus *et al.*, 1996), the contribution of alternative splicing to such localised expression has not been thoroughly investigated. Since an alternative splice insert of the BK channel, SV1, has been shown to cause retention/ retrieval of the BK channel to the endoplasmic reticulum (Zarei *et al.*, 2004), do similar modes of splice variant- specific regulation exist to determine the trafficking of other α-subunits to the cell surface? Additionally, since heteromeric assembly of differentially spliced BK channel α-subunits has been shown to influence channel regulation (Tian *et al.*, 2004), does such regulation occur for subcellular localisation, where alternatively spliced α-subunits may influence the expression of BK channels in which they are included?

Secondly, what is the differential tissue distribution of BK channel alternative splice variants? Alternative splicing of the BK channel provides functionally distinct BK channels in different tissues (Oberholtzer, 1999, Saito *et al.*, 1997), however the distribution of splice variants across tissues has not been well characterised.

Thirdly, given the significance of regulated neuronal signalling during development of the central nervous system, and since BK channels contribute to synaptic release and action potential shaping and frequency (Raffaelli *et al.*, 2004, Miranda *et al.*, 2003, Hu *et al.*, 2001), does alternative splicing of the BK channel contribute to regulation of neuronal excitability in order to facilitate this process? Since a neuron-specific splice variant of the BK channel has been observed during *Xenopus* embryogenesis (Kukuljan *et al.*, 2003), does such developmentally- regulated splicing also occur in mammalian systems?

Finally, dynamic alternative splicing of the BK channel in the adrenal gland has been shown to occur in response to chronic stress in tree shrews (McCobb *et al.*, 2003), and expression of BK channel alternative splice variants in the pituitary gland was demonstrated to be subject to steroidal regulation (Mahmoud and McCobb, 2004). However, the regulation of BK channel splicing in other tissues of the HPA axis, as well as other steroid- sensitive brain regions, in response to physiological challenge in the mouse is unclear.

This thesis aims to test the following hypotheses:

1) That alternative splicing can influence the subcellular localisation and assembly of the BK channel, using alternatively spliced mouse BK channel α-subunits as a model for examining differential subcellular localisation.
2) That BK channel alternative splice variants are differentially expressed in different tissues, and that splice variant expression can be dynamically

regulated, for example during development or in response to physiological challenge.

Cloned murine BK channel alternative splice variants and BK channel alternative splice variant expression in mouse tissues were used as the model for studies throughout this thesis.

1-5-2 Synopsis of chapters

In chapter 3, visualisation of the subcellular localisation of BK channel alternative splice variants is investigated. BK channels fused at the C-terminus with fluorescent proteins are used in order to study the effects of inclusion of different alternative splice inserts on surface expression of the BK channel in mammalian cell lines, and examine the effects of endogenous BK channel trafficking mechanisms on these fusion proteins. Additionally, the simultaneous colocalisation of BK channel α-subunit alternative splice variants labelled with spectrally distinct fluorescent proteins is examined, and the use of these fusion proteins as tools for analysis of heteromeric assembly of differentially- spliced BK channel α-subunits is also investigated.

In chapter 4, real time PCR assays are designed and optimised in order to facilitate the rapid, highly specific and sensitive detection and quantitation of expression of BK channel alternative splice variants. These are then applied to screen mouse tissues in order to examine the relative expression levels of five known BK channel alternative splice variants, at splice site C2, throughout the animal.

The real time PCR assays for BK channel alternative splice variants are then applied in chapter 5, in order to investigate regulated changes in splicing during development. Tissues of the mouse CNS at several embryonic and early postnatal stages are assayed for the presence of the STREX and ZERO BK channel α-subunits, in order to observe whether the expression of these two alternative splice variants changes over the course of development.

Chapter 6 addresses the regulation of BK channel alternative splicing in response to physiological challenge. Expression of the STREX BK channel alternative splice variant is investigated during two different chronic stress paradigms, as well as pharmacological and surgical manipulation of glucocorticoid levels. Real time PCR is used to investigate whether perturbations of HPA axis activity can alter the expression of the STREX BK channel alternative splice variant in the mouse, in tissues of the HPA axis, as well as other steroid- responsive brain regions.

Finally, chapter 7 summarises findings of this study, and suggests future experiments based on questions arising from the results obtained.

Chapter Two:

Materials and methods

2-1 Suppliers of materials

2-1-1 Chemicals

Unless stated otherwise, all chemicals were supplied by Sigma-Aldrich Co. Ltd, Poole, Dorset, UK, and were of the highest grade available.

2-1-2 Molecular biology and cell culture Reagents

Applied Biosystems (UK), Warrington, Cheshire, UK

Taqman® real time PCR primer and probe sets

Taqman® universal PCR master mix

Mouse BK channel 'Assay on Demand' ready-mixed 20x primer and probe set, assay ID **Mm00516078_m1**

BD Biosciences Clontech, Palo Alto, CA, USA

BD Living Colours™ pHcRed-N1 vector

Biogene Ltd., Kimbolton, Cambridgeshire, UK

Real time PCR master mix including Hotstart Taq and ROX

Bioline Ltd., London, UK

Hyperladder™ I quantitative DNA ladder

Bio-Rad Laboratories Ltd., Hemel Hempstead, Hertfordshire, UK

Gel electrophoresis power supply

Gibco™ Invitrogen Corporation, Paisley, UK

Mammalian cell culture media and reagents

Harlan Sera-Lab Ltd., Loughborough, Leicestershire, UK

Foetal Calf serum

Helena Biosciences Europe, Sunderland, Tyne & Wear, UK

Agarose (Calbiochem)

Pellet Paint co-precipitant (Novagen)

Merck Biosciences Ltd., Beeston, Nottingham, UK

Mowiol 4-88 reagent

Molecular Probes Inc., Eugene, OR, USA

TO-PRO 3 Iodide nucleic acid stain

MWG Biotech AG, Ebersberg, Germany

PCR primers

Sequencing of DNA

Pharmacia Diagnostics AB, Uppsala, Sweden

Gel electrophoresis tanks

Promega Ltd., Southampton, UK

Restriction enzymes, T4 DNA ligase,

Roche Diagnostics GmbH, Mannheim, Germany

Expand High Fidelity PCR System

2-1-3 Antibodies

Autogen Bioclear UK Ltd., Calne, Wiltshire, UK

Goat Anti EEA1 polyclonal.

BD Biosciences, Oxford, UK

Mouse anti ERp72 monoclonal

Mouse anti GM130 monoclonal

Molecular Probes Inc., Eugene, OR, USA

Donkey Anti-Goat IgG (H+L), Alexa Fluor® 647 conjugate

Donkey Anti-Mouse IgG (H+L), Alexa Fluor® 647 conjugate

2-2 Molecular biology protocols

2-2-1 Isolation of RNA from mammalian cells (QIAgen RNeasy Mini Kit)

Cells were grown in tissue culture, typically on 6- or 12- well plates. Culture medium was completely aspirated, then the cells were lysed directly in the wells of the culture plate, and RNA harvested using the QIAgen RNeasy Mini Kit according to the manufacturer's instructions. RNA was also harvested from homogenised whole animal tissues using the QIAgen RNeasy Mini Kit, according to the manufacturer's instructions.

2-2-2 Reverse transcription

20µl reactions were prepared on ice, each containing 1x RT buffer (QIAgen), 0.5mM of each dNTP, 1µM oligo-dT primer, 10 U of RNasin (Promega), 4 U of Omniscript reverse transcriptase (QIAgen) and 2µg of RNA. These were incubated for 60 min at 37°C, then cDNA products stored at -20°C.

2-2-3 Miniprep alkaline lysis for plasmid DNA isolation

Individual bacterial colonies were seeded, using a sterile pipette tip, into 5ml of LB medium, then incubated overnight at 37°C with 200rpm shaking. 1.5ml of each culture was transferred into a 1.5ml microcentrifuge tube, and centrifuged at 12000 x *g* for 30 s. The LB broth was then completely aspirated from the pellet, which was resuspended by vortexing in 250µl solution 1 (10mM Tris, 1mM EDTA, 0.1mg/ml RNAse A, pH 8.0). After 5 min incubation at room temperature, 250µl solution 2 (0.2M NaOH, 1% SDS) was added, and the solutions mixed by inverting. Within 5 min of this, 300µl of solution 3 (3M K^+, 5M acetate) was added, and the solutions

mixed by inverting before incubation for 5 min at -20°C. After incubation, the solutions were centrifuged at 12000 *g* for 5 min, and the supernatant transferred to fresh tubes, to which 800µl of 25:24:1 (v/v) phenol: chloroform: isoamyl alcohol was added. These were vortexed, then centrifuged at 12000 *g* for 2 min. The upper aqueous phase of the supernatant was transferred to a fresh tube and 800µl isopropanol was added. The solution was then mixed by inverting before incubation at -20°C for 3 min. Following this incubation, the solutions were centrifuged at 12000 *g* for 30 min, and the supernatant was completely aspirated. DNA pellets were then washed by adding 50µl 70% ethanol and centrifuging at 12000 *g* for 30 s, then resuspended in 50µl solution 1 by heating at 70°C for 5 min.

2-2-4 Maxiprep alkaline lysis for plasmid DNA isolation

100µl of an overnight 5ml culture, or a single colony picked using a sterile pipette tip, was seeded into 100ml LB medium containing the correct antibiotic for plasmid selection. This was incubated overnight at 37°C with shaking, then plasmid DNA was harvested using the QIAfilter plasmid Maxiprep kit (QIAGEN) according to the manufacturer's instructions.

2-2-5 Quantitation of DNA/ RNA

A 1/200 dilution of the DNA or RNA sample in DEPC H2O was prepared and its absorbance at 260 and 280nm measured using a UV spectrophotometer. Purity was assessed using the ratio of A_{260}/A_{280}- an ideal ratio of 1.8 indicating pure dsDNA, and a ratio of 2 indicating pure RNA, whilst lower ratios were indicative of contamination with other nucleic acids or protein. To calculate the concentration,

where an OD_{260} of 1 indicates DNA at a concentration of 50µg/ml, the formula was applied:

OD_{260} x 50µg/ml x dilution factor = [DNA] (µg/ml)

whilst an OD_{260} of 1 for RNA indicates 40µg/ml:

OD_{260} x 40µg/ml x dilution factor = [RNA] (µg/ml)

2-2-6 Standard PCR conditions

PCR was carried out in 50µl reactions, containing 1 U of Taq DNA polymerase (Promega), 1x reaction buffer (Promega), 0.2mM each of dATP, dCTP, dTTP and dGTP, 1.5mM $MgCl_2$ and 1µM each of forward and reverse primers. Reactions were generally run for 1 min. at 95°C, then 40 cycles, using annealing temperatures appropriate to the primers' calculated T_m (assessed using the formula **T_m = 4 x (G+C) + 2 x (A+T)**) and 72°C extension phases according to the length of the amplicon, approximately 1 min per kb, followed by 10 min. at 72°C after the final cycle.

2-2-7 DNA agarose gel electrophoresis

A 1% agarose (w/v) gel was prepared in 50 or 100ml of 1x TBE buffer (45mM Tris-base, 45mM Boric acid, 2mM EDTA, pH 8.0), depending on number of samples. If the expected size of the DNA fragment was less than 300bp, the percentage of agarose was increased, up to 4% to increase band definition when imaging under UV transillumination. 0.5µl ethidium bromide was added per 10ml of gel, and mixed by swirling. DNA samples were mixed with 5µl of loading dye (10x recipe for 100ml: 60% glycerol (v/v), 0.25% bromophenol blue (w/v), 33% 150mM Tris (pH7.6) (v/v) in H_2O), loaded, and run for 20-30 min. at 170V using a Bio-Rad model 200/2.0 power supply and Pharmacia GNA-100 gel electrophoresis apparatus.

2-2-8 Transformation of chemically competent *E.coli*

50µl aliquots of chemically competent *E.coli* were removed from storage at -70°C and thawed on ice. 10ng of plasmid DNA was added, then the mixture was incubated on ice for 20 min. Subsequently, cells were heat-shocked at 42°C for 45 s, and 500µl of LB medium was added. The mixture was incubated for 30-45 min at 37°C in a shaking incubator, at 200rpm, then 200µl of cells were plated onto selective agar containing the appropriate antibiotic and incubated overnight at 37°C.

2-2-9 Selection of bacterial colonies for production of plasmid DNA

Individual colonies grown on selective agar were picked using a sterile pipette tip, and touched onto a new selective agar plate, then dipped vigorously into a 50µl PCR reaction containing primers specific to the plasmid DNA construct of interest. The selected colonies were grown overnight, and those that were shown by PCR to contain the correct insert were again picked using a sterile pipette tip, and inoculated into 100ml of selective medium. This was incubated overnight at 37°C in a shaking incubator, at 200rpm.

2-2-10 Restriction digest

20µl reactions were prepared, each containing 2-10 U of the respective restriction enzyme (Promega, Roche) in the appropriate buffer (Promega, Roche) diluted to 1x with DEPC H_2O, and 0.2-1µg of DNA sample. These were then incubated at the optimum temperature for 1-4 hours. DNA gel electrophoresis was used to confirm sizes of digested fragments, which were then purified using the QIAgen QIAEX II gel extraction kit according to the manufacturer's instructions.

2-2-11 Sequential double restriction digest

The enzyme whose corresponding buffer contained the lowest salt concentration was used first. A 20µl reaction was prepared containing 2-10 U of the first restriction enzyme (Promega, Roche) in the appropriate buffer (Promega, Roche) diluted to 1x in DEPC H_2O, and 1-5µg of DNA sample. This was incubated at the appropriate temperature for 1-4 hours. Following this, 24µl DEPC H_2O was added to dilute the first enzyme's buffer, 5µl of the appropriate 10x buffer, and 2-10 U of the second enzyme were added to give a total volume of 50µl. The reaction was then incubated at the appropriate temperature for the second enzyme for 1-4 hours, followed by DNA gel electrophoresis and fragment recovery as described for the single digest.

2-2-12 Generation of fluorescent BK channel constructs

2-2-12-1 Design of primers to add restriction sites to BK channel ZERO variant

A number of mammalian expression vectors were previously generated, encoding several alternatively spliced variants of the BK channel. In order to create an expression construct containing the ZERO BK channel splice variant, conjugated to a far-red fluorescent protein, PCR primers were generated, which flanked the full-length channel sequence, and added a unique restriction site to either end of the channel, corresponding to sites contained in the MCS of the pHcRed-N1 mammalian expression vector. Restriction sites chosen were *Kpn*I and *BamH*I.

The primers were designed such that when the channel was inserted into the vector using these sites, the sequence would be in-frame with that of the HcRed protein, with no intervening stop codons. Since an extra overhang is required for efficient

enzyme activity when the restriction site is at the end of a short DNA molecule (Moreira and Noren, 1995), extra bases were added to the primers at the appropriate end. The primer sequences were as follows:

Forward: 5'-CA *KpnI* GGTACC **ATGGATGCGCTCATCATA**

Reverse: 5'-AT *BamHI* GGATCC A **AACATTCATCTTCAACTT**

BK channel sequence is shown in bold, and the restriction sites are underlined.

2-2-12-2 Generation of insert containing full-length ZERO BK channel

15ng of ZERO-HA-pcDNA3.1 was used as a template in order to generate the full-length *Kpn*I-BK channel-*BamH*I insert. A 50µl PCR reaction was prepared using the Expand High Fidelity PCR system protocol (Roche) as follows:

ZERO-HA-pcDNA3.1	15ng
Expand High Fidelity buffer	5µl
Forward primer (10pmol/µl)	1µl
Reverse primer (10pmol/µl)	1µl
dNTP (10mM each nucleotide)	1µl
Expand High Fidelity enzyme mix	0.75µl
DEPC H_2O	40µl

This was cycled using the following parameters:

1min. at 95°C, 40 x (30s at 95°C, 30s at 62°C then 4min. at 72°C), 10min at 72°C

The correct product length of approximately 3.6Kb was confirmed by electrophoresis on a 1% (w/v) agarose gel, by comparison with Hyperladder I 1Kb markers (Bioline) (fig. 2-1), then the resulting band was excised as quickly as possible to minimise degradation due to UV exposure. The PCR product was then purified from the gel slice using the QIAgen QIAEX II gel extraction kit, according to the manufacturer's

Figure 2-1

ZERO-HcRed-N1 construct generation

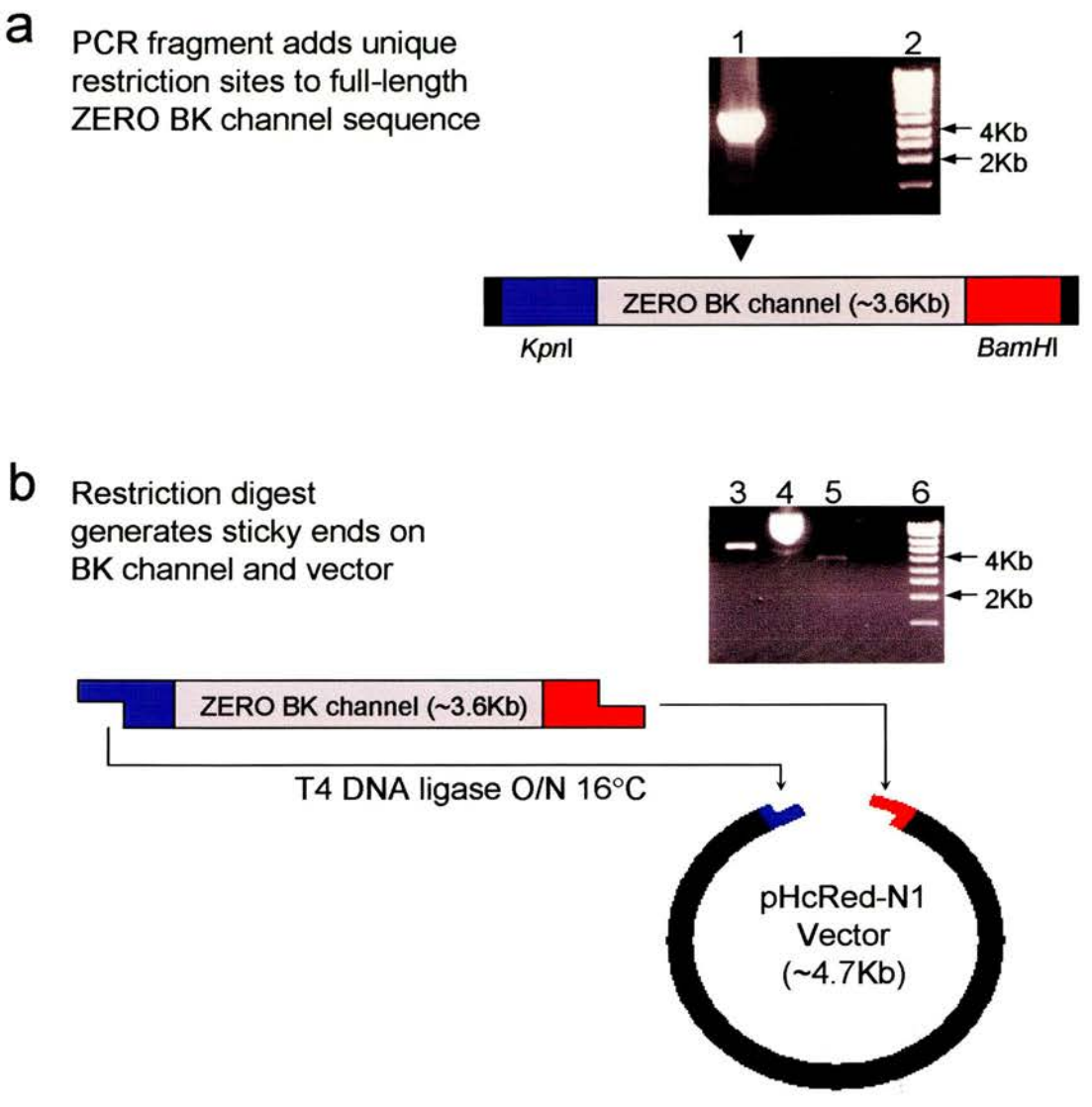

Figure 2-1 ZERO-HcRed-N1 construct generation

a) PCR was used to add *Kpn*I (blue) and *BamH*I (red) restriction sites, corresponding to those in the MCS of the pHcRed-N1 vector, to the ends of the full- length ZERO BK channel sequence, then correct fragment size (~3.6Kb) confirmed by electrophoresis on a 1% (w/v) agarose gel (lane 1) relative to Hyperladder I DNA markers (lane 2). Both pHcRed-N1 vector and the ZERO BK channel PCR fragment were then sequentially digested with *Kpn*I and *BamH*I **(b)** to generate sticky ends, then run on a 1% (w/v) agarose gel. Lane 3 shows digested pHcRed-N1, compared with uncut vector (lane 4), whilst lane 5 shows digested ZERO PCR fragment. Fragment sizes were again compared with Hyperladder I DNA markers (lane 6). Following electrophoresis, the digested ZERO PCR fragment and cut vector were purified from the gel and ligated overnight at 16°C.

protocol (QIAGEN). The resulting PCR fragment generated was a full-length ZERO BK channel sequence, flanked by unique 5' *Kpn*I and 3' *BamH*I restriction sites (fig. 2-1).

2-2-12-3 Generation of ZERO-HcRed-N1

1µg of the ZERO *Kpn*I/*BamH*I insert and 1µg of the pHcRed-N1 vector were included in separate 20µl double restriction digests using *Kpn*I and *BamH*I in MULTI-CORE buffer (Promega). These were incubated at 37°C for 4h then the entire reactions were electrophoresed on a 1% (w/v) agarose gel (fig. 2-1). Bands containing the cut vector and insert were excised and purified using the QIAEX II gel extraction kit (QIAGEN) according to the manufacturer's protocol, then 10% of the DNA was electrophoresed on a 1% (w/v) agarose gel to confirm recovery.

The *Kpn*I/ *BamH*I digested full-length ZERO insert and pHcRed vector were ligated overnight at 16°C, in 10µl reactions, containing vector and insert fragments at 1:1 or 1:3 molar ratios, with 1 U of T4 DNA ligase (Promega) in 1x ligase buffer (Promega), according to the manufacturer's instructions (fig. 2-1), then 5µl of each reaction was transformed into 50µl of TOP10 *E.coli* (Invitrogen) according to the manufacturer's instructions. Colonies were PCR screened using primers specific to the splice site 1-3 region of the BK channel. A positive result was indicated by a band approximately 600bp in size, as determined by electrophoresis on a 1% (w/v) agarose gel. This colony was then seeded into a 100ml overnight culture for Maxiprep. The correct generation of the ZERO-HcRed-N1 construct was confirmed by sequencing carried out by MWG Biotech, Mannheim, Germany.

2-2-12-4 Generation of STREX-HcRed-N1

In order to generate a construct encoding a full-length BK channel containing the STREX BK channel alternative splice variant, STREX-HA-pcDNA3 and ZERO-HcRed-N1 were restriction digested using *Kpn*I and *Blp*I, to generate a ~2.4Kb insert fragment containing sequence from the N-terminal of the BK channel, up to the *Blp*I restriction site downstream of splice site 2, which included the STREX exon, and a ~5.8Kb HcRed-N1 vector containing the c-terminal BK channel sequence downstream of the *Blp*I site. This was run on a 1% (w/v) agarose gel, to confirm digestion, then excised and purified. Following recovery, insert and vector fragments were ligated overnight at 16°C, and used to transform TOP10 *E.coli*. Colonies were screened for presence of STREX, then one colony containing the correctly- ligated construct was used to seed a 100ml culture for maxiprep, as described previously

2-2-13 Preparation of DNA for sequencing

2µl of Pellet Paint co-precipitant (Novagen) was added to 2µg of DNA, followed by 0.1 volume of 3M Na Acetate. This was mixed briefly, then 2 volumes of 100% ethanol were added before vortexing. The mixture was incubated at room temperature for 2 min, then the sample was centrifuged at 14000 x *g* for 5 min. Supernatant was removed, then 200µl 70% (v/v) ethanol was added to the pellet before briefly vortexing and centrifuging at 14000 x *g* for 5 min. Following this, the supernatant was removed, and 200µl of 100% ethanol added before vortexing and centrifuging at 14000 x *g* for 5 min. The supernatant was removed, and the pellet allowed to air dry for 10-15 min

2-3 Real-time PCR protocols

2-3-1 Design of real-time PCR Taqman primer and probe sets

The Primer Express program, version 2.0 (Applied Biosystems © 2000- 2003), was used to design primers and probes for use in the Taqman assay. Following the standard Primer Express parameters, the forward and reverse primers were designed to be between 9 and 40 bases in length, with T_m of 58-60°C, G/C content of 30-80% and a maximal T_m difference of 2°C. The T_m of the Taqman probe was 8-10°C higher than that of the primer pair, and potential probe sequences possessing a 5' guanine were excluded, as this causes unwanted quenching of fluorescence from the reporter dye. In most cases, the forward or reverse primer was designed to span an exon junction with an overhang of 3 bases at its 3' end. This was sufficient to cause mispriming if the final 3 bases were mismatched, and thus preserve specificity (Kwok, 1990). In the case of the STREX BK channel alternative splice variant, the sequence at either end of the splice insert was unsuitable for correct primer design. Therefore, the entire Taqman amplicon was designed within the insert itself.

2-3-2 Real-time PCR assay standard conditions

Reactions were performed in 25µl, in ABI Prism 96-well optical reaction plates. Each reaction contained 1x Biogene real-time PCR master mix (containing Hotstart Taq DNA polymerase, optimised reaction buffer including ROX passive reference, 5mM final concentration $MgCl_2$ and nucleotides), 500nM final concentration of forward and reverse primers, and 300nM final concentration of 5' FAM (6-carboxyfluorescein), 3' TAMRA (6-carboxytetramethylrhodamine)-labelled Taqman probe. Reactions were run using Applied Biosystems' universal thermal cycling parameters:

2 min hold at 50°C, 10 min hold at 95°C for Taq polymerase activation, then 40 x (15s at 95°C and 1 min at 60°C) cycles.

2-3-3 Standard curves for real-time PCR Taqman primer and probe sets

A logarithmic dilution of plasmid DNA in DEPC H_2O containing a single BK channel splice variant was prepared over a concentration range of 2ng- 0.2fg per 5µl in order to minimise pipetting errors. These standard samples were run in triplicate on an ABI Prism 96- well optical reaction plate as 25µl reactions with 1x Biogene real-time PCR master mix and the Taqman probe/ primer set specific to the splice variant being tested, using Applied Biosystems' standard thermal cycling parameters. Ct values were recorded and plotted against log starting concentration.

2-3-4 Competition assay for Taqman primer and probe sets

This assay was used to confirm the specificity of the Taqman primer and probe sets. 25µl triplicate reactions were prepared as for generation of standard curves, and an additional 20pg of plasmid DNA containing an alternatively spliced variant of the BK channel was added to each sample. The reactions were then run using Applied Biosystems' standard thermal cycling parameters.

2-3-5 Real-time PCR screening of mouse cDNA arrays

cDNA from whole-mouse and mouse brain Rapid-scan gene expression panels (Origene) was resuspended by adding 25µl DEPC H_2O to each well (containing 2ng total cDNA, normalised to β-actin), then incubating on ice for 30 min. 5µl (0.4ng cDNA) of each sample was incorporated into a 25µl reaction containing 1x Biogene

real-time PCR master mix, and the Taqman primer/ probe set specific to one BK channel splice variant. A triplicate logarithmic dilution over the range of 2ng-0.2fg of plasmid DNA, containing the splice variant being screened for, was run simultaneously to generate a standard curve, to enable quantitation of the samples. Reactions were run on an ABI Prism 96-well optical reaction plate, using Applied Biosystems' standard thermal cycling parameters.

2-3-6 Quantitation of starting material in a real-time PCR assay

Quantitation of samples was carried out using Applied Biosystems' ABI Prism 7000 SDS software, version 1.1 (Applied Biosystems © 2000- 2003) which generates amplification curves of fluorescence against PCR cycle number, which can be used to calculate the starting DNA concentration in unknown samples. In each run, a triplicate standard curve was incorporated. Samples were considered negative if their fluorescence did not cross the threshold value after 40 cycles of amplification. For each sample, a Ct value was defined as the cycle number at which the fluorescence increased above the threshold. Using slope and intercept values generated from the standard curve, this value was incorporated into the straight-line equation y=mx+c, where Ct = slope x log concentration + intercept, and from this:

concentration = 10^(Ct – intercept) / slope.

2-4 Mammalian cell culture protocols

2-4-1 Standard cell culture passage protocol

HEK293, PC12 and MDCK cells were used, over a passage range of 18-45. Cells were maintained in DMEM + L-glutamine + 10% (v/v) FCS (no antibiotic), in 75cm^2 flasks, at 37°C in 95% (v/v) air, 5% (v/v) CO_2, and passaged every 3-4 days at 70-

80% confluency. The medium was removed and discarded, and cells washed using 2ml of HBSS + 0.1% (v/v) EDTA. This was removed, then 0.5-1ml of Trypsin-EDTA was added and cells incubated at 37°C for 1-2 min. The flask was gently tapped to detach the cells, which were then resuspended in 6ml of DMEM + 10% FCS by triturating up and down slowly using a 10ml sterile disposable pipette. Once cells were fully resuspended, 1ml of cells was added to 11ml DMEM +10% FCS in a new sterile $75cm^3$ tissue culture flask.

2-4-2 Transfection of cells using lipofectamine 2000

Cells were cultured on coverslips in a sterile 12 well tissue culture plate, in 1ml DMEM + 10% (v/v) FCS per well, without antibiotics, at 37°C, in 95% (v/v) air, 5% (v/v) CO_2, until 40% confluent. For each transfection reaction, 1μg DNA and 3μl lipofectamine 2000 (Invitrogen) were each diluted separately in 50μl DMEM without serum, and incubated for <5 min. They were then combined, mixed gently, and incubated for 20 min. Following this incubation, 100μl of the DNA-lipofectamine 2000 complexes in DMEM were added directly into the well. Cells were subsequently incubated for 96h at 37°C in 95% (v/v) air, 5% (v/v) CO_2, then fixed and mounted using Mowiol.

2-5 Imaging

2-5-1 Fixing and mounting of cells

24-96h after transfection, the medium was aspirated and the cells washed twice with 1ml 1 x PBS containing 2mM $CaCl_2$. The cells were then incubated in 1ml 4% (w/v) paraformaldehyde in PBS for 20 min. The paraformaldehyde was aspirated and cells washed twice in 1 x PBS, then quenched for 10 min in 1ml PBS containing 50mM

NH_4Cl. After quenching, the cells were washed twice in 1ml 1 x PBS. Coverslips were dipped in distilled H_2O, dried briefly to remove excess H_2O, then mounted onto slides using Mowiol, and left to dry overnight before imaging.

2-5-2 Indirect immunofluorescence

Cells were plated onto 16mm coverslips in a 12-well tissue culture plate, 24h before transfection. 24-96h after transfection, the medium was aspirated, and the cells washed twice with 1ml 1 x PBS. Following this, 1ml of fixative (4% paraformaldehyde/ 0.3% triton x-100 in PBS) was added and the cells incubated overnight at 4°C. The next day, the fixative was aspirated and replaced with 1ml 4% paraformaldehyde before incubation for 10 min at room temperature. Cells were then washed twice with 1ml PBS/ 0.2% fish skin gelatin (FSG). 1ml of PBS/ 2% BSA/ 0.05% Tween was added and the cells incubated for 1h, then washed twice with 1ml PBS/ FSG. Coverslips were then placed face down on parafilm into 150-200µl of the appropriate primary antibody, diluted in PBS/ FSG, for 1h. Coverslips were then returned to the 12-well plate and washed 5 times with 1ml PBS/ FSG with agitation. 1ml of the appropriate secondary antibody diluted in PBS/ FSG was added to each well, and the plate was incubated for 30 min in the dark, to prevent photobleaching of the fluorescent label of the secondary antibody. Following this, the coverslips were washed 5x with 1ml PBS/ FSG with agitation, then rinsed in distilled H_2O and mounted onto slides using Mowiol. Alternatively, if nuclear staining was required, 0.5ml of a 1:7000 dilution of TOPRO 3 in PBS was added after the secondary antibody was washed off. Cells were incubated for 10 s, then the dye was aspirated and coverslips washed 5x with 1ml PBS/ FSG then rinsed in distilled H_2O, mounted onto slides using Mowiol and dried for 24h before imaging.

2-5-3 Imaging of fluorescently-labelled cells

Images were acquired using a Zeiss Axioskop laser scanning confocal microscope (LSM510), with a plan- achromat x 63/ 1.4 oil immersion objective lens, at 1024 x 1024 resolution, as an average of 4 scans per line, scanning through the centre of the cells. In the case of MDCK cells, stacks of images were taken vertically at 0.2μm intervals, to investigate potential localisation of transfected channels to either apical or basal surfaces. EGFP and AlexaFluor 488 images were obtained using argon2 laser excitation at 488nm, collecting fluorescence through a band pass 500-550nm filter. HcRed images were obtained using HeNe1 laser excitation at 543nm, and fluorescence collected through a band pass 515-615nm filter. TOPRO and Alexa 647 images were obtained using HeNe2 laser excitation at 633nm, and fluorescence collected through a long- pass 650nm filter.

2-5-4 Analysis of images

Images of fixed cells taken using confocal microscopy were viewed using the Zeiss LSM image browser software, version 3.1.0.99 (Carl Zeiss GMBH © 1997- 2001). In all cases, the membrane was defined as the outer edge of the cell, which was confirmed by visualisation using the transmitted image, and analysis was performed on scans through the centre of the cells. This was especially significant for the analysis of fluorescent expression in MDCK cells, since a scan taken through the villi at the apical surface of the cells can resemble intracellular trapping of the fluorescent label (fig. 2-2). In each random field of view, cells were assessed for four different types of fluorescent labelling- either membrane, diffuse, trapped or perinuclear. These categories were not mutually exclusive, and were defined as: robust, bright fluorescence around the edge of the cell; diffuse staining of the cytoplasm; discrete bright intracellular puncta and bright fluorescence in a ring

Figure 2-2
Imaging of polarised MDCK cells growing in a monolayer

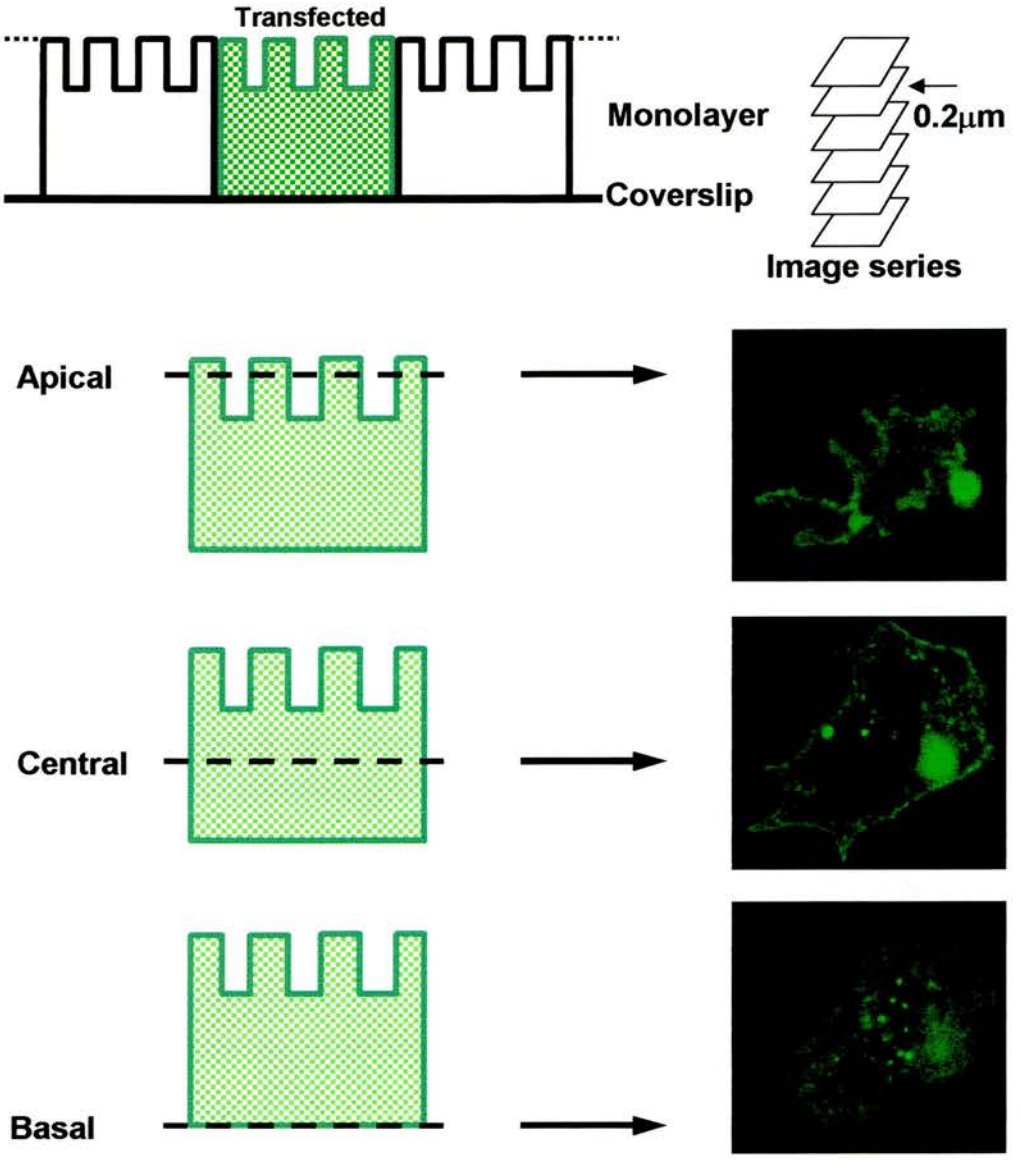

Figure 2-2 Imaging of polarised MDCK cells growing in a monolayer

MDCK cells were transfected, then grown until ~100% confluent. In order to assess polarisation of expression of fluorescent protein, vertical series of images were taken at ~0.2μm intervals through the cell. In order to correctly assess membrane expression, images from the centre of the cell were used.

around the edge of the nucleus, respectively (fig. 2-3). The number of cells in which each type of fluorescent labelling was observed was expressed as a percentage of the total number of fluorescently- labelled cells in one field of view. In cases where EGFP, HcRed or Alexa dye fluorescence were colocalised with each other, this was determined visually and also using fluorescent profiling, by measuring fluorescence in 0.02μm intervals along a straight line through the cell in the X-Y plane, intersecting the area of interest. Simultaneous peaks of fluorescence for the fluorescent proteins or dyes were indicative of colocalisation.

2-6 Mouse behavioural experiment protocols

The following behavioural experiments were carried out by Dr. Dóra Zelena and colleagues, at the Institute of Experimental Medicine, Budapest, Hungary, in accordance with ethical guidelines set by the Hungarian Council for Animal Care. RNA isolation from whole mouse tissues was carried out using the QIAgen RNeasy Mini Kit as described previously, and cDNA was generated using QIAgen Omniscript reverse transcriptase, as described previously.

2-6-1 General protocol

Male NMRI mice (Charles River, Hungary) were acclimatised for a minimum of 10 days in a 13h light/ 11h dark cycle, with food and water *ad libitum*, at 21 ± 1°C, in a humidity- controlled environment, with 3-5 animals per cage. All treatments were applied for 14 days, and animals sacrificed on day 15. Weight of each animal was measured at 3-4 day intervals, and post- decapitation, thymus and adrenal weight was also recorded. For decapitation, 2 or more mice were taken on each occasion in order to avoid inducing acute isolation stress. Trunk blood was collected into tubes on ice, containing K_2- EDTA, centrifuged, then stored at –20°C until measurement of

Figure 2-3
Analysis of confocal microscopy images

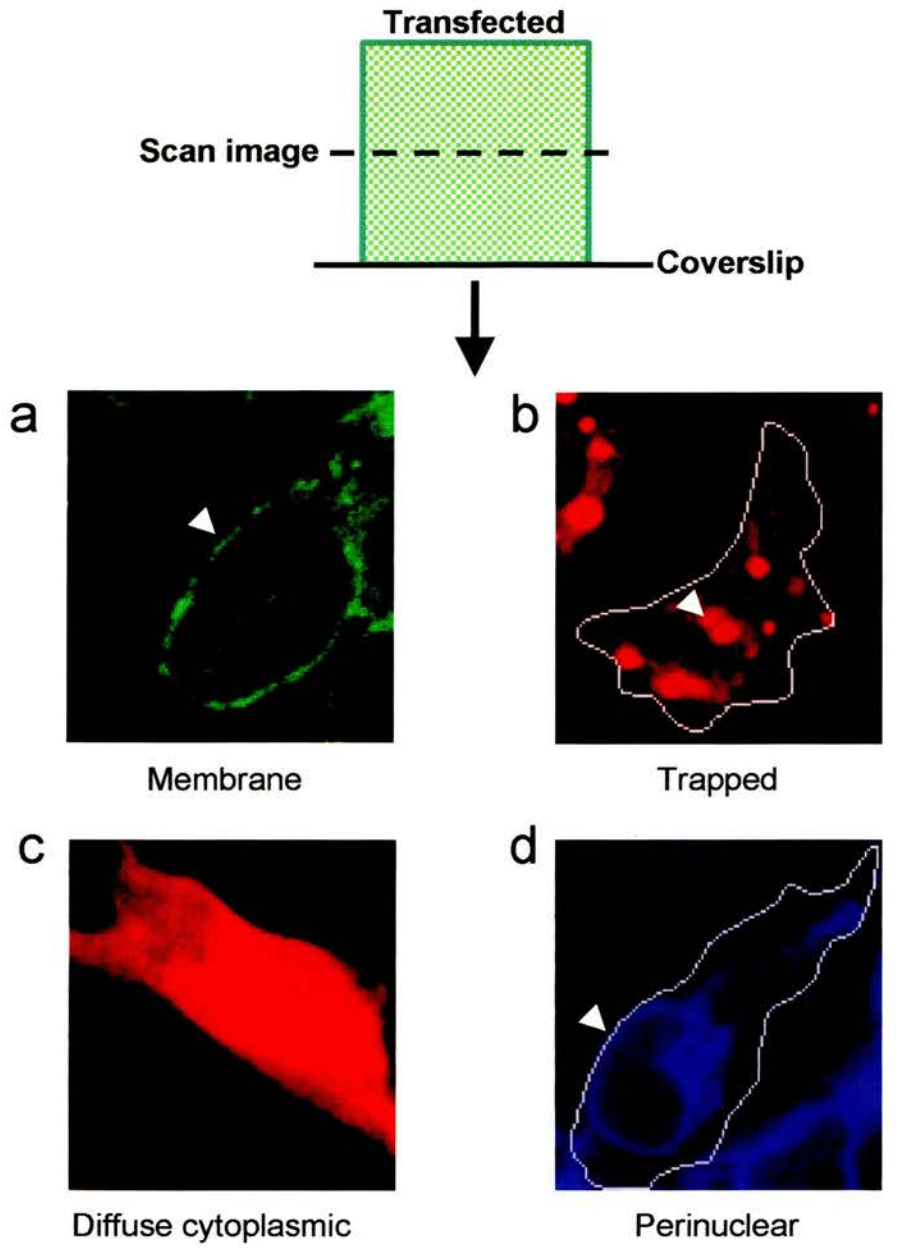

Figure 2-3 Analysis of confocal microscopy images

Representative images of each of the four different types of fluorescent labelling, showing **a)** membrane expression (white arrow), **b)** trapped punctate expression (white arrow), **c)** diffuse cytoplasmic expression and **d)** perinuclear expression (white arrow). All images were taken through the centre of the cell, acquired 72-96h after transfection.

hormones by radioimmunoassay. Adrenal gland, anterior pituitary, hypothalamus, hippocampus and cerebellum were removed and immediately frozen on dry ice, and stored at –70°C. RNA was isolated from each tissue, and cDNA was synthesised from this.

2-6-2 Adrenalectomy

Mice were anaesthetised with ketamine- xylasine, and following this were bilaterally adrenalectomised from a dorsal approach. Animals were handled as per the general protocol, but were given 0.9% saline to drink in addition to tap water.

2-6-3 Dexamethasone

Mice were given 5μg/ ml dexamethasone in their drinking water, initially dissolved in ethanol, and diluted to 1% final ethanol concentration

2-6-4 Rat stress

Mice were placed in separate cages, without food or water, then rats in plexiglass cages with grid floors were placed on top of the cages in which mice were housed so that the animals could see, hear and smell, but not touch, each other, in a randomised manner of timing (morning, noon, afternoon, during the light phase of the daily cycle), duration (1-3h) and number of stress exposures (1-2 times) over the 14- day experimental period.

2-6-5 Restraint

Restraint stress was induced in mice by placing each animal in a 50ml centrifugation tube (internal diameter 30mm, length 100mm with a 15mm cone at the base, and 5mm breathing hole in the top) for 1h in the morning of each day of the 14- day

experimental period. Animals were sacrificed on day 15, 24h after the last restraint stress session.

2-7 Analysis of data

Data was analysed using the Statview software package, version 5.0.1 (S.A.S. Institute, © 1992- 1998). For imaging data, the percentages of cells displaying each of the fluorescent protein expression criteria - membrane, trapped, diffuse or perinuclear - were calculated for each treatment. Results for each treatment were compared across these three categories and analysed by ANOVA and *post- hoc* tests, with significant differences indicated by p values of less than 0.05 or 0.01 using Student- Newman- Keuls test.

For real-time PCR investigation of BK channel expression, total BK, and also splice variant expression in mouse tissues was quantified relative to a standard curve included in each run, then this was normalised to expression in the 19- day embryo. For statistical comparison of expression in the embryonic stages, results were analysed by ANOVA and *post- hoc* tests, with significant differences indicated by p values below the adjusted level using the Bonferroni/ Dunn test at a significance level of 5% or 1%.

To investigate alternative splicing of the BK channel in the CNS during mouse embryogenesis, the concentrations of the STREX and ZERO BK channel alternative splice variants in each tissue at each developmental stage were used to generate a ratio of splice variant/ total BK channel, and this was expressed as a percentage of that at postnatal day 35 (P35). Results were then analysed by ANOVA and post-hoc

tests, with significant differences indicated by p values below the adjusted level using the Bonferroni/ Dunn test at a significance level of 5% or 1%.

Investigation of alternative splicing of the BK channel in response to manipulation of HPA axis activity in mice was carried out by quantifying total BK channel expression as well as that of the STREX alternative splice variant in each tissue, to generate a STREX/ BK channel ratio, then this was expressed as a percentage. Results were then analysed by ANOVA and *post- hoc* tests, with significant differences indicated by p values of less than 0.05 or 0.01 using Student- Newman-Keuls test. Correlations of mouse corticosterone (CORT) or adrenocorticotrophic hormone (ACTH) with STREX/ BK channel ratio were carried out using Spearman's Rank Correlation test.

Chapter Three:

Expression of fluorescent protein-labelled BK channel alternative splice variants in mammalian cells

3-1 Introduction

3-1-1 Factors influencing subcellular localisation of the BK channel

The cytoplasmic tail region of the BK channel has been shown to be necessary for BK cell surface expression (Wang *et al.*, 2003). In addition to more well-characterised functional changes, such as increased channel sensitivity to Ca^{2+} (Erxleben *et al.*, 2002), it is possible that novel splice inserts in this region may have an effect on membrane targeting, in a similar fashion to those already known to take place in the N-terminal region (Zarei *et al.*, 2001). Alternatively spliced BK α-subunits may take on a regulatory role by heterotetramerisation with other isoforms, as has been observed in other potassium channel types (Ottschytsch *et al.*, 2002), either influencing the overall excitability of the channel or preventing its trafficking to the membrane.

The subcellular localisation of the BK channel may be altered by alternative splicing within the C- terminal region. Zarei and coworkers have reported that for the human BK channel alternative splice variant containing the SV1 insert, normally located within the S1 transmembrane domain of the channel α-subunit, the presence of the nonbasic hydrophobic endoplasmic reticulum retention/ retrieval motif, CVLF, is sufficient to cause retention within the endoplasmic reticulum (Zarei *et al.*, 2004). Additionally, the position within the channel α-subunit of this motif is not critical to its function of inhibition of membrane trafficking, raising the additional possibility that hitherto unknown alternative splice inserts within the cytoplasmic tail region may also alter the channel α-subunit cell surface expression in a similar manner, causing retention of the channel in a particular subcellular compartment.

The α-subunit composition of the channel has been shown to have a regulatory influence on processes such as activation following phosphorylation (Tian *et al.*, 2004), although it is still unknown whether heterotetramerisation of BK channel α-subunits is a mechanism for generating phenotypic diversity in native tissues. Fluorescent protein labelling was used to investigate whether or not multiple alternatively spliced BK channel α-subunits in a single cell can be visualised, and also whether any distinct pattern of subcellular localisation of the channel, attributable to a particular splice variant, may influence the localisation of an alternatively spliced α-subunit.

3-1-2 Establishing a protocol for robust, reproducible expression of fluorescent BK channel fusion proteins

In order to study any changes in the subcellular localisation that may occur as a result of alternative splicing, fluorescent protein labelling of the BK channel in combination with laser scanning confocal microscopy was used. It has been observed that N-terminal labelling with a GFP tag can alter the intrinsic properties of the channel. For example, although hSlo N-terminally labelled with GFP formed functional channels when expressed transiently in HEK293 cells, its voltage dependence and calcium sensitivity was altered (Meyer and Fromherz, 1999). In the studies reported in this chapter, all fluorescent labels were placed at the C-terminus of the α-subunits. This approach has previously been used to visualise the BK channel, using GFP fused in- frame to the C- terminus of the ZERO BK channel splice variant (Myers *et al.*, 1999). C- terminal labelling of the channel did not appear to affect the targeting of the protein, or its functional properties. Since

exogenous factors are not required for fluorescence of EGFP, visualisation of dynamic movement of the protein between subcellular compartments within living cells is possible, unlike other methods such as indirect immunofluorescence where reagents must be introduced into permeabilised cells.

BK channel STREX and ZERO constructs, with EGFP fused in- frame to the C-terminus, had been made previously by MJS lab members. However in order to simultaneously visualise the localisation of more than one splice variant, and thus enable the study of possible colocalisation and/ or heterotetramerisation of different BK channel isoforms, it was necessary to generate a construct that would result in the expression of the channel as a fusion protein labelled with a fluorescent protein whose emission wavelength was spectrally distinct from that of EGFP. For such studies, HcRed was chosen, since its peak emission wavelength is well separated from that of EGFP. In addition, it does not form aggregates as has been reported for another candidate label, DsRed (Gavin *et al.*, 2002, Lauf *et al.*, 2001) which if present, would prevent the accurate localisation of the labelled channels.

Initial investigations for the EGFP and HcRed BK channel fusion proteins were carried out in HEK293 cells, which do not express endogenous BK channels (Shipston *et al.*, 1999), and are widely used in the analysis of ion channel properties and regulation since they can express recombinant proteins efficiently and at a high level. In order to investigate the expression pattern of the fluorescent protein-labelled BK channel constructs, and confirm their use as markers for channel subcellular localisation, it was first necessary to express them in the absence of any

endogenous BK α-subunits. The presence of any novel endogenous channel splice variants, whose surface expression might differ greatly from that of the fluorescent constructs, could potentially interfere with the expression of the latter, in the event that heterotetramerisation of the α-subunits should occur, thereby interfering with results. Once a protocol was established for the robust and reproducible expression of the fluorescent protein- labelled BK channel α-subunits in a cell line lacking endogenous BK channels, the next stage would be to investigate the effect of the presence of fluorescently- labelled alternative splice variants in cells which possess endogenous BK channel splice variants. This would allow potential preferential targeting mechanisms to be addressed.

To this end, rat Pheochromocytoma (PC12) cells were chosen as a model system for investigation, since they possess a native BK channel population including both STREX and ZERO splice variants (Saito *et al.*, 1997), and are able to respond to a diverse range of growth factors, hormones and neurotrophins, making them an important cell line for studying the initiation of multiple intracellular signalling pathways by such factors, and the resulting changes in complex processes such as neurite extension, proliferation, differentiation and cell excitability (Vaudry *et al.*, 2002). The changes in morphology and excitability which accompany PC12 cell responses to stimulatory factors may also be accompanied by changes in the expression of ion channels (Grumolato *et al.*, 2003), and the fluorescently- labelled BK channel constructs may therefore be a useful tool for studying possible changes in ion channel distribution during these processes.

In many cell types, BK channels have been found to express in a highly localised manner, particularly at the apical surface of epithelial cells (Sohma *et al.*, 1994, James *et al.*, 1994, Takeuchi *et al.*, 1992). The EGFP and HcRed BK channel fusion proteins would therefore be useful for investigating whether the intrinsic mechanisms for trafficking of the endogenous channels in such a cell system would influence the expression of a transiently transfected BK channel. Madin-Darby Canine Kidney (MDCK) cells were chosen for this investigation since when grown in a monolayer, they polarise to form apical and basal surfaces, with expression of certain proteins being restricted to the apical surface (Vega-Salas *et al.*, 1987, Cohen and Musch, 2003). Other potassium channel types can be expressed in MDCK cells in a polarised manner (Ortega *et al.*, 2000) and it has been shown that the human BK channel splice variant, hSlo, when stably expressed in MDCK cells, localises to the apical surface of the cells (Bravo- Zehnder *et al.*, 2000). The channel can also be expressed basolaterally (Burckhardt and Gogelein, 1992), and it could be speculated that signals for localisation to either, or both polar surfaces might also be introduced by alternative splicing. The fluorescent protein labelled BK channel constructs are therefore useful tools in investigating whether the mechanisms for polarisation of the endogenous channels might affect the expression of transiently- transfected α-subunits, and whether this was influenced by the presence of distinct channel splice variants.

3-2 Results

3-2-1 Expression in HEK293 cells

3-2-1-1 Expression of EGFP and HcRed labelled BK channel splice variants in HEK293 cells

As an initial step to investigate the expression of the BK channel fluorescent fusion proteins in mammalian cells, cDNA constructs were transfected into HEK293 cells using the well- established Lipofectamine method (Invitrogen). Transfection of HEK293 cells was optimised for cells grown on 12-well tissue culture plates, using 1μg of cDNA per well, and transfection efficiency was routinely > 80%. Initial time course experiments at 24, 48, 72 and 96 h determined that 96 h was the optimal time after transfection for visualisation of the BK channel EGFP fluorescence at the cell membrane. Although visible fluorescence could be detected 24 h post- transfection in cells transfected with ZERO-EGFP and STREX-EGFP, the level of channels expressing at the plasma membrane was maximal between 72 and 96 h. Therefore, the 96 h timepoint was used for data analysis in the majority of the subsequent investigations. In each case, (N= X) represents the number of independent experiments carried out, whilst (n= X) represents the number of cells assayed.

In HEK293 cells expressing ZERO-EGFP, 32.6 ± 7.1% (N=12, n= 492) of transfected cells displayed robust plasma membrane expression as defined in the methods section. Membrane expression was largely uniform across the plasma membrane, as shown in figure 3-1. The trapping of EGFP fluorescence in bright intracellular 'puncta' was observed in 29.8 ± 8.1% of transfected cells, typically distributed in a random pattern throughout the cell, average diameter 2.9 ± 0.2μm

(N= 3, n= 62). A diffuse cytoplasmic expression was also seen, with nuclear exclusion, in 91.1 ± 4.0% of transfected cells (fig. 3-1).

cDNA constructs encoding -EGFP labelled STREX BK channel α-subunits were expressed in HEK293 cells, in order to investigate whether the cellular distribution of the BK channel α-subunit EGFP fusion protein was modified by the presence of the alternatively spliced STREX insert. These channels are identical to ZERO-EGFP, except for an additional 59 aa insert at alternative splicing site C2, in the intracellular C-terminus. Under parallel transfection conditions robust, uniform plasma membrane expression was observed in 50.8 ± 6.1% (N=16, n= 575) of HEK293 cells transfected with STREX-EGFP, and trapped expression in bright intracellular puncta was observed in 47.2 ± 6.0% of transfected cells. Average puncta size was 3.1 ± 0.3μm (N=3, n= 53). Diffuse cytoplasmic expression was observed in 85.8 ± 7.1% of cells. These data suggest that in HEK293 cells, both ZERO-EGFP and STREX-EGFP are expressed in a similar fashion, as no significant difference was found between these two alternatively spliced α-subunits for the levels of membrane, trapped puncta or diffuse expression (fig. 3-1). Expression of EGFP alone in HEK293 cells is distributed uniformly throughout the cytoplasm, with nuclear exclusion (fig. 3-1).

In contrast, expression of ZERO α-subunits as C- terminally- labelled HcRed fusion proteins resulted in an almost complete loss of plasma membrane targeting. Fluorescent profiles were generated for HEK293 cells expressing ZERO-EGFP and ZERO-HcRed, by measuring the fluorescence intensity at 0.02μm intervals in a line across the cell, enabling further visualisation of the subcellular localisation of the BK

Figure 3-1
Expression of ZERO-EGFP or STREX-EGFP BK channel constructs in HEK293 cells

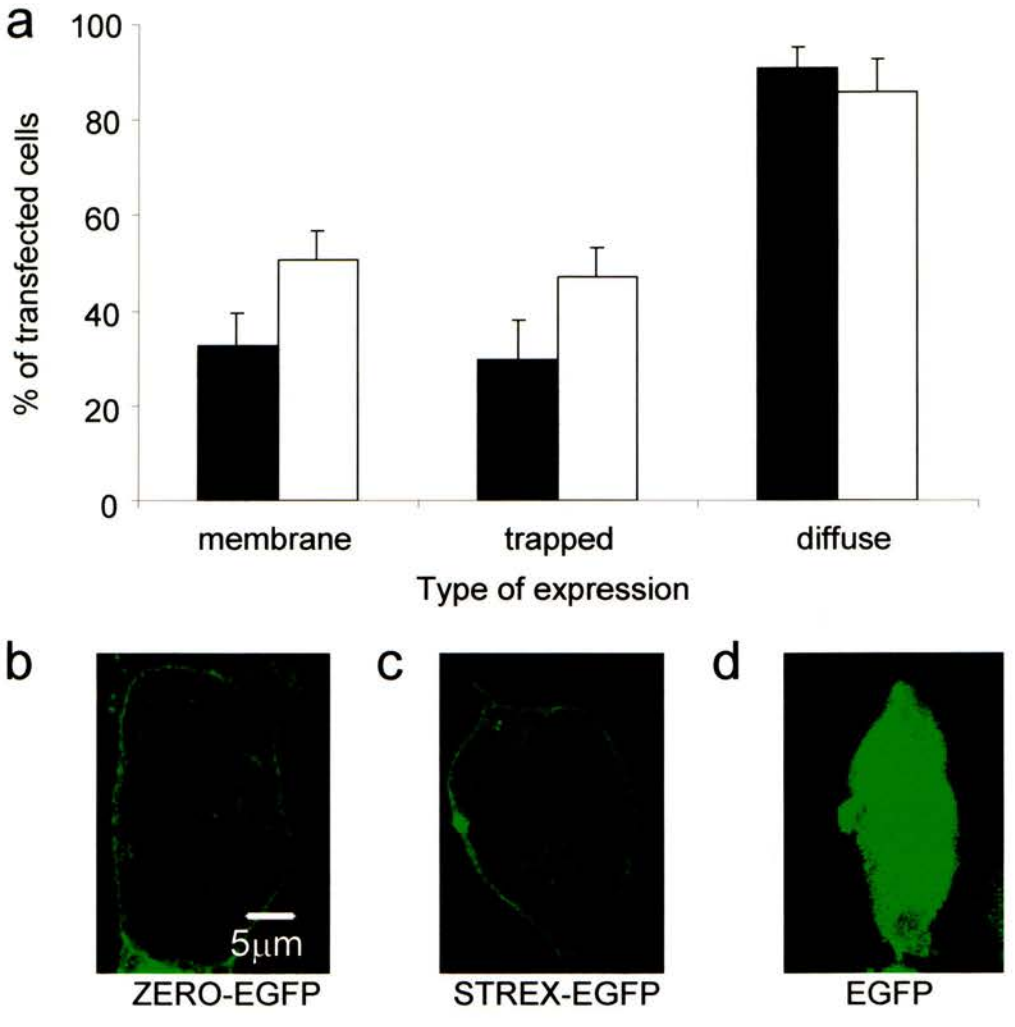

Figure 3-1 Expression of ZERO-EGFP or STREX-EGFP BK channel constructs in HEK293 cells

a) Data shown as a mean percentage of total transfected cells per field of view (± SEM), for each of the three types of fluorescent expression in HEK293 cells singly transfected with ZERO-EGFP (closed bars, N= 12, n= 492) or STREX-EGFP (open bars, N= 16, n= 575). Representative images are shown of HEK293 cells expressing **b)** ZERO-EGFP, **c)** STREX-EGFP and **d)** EGFP alone respectively, taken 96 h after transfection.

channel α-subunit fusion proteins (fig. 3-2), with peaks of fluorescence indicating localisation of the proteins. Fluorescent labelling at the plasma membrane was present in only 7.9 ± 2.5% (N= 17, n= 712) of cells expressing ZERO-HcRed (fig. 3-3); this was significantly lower than in cells transfected with ZERO-EGFP ($p< 0.05$). In addition, trapped expression increased significantly to 78.7 ± 5.5% ($p< 0.01$), and was characterised by bright intracellular puncta distributed randomly throughout the cytoplasm, average diameter 3.3 ± 0.2μm (N= 3, n= 123). Diffuse cytoplasmic expression was also observed in 61.6 ± 9.2 % of cells, although this was not significantly different to that seen in cells expressing ZERO-EGFP.

To investigate whether or not the reduction of membrane expression and trapping in intracellular puncta was a property unique to the -HcRed labelled ZERO BK channel splice variant, the alternatively spliced STREX BK channel α-subunit was also fused at the C- terminus with HcRed, and expressed in HEK293 cells. A similar pattern to that observed for the -HcRed labelled ZERO α-subunits occurred (fig. 3-4)- plasma membrane expression of the channel was observed in 21.2 ± 5.2% (N= 8, n= 452) of transfected cells (fig. 3-3); this was significantly lower than for STREX-EGFP ($p< 0.01$). In addition, trapped expression increased significantly ($p< 0.05$) to 74.9 ± 7.8% of transfected cells, when compared to STREX-EGFP, and was again characterised by bright intracellular puncta, average diameter 3.6 ± 0.2μm (N= 3, n= 165). Diffuse cytoplasmic expression, excluded from the nucleus, was observed in 97.2 ± 2.1% of cells, although this was not significantly different to that observed for STREX-EGFP expressed in HEK cells in parallel conditions.

Figure 3-2
Fluorescent profile of ZERO-EGFP or ZERO-HcRed in HEK293 cells

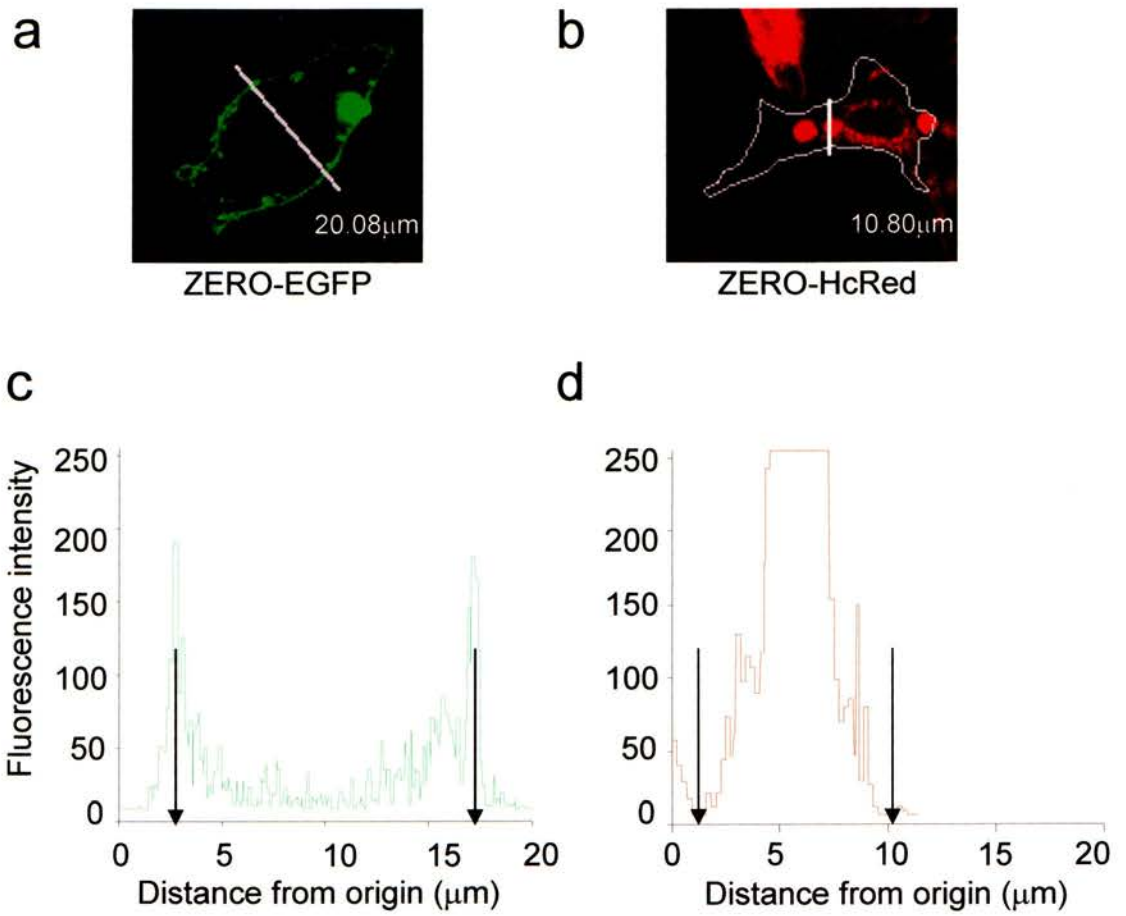

Figure 3-2 Fluorescent profile of ZERO-EGFP or ZERO-HcRed in HEK293 cells

Fluorescence was measured at 0.02μm intervals along a line through HEK293 cells expressing **(a)** ZERO-EGFP and **(b)** ZERO-HcRed (outline of cell is shown in grey) 96h after transfection. Fluorescent profile is expressed as fluorescence intensity (0- 255) against distance (μm) from origin of line scan for HEK293 cells expressing **(c)** ZERO-EGFP, where peak fluorescence (green trace) can be seen at the membrane (arrows) and **(d)** ZERO-HcRed, where no fluorescence (red trace) is seen at the membrane (arrows) but is localised in a punctate manner, inside the cell.

Figure 3-3
Expression of ZERO-HcRed or STREX-HcRed BK channel constructs or pHcRed in HEK293 cells

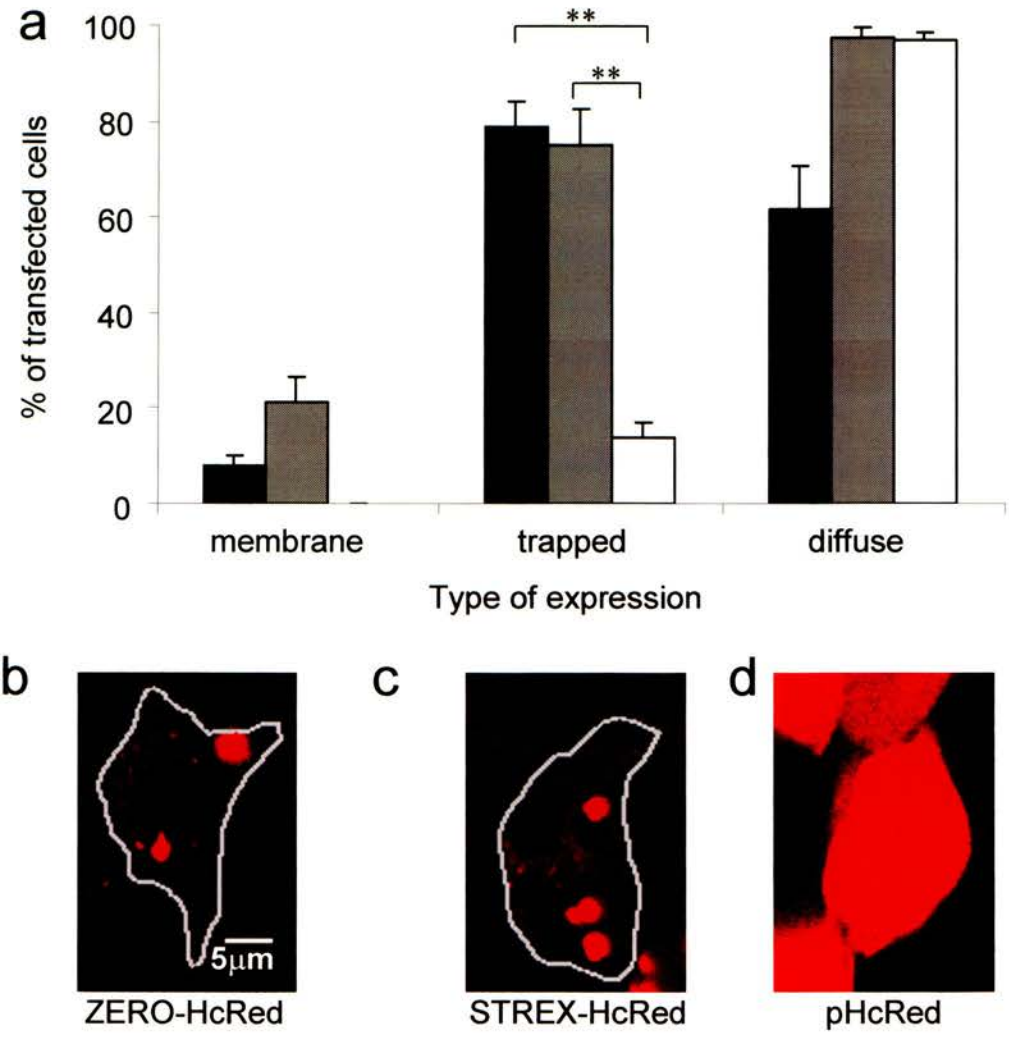

Figure 3-3 Expression of ZERO-HcRed or STREX-HcRed BK channel constructs or pHcRed in HEK293 cells

a) Data shown as a mean percentage of total transfected cells per field of view (± SEM), for each of the three types of fluorescent expression in HEK293 cells singly transfected using ZERO-HcRed (closed bars, N= 17, n= 712), STREX-HcRed (hatched bars, N= 8, n= 452) and pHcRed (open bars, N= 17, n= 727). Also shown are representative images for HEK293 cells expressing **b)** ZERO-HcRed, **c)** STREX-HcRed (outlines of cells shown in grey) and **d)** pHcRed taken 96 h after transfection.

Figure 3-4
Fluorescent profile of STREX-EGFP or STREX-HcRed in HEK293 cells

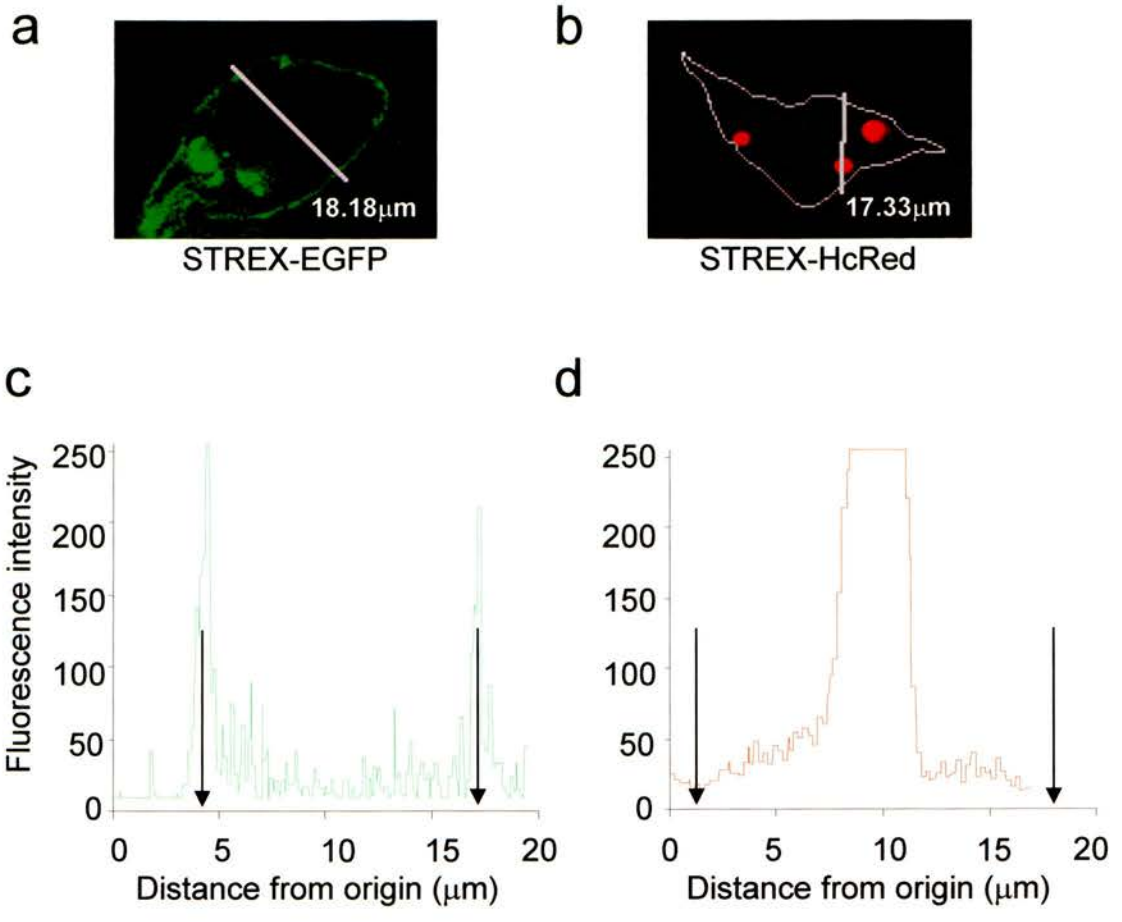

Figure 3-4 Fluorescent profile of STREX-EGFP or STREX-HcRed

Fluorescence was measured at 0.02μm intervals along a line through HEK293 cells expressing **(a)** STREX-EGFP and **(b)** STREX-HcRed (outline of cell is shown in grey) 96h after transfection. Fluorescent profile is expressed as fluorescence intensity (0- 255) against distance (μm) from origin of line scan for HEK293 cells expressing **(c)** STREX-EGFP, where peaks in fluorescence (green trace) can be seen at the membrane (arrows) and **(d)** STREX-HcRed, where no fluorescence (red trace) is seen at the membrane (arrows) but is localised in a punctate manner, inside the cell.

HEK293 cells were transfected with pHcRed-N1, which encodes the HcRed protein by itself, in order to investigate whether the trapping of the ZERO-HcRed α-subunits was a result of the HcRed fusion protein *per se*. In the transfected cells, fluorescence was uniformly distributed throughout the cell, in a similar manner to that observed for EGFP alone. Membrane, trapped and diffuse expression were 0%, 13.6 ± 3.2% and 96.9 ± 1.7% respectively (N= 17, n= 727). Trapping of HcRed alone was significantly lower ($p< 0.01$) than for either ZERO-HcRed or STREX-HcRed alone (fig. 3-3), and this suggests that HcRed itself does not undergo the oligomerisation and aggregation that have been reported for another red fluorescent protein variant, DsRed (Gavin *et al.* 2002). The trapping of the ZERO-HcRed α-subunits is therefore likely to be a function of the channel- HcRed fusion protein, as opposed to an effect of HcRed alone. It might be possible that the observed puncta are composed only of the HcRed protein alone, which may have been cleaved from the channel post-translation. However, as HcRed expressed alone results in a uniform fluorescence throughout the cell, this is most unlikely to be the case.

Whilst precluding the use of BK channel- HcRed fusion proteins to investigate the channel α-subunit expression and distribution in mammalian cells, these data suggest that they may be useful in providing a valuable, genetically encodable dominant-negative suppressor of BK channel α-subunit cell surface expression. To investigate this hypothesis, subsequent studies were performed to analyse the cellular distribution of the fusion proteins in HEK293 cells following cotransfection with BK channel α-subunit- EGFP and BK α subunit- HcRed constructs.

3-2-1-2 Homomeric assembly of fluorescently- labelled BK channel α-subunits in HEK293 cells

BK channel α-subunits assemble as tetramers to form functional channels (Tian *et al.*, 2004, Brelidze *et al.*, 2003). Since the increased trapping and decreased membrane expression of ZERO- HcRed was shown to be a result of the fusion protein, rather than HcRed alone, this suggests that there are at least two possible mechanisms for the trapping of the channel- HcRed proteins; i) single HcRed fusion proteins are incorrectly folded, therefore cannot be assembled into tetramers, and transported to the plasma membrane, or ii) the fusion proteins are capable of tetramerisation, however the subsequent channel tetramer is incorrectly targeted- in this case, the BK channel α-subunit HcRed fusion protein may be acting as a dominant negative suppressor of cell surface expression. In the case of the former, in cells coexpressing both EGFP and -HcRed labelled BK channel α-subunits, trapping should only be observed for the -HcRed labelled fusion proteins. However if tetramerisation is possible, the -HcRed labelled α-subunits may cause trapping of the channel- EGFP fusion proteins. Alternatively, they might be 'rescued' by the latter, allowing delivery of the -HcRed labelled α-subunits to the cell surface. In both of these cases, colocalisation of EGFP and HcRed fluorescence in intracellular puncta or at the plasma membrane would be observed.

Cotransfection of ZERO-EGFP with ZERO-HcRed resulted in a significant ($p< 0.01$) reduction of ZERO-EGFP plasma membrane expression to 9.9 ± 2.7% (N= 10, n= 454) of transfected cells, compared to 32.6 ± 7.1% for ZERO-EGFP alone (fig. 3-5). The trapping of ZERO-EGFP and ZERO-HcRed fusion proteins in intracellular

Figure 3-5
Coexpression of ZERO-EGFP with ZERO-HcRed or STREX-HcRed in HEK293 cells

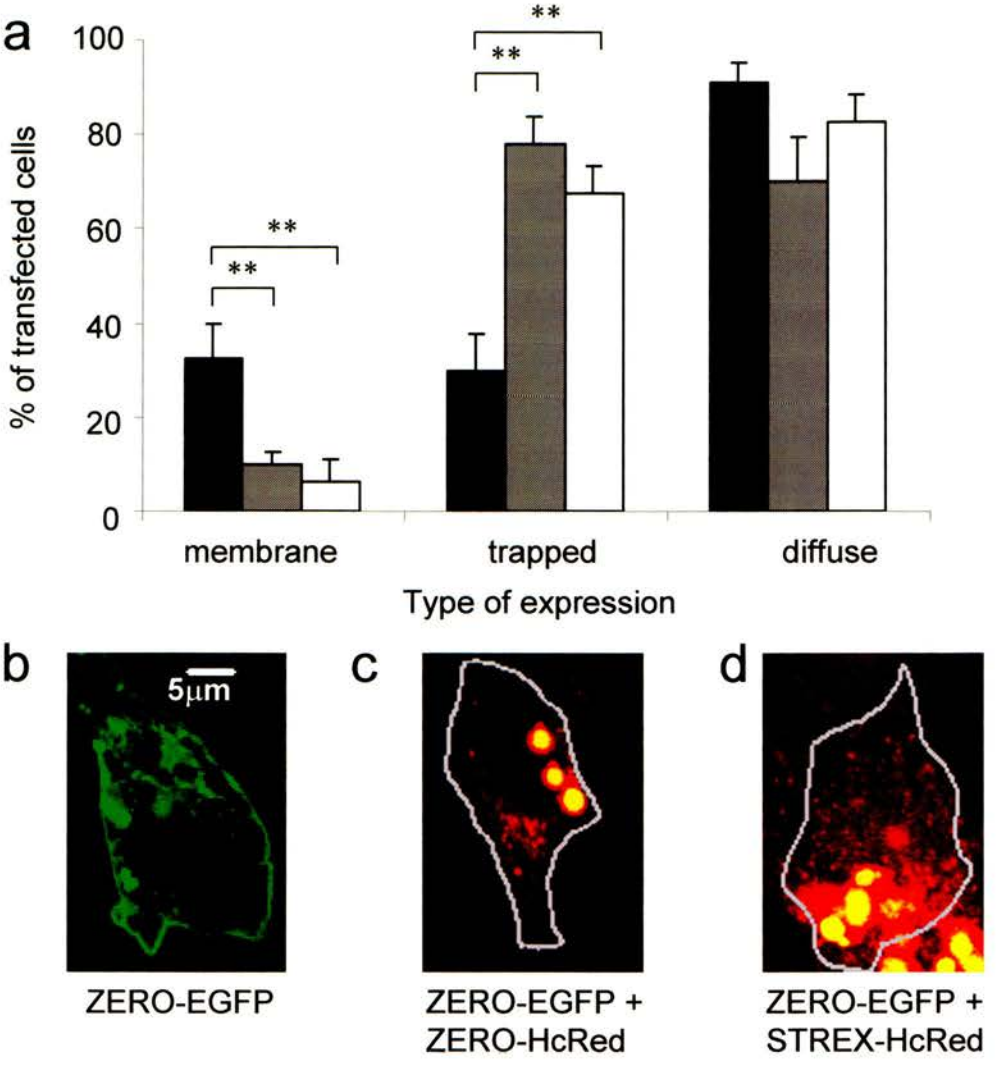

Figure 3-5 Coexpression of ZERO-EGFP with ZERO-HcRed or STREX-HcRed in HEK293 cells

a) Data shown as a mean percentage of total transfected cells per field of view for each of the three types of fluorescent expression in HEK293 cells singly transfected with ZERO-EGFP (closed bars, N= 12, n= 492), cotransfected with ZERO-EGFP and ZERO-HcRed (crossed bars, N= 10, n=454) or cotransfected with ZERO-EGFP and STREX-HcRed (open bars, N= 7, n= 283). Representative images of HEK293 cells expressing **b)** ZERO-EGFP, **c)** coexpressing ZERO-EGFP and ZERO-HcRed, and **d)** coexpressing ZERO-EGFP and STREX-HcRed (outlines of cells shown in grey), taken 96 h after transfection. In cotransfected cells, colocalisation of EGFP and HcRed fluorescence is shown in yellow. (* = $p<0.05$, ** = $p<0.01$ ANOVA with post- hoc test Student- Newman- Keuls).

puncta significantly increased to 78.3 ± 5.5% compared to 29.8 ± 8.1% for singly transfected ZERO- EGFP ($p < 0.01$). Strong overlapping peaks of fluorescence for both EGFP and HcRed were observed in the fluorescent profiles for cells expressing ZERO-EGFP and ZERO-HcRed, suggesting that these two fluorescent protein-labelled BK channel α-subunits were colocalised in these trapped puncta (fig. 3-6), which had an average diameter of 2.9 ± 0.1μm (N=3, n= 162). The level of diffuse expression was 70.3 ± 9.5% for cotransfected cells, and 91.1 ± 4.0% for ZERO-EGFP alone. This suggests that ZERO-HcRed is able to form dimers or tetramers with ZERO-EGFP in HEK293 cells, and it appears that ZERO-HcRed behaves as a dominant negative suppressor of cell surface expression for homomeric channels of the same splice variants.

In order to test whether STREX-HcRed acted as a dominant negative suppressor of cell surface expression when coexpressed with the STREX-EGFP fusion protein HEK293 cells were cotransfected using both STREX-EGFP and STREX-HcRed. A significant ($p< 0.01$) suppression of plasma membrane expression was observed in the cotransfected cells, where 16.5 ± 6.4% (N= 9, n= 452) of cells had fluorescent labelling of the plasma membrane, as opposed to 50.8 ± 6.1% for STREX-EGFP alone (fig. 3-7). Trapped expression increased significantly ($p < 0.05$) from 47.2 ± 6.0% for STREX-EGFP alone, to 76.4 ± 4.5% in cotransfected cells. STREX-EGFP and STREX-HcRed colocalised into bright intracellular puncta (fig. 3-6), in a similar manner to that observed for STREX-HcRed alone. Average puncta diameter was 2.7 ± 0.2μm (N=3, n= 83). Diffuse cytoplasmic expression was still present in 93.6 ±

Figure 3-6
Fluorescent profile of HEK293 cells cotransfected with ZERO-EGFP/ ZERO-HcRed or STREX-EGFP/ STREX-HcRed

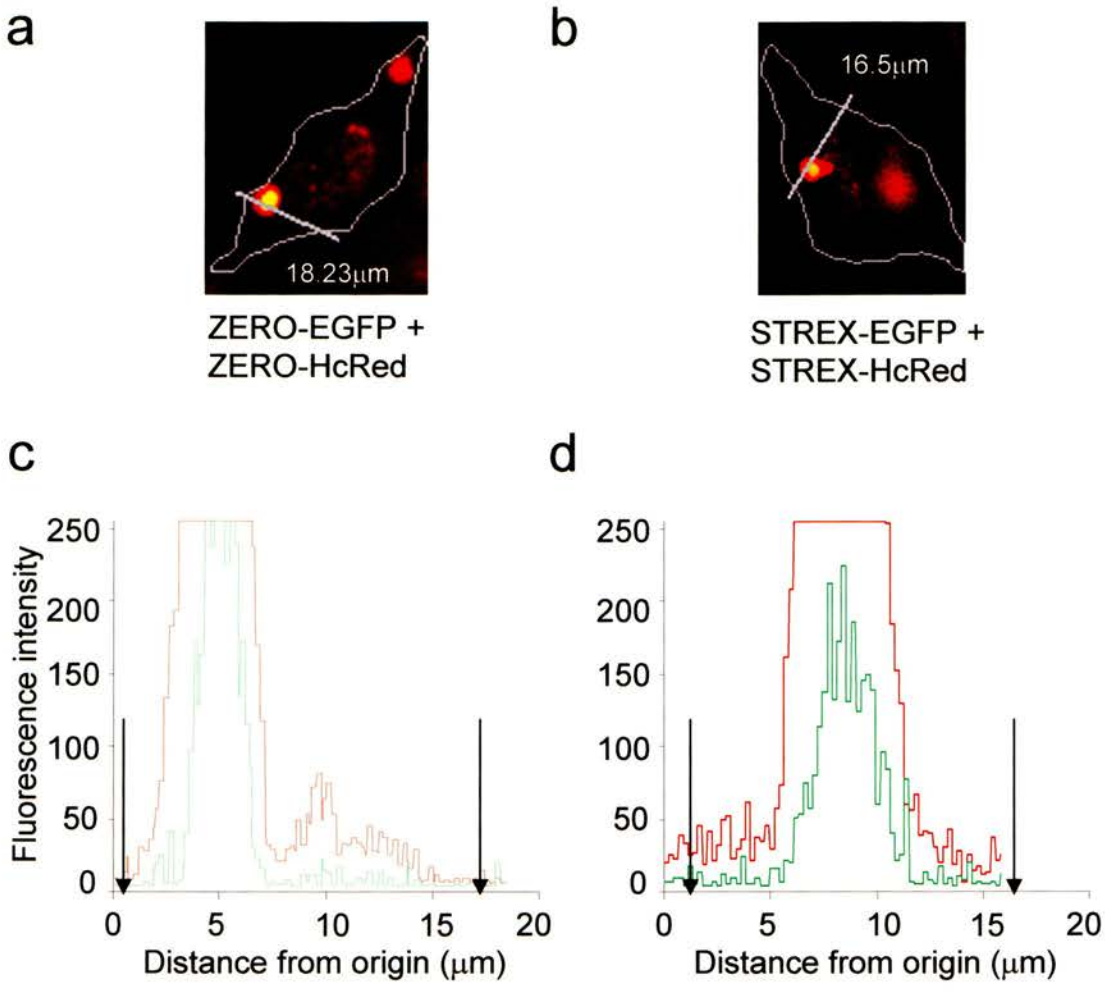

Figure 3-6 Fluorescent profile of HEK293 cells cotransfected with ZERO-EGFP/ ZERO-HcRed or STREX-EGFP/ STREX-HcRed

Fluorescence was measured at 0.02μm intervals along a line through HEK293 cells cotransfected with either **(a)** ZERO-EGFP and ZERO-HcRed or **(b)** STREX-EGFP and STREX-HcRed. The outline of the cell membrane is shown in grey. Fluorescent profile is expressed as fluorescence intensity (0-255) against distance from origin of line scan for HEK293 cells coexpressing **(c)** ZERO-EGFP and ZERO-HcRed or **(d)** STREX-EGFP and STREX-HcRed. In images, colocalisation of EGFP and HcRed fluorescence is shown in yellow. In each case, EGFP (green trace) and HcRed (red trace) fluorescence cannot be seen at the plasma membrane, but instead colocalise within the cell in a punctate manner.

Figure 3-7
Coexpression of STREX-EGFP with STREX-HcRed or ZERO-HcRed in HEK293 cells

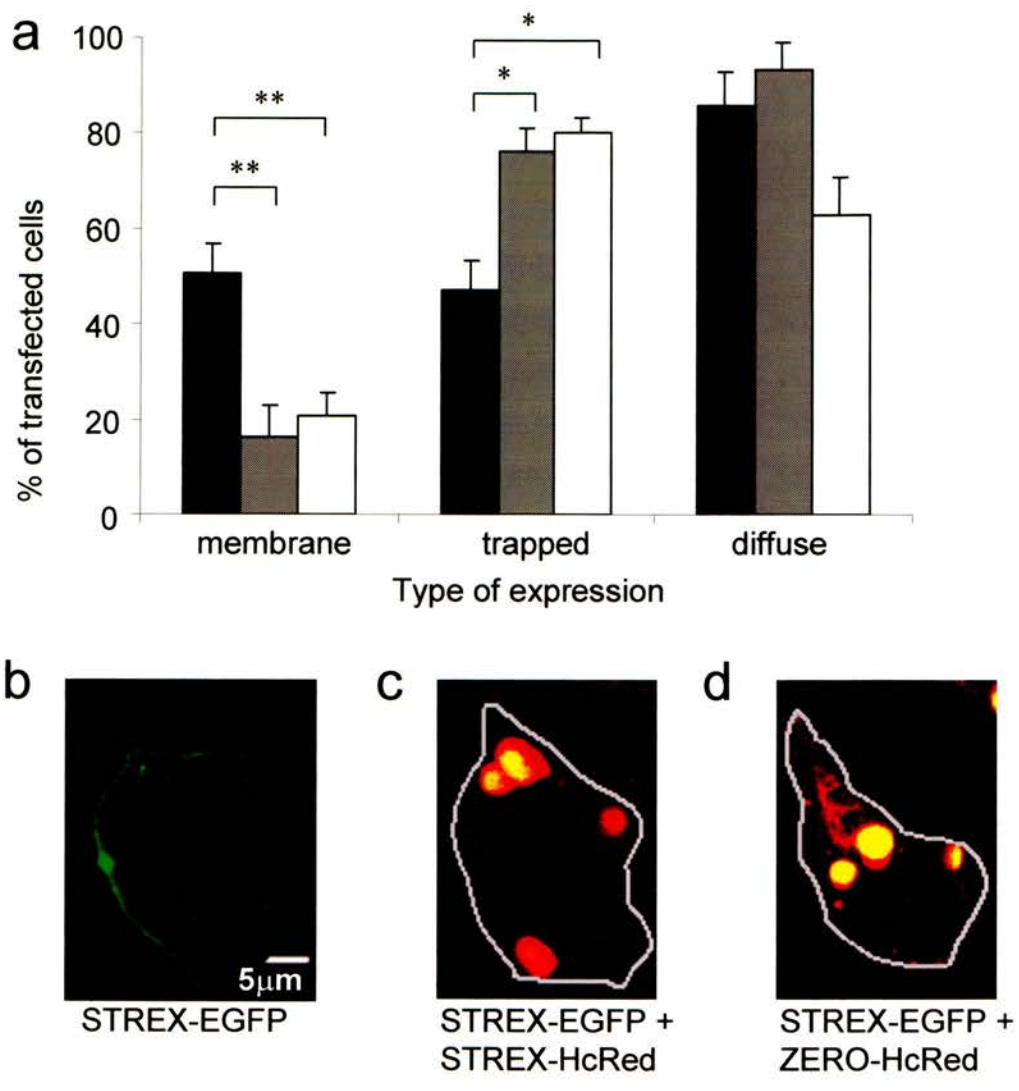

Figure 3-7 Coexpression of STREX-EGFP with STREX-HcRed or ZERO-HcRed in HEK293 cells

a) Data shown as a mean percentage of total transfected cells per field of view for each of the three types of fluorescent expression in HEK293 cells singly transfected with STREX-EGFP (closed bars, N= 16, n= 575), cotransfected with STREX-EGFP and STREX-HcRed (crossed bars, N= 9, n=452) or cotransfected with STREX-EGFP and ZERO-HcRed (open bars, N= 17, n= 763). Representative images of HEK293 cells expressing **b)** STREX-EGFP, **c)** coexpressing STREX-EGFP and STREX-HcRed, and **d)** coexpressing STREX-EGFP and ZERO-HcRed (outlines of cells shown in grey), taken 96 h after transfection. In cotransfected cells, colocalisation of EGFP and HcRed fluorescence is shown in yellow. (* = $p<0.05$, ** = $p<0.01$ ANOVA with post- hoc test Student- Newman- Keuls).

5.7% of cells, and this was not significantly different to that observed for STREX-EGFP alone.

To exclude the possibility that the HcRed protein itself causes the trapping of -EGFP labelled BK channel α-subunits, and to demonstrate that α-subunit multimerisation is required for the dominant negative effect of the BK channel α-subunit- HcRed constructs, ZERO-EGFP was cotransfected into HEK293 cells with pHcRed-N1. Plasma membrane expression of ZERO-EGFP in the presence of HcRed was not significantly different to that of ZERO-EGFP alone- 19.8 ± 7.2% (N= 7, n= 279) as opposed to 32.6 ± 7.1% for singly- transfected ZERO-EGFP. Trapped and diffuse cytoplasmic expression were also present in 14.2 ± 6.0% and 97.3 ± 1.3% of transfected cells respectively, and these were not significantly different compared to ZERO-EGFP alone- 29.8 ± 8.6% and 91.1 ± 4.0% of cells respectively (fig. 3-8).

STREX-EGFP was also cotransfected into HEK293 cells with pHcRed-N1. Plasma membrane expression of STREX-EGFP in the presence of HcRed was not significantly different to that in cells expressing STREX-EGFP alone, at 48.2 ± 4.8% (N= 17, n= 1011) compared to 50.8 ± 6.1% respectively. Paradoxically, the level of trapped STREX-EGFP in the cotransfected cells fell significantly to 12.3 ± 2.9% compared with 47.2 ± 6.0% for STREX-EGFP alone ($p < 0.01$). The level of diffuse expression in the cotransfected cells, 90.3 ± 4.5% was comparable to that of the STREX-EGFP singly transfected cells, 85.8 ± 7.1% (fig. 3-9).

Figure 3-8
Coexpression of ZERO-EGFP with pHcRed in HEK293 cells

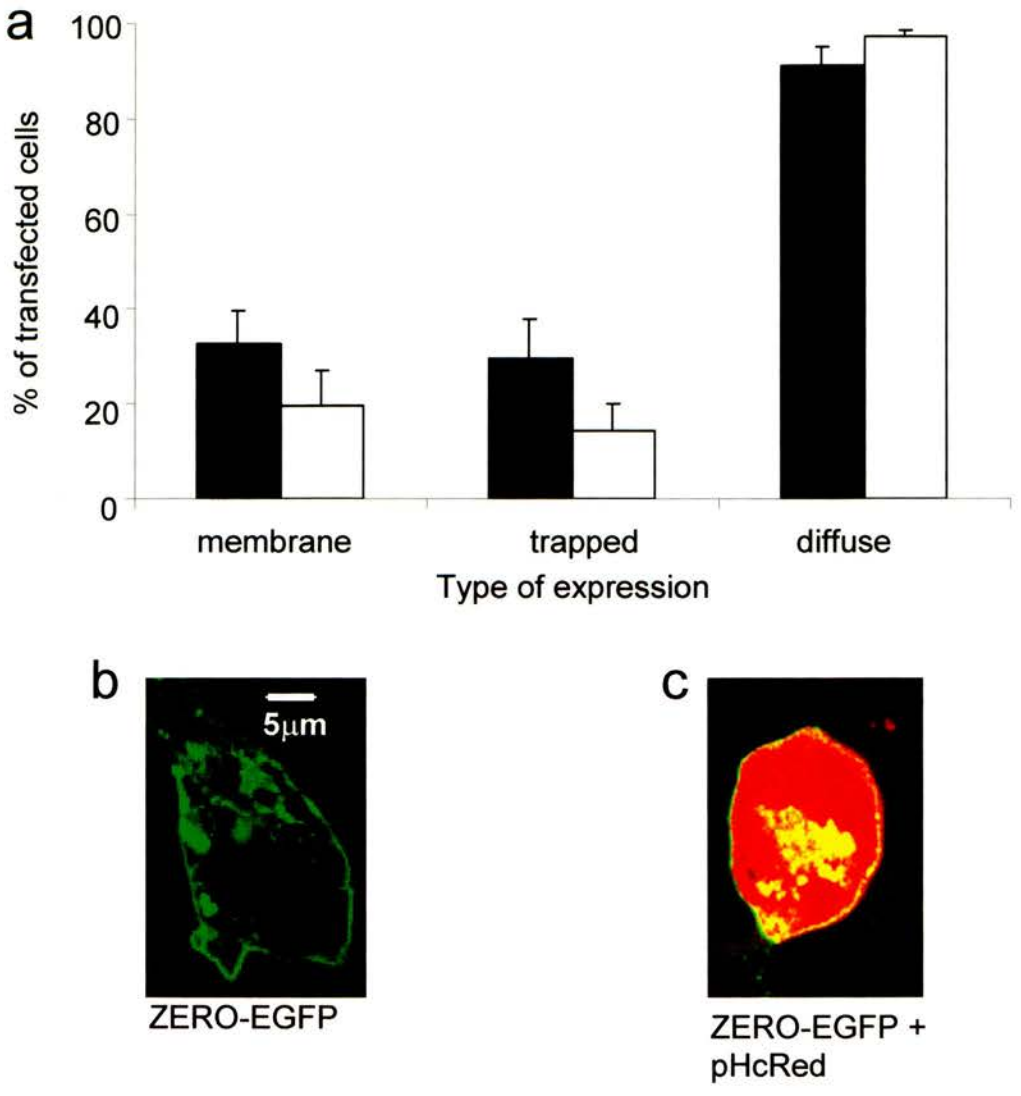

Figure 3-8 Coexpression of ZERO-EGFP with pHcRed in HEK293 cells

a) Data shown as mean percentage of total transfected cells per field of view (± SEM) for each of the three types of fluorescent expression in HEK293 cells transfected with ZERO-EGFP alone (closed bars, N= 12, n= 492), or ZERO-EGFP cotransfected with pHcRed (crossed bars, N= 7, n= 279). Representative images of cells are also shown for **b)** ZERO-EGFP and **c)** ZERO-EGFP cotransfected with pHcRed, taken 96 h after transfection. In cotransfected cell, colocalisation of EGFP and HcRed fluorescence is shown in yellow.

Figure 3-9
Coexpression of STREX-EGFP with pHcRed in HEK293 cells

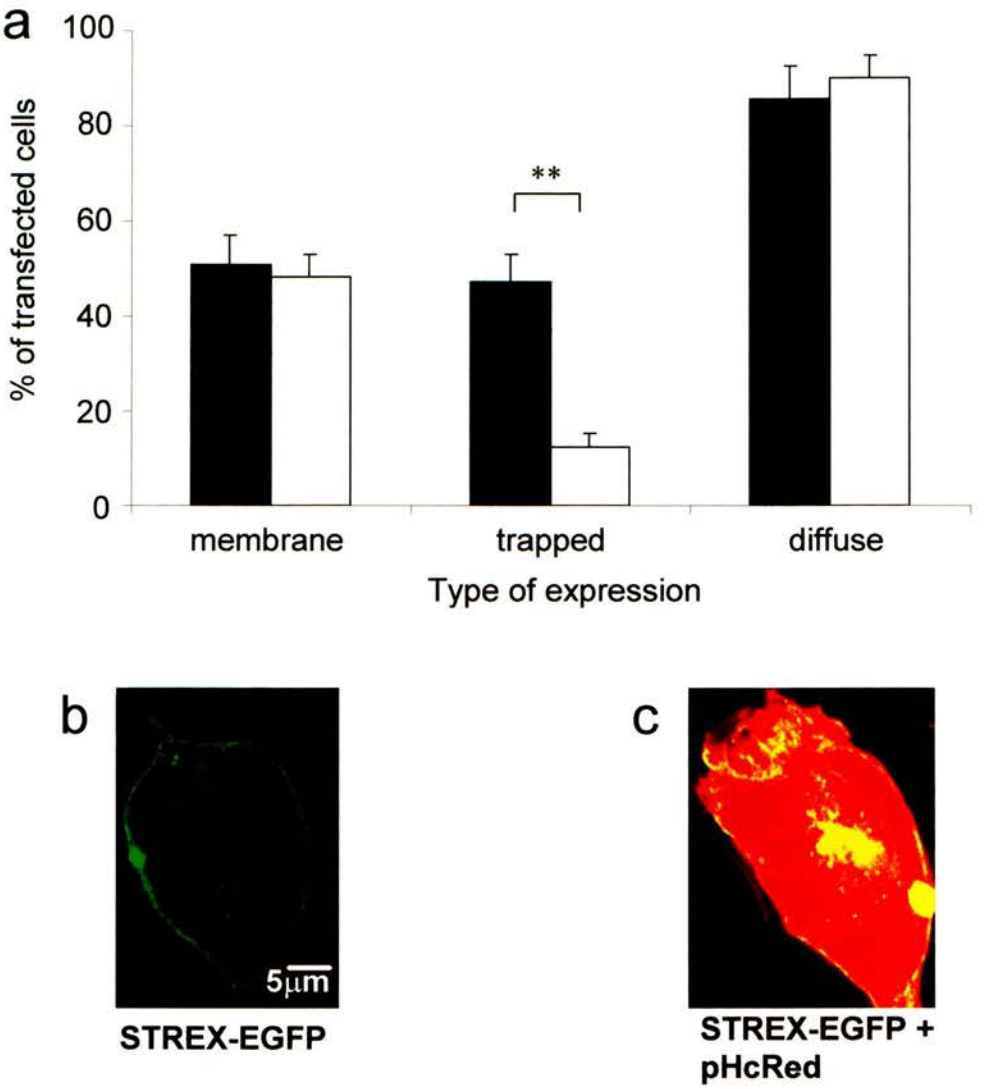

Figure 3-9 Coexpression of STREX-EGFP with pHcRed in HEK293 cells

a) Data shown as mean percentage of total transfected cells per field of view (± SEM) for each of the three types of fluorescent expression in HEK293 cells transfected with STREX-EGFP alone (closed bars, N= 16, n= 575), or STREX-EGFP cotransfected with pHcRed (crossed bars, N= 17, n= 1011). Representative images of cells are also shown for **b)** STREX-EGFP and **c)** STREX-EGFP cotransfected with pHcRed, taken 96 h after transfection. In cotransfected cell, colocalisation of EGFP and HcRed fluorescence is shown in yellow. (** = $p<0.01$ ANOVA with post- hoc test Student- Newman- Keuls).

3-2-1-3 Heteromeric assembly of fluorescently- labelled BK channel α-subunits in HEK293 cells

To investigate whether or not the presence of the ZERO-HcRed construct would affect the cellular distribution of another fluorescently- labelled BK channel splice variant, ZERO-HcRed was coexpressed in HEK293 cells with STREX-EGFP. This resulted in a significant ($p< 0.01$) suppression of plasma membrane expression of STREX-EGFP, from 50.8 ± 6.1% for STREX-EGFP expressed alone, to 20.7 ± 5.0% (N= 17, n= 763) for the STREX-EGFP and ZERO-HcRed cotransfected cells (fig. 3-7). Trapped expression increased significantly from 47.2 ± 6.0% for STREX-EGFP alone, to 80.1 ± 3.0% for STREX-EGFP cotransfected with ZERO-HcRed ($p< 0.05$). Average diameter of the trapped puncta was 2.2 ± 0.2μm (N=3, n= 69), and again strong overlapping peaks for EGFP and HcRed in the fluorescence profiles for cells expressing STREX-EGFP and ZERO-HcRed, suggest that these two fluorescently-labelled BK channel α-subunits are colocalised within these puncta (fig. 3-10). Diffuse cytoplasmic expression fell slightly from 85.8 ± 7.1% for singly transfected STREX-EGFP to 63.2 ± 7.8% in the cotransfected cells, but this was not a significant difference.

HEK293 cells were cotransfected using ZERO-EGFP and STREX-HcRed, in order to investigate whether the latter could cause the suppression of membrane expression of the ZERO BK channel variant. The level of membrane expression in the cotransfected cells was reduced to 6.4 ± 4.6% (N= 7, n= 283), significantly ($p< 0.01$) lower than for ZERO-EGFP alone, where 32.6 ± 7.1 of cells had fluorescent membrane labelling (fig. 3-5). There was also a significant ($p< 0.01$) increase in the

Figure 3-10
Fluorescent profile of HEK293 cells cotransfected with STREX-EGFP/ ZERO-HcRed or ZERO-EGFP/ STREX-HcRed.

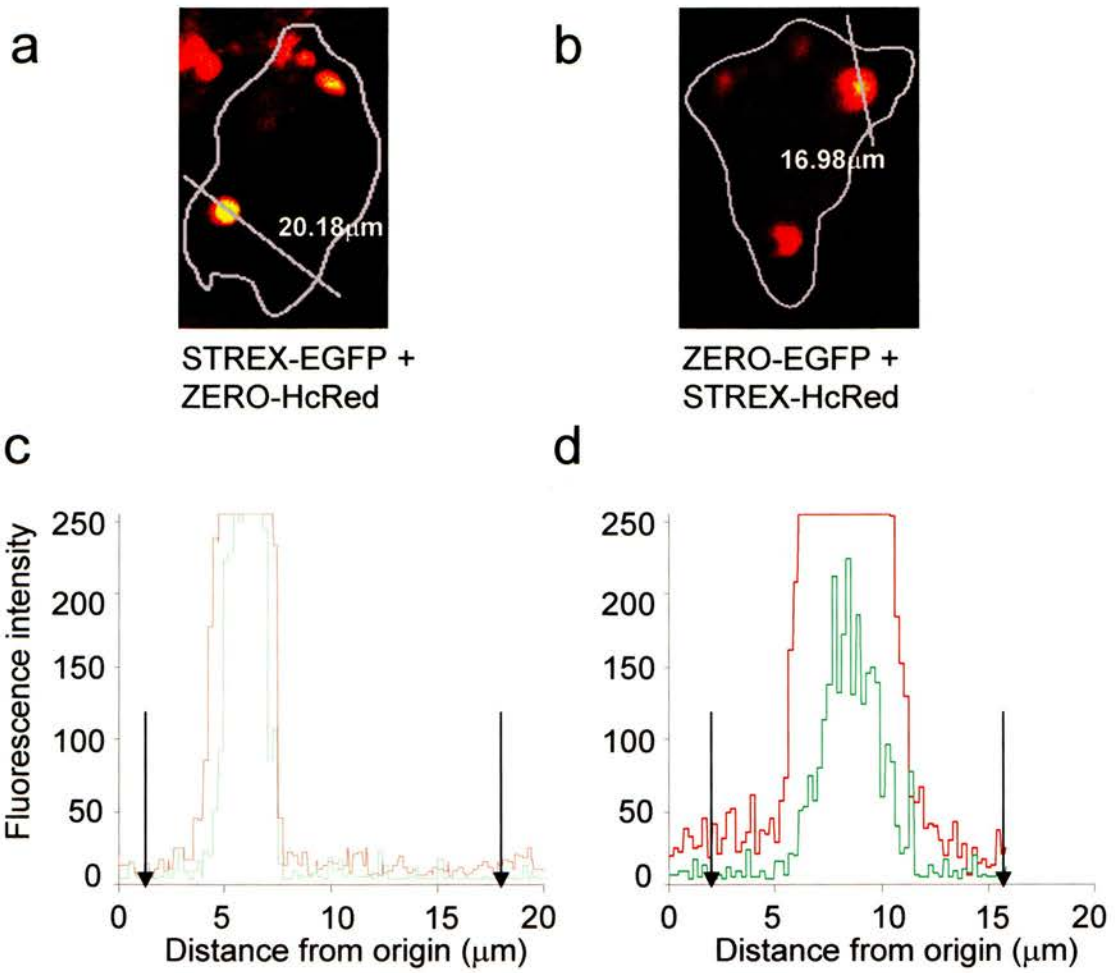

Figure 3-10 Fluorescent profile of HEK293 cells cotransfected with STREX-EGFP/ ZERO-HcRed or ZERO-EGFP/ STREX-HcRed.

Fluorescence was measured at 0.02μm intervals along a line through HEK293 cells cotransfected with either **(a)** STREX-EGFP and ZERO-HcRed or **(b)** ZERO-EGFP and STREX-HcRed. The outline of the cell membrane is shown in grey. Fluorescent profile is expressed as fluorescence intensity (0-255) against distance from origin of line scan for HEK293 cells coexpressing **(c)** STREX-EGFP and ZERO-HcRed or **(d)** ZERO-EGFP and STREX-HcRed. In images, colocalisation of EGFP and HcRed fluorescence is shown in yellow. In each case, EGFP (green trace) and HcRed (red trace) fluorescence cannot be seen at the plasma membrane, but instead colocalise within the cell in a punctate manner.

amount of trapping, characterised by bright intracellular puncta, present in 67.8 ± 5.7% of cotransfected cells, as opposed to 29.8 ± 8.1% of cells singly transfected using ZERO- EGFP. Again, in the cotransfected cells, both ZERO-EGFP and STREX-HcRed were colocalised in the large trapped puncta (fig. 3-10), the average diameter of which was 3.1 ± 0.1μm (N= 3, n= 149).

Taken together, these data suggest that the BK channel splice variant α-subunits can assemble as heteromultimers, and that ZERO-HcRed and STREX-HcRed may act as a dominant negative α-subunit for cell surface expression of BK channel α-subunit splice variants in HEK293 cells.

3-2-1-4 Expression of -HA tagged BK channel alternatively spliced α-subunits in HEK293 cells

In order to preclude the possibility that the pattern of expression seen for the -EGFP labelled BK channel α-subunit fusion proteins was a result of EGFP itself, for example by causing incorrect folding of the cytoplasmic tail of the channel, or altered trafficking due to the relatively large size (229aa) of the label at the C-terminus, constructs were used that would cause expression of BK channel α-subunits labelled at the C- terminus with the HA epitope (9aa in length).

HEK293 cells were transfected with cDNA encoding BK channel α-subunits, with a C- terminal HA epitope tag. 96 h after transfection, the cells were fixed, then immunostained using a rabbit polyclonal anti- HA primary antibody, followed by an

anti- rabbit secondary antibody labelled with the Alexa- 488 or -647 fluorescent dye, then imaged as for the EGFP and HcRed BK channel α-subunit fusion proteins.

In HEK293 cells expressing ZERO-HA, robust labelling of the plasma membrane was observed in 48.3 ± 5.2% (N= 5, n= 60) of transfected cells, whilst trapped fluorescence in bright intracellular puncta was observed in 67.9 ± 9.7% of transfected cells. Diffuse cytoplasmic expression was observed in 97.8 ± 2.2% of transfected cells. No significant difference was observed between either the membrane or diffuse cytoplasmic expression of ZERO-HA compared to ZERO-EGFP, however the trapped expression in bright intracellular puncta for ZERO-HA was significantly higher ($p < 0.01$) than that of ZERO-EGFP (29.8 ± 8.1% of transfected cells) (fig. 3-11).

In order to observe whether there was any difference in expression of an alternatively spliced BK channel α-subunit when labelled with HA instead of EGFP, cDNA constructs encoding -HA labelled STREX BK channel α-subunits were expressed in HEK293 cells. Robust, uniform plasma membrane expression was observed in 68.1 ± 4.4% (N= 8, n= 118) of transfected cells. Trapped expression in bright, intracellular puncta was observed in 38.0 ± 8.5% of transfected cells, and diffuse cytoplasmic expression was seen in 95.0 ± 2.7% of transfected cells. No significant difference was observed for either membrane, trapped or diffuse cytoplasmic expression when compared to those of STREX-EGFP (fig. 3-12). These data suggest that the presence of a large C-terminal label, such as EGFP does not affect the membrane trafficking of BK channel alternative splice variants. Although the amount

Figure 3-11
Comparison of expression of ZERO-EGFP or ZERO-HA in HEK293 cells

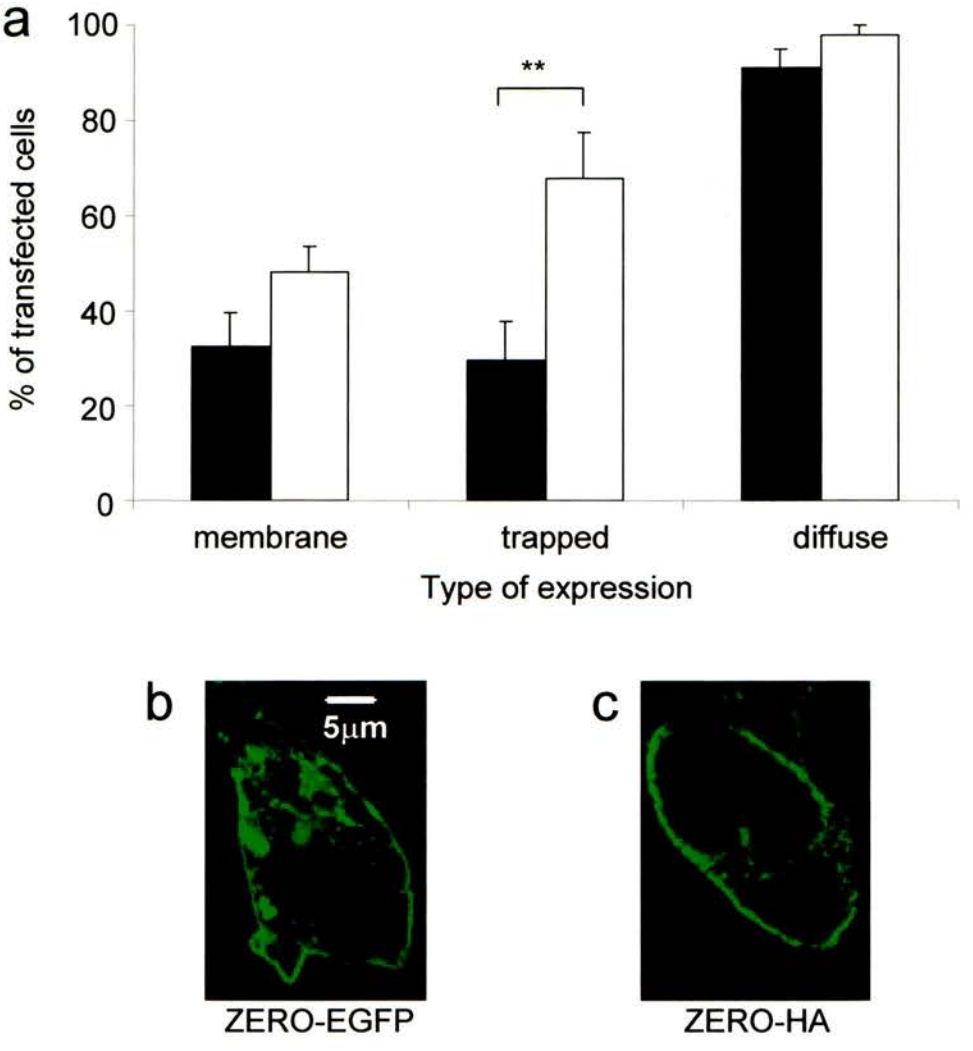

Figure 3-11 Comparison of expression of ZERO-EGFP or ZERO-HA in HEK293 cells

a) Data shown as a mean percentage of total transfected cells per field of view for HEK293 cells expressing ZERO-EGFP (closed bars, N= 12, n= 492) and ZERO-HA (open bars, N= 5, n= 60). Representative images are also shown of HEK293 cells expressing **b)** ZERO-EGFP and **c)** ZERO-HA. (** = $p < 0.01$ ANOVA with post- hoc test Student- Newman- Keuls).

Figure 3-12
Comparison of expression of STREX-EGFP or STREX-HA in HEK293 cells

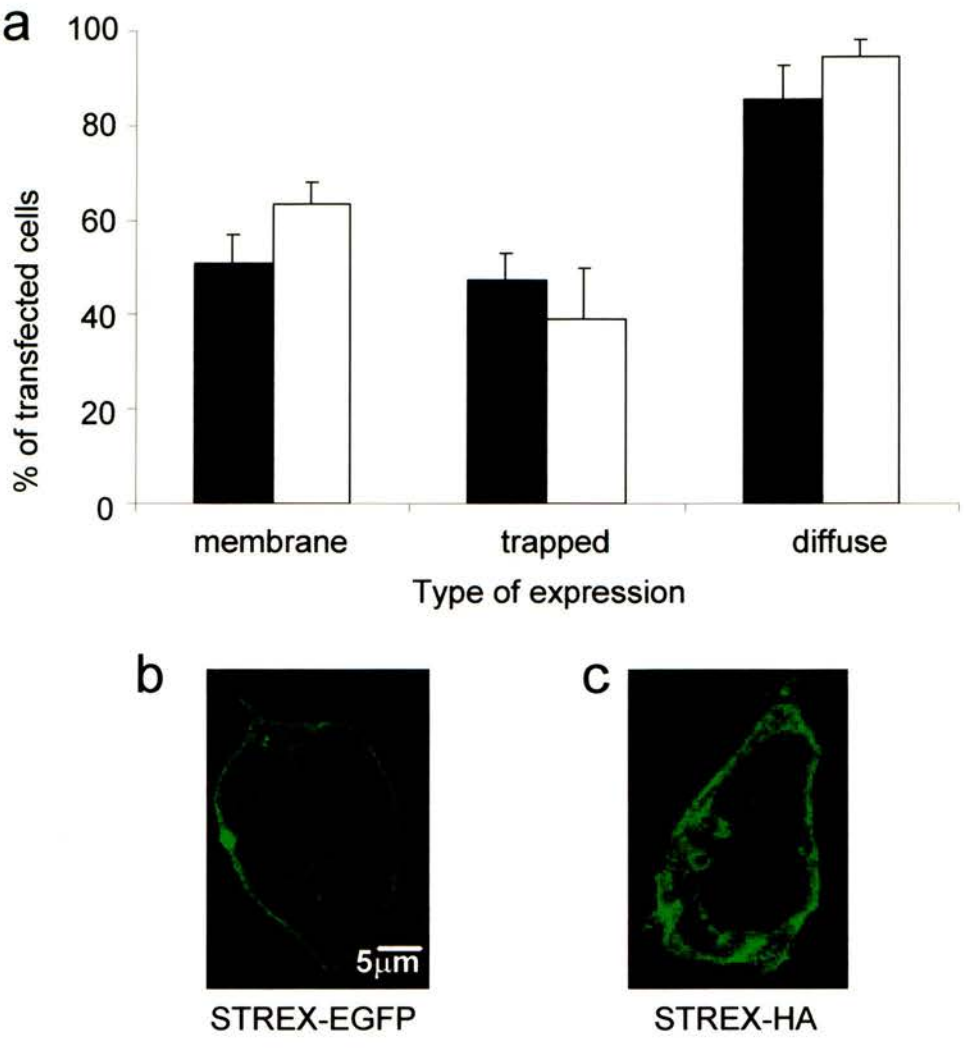

Figure 3-12 Comparison of expression of STREX-EGFP or STREX-HA in HEK293 cells

a) Data shown as a mean percentage of total transfected cells per field of view for HEK293 cells expressing STREX-EGFP (closed bars, N= 16, n= 575) and STREX-HA (open bars, N= 8, n= 118). Representative images are also shown of HEK293 cells expressing **b)** STREX-EGFP and **c)** STREX-HA.

of trapped punctate expression observed in cells transfected with ZERO-HA was significantly higher than that of ZERO-EGFP, this was not accompanied by a significant reduction in membrane expression, and it may be the case that the overall expression level is higher for the ZERO-HA cDNA construct, therefore use of the -EGFP labelled ZERO BK channel fusion protein may be preferable to ZERO-HA due to the reduced trapping.

3-2-1-5 Homomeric assembly of -HA and -HcRed labelled BK channel α-subunits in HEK293 cells

Having previously observed that the ZERO-HcRed fusion protein reduced the membrane expression of ZERO-EGFP when coexpressed in HEK293 cells, and that STREX-HcRed reduced the membrane expression of STREX-EGFP, these experiments were repeated in order to address whether the -HcRed labelled BK channel alternative splice variants would also prevent the membrane expression of the -HA labelled channel α-subunits.

Cotransfection of ZERO-HA with ZERO-HcRed resulted in a significant reduction in membrane labelling ($p< 0.05$) to 13.4 ± 8.2% (N= 4, n= 81) of transfected cells, compared with 48.3 ± 5.2% for ZERO-HA alone. No significant difference was observed in the amount of intracellular puncta, seen in 86.9 ± 5.9% of transfected cells, compared to that of ZERO-HA alone (67.9 ± 9.7% of transfected cells) or diffuse cytoplasmic expression, seen in 93.8 ± 2.9% of transfected cells, compared to that of ZERO-HA alone (97.8 ± 2.2% of transfected cells) (fig. 3-13).

Figure 3-13
Expression of ZERO-HA and coexpression of ZERO-HA with ZERO-HcRed or STREX-HcRed in HEK293 cells

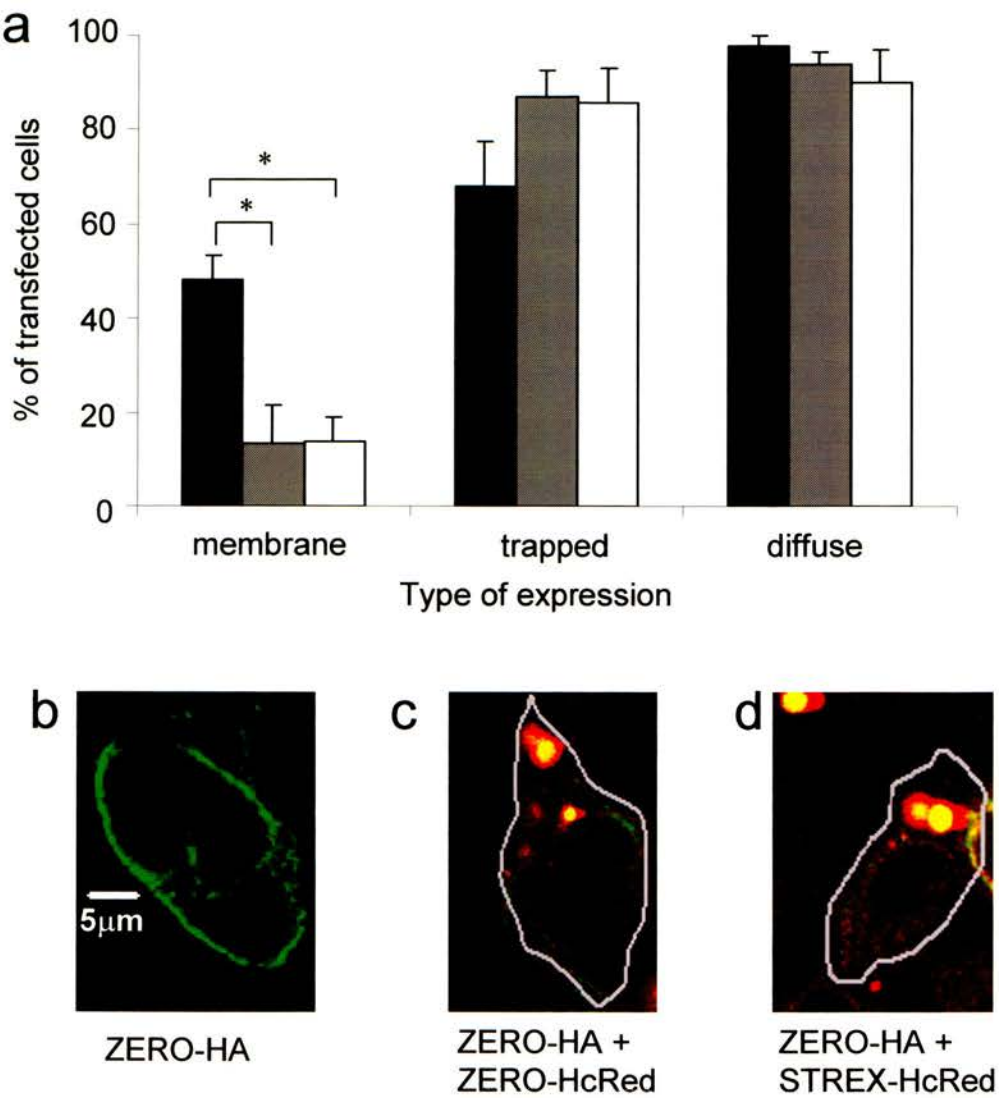

Figure 3-13 Expression of ZERO-HA and coexpression of ZERO-HA with ZERO-HcRed or STREX-HcRed in HEK293 cells

a) Data shown as a mean percentage of total transfected cells per field of view for each of the three types of fluorescent labelling in HEK 293 cells singly transfected with ZERO-HA (closed bars, N= 5, n= 60), cotransfected with ZERO-HA and ZERO-HcRed (crossed bars, N= 4, n= 81) or cotransfected with ZERO-HA and STREX-HcRed (open bars, N=3, n=42). Representative images of cells are also shown for **b)** ZERO-HA, **c**) ZERO-HA cotransfected with ZERO-HcRed and **d**) ZERO-HA with STREX-HcRed (outlines of cells shown in grey). In cotransfected cells, colocalisation of fluorescence is shown in yellow. (* = $p<0.05$ ANOVA with post- hoc test Student- Newman- Keuls).

HEK293 cells were then cotransfected with STREX-HA and STREX-HcRed in order to test whether cell surface expression of STREX-HA would be reduced when coexpressed with STREX-HcRed. Plasma membrane labelling was observed in 32.0 ± 3.5% (N= 5, n= 97) of transfected cells, significantly lower ($p< 0.01$) than STREX-HA alone (68.1 ± 4.4% of transfected cells). Trapping of the fusion proteins in intracellular puncta was observed in 64.6 ± 9.0% of cells. This was significantly higher ($p< 0.05$) than for STREX-HA alone (38.0 ± 8.5% of transfected cells). Diffuse cytoplasmic expression was observed in 82.7 ± 8.7% of cells, although this was not significantly different to that observed for STREX-HA alone (fig. 3-14).

Taken together, these data suggest that the -HA labelled BK channel α-subunits behave in a similar fashion to the -EGFP labelled BK channel α-subunits when cotransfected with ZERO-HcRed and STREX-HcRed, which are able to act as dominant- negative suppressors of cell surface expression for homomeric assembly with the same splice variants.

3-2-1-6 Heteromeric assembly of -HA and -HcRed labelled BK channel α-subunits in HEK293 cells

HEK293 cells were cotransfected with ZERO-HA and STREX-HcRed, in order to address whether the latter could form multimers with an alternatively spliced BK channel α-subunit labelled at the C- terminus with HA, thus affecting the surface expression in a similar manner to that observed when ZERO-EGFP and STREX-HcRed were coexpressed. Plasma membrane expression of ZERO-HA fell significantly ($p< 0.05$), and was observed in 13.6 ± 5.2% (N= 3, n= 42) of transfected

Figure 3-14
Expression of STREX-HA and coexpression of STREX-HA with STREX-HcRed or ZERO-HcRed in HEK293 cells

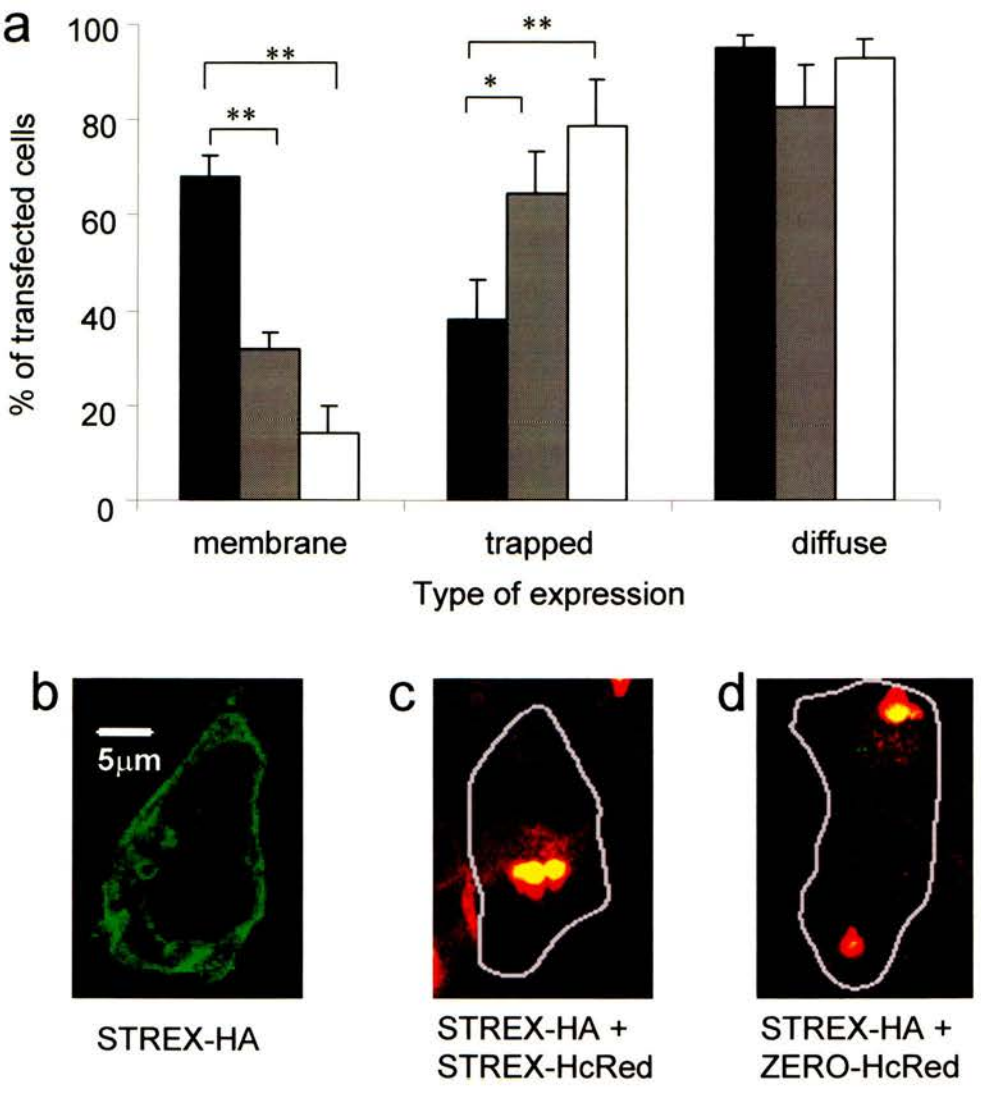

Figure 3-14 Expression of STREX-HA and coexpression of STREX-HA with STREX-HcRed or ZERO-HcRed in HEK293 cells

a) Data shown as a mean percentage of total transfected cells per field of view for each of the three types of fluorescent labelling in HEK 293 cells singly transfected with STREX-HA (closed bars, N= 8, n= 118), cotransfected with STREX-HA and STREX-HcRed (crossed bars, N= 5, n= 97) or cotransfected with STREX-HA and ZERO-HcRed (open bars, N= 4, n= 67). Representative images are also shown for cells expressing **b)** STREX-HA, **c**) STREX-HA coexpressed with STREX-HcRed and **d**) STREX-HA with ZERO-HcRed (outlines of cells shown in grey). In cotransfected cells, colocalisation of fluorescence is shown in yellow. (* = $p<0.05$, ** = $p<0.01$ ANOVA with post-hoc test Student- Newman- Keuls).

cells, compared to 48.3 ± 5.2% for ZERO-HA alone. Trapped expression was observed in 85.8 ± 7.4% of transfected cells, and was not significantly higher than in cells transfected with ZERO-HA alone. Diffuse cytoplasmic expression was observed in 90.1 ± 7.1% of transfected cells, and again there was no significant difference when compared with ZERO-HA alone (fig. 3-13).

In order to investigate whether expression of ZERO-HcRed would also affect the cellular distribution of an -HA labelled STREX BK channel α-subunit, HEK293 cells were cotransfected with STREX-HA and ZERO-HcRed. Plasma membrane expression of STREX-HA was significantly reduced ($p< 0.01$) to 14.0 ± 5.8% (N= 4, n= 67) of cotransfected cells, compared to 68.1 ± 4.4% for STREX-HA alone. Trapped expression significantly increased ($p< 0.01$) to 78.6 ± 9.7% of transfected cells, compared with 38.0 ± 8.5% for STREX-HA alone. Diffuse cytoplasmic expression was observed in 92.8 ± 4.4% of transfected cells, and this was not significantly different to that observed for STREX-HA alone (fig. 3-14).

3-2-1-7 Expression of the -HcRed labelled BK channel ZERO alternative splice variant in HEK293 cells stably expressing STREX-HA

In all of the cases where the EGFP and -HA labelled BK channel α-subunit alternative splice variants were coexpressed with ZERO-HcRed, the presence of the latter was found to cause profound disruption of the normal membrane expression of the channels. Although this dominant- negative effect has been observed for newly-synthesised channels, it was unclear whether, as well as multimerisation with other BK channel α-subunits to cause their retention within the cytoplasm, it was possible

that ZERO-HcRed could, by a hitherto unknown mechanism, cause the retrieval of channels which had previously been trafficked to the membrane.

In order to investigate the effect of the ZERO-HcRed fusion protein on an alternatively spliced BK channel α-subunit already localised to the cell membrane, HEK293 cells were stably transfected with STREX-HA. Cells were split and plated onto glass coverslips in 12-well plates, then grown until 40% confluent, and transfected with ZERO-HcRed. Cells were then fixed, immunostained with rabbit anti-HA in conjunction with an Alexa-488- conjugated donkey anti- rabbit secondary antibody, and mounted 24h, 48h, 72h, 96h and 1week after transfection, then imaged and analysed as before. Cells which were not transfected with ZERO-HcRed were immunostained in the same manner at the same timepoints.

No significant differences were found, at any timepoint, when comparing the membrane expression of HEK293 cells stably expressing STREX-HA with that of cells stably expressing STREX-HA which had also been singly- transfected with ZERO-HcRed. For STREX-HA only, membrane expression was observed in 61.3 ± 5.9% (24h), 70.5 ± 6.6% (48h), 63.5 ± 10.2% (72h), 65.5 ± 13.5% (96h) and 54.3 ± 10.1% (1wk) (N=3, n= 125, 118, 107, 130, and 111 respectively) of transfected cells, whilst in those also expressing ZERO-HcRed, membrane expression was observed in 41.1 ± 3.9% (24h), 39.6 ± 10.2% (48h), 40.8 ± 2.5% (72h), 38.3 ± 16.6% (96h) and 60.0 ± 25.3% (1wk) (N=3, n= 37, 67, 91, 73 and 58 respectively) of transfected cells. Membrane expression in HEK293 cells stably expressing STREX-HA was also found not to change significantly across the five timepoints. Additionally, no

significant differences were found when membrane expression of cells stably expressing STREX-HA which were also cotransfected with ZERO-HcRed, was compared across the five timepoints.

When comparing trapping of the BK channel α-subunit fusion proteins in bright intracellular puncta, no significant differences were found across the five timepoints for HEK293 cells stably expressing STREX-HA, and this was also the case for the stably- transfected cells expressing STREX-HA which were also transiently-transfected with ZERO-HcRed. For STREX-HA alone, trapped punctate expression was observed in 69.7 ± 16.9% (24h), 58.1 ± 6.5% (48h), 78.1 ± 6.1% (72h), 43.2 ± 6.7% (96h) and 51.3 ± 6.9% (1wk) of transfected cells. For STREX-HA stable and ZERO-HcRed transfected cells, trapped punctate expression was seen in 86.2 ± 1.6% (24h), 92.0 ± 6.1% (48h), 84.6 ± 10.1% (72h), 86.2 ± 7.0% (96h) and 84.2 ± 8.5% (1wk) of transfected cells. The only significant difference observed was at the 96h timepoint, where STREX-HA only cells had significantly lower trapped punctate expression than those also expressing ZERO-HcRed ($p < 0.05$).

Diffuse cytoplasmic expression was observed in 77.8 ± 11.4% (24h), 69.4 ± 5.0% (48h), 72.0 ± 12.3% (72h), 94.9 ± 5.1% (96h) and 95.1 ± 3.8% (1wk) of transfected cells stably expressing STREX-HA alone. In cells stably expressing STREX-HA which had been singly transfected with ZERO-HcRed, diffuse cytoplasmic expression was observed in 92.6 ± 7.4% (24h), 73.3 ± 19.3% (48h), 89.8 ± 6.0% (72h), 87.2 ± 6.6% (96h) and 75.9 ± 20.0% (1wk) of transfected cells. No significant differences were observed across the five timepoints for cells stably expressing

STREX-HA alone, nor for cells which were also expressing ZERO-HcRed. When diffuse cytoplasmic expression was compared between the cells stably expressing STREX-HA alone, or in conjunction with transiently- transfected ZERO-HcRed, again no significant differences were found (fig. 3-15).

3-2-1-8 Indirect immunofluorescence assay for Golgi apparatus and endosome in cells transfected using ZERO-HcRed

In order to establish the stage of post-translational processing at which the ZERO-HcRed protein is being trapped, indirect immunofluorescence assays were carried out using either mouse monoclonal anti-GM130 to detect the Golgi apparatus, goat anti-EEA1 to detect endosomes, or anti- LAMP1 to detect lysosomes. In HEK293 cells transfected with ZERO-HcRed, and immunostained with anti- LAMP1 in conjunction with an Alexa- 488- conjugated anti mouse secondary antibody, the bright intracellular puncta observed for ZERO-HcRed appeared independently of the fluorescent labelling of the lysosome (fig. 3-16), indicating that the trapping of the Zero-HcRed fusion protein does not occur in this intracellular compartment. Indirect immunofluorescence of the Golgi apparatus, using anti-GM130 in conjunction with an alexa-647- conjugated anti- mouse secondary antibody did not cause labelling of the regions in which ZERO-HcRed was localised, whilst structures resembling the Golgi apparatus were stained in a highly selective manner (fig. 3-16).

Figure 3-15
Expression of ZERO-HcRed in HEK293 cells stably expressing STREX-HA

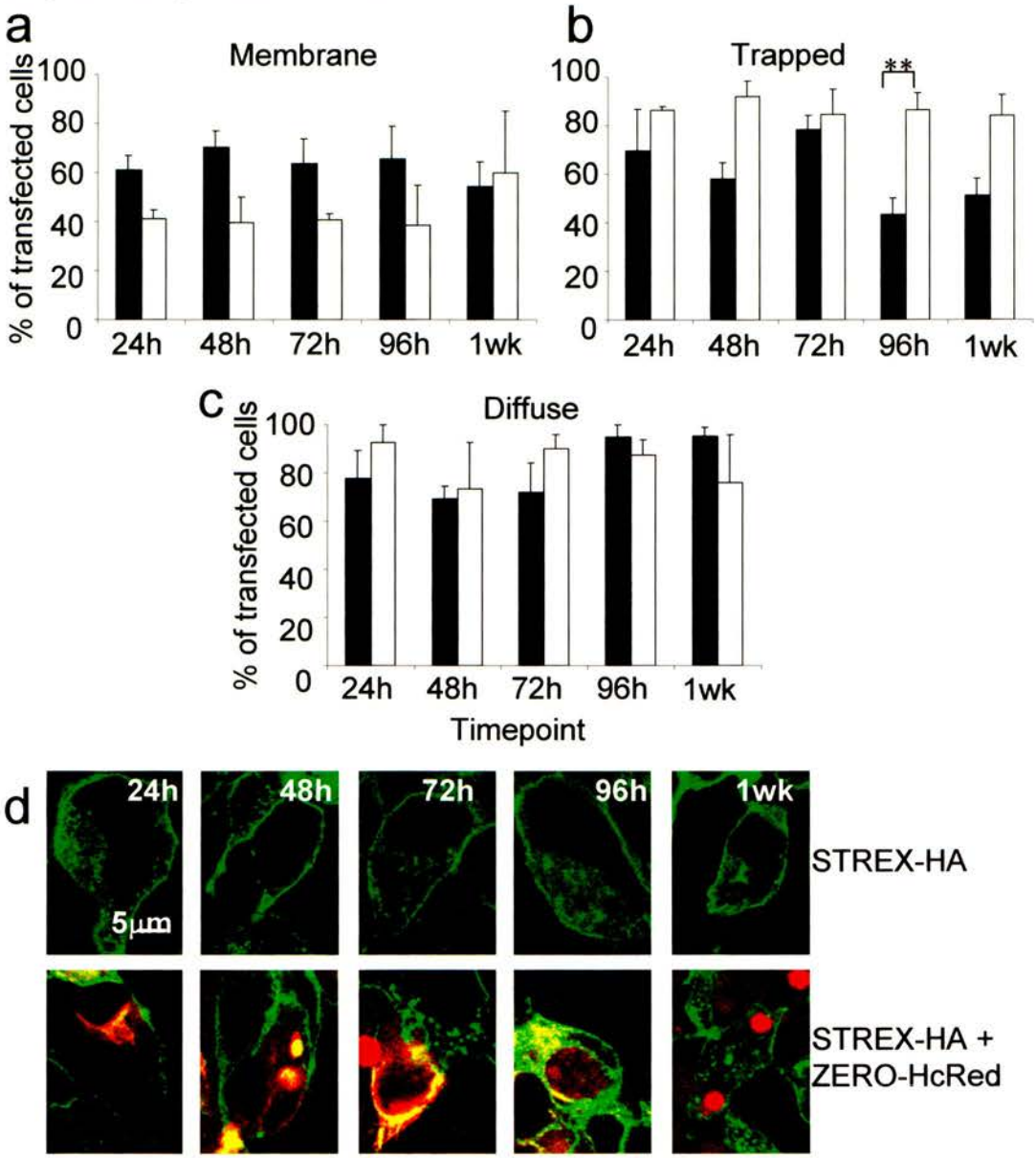

Figure 3-15 Expression of ZERO-HcRed in HEK293 cells stably expressing STREX-HA

Data shown for HEK293 cells stably transfected with STREX-HA (closed bars, N=3, n= 125 (24h), 118 (48h), 107 (72h), 130 (96h), and 111 (1wk)) and stably transfected with STREX-HA, expressing transiently transfected ZERO-HcRed (open bars, N=3, n= 37 (24h), 67 (48h), 91 (72h), 73 (96h) and 58 (1wk)). Showing **a)** membrane expression, **b)** trapped expression and **c)** diffuse expression. **d)** Representative images for HEK293 cells stably expressing STREX-HA (top row) and expressing STREX-HA with ZERO-HcRed (bottom row) at each timepoint are shown. In cotransfected cells, colocalisation of fluorescence is shown in yellow. (** = $p<0.01$ ANOVA with post- hoc test Student- Newman- Keuls).

Figure 3-16
Indirect immunofluorescence against lysosome, golgi apparatus and early endosome in HEK293 cells expressing ZERO-HcRed

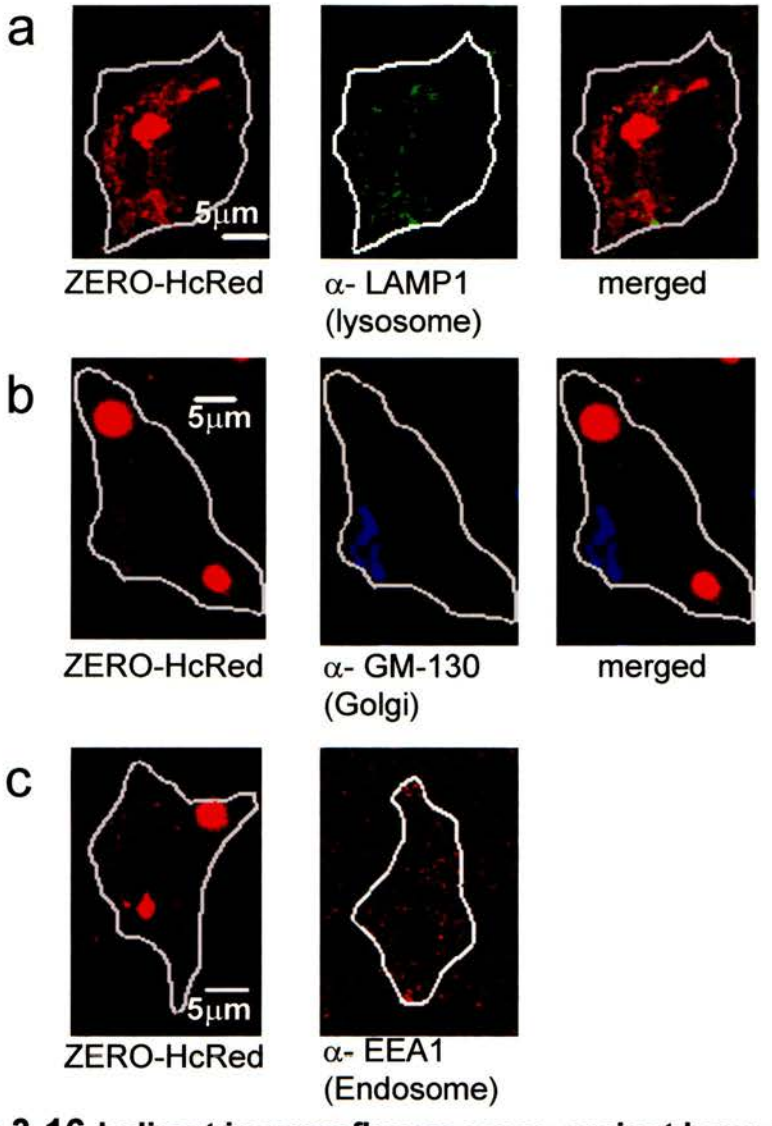

Figure 3-16 Indirect immunofluorescence against lysosome, golgi apparatus and early endosome in HEK293 cells expressing ZERO-HcRed

HEK293 cells expressing ZERO-HcRed and stained using **a)** mouse monclonal anti-LAMP1 (Using Alexa-488- conjugated secondary antibody) or **b**) mouse monoclonal anti-GM130 (using Alexa-647- conjugated secondary antibody) HcRed and Alexa dye fluorescence are shown separately for each cell (first and second panels respectively) then merged (third panel). **c)** Comparison of ZERO-HcRed expression against staining with goat anti- EEA1 (using Alexa-568-conjugated secondary antibody) in an untransfected cell. Outlines of cells are shown in grey.

3-2-1-9 Coexpression of ZERO-HcRed with an -EGFP labelled non- BK channel membrane protein in HEK293 cells

To confirm that ZERO-HcRed causes intracellular retention and trapping, specifically by multimerisation with the alternatively spliced EGFP and -HA labelled BK channel α-subunits, HEK293 cells were transfected singly with the membrane protein syntaxin-1A, which was labelled with EGFP. 96h after transfection, fluorescent labelling at the plasma membrane was observed in 41.6 ± 6.4% (N= 5, n= 199) of transfected cells. Trapped intracellular puncta were observed in 47.3 ± 8.7%, and diffuse cytoplasmic expression was observed in 42.8 ± 14.9% of transfected cells.

As a control in order to preclude the possibility that the HcRed protein would interfere with normal membrane expression of the syntaxin-1A-EGFP fusion protein, HEK293 cells were cotransfected with syntaxin-1A-EGFP and pHcRed. Fluorescent labelling at the plasma membrane was observed in 65.8 ± 12.4% (N= 5, n= 94) of transfected cells, intracellular punctate trapping was seen in 48.2 ± 18.0%, and diffuse cytoplasmic expression observed in 70.4 ± 17.1% of transfected cells. No significant differences were observed in membrane, trapped or diffuse fluorescence in cells expressing either syntaxin-1A-EGFP alone, or coexpressed with HcRed, suggesting that the latter does not interfere with the expression of this -EGFP labelled membrane protein.

When syntaxin-1A-EGFP was coexpressed in HEK293 cells with ZERO-HcRed, membrane expression was not significantly altered compared to syntaxin-1A-EGFP;

fluorescent labelling of the plasma membrane was observed in 27.4 ± 10.0% (N= 5, n= 129) of transfected cells. However, this was significantly lower than membrane expression of syntaxin-1A-EGFP coexpressed with HcRed ($p< 0.05$). Trapped punctate expression was observed in 88.2 ± 5.4% of transfected cells, significantly higher than for either syntaxin-1A-EGFP alone or syntaxin-1A-EGFP coexpressed with HcRed. Diffuse cytoplasmic expression, seen in 68.1 ± 13.0% of transfected cells, was not significantly different to that observed in cells expressing syntaxin-1A-EGFP alone, or coexpressed with HcRed (fig. 3-17).

Although the trapped expression in cells coexpressing syntaxin-1A-EGFP with ZERO-HcRed was significantly higher than for syntaxin-1A-EGFP alone, EGFP and HcRed fluorescence was frequently not colocalised in puncta, unlike those seen in cells coexpressing STREX-EGFP with ZERO-HcRed. Additionally, the membrane expression of cells coexpressing syntaxin-1A-EGFP with ZERO-HcRed did not fall significantly compared to syntaxin-1A-EGFP alone, and again this was dissimilar to the pattern observed for cells coexpressing STREX-EGFP with ZERO-HcRed. It therefore appears that whilst -EGFP labelled BK channel α-subunit fusion proteins, when coexpressed with ZERO or STREX-HcRed, are not trafficked correctly to the membrane, and are instead predominantly retained in large intracellular puncta with the -HcRed labelled α-subunits, an -EGFP labelled non- BK channel membrane protein can still be trafficked to the cell surface when coexpressed with the latter.

Having successfully expressed the EGFP and -HA labelled BK channel α-subunit alternative splice variants in HEK293 cells, demonstrating the viability of the ZERO

Figure 3-17
Coexpression of Syntaxin-1A-EGFP with pHcRed or ZERO-HcRed in HEK293 cells

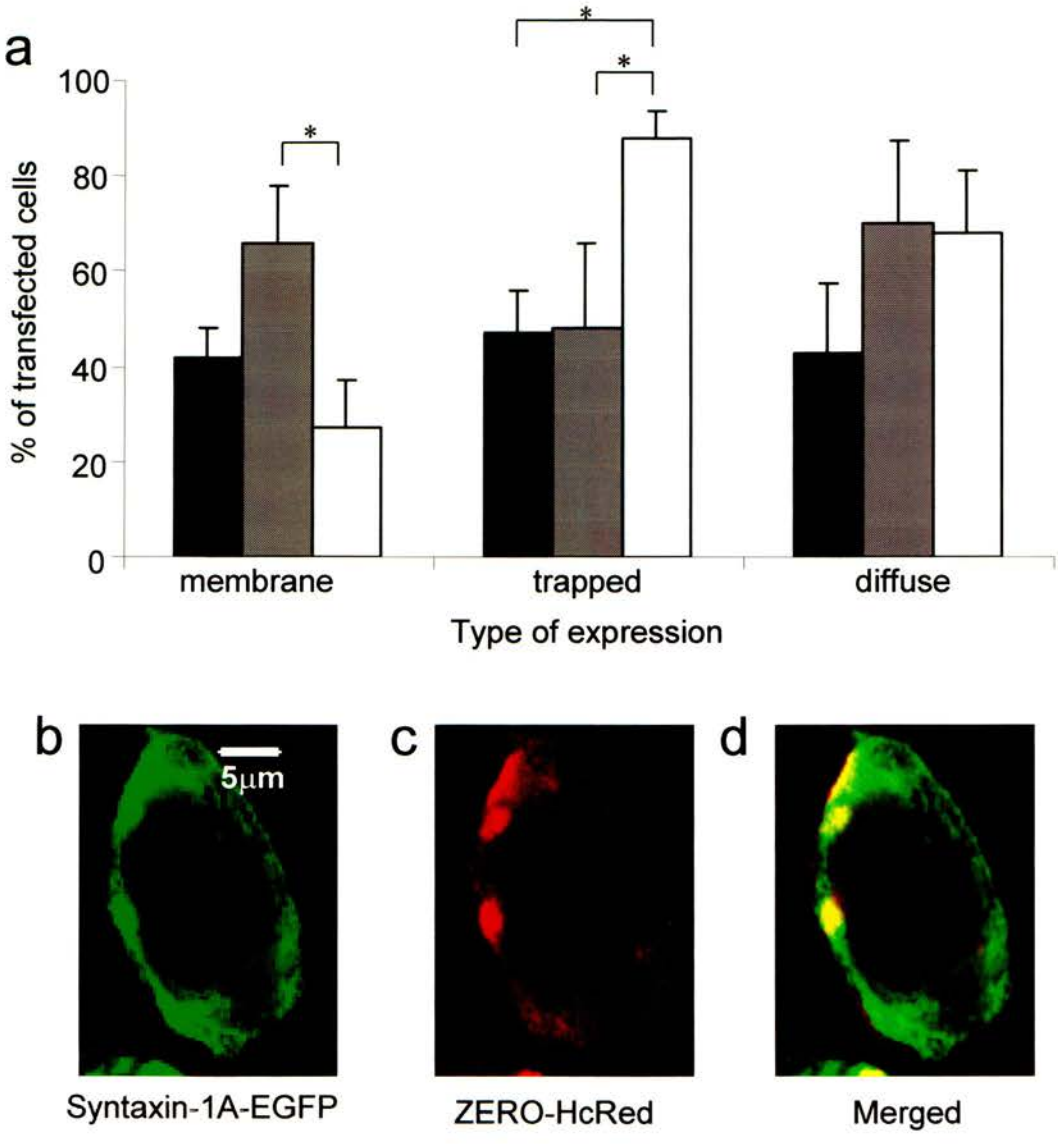

Figure 3-17 Coexpression of Syntaxin-1A-EGFP with pHcRed or Zero-HcRed in HEK293 cells

a) Data shown as a mean percentage of total transfected cells per field of view for each of the three types of expression in HEK293 cells expressing syntaxin-EGFP (closed bars, N= 5, n= 199), coexpressed with pHcRed (crossed bars, N= 5, n= 94) or coexpressed with ZERO-HcRed (open bars, N= 5, n= 129). **b)** shows syntaxin-1A-EGFP only in a HEK293 cell coexpressing syntaxin-1A-EGFP with ZERO-HcRed. **c)** shows ZERO-HcRed only in the same cell. **d)** shows the merged image. Colocalisation of EGFP and HcRed fluorescence is shown in yellow. (* = $p<0.05$ ANOVA with post- hoc test Student- Newman- Keuls).

and STREX-EGFP fusion proteins in visualising BK channel expression, and observed the novel, dominant- negative effect on membrane trafficking observed for ZERO and STREX-HcRed, these experiments were repeated in PC12 cells, where endogenous BK channel expression is also present, in order to investigate the possibility that the mechanisms for trafficking the native channels might affect the expression of the -EGFP fused BK channel alternative splice variants, and whether the dominant- negative effect of ZERO-HcRed and STREX-HcRed could be reversed or reduced.

3-2-2 Expression in PC12 cells

3-2-2-1 Expression of EGFP and HcRed labelled BK channel constructs in PC12 cells

The BK channel alternative splice variants fused at the C- terminus with the different fluorescent proteins, were expressed in PC12 cells to investigate whether or not the membrane trafficking of the EGFP labelled BK channel constructs would be altered when expressed on a background of the native population of channels in PC12 cells, and also whether the endogenous mechanisms for BK channel trafficking might provide a 'rescue' function for the -HcRed labelled ZERO and STREX channel α-subunits, restoring plasma membrane expression.

PC12 cells were cultured as described in the methods section, and plated onto coverslips 24 h before transfection with 1μg cDNA per well. Although the transfection efficiencies were consistently < 5%, the general patterns of expression within transfected cells for each construct were similar to those observed in HEK293

cells. Plasma membrane expression was observed in 58.3 ± 16.9% (N= 6, n= 30) of PC12 cells expressing ZERO-EGFP. The randomly distributed punctate trapped expression was seen in 3.3 ± 3.3% of these cells, and was significantly lower ($p< 0.05$) than in HEK293 cells transfected using ZERO-EGFP. Diffuse expression throughout the cytoplasm was seen in 100% of cells, and the fluorescent protein was excluded from the nucleus (fig. 3-18).

In PC12 cells transfected using the STREX-EGFP construct, a similar pattern of expression was observed to that in HEK293 cells; 63.3 ± 12.6% (N= 5, n= 28) of transfected cells displayed plasma membrane expression, whilst in 34.7 ± 17.2%, intracellular trapping of STREX-EGFP was seen in a random distribution. Again, diffuse cytoplasmic expression was observed, in 89.3 ± 6.9% of transfected cells and was excluded from the nucleus (fig. 3-18). As in HEK293 cells, no significant difference in the expression or distribution of these two alternatively spliced BK channel α-subunits was observed.

The extreme deviation away from the pattern of fluorescence predicted using the –EGFP labelled channel α-subunits, as observed in HEK293 cells expressing the ZERO-HcRed construct, was recapitulated in PC12 cells transfected with ZERO-HcRed under parallel conditions. In this case, plasma membrane expression was abolished (N= 5, n= 22) compared to ZERO-EGFP ($p< 0.05$), whilst large randomly distributed puncta of fluorescent expression were seen in a significantly higher number of cells- 79.3 ± 12.2% as opposed to 3.3 ± 3.3% for ZERO-EGFP ($p< 0.01$).

Figure 3-18
Expression of ZERO-EGFP or STREX-EGFP BK channel constructs in PC12 cells

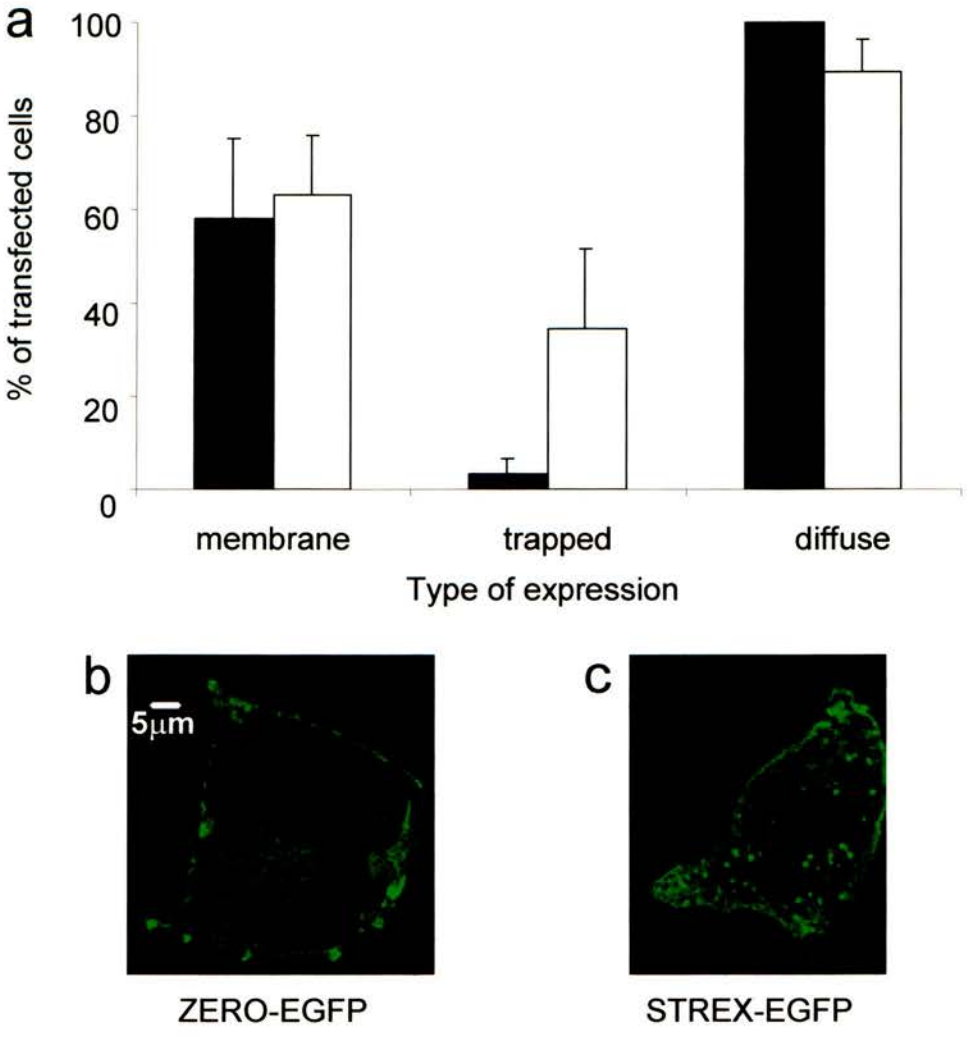

Figure 3-18 Expression of ZERO-EGFP or STREX-EGFP BK channel constructs in PC12 cells

a) Data shown as a mean percentage of total transfected cells per field of view (± SEM), for each of the three types of fluorescent expression in PC12 cells singly transfected with ZERO-EGFP (closed bars, N= 6, n= 30) or STREX-EGFP (open bars, N= 5, n= 28). Representative images are shown of PC12 cells expressing **b)** ZERO-EGFP and **c)** STREX-EGFP, taken 96 h after transfection.

Diffuse cytoplasmic expression was present in 48.8 ± 17.6% of cells, significantly less than for ZERO-EGFP ($p< 0.05$) (fig. 3-19).

In order to test whether the disruption of membrane expression of the –HcRed labelled channels was a property of the HcRed fluorescent protein itself, PC12 cells were transfected using the pHcRed-N1 plasmid. No membrane fluorescence was observed in the transfected cells (N= 5, n= 33), and trapped fluorescence was also absent. The latter was significantly lower than for PC12 cells expressing ZERO-HcRed alone ($p< 0.01$). Bright diffuse cytoplasmic expression was present in 100% of cells, significantly higher than for ZERO-HcRed alone ($p< 0.05$), further reinforcing the observations made for similarly transfected HEK293 cells- that the extreme trapping is a function of the ZERO-HcRed α-subunit itself, rather than a property of the HcRed protein alone (fig. 3-19).

3-2-2-2 Homomeric assembly of fluorescently- labelled BK channel α-subunits in PC12 cells

PC12 cells were cotransfected with ZERO-EGFP and ZERO-HcRed. Plasma membrane expression of the ZERO-EGFP BK channel α-subunits was abolished (N= 3, n= 11); a significant reduction in comparison to cells transfected with ZERO-EGFP alone ($p< 0.05$). The trapping of channels in large, bright intracellular puncta was observed in 100% of transfected cells, significantly ($p< 0.01$) higher than for ZERO-EGFP alone, where intracellular trapping of fluorescent protein was seen in only 3.3 ± 3.3% of cells. Diffuse cytoplasmic expression was also seen, in 54.8 ±

Figure 3-19
Expression of ZERO-HcRed BK channel construct and pHcRed in PC12 cells

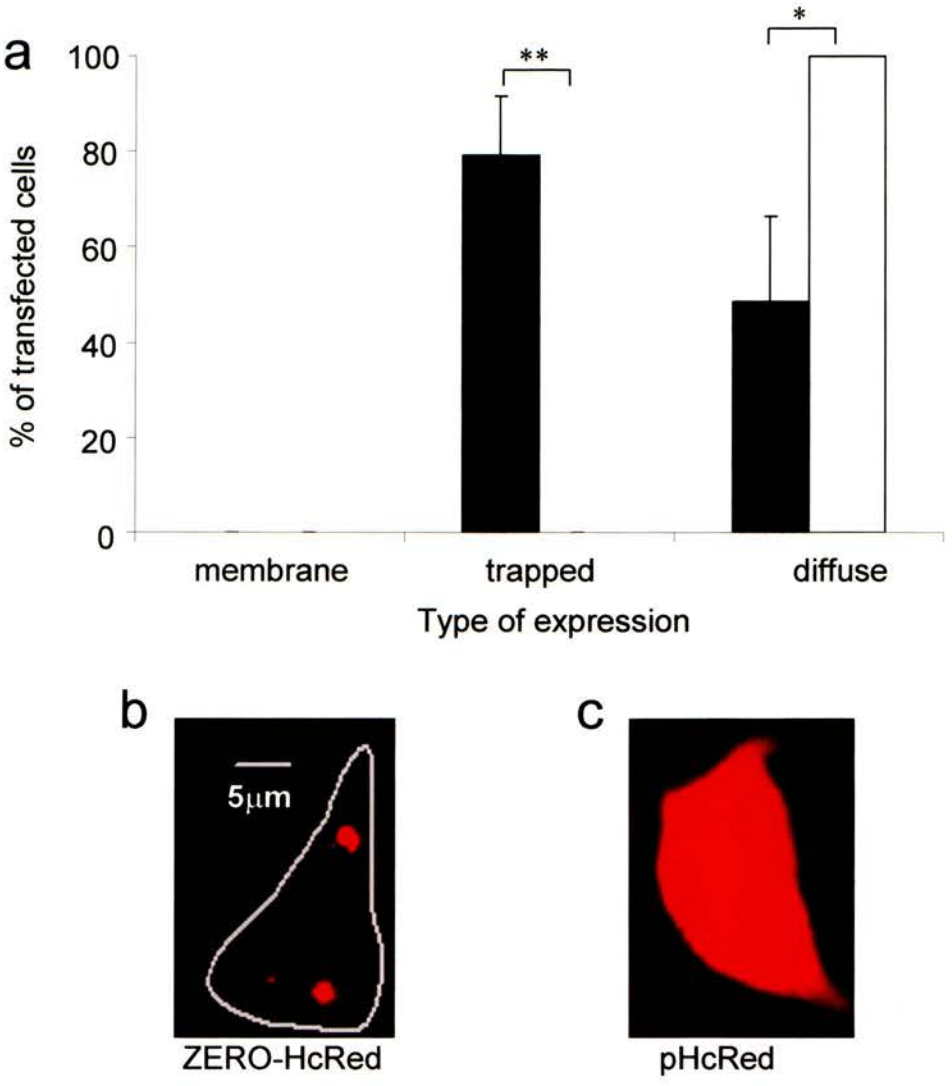

Figure 3-19 Expression of ZERO-HcRed BK channel construct and pHcRed in PC12 cells

a) Data shown as a mean percentage of total transfected cells per field of view (± SEM), for each of the three types of fluorescent expression in PC12 cells singly transfected using ZERO-HcRed (closed bars, N= 5, n= 22) and pHcRed (open bars, N= 5, n= 33). Representative images are also shown for PC12 cells expressing **b)** ZERO-HcRed and **c)** pHcRed, taken 96 h after transfection.

24.9% of cotransfected cells, although this was not significantly different to that observed in PC12 cells singly transfected with ZERO-EGFP (100%) (fig. 3-20)

Results of cotransfection in HEK293 cells previously showed that the HcRed protein itself was not responsible for the dominant- negative effect on cell surface expression and increased intracellular trapping exerted by the ZERO-HcRed and STREX-HcRed BK channel α-subunit fusion proteins on the -EGFP fused alternative splice variants. To investigate whether this was also the case when expressed in a cell line which produces endogenous BK channels, ZERO-EGFP was cotransfected with pHcRed into PC12 cells. EGFP expression at the plasma membrane was observed in 71.4 ± 12.8% (N= 4, n= 26) of transfected cells, and was not significantly different to that seen in cells singly transfected with ZERO-EGFP. Trapped expression was observed in 30.8 ± 10.8% of transfected cells, and diffuse expression was seen in 100% of transfected cells. Neither of these were significantly different to expression of singly-transfected ZERO-EGFP (fig. 3-20).

The plasma membrane EGFP expression in PC12 cells cotransfected with STREX-EGFP and pHcRed was significantly lower ($p < 0.05$) than that for STREX-EGFP alone- 29.7 ± 7.8% (N=6, n=26) as opposed to 63.3 ± 12.6%. However, STREX-EGFP cotransfected with pHcRed did not appear to mimic the trapping observed in the STREX-EGFP/ ZERO-HcRed cotransfections, since the reduction in membrane expression was not accompanied by a significant increase in observed large trapped puncta. In fact, in the cotransfected PC12 cells, the level of large bright puncta observed was lower, although it was not significantly different- 8.6 ± 4.3%, as

Figure 3-20
Coexpression of ZERO-EGFP with pHcRed or ZERO-HcRed in PC12 cells

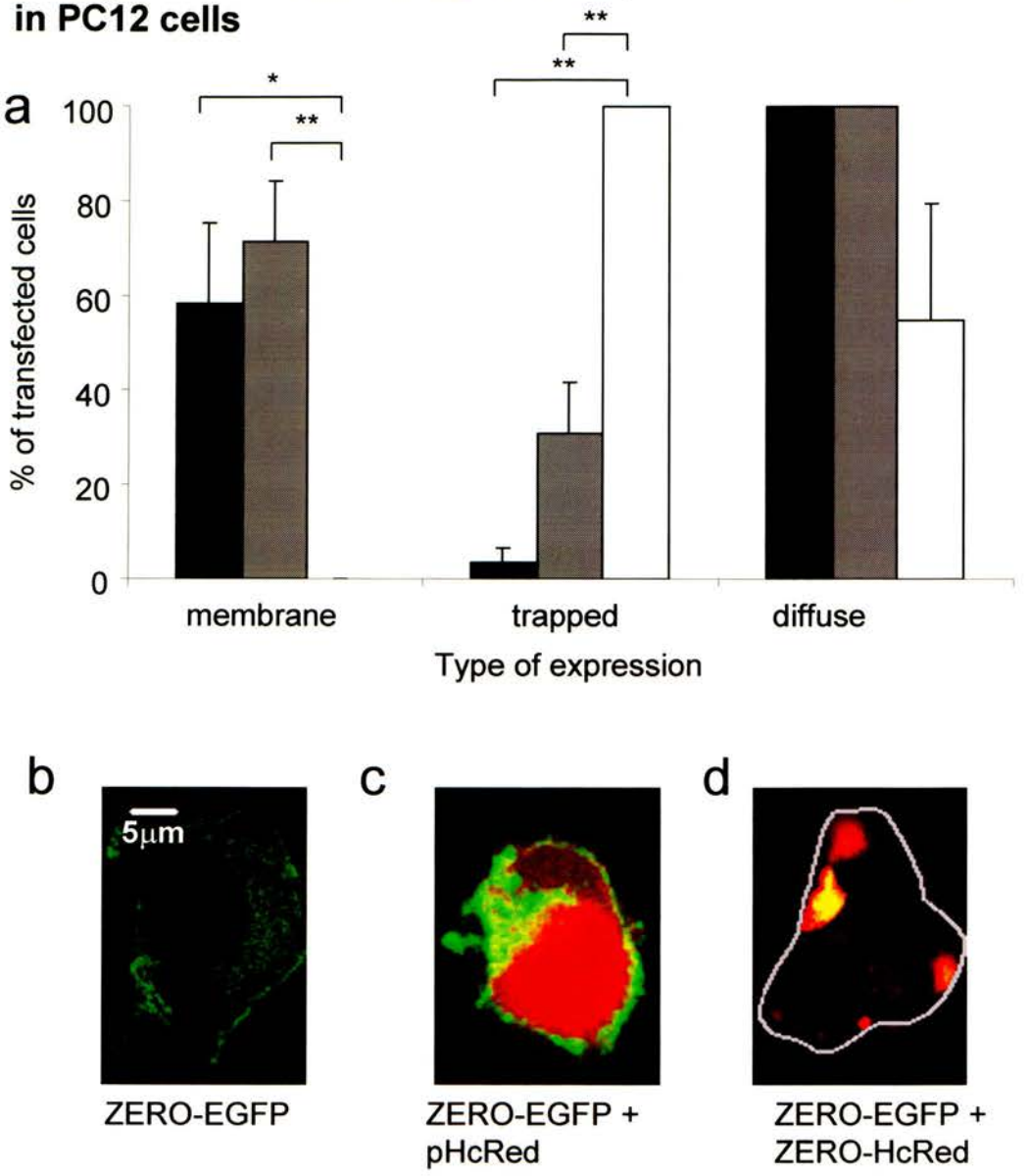

Figure 3-20 Coexpression of ZERO-EGFP with pHcRed or ZERO-HcRed in PC12 cells

a) Data shown as a mean percentage of total transfected cells per field of view (±SEM) for each of the three types of fluorescent expression in PC12 cells transfected with ZERO-EGFP alone (closed bars, N= 6, n= 30), ZERO-EGFP cotransfected with pHcRed (crossed bars, N= 4, n= 26) or ZERO-EGFP cotransfected with ZERO-HcRed (open bars, N= 3, n=11). Representative images are shown for **b)** ZERO-EGFP cotransfected with **c)** pHcRed, or **d)** ZERO-HcRed (outline of cell shown in grey), taken 96h after transfection. In cotransfected cells, colocalisation of EGFP and HcRed fluorescence is shown in yellow. (* = $p < 0.05$, ** = $p < 0.01$ ANOVA with post- hoc test Student-Newman- Keuls).

opposed to 34.7 ± 17.2% for STREX-EGFP alone- a similar effect to that seen in cotransfected HEK293 cells under the same conditions. When coexpressed with pHcRed in HEK293 cells, STREX EGFP underwent significantly less trapping than when expressed alone. One possible explanation for this is that the net amount of STREX-EGFP being produced is lower than when singly expressed, therefore increased efficiency of trafficking to the membrane may occur, as opposed to STREX-EGFP alone, where a high level of expression may cause trapping of the channel resulting in inhibition of surface expression. Diffuse cytoplasmic expression was observed in 94.2 ± 4.2% of transfected cells, as opposed to 89.3 ± 6.9% for STREX-EGFP alone (fig. 3-21).

3-2-2-3 Heteromeric assembly of fluorescently- labelled BK channel α-subunits in PC12 cells

The novel dominant- negative effect of the ZERO-HcRed α-subunit on the plasma membrane expression of an alternatively spliced BK channel α-subunit that was observed in HEK293 cells, also occurred in PC12 cells. Plasma membrane expression fell significantly ($p < 0.05$) to 5.0 ± 5.0% ($N = 4$, $n = 13$) in PC12 cells cotransfected with ZERO-HcRed and STREX-EGFP, compared to 63.3 ± 12.6% for STREX-EGFP alone. Trapped expression in the cotransfected cells rose significantly to 100% as opposed to 34.7 ± 17.2% for singly- transfected STREX-EGFP ($p < 0.01$). In this case, both HcRed and EGFP fluorescence were present in these puncta, reinforcing the notion that formation of heterodimers or heterotetramers occurs, and that their trafficking to the plasma membrane is disrupted by the presence of a

Figure 3-21
Coexpression of STREX-EGFP with pHcRed or ZERO-HcRed in PC12 cells

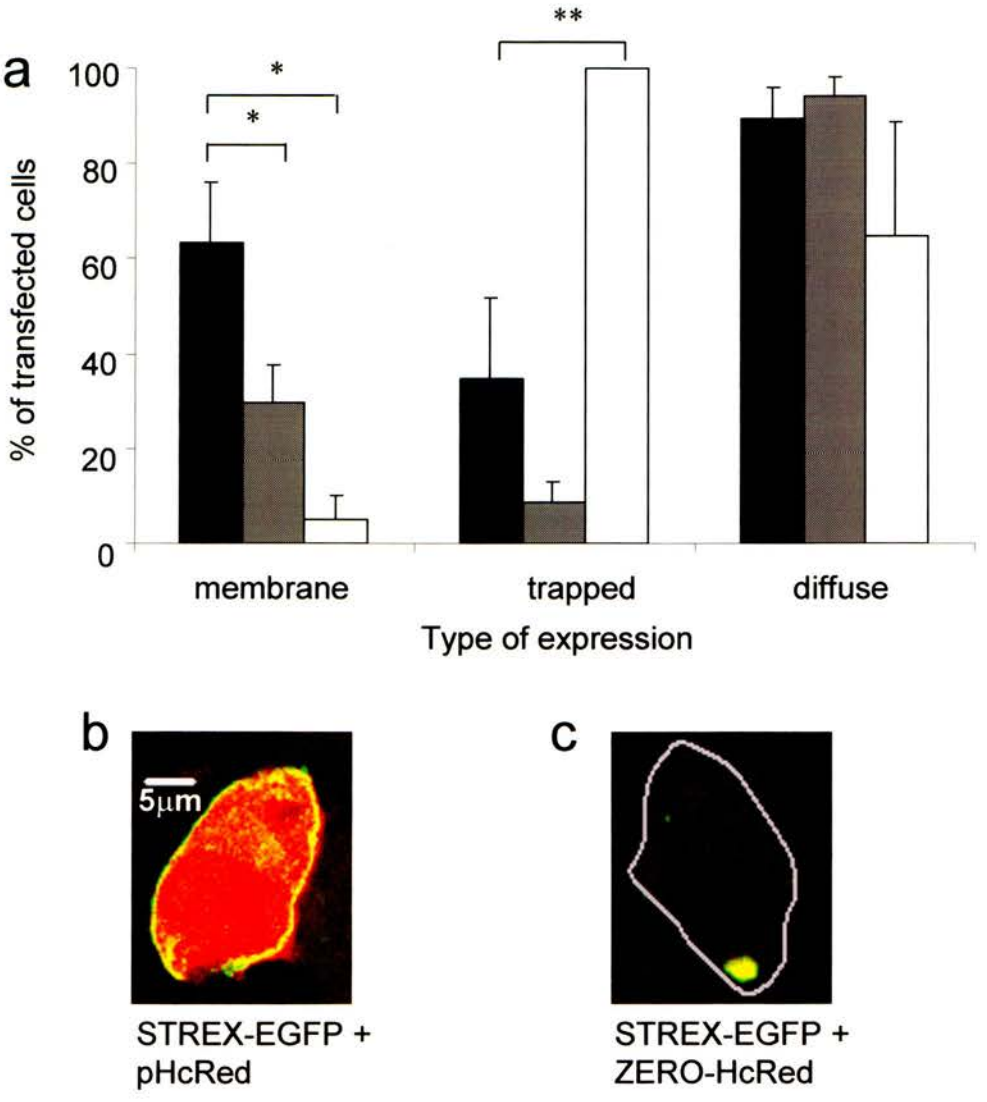

Figure 3-21 Coexpression of STREX-EGFP with pHcRed or ZERO-HcRed in PC12 cells

a) Data shown as a mean percentage of total transfected cells per field of view (±SEM) for each of the three types of fluorescent expression in PC12 cells transfected with STREX-EGFP alone (closed bars, N= 5, n= 28) or STREX-EGFP cotransfected with pHcRed (crossed bars, N= 6, n= 26) or with ZERO-HcRed (open bars, N= 4, n=13). Representative images are shown for STREX-EGFP cotransfected with **b)** pHcRed or with **c)** ZERO-HcRed (outline of cell shown in grey), taken 96h after transfection. In cotransfected cells, colocalisation of EGFP and HcRed fluorescence is shown in yellow. (* = $p<0.05$, ** = $p<0.01$ ANOVA with post- hoc test Student- Newman- Keuls).

ZERO-HcRed α-subunit. Diffuse cytoplasmic expression was present in 65.0 ± 23.6% of the cotransfected cells (fig. 3-21).

These data generally follow the pattern of observations made in HEK293 cells, suggesting that alternatively spliced BK channel variants may form heteromultimers in PC12 cells, and that the presence of the -HcRed labelled ZERO α-subunit exerts a dominant- negative effect on the plasma membrane expression of channels. It is also likely that this suppression of membrane expression is not affected by the regulatory mechanisms that govern membrane trafficking of the endogenous channels in PC12 cells.

3-2-2-4 Expression of ZERO-HcRed with syntaxin-1A-EGFP in PC12 cells

Previous results in HEK293 cells indicated that membrane expression of syntaxin-1A-EGFP was not disrupted by ZERO-HcRed, or the HcRed protein, suggesting that trapping of -EGFP and -HA labelled ZERO and STREX fusion proteins by ZERO-HcRed and STREX-HcRed was likely to be dependent on multimerisation of the BK channel α-subunits. To investigate whether ZERO-HcRed caused specific trapping of other BK channel α-subunits in a cell line with endogenous BK channel expression, syntaxin-1A-EGFP was expressed singly, and coexpressed with HcRed or ZERO-HcRed in PC12 cells. Membrane expression was observed in 28.3 ± 12.8% (N= 5, n= 50) of cells expressing syntaxin-1A-EGFP alone. When syntaxin-1A-EGFP was coexpressed with HcRed or ZERO-HcRed, membrane expression was observed in 40.0 ± 24.5% (N=5, n=9) and 46.7 ± 22.6% (N=5, n=12) of transfected cells

respectively. In both cases, membrane expression was not significantly different to that of syntaxin-1A-EGFP alone. However, the level of trapped expression in PC12 cells expressing syntaxin-1A-EGFP alone, and also coexpressing syntaxin-1A-EGFP with HcRed (27.5 ± 3.7% and 5.0 ± 5.0% respectively) was significantly lower ($p < 0.05$ and $p < 0.01$ respectively) than in cells coexpressing syntaxin-1A-EGFP with ZERO-HcRed, where punctate trapping was observed in 63.3 ± 15.3% of transfected cells. No significant difference was observed in the diffuse cytoplasmic expression in PC12 cells expressing syntaxin-1A-EGFP alone (89.1 ± 5.4% of transfected cells) with that of cells coexpressing syntaxin-1A-EGFP with HcRed or ZERO-HcRed (100 ± 0% and 80.0 ± 12.3% of transfected cells, respectively) (fig. 3-22).

Although the trapping of fluorescent proteins in intracellular puncta increased in PC12 cells when syntaxin-1A-EGFP was coexpressed with ZERO-HcRed compared with syntaxin-1A-EGFP alone, or coexpressed with the HcRed fluorescent protein, it is likely that no interaction occurs between the syntaxin-1A-EGFP and ZERO-HcRed fusion proteins, since a concomitant reduction in plasma membrane expression of syntaxin-1A-EGFP would also be predicted, however no significant difference was observed in this case.

Having observed the behaviour of the fluorescent BK channel fusion proteins in both the presence and absence of native BK channel α-subunits, the fluorescent BK channel constructs were used to study the effect of expression in a model cell system where discrete localisation of the endogenous BK population can occur. In this situation, certain alternative splice variants might be expressed more strongly in a

Figure 3-22
Coexpression of Syntaxin-1A-EGFP with pHcRed or ZERO-HcRed in PC12 cells

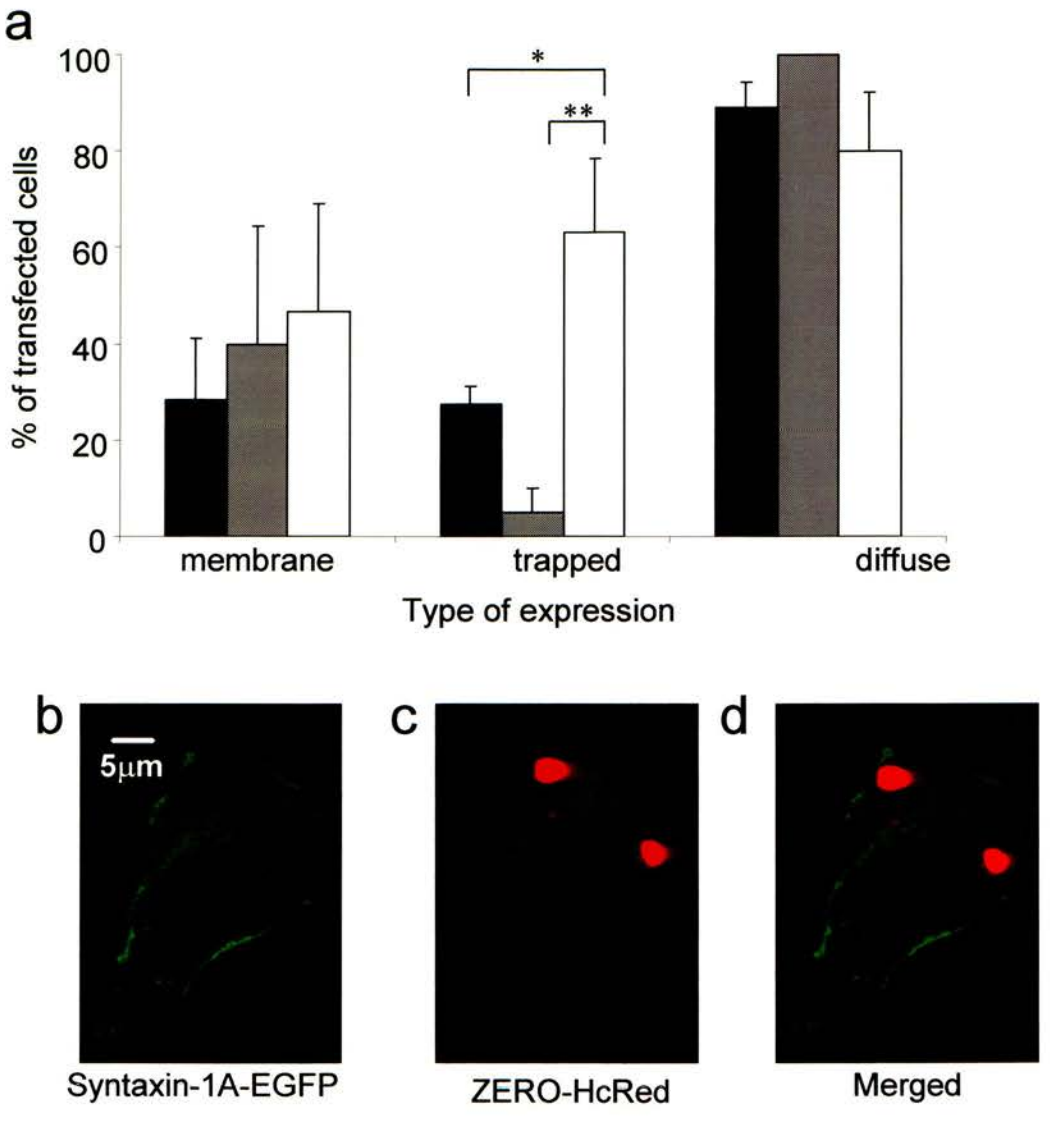

Figure 3-22 Coexpression of Syntaxin-1A-EGFP with pHcRed or Zero-HcRed in PC12 cells

Data shown as a mean percentage of total transfected cells per field of view for each of the three types of expression in PC12 cells expressing sytnaxin-1A-EGFP alone (closed bars, N= 5, n= 50), coexpressed with pHcRed (crossed bars, N= 5, n=9) or coexpressed with ZERO-HcRed (open bars, N= 5, n= 12). **b)** shows syntaxin-1A-EGFP only in a PC12 cell coexpressing syntaxin-1A-EGFP with ZERO-HcRed. **c)** shows ZERO-HcRed only, in the same cell. **d)** shows the merged image. (* = $p< 0.05$, ** = $p< 0.01$ ANOVA with post- hoc test Student-Newman- Keuls).

localised manner than others, therefore the fluorescent BK channel constructs would be useful tools for observing any changes in the subcellular localisation of transfected channels as a result of being expressed in these circumstances. To investigate this possibility, MDCK cells were used, as polarised apical expression of both endogenous, and also transfected BK channels has been reported (Bolivar and Cereijido, 1987, Bravo- Zehnder *et al.*, 2000) in this cell line.

3-2-3 Expression in MDCK cells

3-2-3-1 Expression of -EGFP and -HcRed labelled BK channel constructs in MDCK cells

MDCK cells were cultured, and plated onto glass coverslips as described in the methods section, 24 h before transfection using Lipofectamine 2000 with 1μg of cDNA per well. As for PC12 cells, the transfection efficiency was generally < 5%. Since MDCK cells become polarised when growing in a monolayer, with localisation of ion channels to either basal or apical surfaces having been reported, it was necessary to ensure that any images for analysis taken from MDCK cells grown to ~100% confluency were representative of expression at the membrane. To this end, all images of expression of the BK channel -EGFP and -HcRed fusion proteins were taken through the centre of the cells, below the apical villi, as shown in methods figure 2-1, since the three- dimensional nature of the projections from the apical surface can cause a cross- section through this region to resemble discrete trapped puncta.

In MDCK cells transfected using the ZERO-EGFP construct, plasma membrane expression was observed in 11.9 ± 9.1% (N= 12, n= 22). Trapped punctate expression was seen in 48.8 ± 12.9% of cells, whilst diffuse cytoplasmic expression was observed in 97.6 ± 2.5% of cells. In cells transfected using STREX-EGFP, plasma membrane expression was present in 86.5 ± 7.7% of cells (N= 13, n= 23). This was significantly higher than that observed in the cells expressing ZERO-EGFP ($p< 0.01$). Randomly distributed punctate fluorescent expression was seen in 75.0 ± 9.9% of transfected cells, whilst diffuse cytoplasmic expression, with nuclear exclusion, was observed in 69.2 ± 12.4% (fig. 3-23). Although there was a significant difference in the membrane expression of ZERO-EGFP compared with STREX-EGFP, no significant difference was found for the level of trapped puncta or diffuse expression between these two alternatively spliced BK channel α-subunits (fig. 3-23).

In MDCK cells expressing ZERO-HcRed, no membrane targeting of the fluorescently- labelled α-subunit was observed (fig. 3-24) (N=8, n=26). The level of trapped fluorescence rose to 100%, significantly higher than for ZERO-EGFP ($p< 0.01$), and this was again characterised by large bright intracellular puncta as were observed in HEK293 and PC12 cells expressing ZERO-HcRed. In 62.5 ± 15.7% of MDCK cells expressing ZERO-HcRed, diffuse cytoplasmic fluorescence, with nuclear exclusion, was observed, and this was not significantly different from that seen in cells expressing ZERO-EGFP or STREX-EGFP.

Figure 3-23
Expression of STREX-EGFP or ZERO-EGFP BK channel constructs in MDCK cells

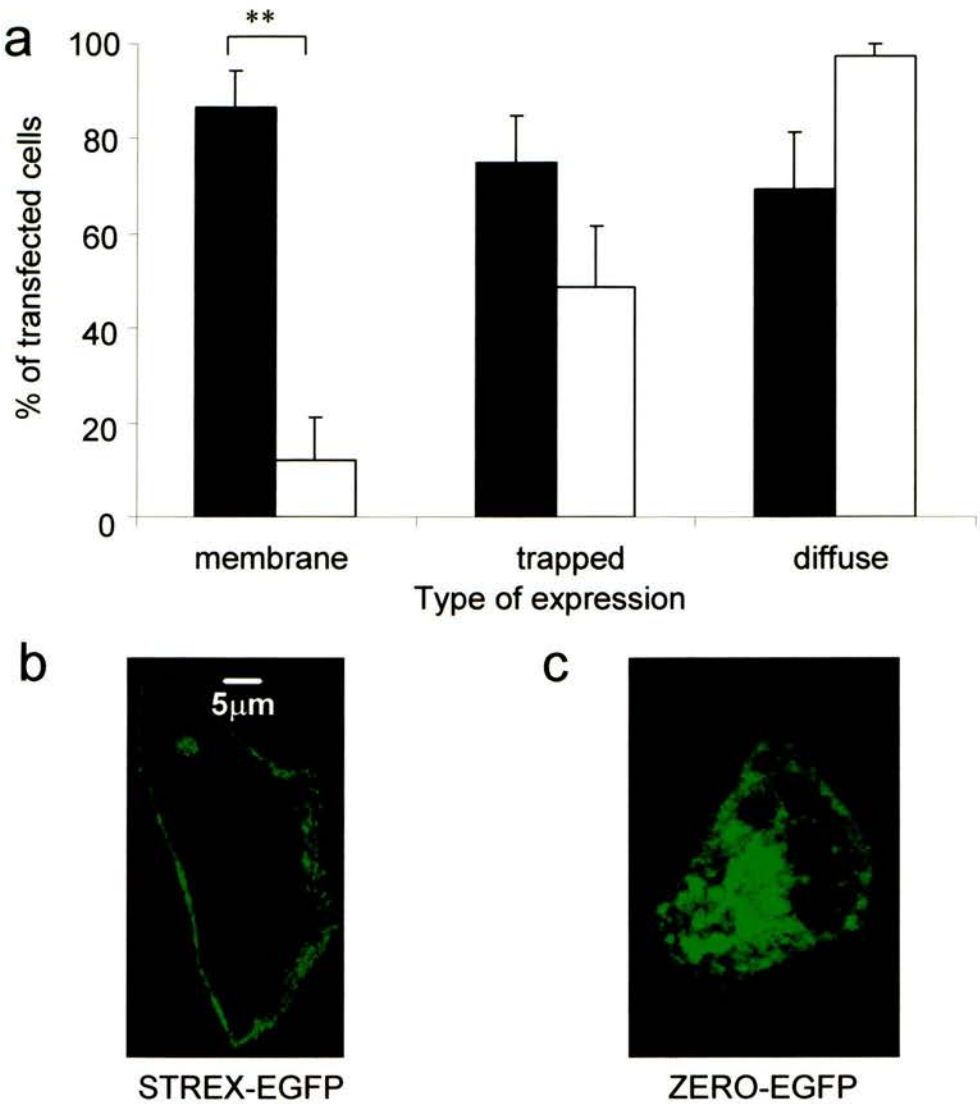

Figure 3-23 Expression of STREX-EGFP or ZERO-EGFP BK channel constructs in MDCK cells

a) Data shown as a mean percentage of total transfected cells per field of view (± SEM) for each of the three types of fluorescent expression in MDCK cells singly transfected with STREX-EGFP (closed bars, N= 13, n= 23) or ZERO-EGFP (open bars, N= 12, n= 22.) Representative images are shown of MDCK cells expressing **b)** STREX-EGFP and **c)** ZERO-EGFP, taken 96 h after transfection. (** = $p<0.01$ ANOVA with post- hoc test Student- Newman- Keuls).

Figure 3-24
Expression of ZERO-HcRed or STREX-HcRed BK channel constructs or pHcRed in MDCK cells

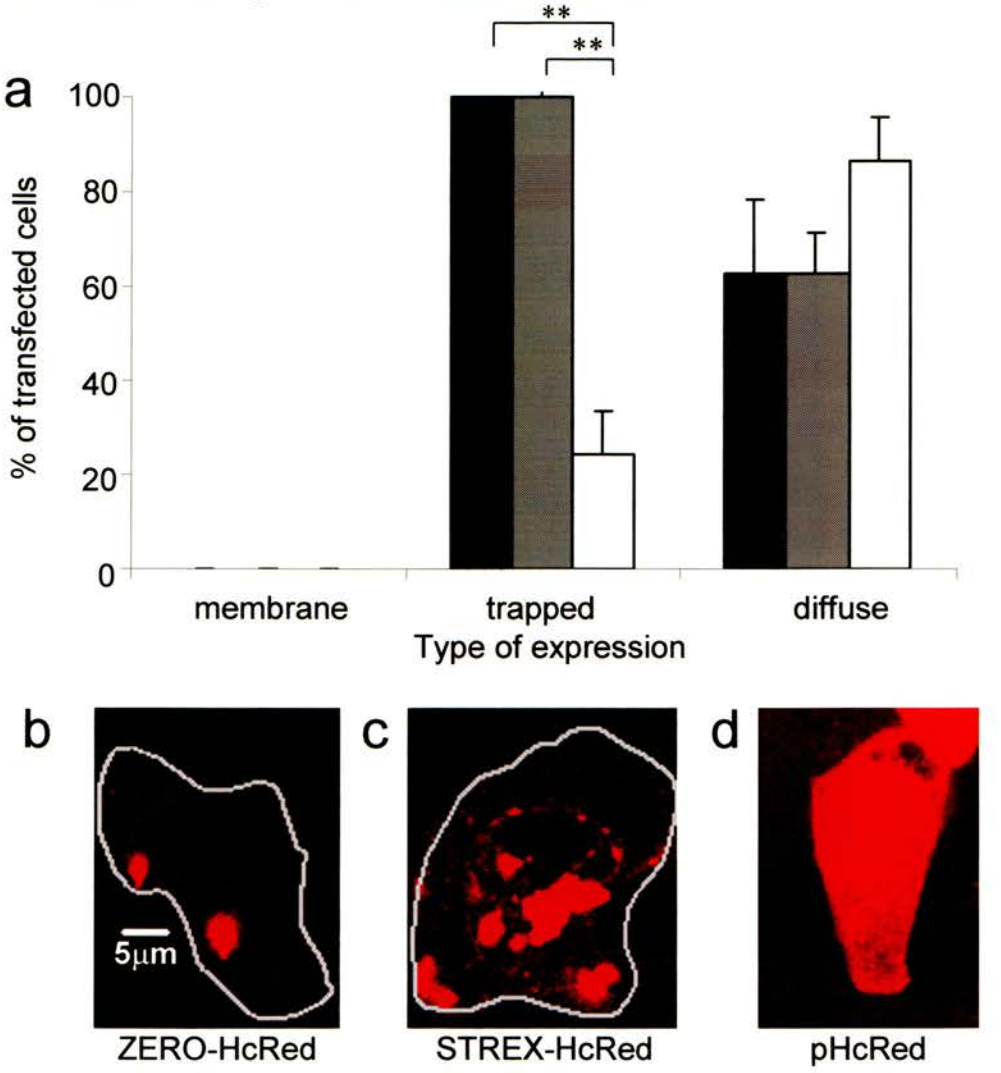

Figure 3-24 Expression of ZERO-HcRed or STREX-HcRed BK channel constructs or pHcRed in MDCK cells

a) Data shown as a mean percentage of total transfected cells per field of view (± SEM) for each of the three types of fluorescent expression in MDCK cells singly transfected using ZERO-HcRed (closed bars, N= 8, n= 26), STREX-HcRed (crossed bars, N= 8, n= 20) or pHcRed (open bars, N= 7, n= 202). Representative images are also shown for MDCK cells expressing **b)** ZERO-HcRed **c)** STREX-HcRed (outlines of cells shown in grey) and **d)** pHcRed, taken 96 h after transfection.

No membrane expression was observed in MDCK cells transfected with STREX-HcRed (fig. 3-24) (N=8, n= 20); this was significantly lower than for STREX-EGFP alone ($p< 0.01$). Trapped expression, characterised by large bright intracellular puncta was present in all cells, although this was not significantly different ($p> 0.05$) to MDCK cells expressing STREX-EGFP, where trapping was present in 75.0 ± 9.9% of transfected cells. Diffuse cytoplasmic expression, with nuclear exclusion, was observed in 62.5 ± 18.3% of cells, but again this was not significantly different when compared to STREX-EGFP.

The HcRed protein was expressed alone in MDCK cells in order to confirm findings from HEK293 and PC12 cells, where it was shown not to aggregate into large intracellular puncta, unlike ZERO-HcRed (fig. 3-24). Again, no fluorescent labelling of the plasma membrane was found, although some trapping of the fluorescent protein was observed in 24.4 ± 9.0% of cells expressing HcRed (N=8, n= 202). This was significantly lower ($p< 0.01$) than for MDCK cells expressing either ZERO-HcRed or STREX-HcRed alone. Bright, uniform fluorescence was seen in 86.4 ± 9.1% of transfected cells, again reinforcing the notion that the trapping of ZERO-HcRed BK channel α-subunits is a property unique to this particular fluorescent protein-labelled subunit, and not a result of the presence of HcRed *per se*.

3-2-3-2 Homomeric assembly of fluorescently- labelled BK channel α-subunits in MDCK cells

In order to test whether the ability of the ZERO-HcRed BK channel α-subunit to disrupt correct membrane targeting of other fluorescent protein- labelled BK channel

α-subunits could be reproduced in a polarised epithelial cell line, MDCK cells were cotransfected using ZERO-EGFP and ZERO-HcRed. Again, ZERO-HcRed appeared to act as a dominant- negative suppressor of membrane expression, as no visible fluorescence (either of EGFP or HcRed) was observed at the plasma membrane in transfected cells (N= 10, n= 14). The level of trapped fluorescence rose to 100% in the cotransfected cells, significantly higher than that observed for ZERO-EGFP alone ($p< 0.05$), and this was again characterised by large intracellular puncta of fluorescence. Diffuse cytoplasmic expression was also observed, in 40.0 ± 16.3% of cotransfected cells. This was significantly lower than for ZERO-EGFP alone ($p< 0.05$) (fig. 3-25).

STREX-EGFP was coexpressed in MDCK cells with pHcRed, in order to confirm the requirement of α-subunit multimerisation for the dominant- negative effect of the BK channel- HcRed fusion proteins, and that the HcRed protein itself is not responsible for cytoplasmic trapping of the BK channel α-subunits. EGFP fluorescent labelling of the plasma membrane was observed in 80.0 ± 20.0% of cells (N=5, n= 10). This was not significantly different to the level of membrane expression seen in MDCK cells transfected with STREX-EGFP alone. Trapped expression was present in 25 ± 11.2% of transfected cells, and this was significantly lower than the level of trapped expression seen for STREX-EGFP alone ($p< 0.01$). This follows the pattern observed in HEK293 and PC12 cells, and it may be the case that although the overall level of protein expression remains the same at this timepoint for cells cotransfected with STREX-EGFP and pHcRed as for STREX-EGFP alone, a lower amount of STREX-EGFP is synthesised, and as a result the

Figure 3-25
Coexpression of ZERO-EGFP with ZERO-HcRed in MDCK cells

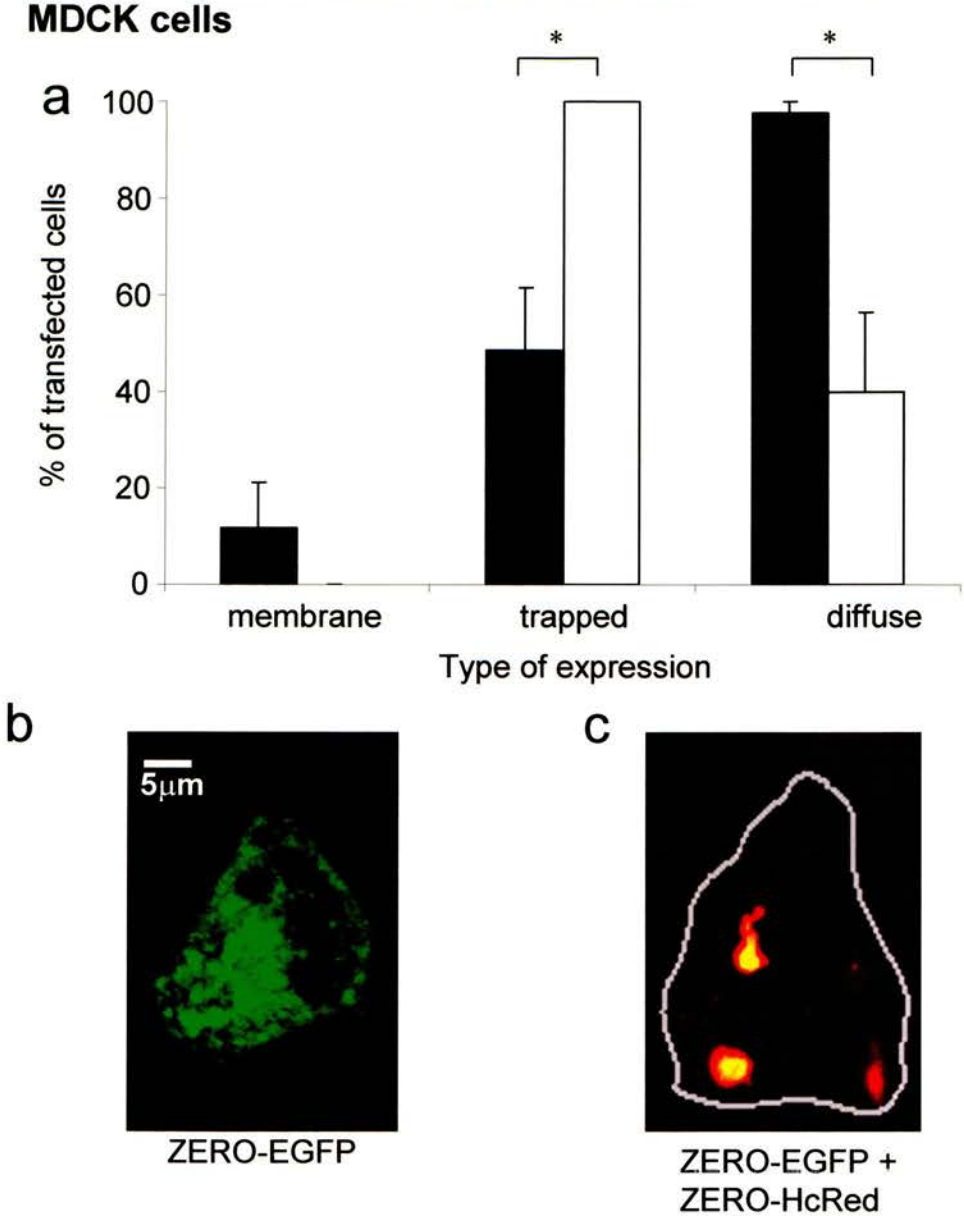

Figure 3-25 Coexpression of ZERO-EGFP with ZERO-HcRed in MDCK cells

a) Data shown as a mean percentage of total transfected cells per field of view for each of the three types of fluorescent expression in MDCK cells singly transfected with ZERO-EGFP (closed bars, N= 12, n= 22) or cotransfected using ZERO-EGFP and ZERO-HcRed (open bars, N= 10, n= 14). **b)** Representative image of MDCK cell expressing ZERO-EGFP and **c)** MDCK cell coexpressing ZERO-EGFP and ZERO-HcRed (outline of cell shown in grey), taken 96 h after transfection. In cotransfected cell, colocalisation of EGFP and HcRed fluorescence is shown in yellow. (* = $p<0.05$ ANOVA with post- hoc test Student- Newman- Keuls).

fusion protein is trafficked correctly to the membrane without saturating the expression/ trafficking machinery, which might otherwise result in trapping. Diffuse cytoplasmic expression was present in 100% of MDCK cells coexpressing STREX-EGFP and pHcRed, and this was not significantly elevated above that for STREX-EGFP expressing alone (fig. 3-26).

3-2-3-3 Heteromeric assembly of fluorescently- labelled BK channel α-subunits in MDCK cells

The ability of ZERO-HcRed to suppress membrane expression of an alternatively spliced BK channel α-subunit was observed in MDCK cells cotransfected using STREX-EGFP with ZERO-HcRed. Plasma membrane expression of STREX-EGFP was seen in 6.7 ± 5.1% (N= 10, n= 27) of the cotransfected cells, significantly less than for STREX-EGFP alone ($p< 0.01$). Trapped fluorescent expression was observed in 93.3 ± 6.7% of cotransfected cells, and again the EGFP and HcRed fluorescence colocalised into large intracellular puncta suggesting that multimerisation of the two BK channel α-subunit variants is occurring, and that when ZERO-HcRed is assembled in multimers with STREX-EGFP, its presence may cause incorrect surface trafficking. Diffuse cytoplasmic expression was also seen in 52.2 ± 16.1% of cotransfected cells, although this was not significantly different from that observed for STREX-EGFP alone (fig. 3-26).

Figure 3-26
Coexpression of STREX-EGFP with pHcRed or ZERO-HcRed in MDCK cells

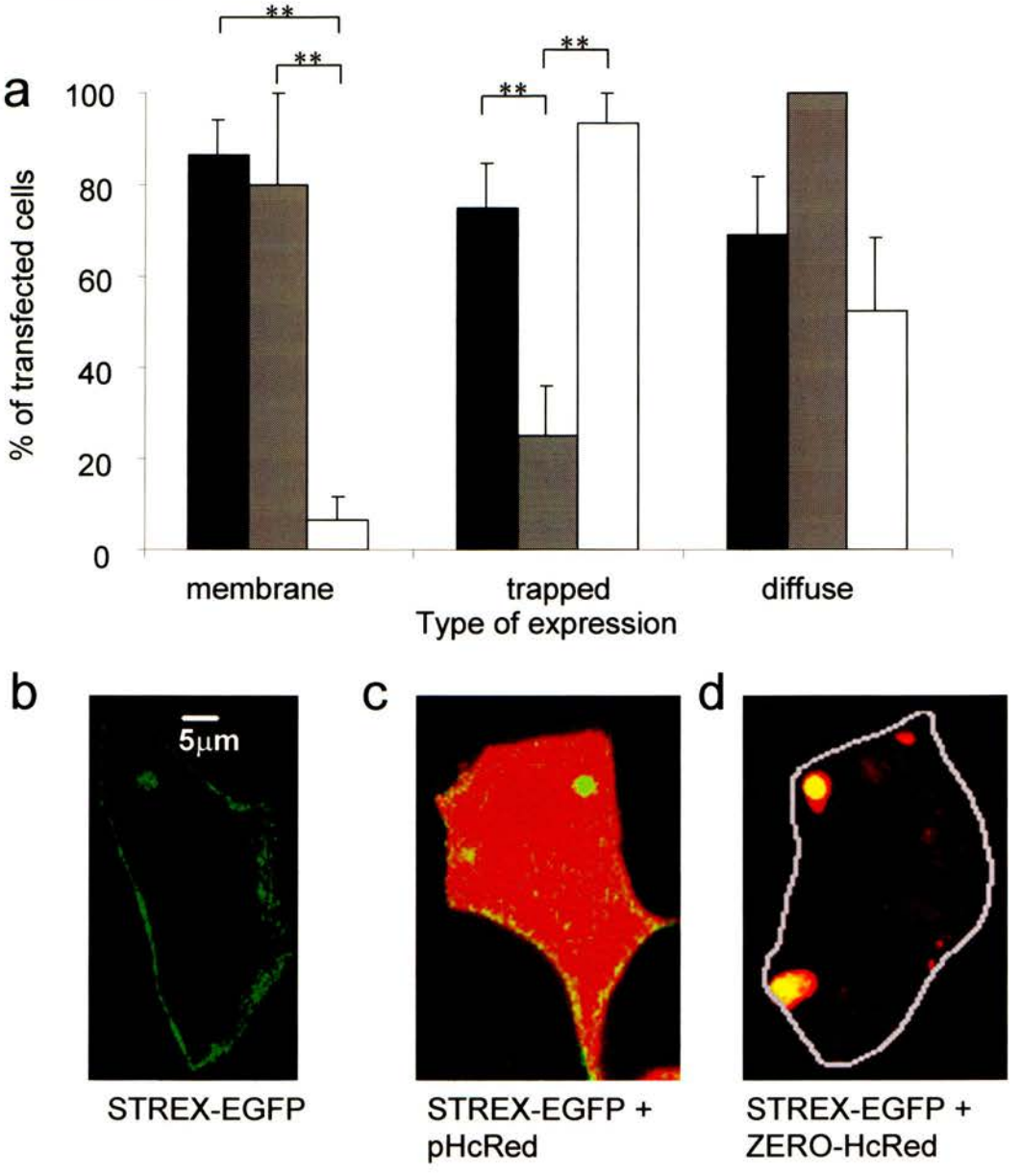

Figure 3-26 Coexpression of STREX-EGFP with pHcRed or ZERO-HcRed in MDCK cells

a) Data shown as a mean percentage of total transfected cells per field of view for the three types of fluorescent expression in MDCK cells singly transfected with STREX-EGFP alone (closed bars, N= 13, n= 23), and cotransfected with either pHcRed (crossed bars, N= 5, n=10) or ZERO-HcRed (open bars, N=10 , n=27) . Representative images are shown for **b)** STREX- EGFP cotransfected with **c)** pHcRed or **d)** ZERO-HcRed (outline of cell shown in grey), taken 96 h after transfection. In cotransfected cells, colocalisation of EGFP and HcRed fluorescence is shown in yellow. (** = $p<0.01$ ANOVA with post- hoc test Student- Newman-Keuls).

3-2-4 Expression of an -HA labelled, novel, truncated BK channel alternative splice variant in HEK293 cells

A recently discovered BK channel alternative splice variant, Δe23, is expressed as a truncated α-subunit, with the truncation occurring at exon 23, within the C- terminal tail region. Although splice inserts containing specific retention/ retrieval signals have been found to alter cell surface expression of the channel (Zarei *et al.*, 2004), this truncated variant allows investigation of the possibility that sections of the C-terminus which had not been previously shown to be involved in channel trafficking may have an effect. To this end, a cDNA construct, Δe23-HA, was generated which would cause the expression of the truncated channel fused at the C- terminus with the HA epitope, enabling the use of indirect immunfluorescence to observe any potential changes in the subcellular localisation of this novel splice variant.

In HEK293 cells transfected with Δe23-HA, labelling of the plasma membrane was observed in 4.2 ± 1.6% (N= 3, n= 96) of cells, significantly lower ($p< 0.01$) than HEK293 cells transfected, in parallel, with STREX-EGFP, where membrane labelling was seen in 73.8 ± 14.5% (N= 3, n= 25) of transfected cells. Trapping of the fusion protein in discrete intracellular puncta was observed in 8.7 ± 7.1%, and this was again significantly lower ($p< 0.05$) than that seen in HEK293 cells expressing STREX-EGFP. Although diffuse cytoplasmic expression was also observed in 86.4 ± 8.4% of cells transfected with Δe23-HA, and this was not significantly different to that of STREX-EGFP, in the majority of cells the fluorescent labelling appeared to be localised in a bright ring around the nucleus. 88.9 ± 8.4% of cells transfected with Δe23-HA contained fluorescent labelling in this

perinuclear manner, and this was significantly higher ($p< 0.01$) than for STREX-EGFP alone, where only 15.8 ± 8.4% of transfected cells contained perinuclear labelling (fig. 3-27).

Previous observations indicated that multimerisation of the -HcRed labelled BK channel α-subunit alternative splice variants could cause the suppression of normal membrane trafficking of those labelled with -EGFP, in a dominant- negative manner. Since the subcellular distribution of the Δe23-HA BK channel fusion protein was found to be perinuclear, HEK293 cells were cotransfected with both Δe23-HA and also STREX-EGFP, to investigate whether an alternative splice variant that is normally robustly expressed at the membrane could multimerise with the truncated splice variant, causing both to be trafficked to the membrane. Conversely, the truncated variant might exert a dominant- negative effect on the membrane expression of the STREX- EGFP α-subunit, and subsequently both would be retained in a perinuclear distribution.

In HEK293 cells cotransfected with Δe23-HA and STREX-EGFP, no fluorescent labelling of either Δe23-HA or STREX-EGFP at the plasma membrane was observed ($N= 3$, $n= 49$), and trapped punctate expression was seen in 9.0 ± 9.0% of transfected cells, with both EGFP fluorescence and HA labelling colocalised in bright intracellular puncta. Both membrane and trapped expression were significantly lower ($p< 0.01$) than for HEK293 cells singly- transfected, in parallel, with STREX-EGFP. Diffuse cytoplasmic expression was not significantly altered, and was observed in 93.6 ± 6.4% of Δe23-HA and STREX-EGFP cotransfected cells. However, whilst

Figure 3-27
Expression of Δe23-HA and coexpression of Δe23-HA with STREX-EGFP in HEK293 cells

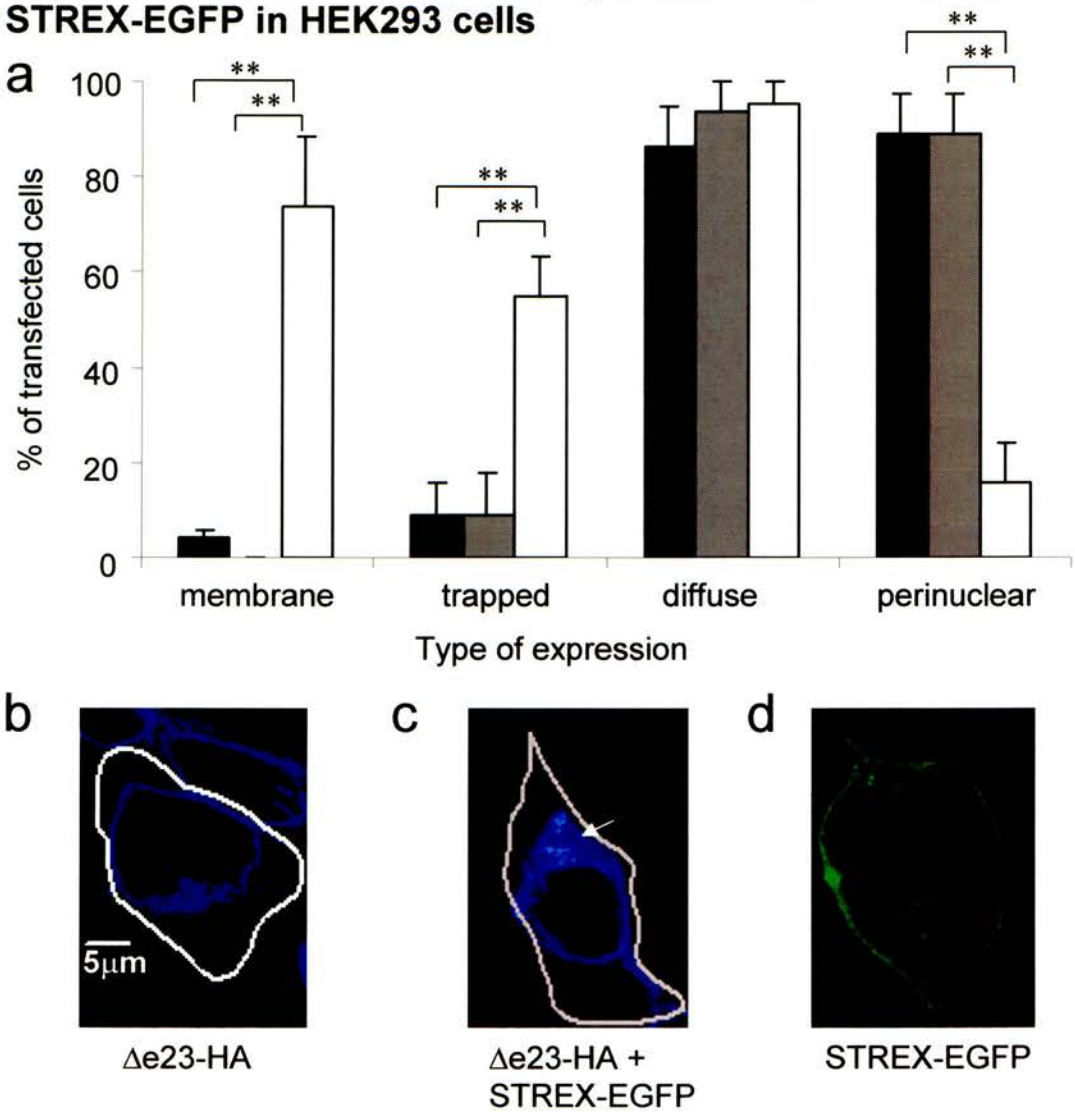

Figure 3-27 Expression of Δe23-HA and coexpression of Δe23-HA with STREX-EGFP in HEK293 cells

a) Data shown as a mean percentage of total transfected cells per field of view for each of four different types of fluorescent labelling in HEK293 cells singly-transfected with Δe23-HA (closed bars, N= 3, n= 96), cotransfected with Δe23-HA and STREX-EGFP (crossed bars, N=3, n= 49) and singly- transfected with STREX- EGFP (open bars, N= 3, n= 25). Representative images are also shown for cells expressing **b)** Δe23- HA, **c)** Δe23-HA cotransfected with STREX-EGFP (outlines of cells shown in grey) and **d)** STREX-EGFP in cotransfected cell, colocalisation of fluorescence is shown in pale green, arrowed. (** = $p<0.01$ ANOVA with post- hoc test Student- Newman- Keuls).

bright, perinuclear fluorescent labelling comprising both Δe23-HA and STREX-EGFP was observed in 89.1 ± 8.2% of cotransfected cells, significantly less perinuclear EGFP labelling was seen in cells singly- transfected with STREX-EGFP where only 15.7 ± 8.4% contained labelling of this type (fig. 3-27).

In summary, a reduction in plasma membrane expression was observed for the ZERO-HcRed and STREX-HcRed constructs in HEK293 cells, and this was also found to affect the membrane trafficking of cotransfected -EGFP and -HA labelled ZERO and STREX α-subunits in a dominant-negative manner. Since the -HA labelled BK channel constructs expressed in a similar manner to those labelled with EGFP, it is unlikely that the EGFP label itself influenced the membrane trafficking of the channel α-subunits. Additionally, the novel truncated BK channel α-subunit alternative splice variant was found to express in a perinuclear manner, and this had a dominant- negative effect on the expression of cotransfected STREX-EGFP, abolishing the normal robust membrane expression of the latter, and significantly increasing the perinuclear expression of EGFP, which was colocalised with fluorescent labelling of the Δe23-HA α-subunits.

3-3 Summary

3-3-1 Subcellular distribution of BK channel fluorescent fusion protein α-subunits

In order to address the question of whether BK channel subcellular localisation can be influenced by alternative splicing at splice site C2, BK α-subunits fused at the C-terminus with two spectrally- distinct fluorescent proteins were used to visually

discriminate between specific alternative splice variants. Additionally, this strategy would also enable the visual study of BK channel α-subunit subcellular localisation *in-vivo* in future studies, since visualisation of these fluorescent fusion proteins is not dependent on permeabilisation and addition of antibodies.

The -EGFP labelled ZERO and STREX BK channel splice variant constructs expressed strongly in HEK293 and PC12 cells, where robust, reproducible membrane expression was observed. No significant differences in subcellular localisation were observed, with channel expression across the entire plasma membrane demonstrating that the ZERO and STREX variants do not modify trafficking. In addition, the presence of endogenous BK channel splice variants in PC12 cells does not modify cell membrane expression. In contrast, ZERO-EGFP plasma membrane expression was significantly lower than that of STREX-EGFP in MDCK cells. Previous studies have indicated that BK channels may be targeted specifically to the basal or apical surfaces of polarised cells (Bravo- Zehnder *et al.*, 2000, Burckhardt and Gogelein, 1992) and it may also be the case that the endogenous trafficking mechanisms of the MDCK cells preferentially target certain splice variants to the cell surface.

Study of subcellular localisation of epitope- tagged channels requires that their expression closely resembles that of channels in nature. Expression of –HA labelled BK channel α-subunits was extremely similar to that of those labelled with –EGFP, therefore it is concluded that the presence of a large fluorescent protein tag fused to the C-terminus of the BK channel α-subunits did not have any deleterious effect on

expression and trafficking of the channel. However, although there was no significant difference in the amount of trapping in intracellular puncta of STREX-HA compared with STREX-EGFP, ZERO-HA was found to cause a significantly higher level of trapping than ZERO-EGFP. It may be the case that ZERO-HA is expressed at a greater rate than ZERO-EGFP and as a result the expression and posttranslational processing machinery becomes saturated more quickly than for the latter, resulting in a higher level of observed trapping. As a consequence of this, ZERO-EGFP may even be preferable to ZERO-HA for use in subsequent experiments requiring visualisation of subcellular localisation of this BK channel alternative splice variant.

An unusual phenotype was observed for the ZERO and STREX BK channel α-subunit alternative splice variants labelled at the C-terminus with HcRed, which were found to be impaired for membrane trafficking, with increased trapping in bright intracellular puncta of the fusion proteins observed in HEK293 cells. This profound disruption of membrane expression was also observed in PC12 and MDCK cells. This suggests that trapping of the fusion proteins was not an artefact of overexpression, and the presence of endogenous BK channels and trafficking mechanisms does not provide a 'rescue' function, for example by multimerisation of ZERO- or STREX-HcRed with endogenous α-subunits. Although both of the –EGFP labelled channel splice variants also caused some degree of trapping in singly-transfected cells, it was distinct from that of ZERO-HcRed and STREX-HcRed in that it was accompanied by both membrane and diffuse expression. It is likely that the trapping observed in the cells singly transfected with ZERO-EGFP and STREX-

EGFP represents fusion proteins at different stages of posttranslational processing, which may be 'in- transit' to the membrane, and is therefore dependent upon overall expression level. This theory is supported by studies suggesting that assembly of subunits in the endoplasmic reticulum operates at only 20-40% efficiency (Ward and Kopito, 1994). Furthermore, recent work by Christianson and Green implicates interplay of assembly and degradation as a regulatory factor in membrane trafficking of oligomeric ion channels (Christianson and Green, 2004). Several possibilities therefore arise when examining the expression of ZERO-HcRed and STREX-HcRed fusion proteins: they may reach a particular stage in posttranslational processing, and are prevented from continuing along the normal trafficking pathway, or alternatively, proteins may be separately targeted to compartments within the cytosol for degradation, either before or after assembly into functional channels.

Trapping of –HcRed labelled ZERO and STREX BK channel α-subunits does not appear to occur during posttranslational processing of the fusion proteins in the Golgi apparatus, since indirect immunofluorescence of the Golgi did not reveal any colocalisation with ZERO-HcRed. Staining of the lysosomal or endosomal compartments did not follow the pattern of large intracellular puncta observed for the -HcRed labelled BK channel α-subunits, therefore these compartments are unlikely to be the location of this trapping. It also seems unlikely that trapping is occurring in the endoplasmic reticulum (ER), since the pattern of expression seen for ZERO-HcRed or STREX-HcRed does not mimic the expected perinuclear appearance of ER- retained material (Zarei *et al.*, 2004), although colocalisation analysis with an ER- specific marker is required to validate this theory. Another target for future

investigation is the proteasome, since it may be the case that incorrect folding of the –HcRed labelled BK channel α-subunits may cause them to be targeted to ubiquitin-dependent proteolytic pathways (Christianson and Green, 2004).

3-3-2 Evidence for homo/ heteromultimerisation of alternatively spliced BK channel α-subunits

Recent evidence showing critical regulatory roles of individual α-subunits within the BK channel tetramer (Tian *et al.*, 2004) led to the hypothesis that assembly of alternative splice variants into heteromultimers is possible, as has been shown for other potassium channel subtypes (Ma *et al.*, 2002). In this way, differential trafficking by particular alternative splice variants may have an effect on other splice variants with which they multimerise, representing a further means of regulating channel populations at the cell surface, and subsequently, membrane excitability. Since the –HcRed labelled BK channel α-subunits caused trapping of the –EGFP and –HA labelled α-subunits in a specific and dominant- negative manner, this provides evidence for heteromeric assembly of BK channel alternative splice variants. Homomultimerisation of fluorescent BK channel α-subunit splice variants was investigated by coexpressing ZERO-HcRed with ZERO-EGFP, or STREX-HcRed with STREX-EGFP. In both cases, coexpression with the –HcRed labelled α-subunit caused a significant reduction in membrane expression of the –EGFP labelled α-subunit, and a concomitant increase in trapping of the fusion proteins in intracellular puncta, where both HcRed and EGFP fluorescence were seen to colocalise. This effect was observed in HEK293, PC12 and MDCK cells, and in the latter two cases the dominant- negative effect of the –HcRed labelled BK channel α-subunits on cell

surface expression appeared to be independent of endogenous channel trafficking mechanisms. The possibility that such abnormal expression was an artefact of the presence of the HcRed protein was precluded, by coexpressing ZERO-EGFP or STREX-EGFP with pHcRed, showing that the HcRed protein is itself unable to cause knockdown of BK channel α-subunit surface expression. In addition to this, in both HEK293 and MDCK cells, when STREX-EGFP was coexpressed with HcRed, the level of trapping of EGFP fluorescence in intracellular puncta was significantly lower compared with STREX-EGFP alone. This reinforces the notion that trapping observed for singly- expressed STREX-EGFP is attributable to a build up of excess fusion protein during posttranslational processing, as when coexpressed with HcRed, less STREX-EGFP is produced, and therefore does not accumulate in the same manner. Any possibility of the presence of multiple fluorescent protein tags causing disruption of normal expression was also precluded, since both ZERO-HcRed and STREX-HcRed were still able to suppress cell surface expression when coexpressed with ZERO-HA and STREX-HA. Additionally, the presence of the ZERO-HcRed fusion protein was found not to alter the membrane expression of coexpressed syntaxin-1A-EGFP in HEK293 cells, indicating the requirement for specific interaction with BK channel α-subunits. Syntaxin-1A can form homodimers, as well as associate with L-type voltage- gated calcium channels (Arien *et al.*, 2003), and has recently been shown to bind to the BK channel. This interaction is not thought to occur solely within the C-terminal tail of the channel (Cibulsky *et al.*, 2005), and it may be the case that interactions occur at multiple sites on the BK channel in order to facilitate this binding. It is possible that the ZERO-HcRed and STREX-HcRed fusion proteins fold incorrectly, thus concealing sites within the BK channel sequence that

normally mediate the interaction with syntaxin-1A. However, coexpression with the –HcRed labelled α-subunits exerts a dominant negative effect on the surface trafficking of other BK channel α-subunits, suggesting that the regions of the channel mediating multimerisation (Quirk and Reinhart, 2001, Jiang *et al.*, 2001) may well be accessible. It is therefore likely that this suppression of membrane expression exerted by ZERO-HcRed and STREX-HcRed is mediated by specific dimer- or homotetramerisation with other BK channel α-subunits, and it appears to be a dominant- negative effect, since assembly with α-subunits that would otherwise be correctly trafficked to the membrane was insufficient to rescue surface expression.

Plasma membrane expression of –EGFP labelled BK channel α-subunits was significantly reduced by coexpression with –HcRed labelled, alternatively spliced α-subunits in HEK293 cells, suggesting that the dominant- negative knockdown of cell surface trafficking by the –HcRed labelled BK channel fusion proteins is not limited to those subunits of the same alternative splice variant, and that heteromeric assembly also occurs. This heteromeric trapping was also observed in PC12 and MDCK cells, where two distinct possibilities arise: firstly, the trapping of the fusion proteins in intracellular puncta may occur independently of the intracellular channels and trafficking mechanisms, and puncta are composed solely of exogenous channel fusion proteins, or secondly the endogenous channels may also be trapped by interaction with the –HcRed labelled α-subunits. In order to investigate these possibilities, additional constructs encoding mutant ZERO-HcRed and STREX-HcRed fusion proteins could be generated, in which the epitope for a BK channel-specific antibody was modified to prevent binding. When these were expressed in

PC12 or MDCK cells, BK channel- specific immunocytochemical labelling in conjunction with a secondary antibody, conjugated to a fluorescent dye that had an emission wavelength spectrally distinct to that of HcRed, would identify endogenous BK channels only, facilitating observation of potential colocalisation.

The absence of knockdown of membrane expression of syntaxin-1A, combined with the knockdown of surface trafficking of other BK channel α-subunits suggests that ZERO-HcRed and STREX-HcRed may affect trafficking of other BK channel α-subunits via multimerisation. However, whilst such an interaction may be suggested by this study, specific assembly of BK channel α-subunits in this manner was not explicitly tested. Further techniques, such as FRET, may be used to investigate close association of coexpressed α-subunits, whilst site- directed mutagenesis of the association domains (Quirk and Reinhart, 2001) of ZERO-HcRed and STREX-HcRed may disrupt the dominant- negative knockdown of surface expression mediated by these fusion proteins on coexpressed BK channel α-subunits. Although ZERO-HcRed and STREX-HcRed may be unuseable in studying membrane localisation of multiple BK channel alternative splice variants, they may be useful tools for investigation of the lifetime of the channel at the cell surface.

3-3-3 Alternative splicing as a modifier of cell surface trafficking

In contrast to the robust membrane expression observed for the ZERO and STREX BK channel α-subunits, the recently- discovered truncated BK channel alternative splice variant, which was fused at the C-terminus with the HA tag, Δe23-HA, was found to localise within HEK293 cells in a perinuclear manner, highly reminiscent of the retention in the endoplasmic reticulum of another BK channel alternative splice variant, reported by Zarei and co-workers (Zarei *et al.*, 2004), which contained a

specific ER retention/ retrieval motif. The perinuclear distribution of Δe23-HA suggests that it becomes retained in the endoplasmic reticulum during processing, but in this case it is likely to be a direct result of this truncated BK channel α-subunit lacking multiple sequences in the C-terminal tail region, which are assessed by the ER during processing, and determine correct export of the protein (Wang *et al.*, 2003). Critically, this regulatory step has been shown to take place *after* multimerisation of the channel, affecting not only homomers of mutant α-subunits lacking these sequences, but also heteromers composed of mutant and wild- type α-subunits (Kwon and Guggino, 2004). The abolition of membrane expression of STREX-EGFP by Δe23-HA supports this theory of trapping via heteromerisation, and since the latter is predominantly expressed at a specific developmental time point, in the 19 day mouse embryo (L. Chen, unpublished data) and in adult cells with low BK channel expression, such as heart and liver (fig. 4-17), it may be the case that this newly- discovered alternative splice variant represents a novel regulatory mechanism for surface expression of BK channels. The restricted expression of the Δe23 truncated BK channel is indicative of such a regulatory role. It is likely that a critical switch in cell excitability occurs at day 19 of murine development. A similar mechanism of regulated BK channel surface expression may occur in the mouse myometrium, where during late pregnancy the number of surface BK channels has been shown to fall, accompanied by a paradoxical rise in BK channel protein expression. Additionally, BK channel protein was seen to localise in a perinuclear manner (Eghbali *et al.*, 2003). These observations are consistent with the concept of BK channel α-subunits with altered trafficking properties being used to reduce cell surface expression by multimerising with other BK channel α-subunits, thereby causing their retention within the processing machinery.

3-3-4 Continued investigation

The ZERO-HcRed and STREX-HcRed fusion proteins appeared to specifically suppress the membrane expression of newly- synthesised α-subunits of the EGFP and -HA labelled BK channel fusion proteins used in this study. Trapping of homo- and heteromeric α-subunits in this dominant- negative manner suggests that whilst ZERO-HcRed and STREX-HcRed may fold incorrectly, they are still able to assemble specifically with other BK channel α-subunits. Although these results preclude their use in visualisation of normal subcellular localisation when coexpressed with -EGFP labelled BK channel alternative splice variants, they may prove useful in knockdown studies to investigate hitherto unknown factors such as the half- life of the BK channel at the cell membrane. A preliminary investigation carried out during this study has indicated that channels must remain in the membrane for at least 7 days, since in HEK293 cells stably transfected to express STREX-HA, membrane expression was still present after expressing ZERO-HcRed for this period, during which any newly- synthesised STREX-HA α-subunits would be multimerised with ZERO-HcRed, and subsequently prevented from reaching the membrane.

Studies of other types of potassium channel implicate not only the subunit composition of channel heteromers with respect to cell surface trafficking (Ma *et al.*, 2002) but also factors such as phosphorylation state (Mirshahi and Logothetis, 2002) therefore this process must be tightly regulated at many levels, in order to correctly control cell excitability. Whilst many of the known mechanisms for ion channel regulation focus on those already at the membrane, future studies will certainly take into account the varied processes governing translocation of the channel proteins to the cell surface.

Chapter Four:

Quantitation of BK channel alternative splice variant expression

4-1 Introduction

4-1-1 Real time PCR

In order to facilitate the study of the expression patterns of BK channel alternative splice variants across tissues, a method was required that could be used to reliably detect and quantify splice variants in very low abundance, as well as being able to discriminate between variants which may only differ in sequence by a few amino acids. An end- point reverse- transcription PCR approach has previously been used by Mahmoud *et al.*, which enabled the accurate relative quantitation of two alternatively- spliced variants of the BK channel (Mahmoud *et al.*, 2002, Lai and McCobb, 2002). However, although detection was possible even at a single- cell level, a high degree of optimisation and a specialised denaturing and electrophoresis protocol were required, with additional correction during intensity analysis to allow for PCR amplicon length and primer efficiency. Although in- situ hybridisation and immunocytochemistry have also been used to detect the relative abundance of BK channels in a number of tissues (Skinner *et al.*, 2003, Pedarzani *et al.*, 2000, Knaus *et al.*, 1996), each bears distinct advantages and disadvantages. The in- situ method allows spatial discrimination of cells expressing the BK channel, but the resolution is not sufficiently high to enable detection of very low- level expression. Whilst indirect immunofluorescence can be used to detect the channel protein, there have been no antibodies published which are specific to individual BK channel alternative splice variants. Thus the real time fluorogenic PCR approach was used, due to its high throughput, specificity, sensitivity, and ability to determine absolute copy number of a target within a sample (Wang and Brown, 1999.).

Real time PCR differs from conventional end-point PCR in that fluorogenic detection chemistries are used to monitor the reaction as it progresses from cycle to cycle, rather than gel electrophoresis and UV visualisation or densitometric analysis of products from finished reactions (Kidd *et al.*, 2000), the major difference being the method used for product quantitation. The real time PCR approach uses the point during cycling at which fluorescence becomes detectable above a user- defined threshold level, during the exponential phase of amplification; the higher the starting concentration of the target, the sooner accumulated product will be detected in the reaction, and neither primers nor probe are at limiting concentrations. In contrast, it is only the plateau phase at the end of amplification which is detected during conventional end- point PCR, at which time the primers or nucleotides may have been exhausted, thus although two products may have had very different starting concentrations, this may not be detectable since both reactions may have reached the plateau phase by the end of the assay.

During real time PCR analysis, detection and quantitation are carried out by computer, in this case using Applied Biosystems 'ABI Prism 7000 Sequence Detection System (SDS)' software version 1.0 (Applied Biosystems, 2001-2002) therefore results are available more quickly than for conventional PCR, and accuracy is also increased since the fluorescence is detected in each well individually. In this way, many of the problems associated with end-point PCR are avoided, such as cross-contamination of wells when loading, uneven gel electrophoresis and inconsistencies in visual analysis of bands on the gel. The risk of cross-contamination between steps is also reduced, as the amplification and quantification

are performed in a 'closed-tube' format. Finally, sensitivity of detection is also higher than that of traditional end-point PCR analysis (Wilhelm and Pingoud, 2003), therefore Real-time PCR is the preferred method for quantitation of samples where the target sequence is present in very low abundance (Bustin, 2000, Swan *et al.*, 1997).

The aim of this chapter was to design and validate real-time PCR assays for a number of different splice variants at splice site C2 of the BK channel and determine their limits of detection. This would allow investigation of unknown samples, generated using mRNA collected from various tissues, where certain BK isoforms might be present as only a small fraction of the overall BK channel population.

A number of different assays have been developed for use in real- time PCR analysis, which produce fluorescence in proportion to the amount of product being formed. This may be direct, where a fluorescent dye binds non-specifically to the dsDNA as product is formed, with enhanced fluorescence compared to the free dye, (for example, the SYBR Green assay). Alternatively this may be indirect, where the dye is bound to a sequence-specific primer or probe, and held in close proximity to a quencher molecule, which suppresses its fluorescence via Förster-type energy transfer (Förster, 1948) until they are separated, either by a conformational change when the primer anneals to its target sequence (for example, Scorpion primers), or when the probe is broken down by exonuclease activity of the PCR enzyme (for example, the Taqman assay) (Wilhelm and Pingoud, 2003). Due to the extra sequence specificity afforded by the Taqman probe over non-specific systems such

as SYBR green, this assay was chosen for our studies. In addition to this, more advanced assays are available when using Taqman analysis- for example detection of single nucleotide polymorphisms by relative quantitation between two differently labelled probes (Livak, 1999, Livak *et al.*, 1995) which may be useful in future screening of tissues for novel BK channel splice variants.

The initial aim of this study was to design and test Taqman real time PCR primer sets specific to five murine BK channel alternative splice variants, as well as a universal BK primer set, each of which could be used to accurately and reproducibly detect and quantify the presence of BK channel splice variants in very low abundance, below the limit of detection for conventional nested end- point PCR, where products would not be visible by agarose gel electrophoresis. Additionally, since the real time PCR method can be used to quantify samples with much greater accuracy than end point PCR, it would be possible to study the relative expression levels of each splice variant across different tissues, or even amongst populations of cells isolated from a tissue, with greater accuracy (Bustin, 2000).

4-1-2 The Taqman assay

The Taqman assay relies on the 5'-3' exonuclease activity of the AmpliTaq Gold ® DNA polymerase. Standard PCR primers are designed for a short amplicon (typically 50 to 150bp in length), and a third 'probe' is designed to target the sequence midway between the primers. Ideally, the primers should target sequence as close to the probe as possible. The 5' end of the probe is labelled with a reporter dye- in this case, FAM™ (6-carboxyfluorescein)- and the non-extendable 3' end is labelled with a

quencher, TAMRA™ (6-carboxytetramethylrhodamine) (Livak *et al.*, 1995). Due to the small physical size of the probe, the reporter and quencher molecules are held together in close proximity, such that energy is transferred from the former to the latter, via Förster- type energy transfer, thus fluorescence of the reporter is suppressed. The probe hybridises to its target sequence during PCR amplification, and is then cleaved by the 5'-3' nucleolytic activity of the DNA polymerase, resulting in the release of the reporter dye, thus fluorescence increases (figure 4-1) and is used as an indirect measure of target amplification. The SDS software records the changes in fluorescence emission intensity from cycle to cycle, and calculates the normalised reporter signal (R_n) by dividing the values by the fluorescent signal from the ROX™ passive reference dye contained in the PCR master mix. This normalisation helps reduce errors arising from pipetting inaccuracy, and enables better comparisons of the reporter signal from well to well. Results are recorded as an 'amplification curve', showing the change in R_n (ΔR_n) from cycle to cycle as the reaction progresses (fig. 4-2).

4-1-3 Quantitation of samples using the Taqman assay

4-1-3-1 Relative standard curve method

During the post-run analysis, a threshold is set above which there is a detectable increase in fluorescence. The point at which each sample's amplification curve crosses the threshold is known as the Ct value. If the PCR reaction is efficient, as the starting concentration of template DNA increases, the Ct will fall in a linear manner. Therefore, by determining the Ct values for a logarithmically diluted series of samples whose starting template concentration is known, a standard curve can be

Figure 4-1
Schematic diagram of the Taqman Assay

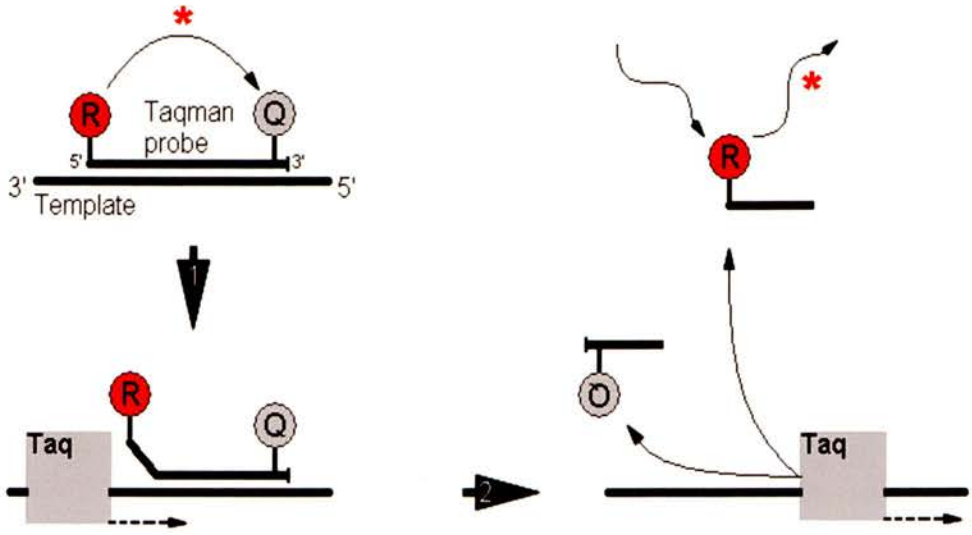

Figure 4-1 Schematic diagram of the Taqman assay

Before amplification, no fluorescence is emitted from the Taqman probe, since the 5' reporter dye (R), FAM (6-carboxyfluorescein), is quenched by the 3' TAMRA (6-carboxytetramethylrhodamine) molecule (Q) due to Förster-type energy transfer. As the Taq DNA polymerase proceeds along the template strand, the 5-3' nuclease activity degrades the probe, releasing the reporter dye. This leads to an increase in fluorescence that can be used to indirectly measure product formation.

Figure 4-2
Generation of standard curves using real time PCR fluorogenic assay

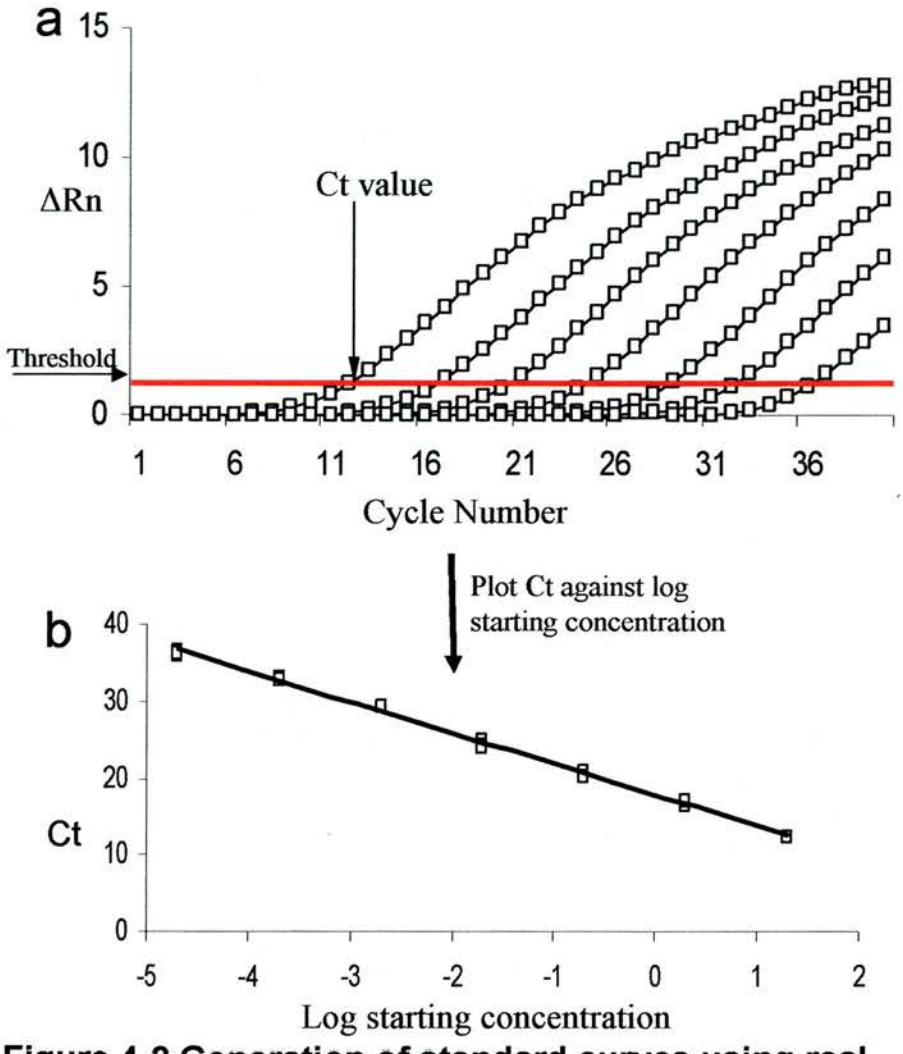

Figure 4-2 Generation of standard curves using real time PCR fluorogenic assay

a) Normalised fluorescence signal, ΔRn, for each logarithmically- diluted sample is plotted against cycle number. The PCR cycle at which the ΔRn for a sample crosses the threshold of detection (red line) is known as the Ct value. **b)** Ct is then plotted against log of starting concentration, generating a standard curve. At 100% efficiency, the slope of the standard curve trendline will be ~-3.23. A high correlation coefficient, above 0.98, indicates that the primers can be used to accurately quantify starting concentration of target in an unknown sample, by extrapolation of its Ct value from the standard curve, when run in parallel conditions.

generated by plotting the Ct values against log starting concentration. If there is good correlation between the trendline and the actual data for the standard curve (i.e. if R^2 is close to 1, e.g. ≥ 0.98), then it can be used to reliably calculate the starting concentrations of unknown samples by extrapolation of their Ct values. In addition to this, the slope of the trendline can be used to calculate the efficiency of the primer and probe set, using the equation:

$$\mathbf{E = 10^{(-1/slope)}}$$

where the maximum theoretical value is 2, indicating that every product is replicated at every cycle of the reaction, and the minimum is 1, which indicates no amplification. As a rough guide, a standard curve slope close to –3.23 indicates a high efficiency (fig. 4-2). The disadvantage of the relative standard curve method is the requirement of a standard curve being generated for every run, however the reduced time taken in optimisation of the assays compared to the comparative Ct method is advantageous.

4-1-3-2 Comparative Ct method

It is possible to carry out quantitation of samples without use of a standard curve in every run. This method is known as the comparative Ct, or ddCt method, and can be used to quantify gene expression in an unknown sample relative to that of a known calibrator, such as an untreated sample, or a tissue where the gene is expressed at a constant level (Dorak, 2005). An endogenous control, such as a housekeeping gene is used to normalise the samples, then the relative difference between the samples is calculated, for example:

ddCt = dCt sample - dCt calibrator

Where the relative expression is expressed as a ratio, ddCt, calculated by subtracting the normalised Ct value of the calibrator from the normalised Ct value of the sample. A plot of Ct versus log input concentration must be generated for both sample and normaliser primer sets in order to validate this method. If the difference in slope between the two plots is less than 0.1, the efficiencies are almost identical, therefore relative quantitation using the comparative Ct method can be carried out (Applied Biosystems, 2001). The comparative Ct method can be carried out for each sample either in single- tube or two- tube formats, with the single tube format requiring reporter dyes with spectrally- resolvable emission wavelengths. This method may be preferable to relative standard curve quantitation since when carried out in single tube format, it compensates for inaccurate pipetting, and has a high throughput. However, it can be time consuming to optimise the assays in terms of primer efficiencies.

4-1-4 General design strategy for BK channel alternative splice variant Taqman assays

Applied Biosystems' Primer Express software, version 2.0.0 was used to design the Taqman primer and probe sets, for use with the Prism 7000 sequence detection system. The BK channel sequence of interest was imported as a text file into Primer Express, and a region highlighted at the start of the potential amplicon as the forward primer. The software was then used to find a compatible reverse primer and probe, according to the following parameters: primers were 9-40 bases in length, with a G/C

content of 30-80%, an optimal T_m of 59°C, and a maximal T_m difference of 2°C between the forward and reverse primers. Those primer pairs with a high degree of complementarity with either themselves or each other were discarded. Amplicon length was between 50 and 250 bp. In addition to this, potential Taqman probes with a guanidine as their 5' base were excluded, as this nucleotide causes quenching of the reporter dye post-cleavage (Giulietti *et al.*, 2001). Finally, it was necessary for the T_m of the Taqman probe to be 10°C higher than that of the primers. It is advantageous to use the Primer Express program since all of the Taqman primer and probe sets that are generated will be compatible with Applied Biosystems' standard thermal cycling parameters (see methods).

Taqman primer sets were designed using Primer Express, specific to five different alternative splice variants of the BK channel (fig. 4-3): ZERO, which has no splice inserts at the C2 alternative splicing site of the channel C-terminal region, IYF, which contains a short, 3 aa insert at position C2, Exon22- a novel 30 aa splice variant recently discovered by Dr. L. Chen, which was only detectable via nested end point PCR in mouse embryo at day 19, STREX, which contains the 59 aa "Stress Regulated Exon" and Δe23, which encodes a truncated channel, with modified surface trafficking properties, also recently discovered by Dr. L. Chen (unpublished data). Since these alternative splice variants all occur at position C2 (fig. 4-4), it was inevitable that several of the primer sequences designed would be common to all of the splice variants being investigated. Therefore, as well as designing primers according to the Primer Express parameters, additional design features were required to ensure that each primer and probe set would amplify only its intended target.

Figure 4-3
Overview of Taqman primer and probe design strategy

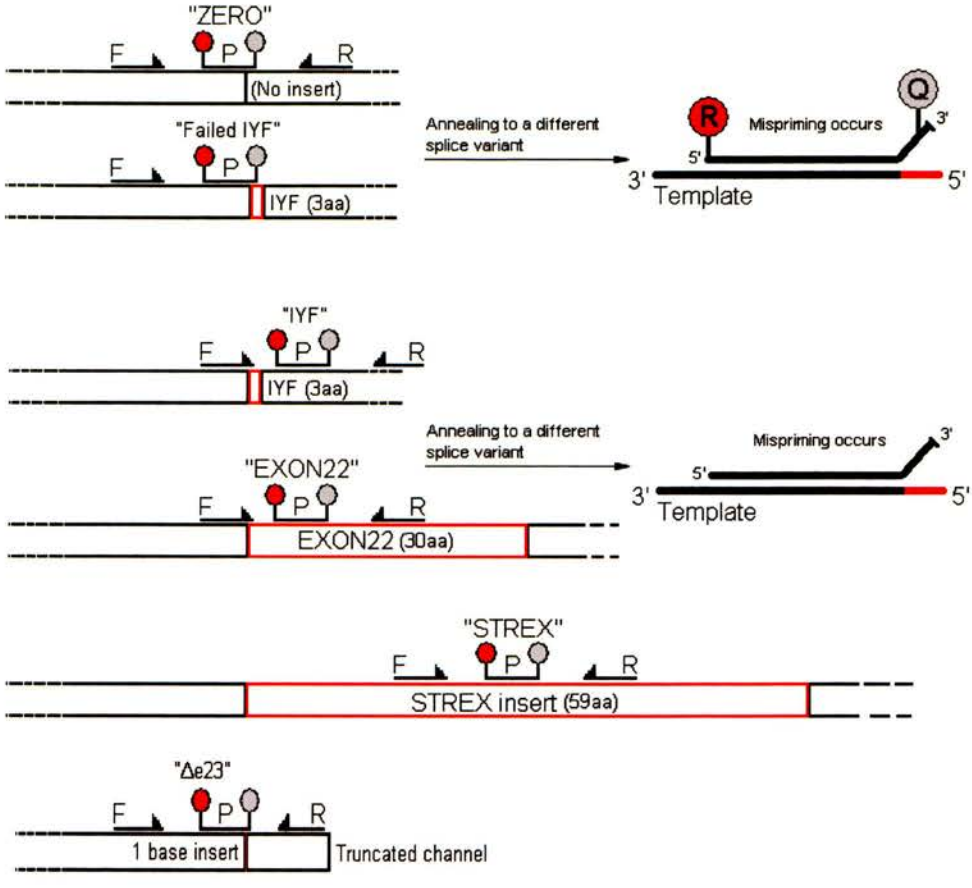

Figure 4-3 Overview of Taqman primer and probe design strategy

Schematic showing locations at which Taqman primer and probe assays annealed to target BK channel alternative splice variant sequences at splice site C2 of the BK channel C-terminus. Taqman primer (F and R- forward and reverse) and probe (P) sets were designed to be specific to the insertless BK alternative splice variant (ZERO), the initial failed IYF primer set (Failed IYF), IYF insert (IYF), the novel Exon 22, STREX insert (STREX) and novel Δe23 truncated channel (Δe23). To preserve specificity, probe or primer sequences were designed with splice- variant specific 3' overhangs. Partial hybridisation of probe or primer to sequence would cause mispriming due to 3' mismatch, preventing amplification.

Figure 4-4
Schematic diagram of BK channel cytoplasmic C-terminal tail showing locations of Taqman primer sites

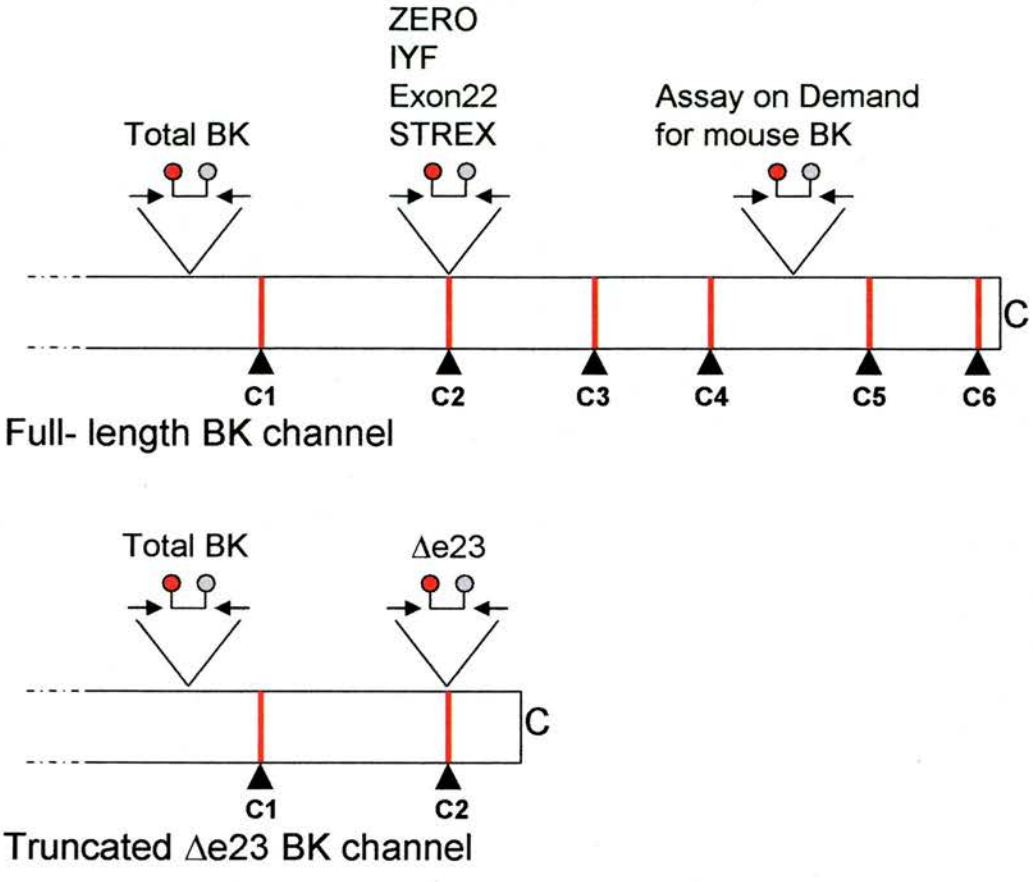

Figure 4-4 Schematic diagram of BK channel cytoplasmic C- terminal tail showing locations of Taqman primer sites

(Not to scale.) The 6 C- terminal sites of alternative splicing are shown (C1- C6). The total BK Taqman real time PCR primer set was designed upstream of the first splicing site, to ensure that all BK channel alternative splice variants could be detected. The splice variant- specific primer sets were all located in and around site C2, whilst Applied Biosystems' Assay on demand primer set for mouse BK channel, assay ID Mm00516078_m1, was designed against sequence downstream of splice site C4.

In general, the design of Taqman assays against the BK channel alternative splice variants included primer sets that would span an exon- exon junction, since it is important to exclude any contaminating trace genomic DNA as template during real time PCR reactions. It was necessary to ensure that amplification would only occur when the primers and probe were completely hybridised to their target, and any partial hybridisation to similar sequences in other splice variants would cause mispriming, and hence no amplification (fig. 4-3). Although ideally all of the primer sets designed would span exon- exon junctions, in some cases, such as for the STREX BK channel splice variant, no suitable primer and probe sets could be found within the nucleotide sequence surrounding the exon junction. In this situation, the length of the STREX insert enabled the design of a Taqman primer and probe set entirely within the exon itself.

In order to test the sensitivity and efficiency of each primer and probe set, a logarithmic dilution of plasmid DNA was prepared, over a concentration range of several orders of magnitude. These samples were then run in triplicate. From the amplification curves, Ct values for each concentration were determined, thereby enabling the generation of a standard curve. From this, the slope was used to predict the efficiency of amplification of these primers' target sequence. All assays were performed using an Applied Biosystems ABI Prism 7000 Sequence Detection System (SDS), and analysed using the ABI Prism 7000 SDS software version 1.0 (Applied Biosystems).

4-2 Results

4-2-1 Design of BK channel alternative splice variant- specific Taqman assays

4-2-1-1 Design of a ZERO BK channel alternative splice variant- specific Taqman assay and standard curve generation

In the case of the ZERO BK channel alternative splice variant, the Taqman probe was designed to span the splice junction at the C2 position within the channel C-terminus (fig. 4-3). Although the sequence at both sides of the splice site is ubiquitous to all of the splice variants being investigated, unless hybridised to the target sequence in ZERO, the probe would have a 3' mismatched overhang, causing mispriming (Kwok, 1990) and preventing amplification.

Triplicate 25µl reactions were set up in 1x Taqman Universal PCR master mix, using the ZERO BK channel Taqman primer and probe set, with a logarithmic dilution of ZERO cDNA over a starting concentration range of 2ng- 20fg, and a standard curve was generated using the Ct values obtained for each starting concentration. Using the slope of the standard curve, the efficiency was calculated to be 1.91, whilst the correlation coefficient was > 0.99. Since there is a high degree of correlation between the standard curve data and the trendline, this indicates that it is possible to accurately predict the concentration of ZERO BK channel in an unknown sample, by extrapolation of its Ct value against the standard curve when assayed in parallel conditions (fig. 4-5).

Figure 4-5
Standard curve generated using the ZERO BK channel splice variant-specific Taqman real time PCR primer and probe set

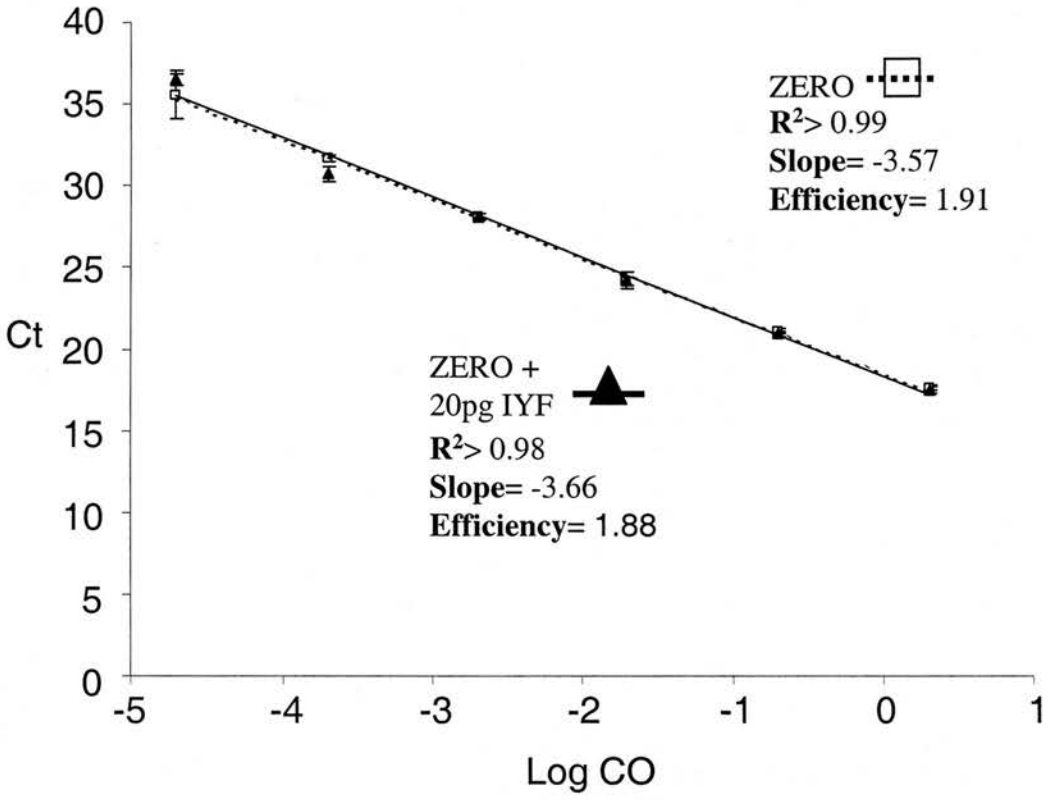

Figure 4-5 Standard curve generated using ZERO BK channel slice variant- specific Taqman real time PCR primer and probe set

ZERO DNA, logarithmically diluted over a starting concentration range from 2ng-20fg was used as a template in 25µl reactions containing the ZERO Taqman primer and probe set in 1x Taqman Universal PCR mastermix (open squares, dashed trendline). The same reactions were also performed in triplicate in the presence of a constant 20pg of IYF DNA as a competing template (filled triangles, solid trendline). Data shown as triplicate Cts for each starting concentration (log scale) ± SEM. Correlation coefficient, slope and calculated efficiency are also shown for each standard curve.

4-2-1-2 Competition standard curve using the ZERO BK channel Taqman assay

In order to preclude the possibility that the ZERO BK channel Taqman assay was able to detect and amplify other alternative splice variants of the channel, a competition assay was designed. Triplicate 25µl reactions performed as before, using ZERO cDNA as template over a starting concentration range of 2ng- 20fg. However, an additional 20pg of IYF cDNA was included in each reaction as a competing template. In the event of amplification occurring as a result of the ZERO BK channel Taqman primers and probe hybridising to the competing sequence, the Ct values obtained for each sample would be artificially low, and this would be especially noticeable in the case of samples containing <20pg of ZERO, causing a lowering of the slope of the standard curve. In this case, it was found that the competing IYF sequence did not cause any extra amplification in the samples, as the efficiency calculated from the slope of the new standard curve was 1.88, similar to that calculated from the standard curve without competition, and the correlation coefficient was again > 0.98 (fig. 4-5). This indicates that the ZERO primer set has a high specificity for the ZERO BK channel alternative splice variant, and it is also able to amplify its target with equal efficiency at an initial starting concentration of 20fg, even where there may be a thousand- fold excess of non- target DNA. In addition to this, no amplification was observed when a run was performed using IYF cDNA alone in a reaction using the ZERO BK channel splice variant- specific Taqman primer set.

4-2-1-3 Design of an IYF BK channel alternative splice variant- specific Taqman assay

When designing the IYF BK channel splice variant- specific Taqman assay for the first time, the probe was designed such that the 3' end spanned the splice junction at site C2, with the last 3 nucleotides annealing to the first 3 within the IYF insert, and the forward and reverse primers located either side of the splice junction. When annealed to a BK splice variant lacking the IYF insert, the 3' overhang of the probe should have been sufficient to cause mispriming, and subsequent lack of amplification. When this primer set was run in triplicate 25µl reactions in 1x Taqman Universal PCR master mix, using a logarithmic dilution of IYF cDNA as template, over a starting concentration range of 2ng- 20fg, and the Ct values used to generate a standard curve, the efficiency was found to be 1.79, and there was a high correlation coefficient between the trendline and data, $R^2 > 0.99$, suggesting that this primer set could be used to accurately quantitate unknown samples over a wide dynamic range by extrapolation of their Ct values against the standard curve (fig. 4-6).

However, when the same reactions were performed again in the presence of 20pg of STREX cDNA as a competing template, the standard curve was disrupted, since at starting concentrations of IYF < 20pg, amplification was masked by that of the STREX cDNA, therefore in these samples, the Ct values reported were artificially low. Under these conditions, the calculated efficiency was 4.35, whilst the correlation coefficient was 0.81. This indicates that this primer set cannot be used to specifically amplify the IYF BK channel alternative splice variant (fig. 4-6).

Figure 4-6
Failed IYF primer design strategy

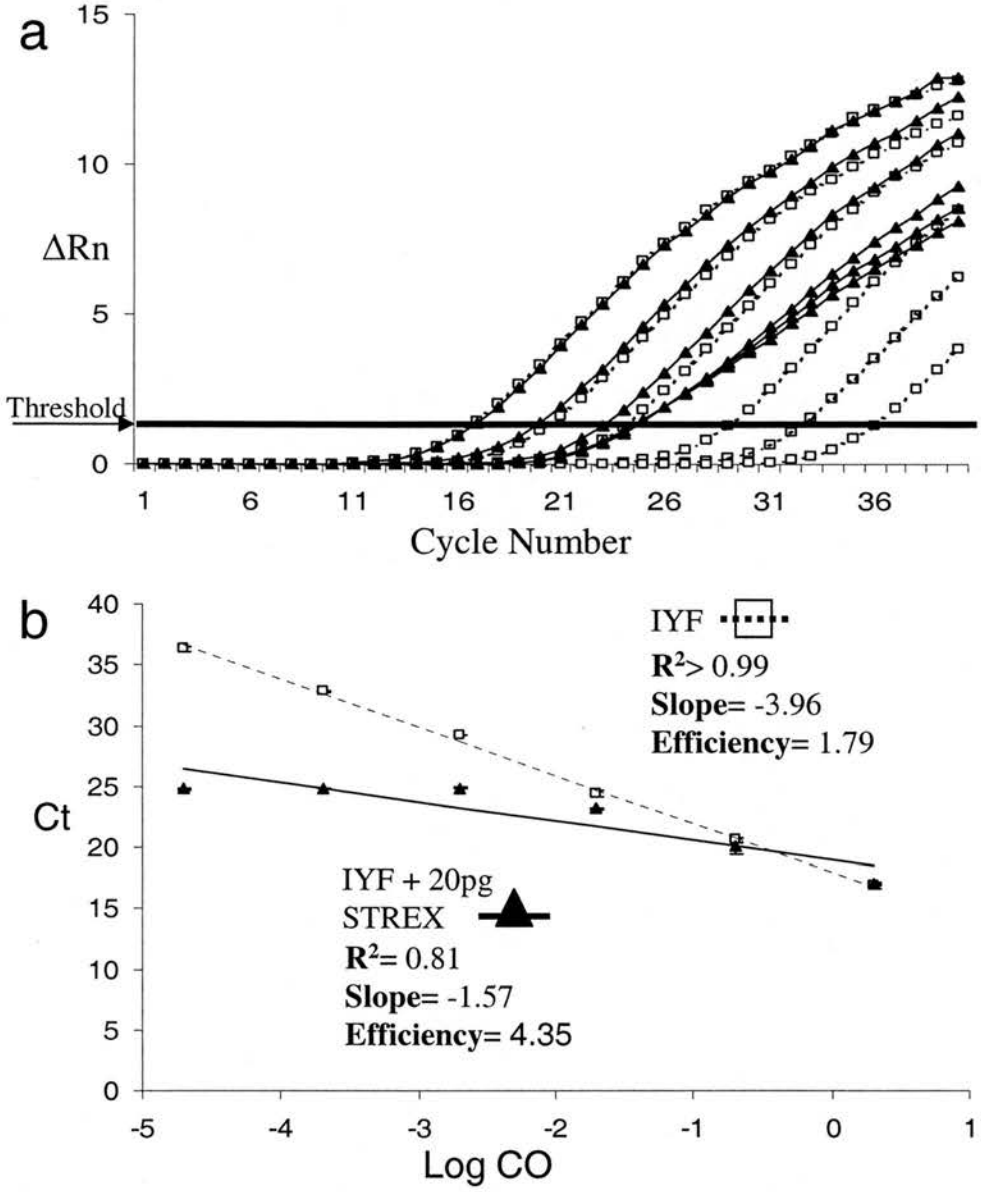

Figure 4-6 Failed IYF Taqman primer design strategy

IYF cDNA was used as a template, logarithmically diluted over a starting concentration range of 2ng- 20fg, in 25µl reactions using the first IYF Taqman primer and probe set. **a)** Although the primers amplified the IYF template over the dynamic range being tested (open squares, dotted trendline), when the same reactions were performed in the presence of 20pg of competing STREX cDNA (filled triangles, solid trendline), the amplification of STREX masked that of the IYF, resulting in artificially low Ct values, and disruption of the standard curve **(b)**.

Since the previous primer set, where the probe was designed to overhang into the IYF insert, was found to amplify not only the IYF BK channel splice variant, but also STREX, a different design strategy was followed in order to generate Taqman assay that was specific to IYF alone. In this case, the forward primer was designed to span the splice junction, with the 3' nucleotides annealing to the start of the IYF insert, the absence of which would again lead to mispriming and subsequent prevention of amplification, due to 3' mismatch of the primer (fig. 4-3). Triplicate 25µl reactions were set up using the IYF BK channel Taqman primer set, in 1x Taqman universal master mix, this time using a logarithmic dilution of IYF cDNA as template, over a starting concentration range of 2ng- 20fg, and the Ct values used to generate a standard curve. The efficiency of this primer set was calculated to be 1.71, whilst the correlation coefficient was > 0.99 (fig. 4-7).

4-2-1-4 Competition standard curve for IYF BK channel Taqman assay

The IYF standard curve was generated as before, but with an additional 20pg of competing STREX template in each reaction. Although as was the case with the original standard curve, the calculated efficiency was found to be slightly lower than for the other primer sets, 1.72, there was still a very high correlation coefficient of > 0.99. It can be concluded that this primer set, although having a lower amplification efficiency than the other Taqman assays, can still be used to reliably quantitate target cDNA in a highly specific manner over a dynamic range of five orders of magnitude, in the presence of a up to a thousand fold excess of competing template sequence (fig. 4-7). When a run was performed using the IYF- specific Taqman primers on STREX cDNA alone, no amplification was observed.

Figure 4-7
Standard curve generated using the IYF- specific Taqman real time PCR primer and probe set

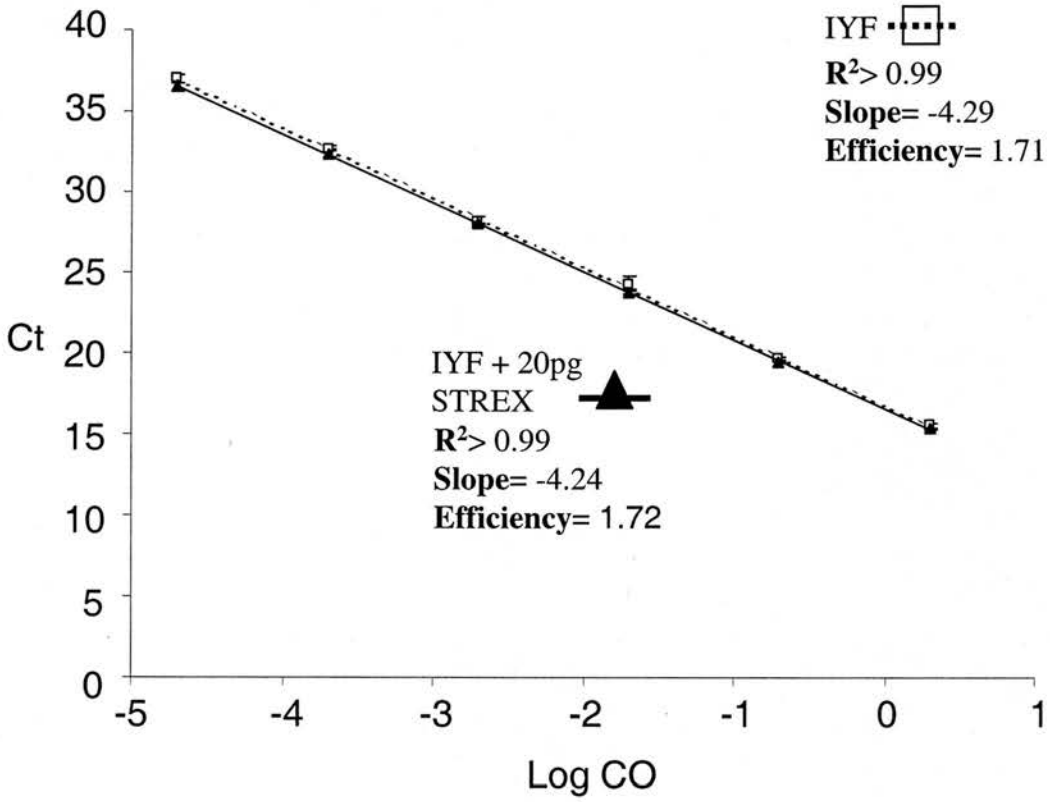

Figure 4-7 Standard curve generated using the IYF-specific Taqman real time PCR primer and probe set

IYF DNA was used as a template, logarithmically diluted over a starting concentration range from 2ng- 20fg, in 25µl reactions containing the IYF-specific Taqman primer and probe set in 1x Taqman Universal PCR master mix (open squares, dashed trendline). The same reactions were also performed in the presence of a constant 20pg of STREX DNA as a competing template (filled triangles, solid trendline). Data shown as triplicate Cts for each starting concentration (log scale) ± SEM. Correlation coefficient, slope and calculated efficiency are also shown.

4-2-1-5 Design of an Exon22 BK channel splice variant- specific Taqman assay

The Exon22 BK channel alternative splice variant was only previously detectable by nested PCR in mouse embryo day 19 cDNA, indicating that if this splice variant is present in other tissues, it is likely to be expressed at very low concentrations. Therefore a Taqman assay against this novel splice variant was generated in order to test for its presence in other tissues, and enable investigation of any potential developmental regulation that might occur. The forward primer of the Taqman primer set was designed to span the splice junction at position C2 of the channel, whilst the probe and reverse primer were designed within Exon22 itself. Triplicate 25µl reactions were prepared using this primer set, in 1x Taqman universal PCR master mix, and run using a logarithmic dilution of Exon 22 cDNA over a starting concentration range of 2ng- 20fg in order to generate a standard curve. From this, the efficiency of the Exon 22 specific Taqman assay was calculated to be 2.01, whilst the correlation coefficient was > 0.99 (fig. 4-8).

4-2-1-6 Competition standard curve for Exon 22 BK channel Taqman assay

A standard curve was generated as before for the Exon 22 Taqman primer set, but this time including 20pg of STREX cDNA as a competing template sequence. The efficiency was unchanged by the presence of the competing template, at 2.03, and the correlation coefficient remained very high, at > 0.99, indicating that it will be possible to use this primer set to accurately predict the starting concentration of Exon 22 in an unknown sample, from its Ct value when run under parallel conditions, and

Figure 4-8
Standard curve generated using the Exon 22- specific Taqman real time PCR primer and probe set

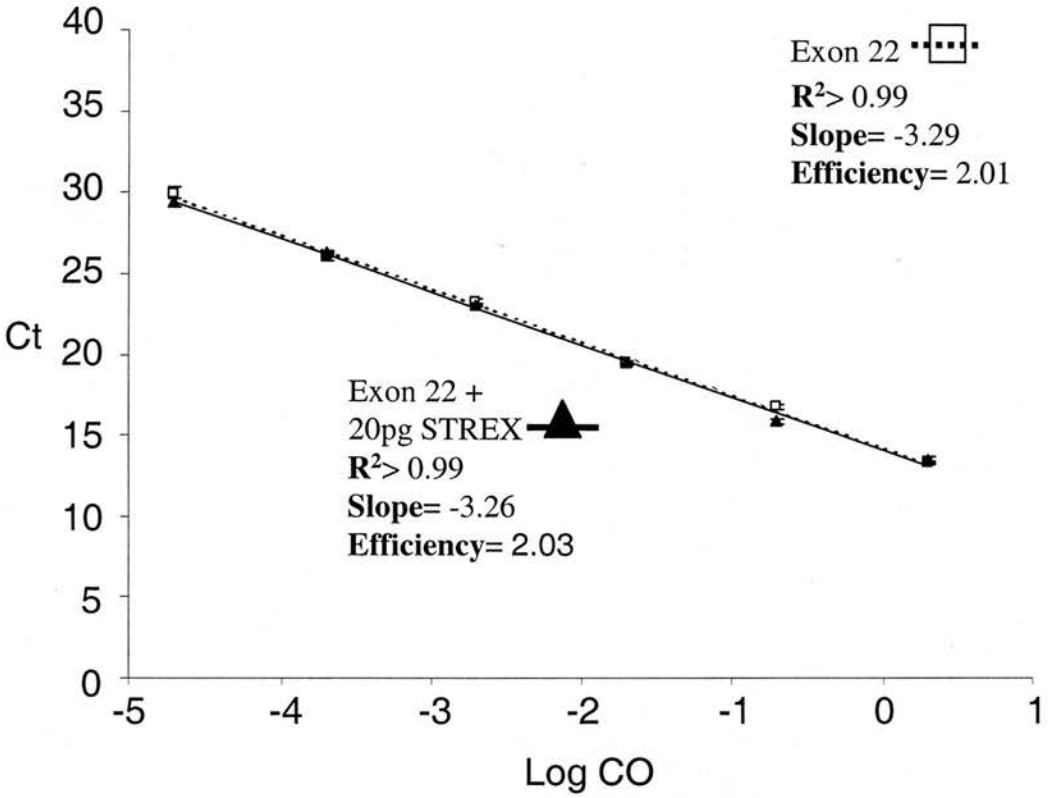

Figure 4-8 Standard curve generated using Exon22-specific Taqman real time PCR primer and probe set

Exon 22 DNA was used as a template, logarithmically diluted over a starting concentration range from 2ng- 20fg, in 25µl reactions containing the Exon 22-specific Taqman primer and probe set in 1x Taqman Universal PCR master mix (open squares, dashed trendline). The same reactions were also performed in the presence of a constant 20pg of STREX DNA as a competing template (filled triangles, solid trendline).Data shown as triplicate Cts for each starting concentration (log scale) ± SEM. Correlation coefficient, slope and calculated efficiency are also shown.

that it has a high degree of specificity, even in the presence of up to a thousand fold excess of competing sequence (fig. 4-8). No amplification was observed when a run was performed using the Exon 22- specific primers on STREX alone.

4-2-1-7 Design of a STREX BK channel alternative splice variant-specific Taqman assay

In general, the strategy applied to primer design was for the Taqman primer and probe sets to span exon/ exon junctions. However, this was not possible in all cases due to the strict criteria applied by the Primer express program when selecting potential amplicons. The 5' and 3' ends of the STREX sequence made it impossible to design a Taqman primer and probe set within the Primer Express parameters that could span the splice junction. Therefore, it was necessary to design the entire amplicon within the STREX insert itself (fig. 4-3). Although this strategy would help to avoid the issue of non- specific amplification occurring due to presence of alternative splice variants containing partially similar sequence, the hybridisation of the Taqman primer and probe set to a single exon could cause problems in cases where samples were contaminated with unwanted genomic DNA. Although this can be eliminated by stringent sample preparation, the increased sensitivity of the real time PCR method means that such contamination at even a low level has to be considered.

Triplicate 25µl reactions were prepared with the STREX- specific Taqman primer set, in 1x Taqman Universal PCR master mix, using a logarithmic dilution of STREX cDNA over a starting concentration range of 2ng- 20fg as template, and a

standard curve generated as before. Using the slope of the standard curve, the efficiency of amplification using this primer set was calculated to be 2.12, whilst there was a very high correlation coefficient between the data and trendline, > 0.99. These data suggest that the STREX- specific Taqman primer set can be used to quantify the starting concentration of STREX in an unknown sample with a high degree of accuracy over a dynamic range of five orders of magnitude (fig. 4-9).

4-2-1-8 Competition standard curve using the STREX BK channel Taqman assay

Although the STREX Taqman primer set does not share any sequence with the other alternatively spliced variants of the BK channel, it was useful to confirm the sensitivity of the primer set by generating a standard curve in the presence of a constant concentration of non- target DNA. The STREX BK channel- specific Taqman primer set was used again to generate a standard curve, this time with a constant 20pg of IYF cDNA present in each reaction. The efficiency was calculated to be 2.07, and the correlation coefficient for this standard curve was > 0.99. From this data, it can be concluded that the STREX Taqman primer and probe set has a high specificity for the STREX BK channel splice variant, and that it is also able to amplify its target with equal efficiency at a starting concentration of 20fg, even where there may be a hundred thousand- fold excess of non- target DNA present (fig. 4-9). No amplification was observed when the STREX- specific Taqman primers were used to assay IYF cDNA alone.

Figure 4-9
Standard curve generated using STREX- specific Taqman real time PCR primer and probe set

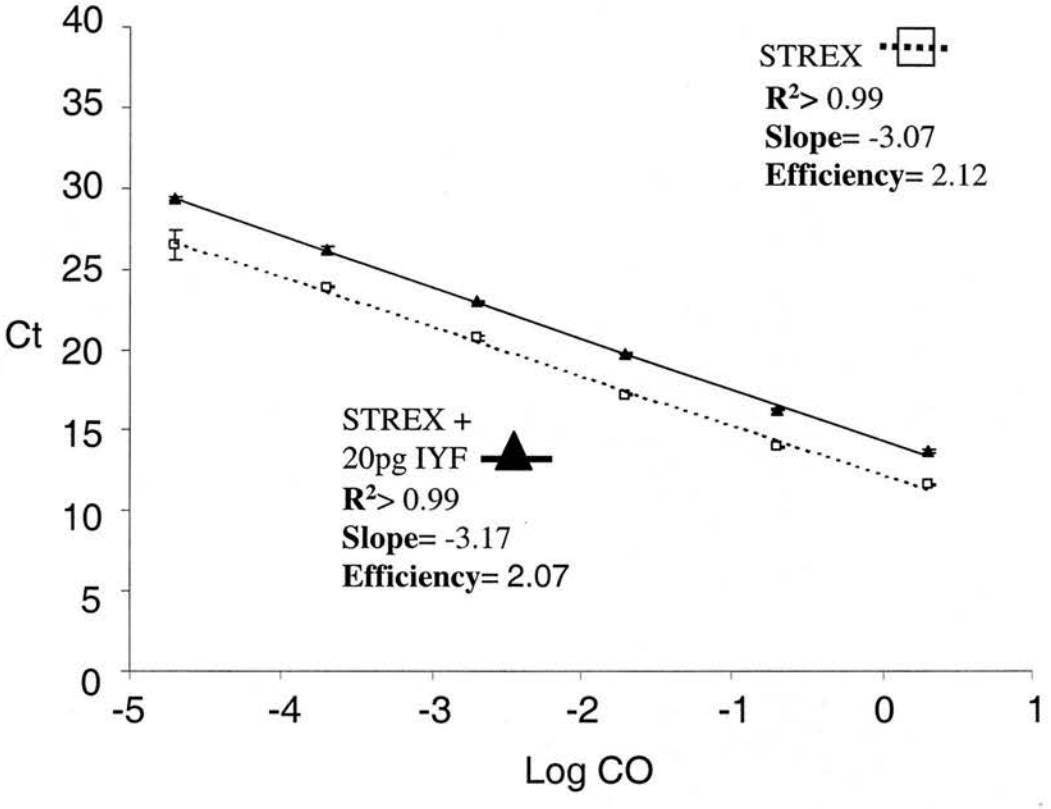

Figure 4-9 Standard curve generated using STREX-specific Taqman real time PCR primer and probe set

Using a logarithmic dilution of STREX DNA, over seven orders of magnitude, with starting quantities of 2ng- 20fg as template, triplicate 25µl reactions were run using the STREX Taqman primer and probe set, in 1x Taqman Universal PCR mastermix (open squares, dashed trendline). The same reactions were also performed in the presence of a constant 20pg of IYF DNA as a competing template (filled triangles, solid trendline). Data shown as triplicate Cts for each starting concentration (log scale) ± SEM. Correlation coefficient, slope and calculated efficiency are also shown.

4-2-1-9 Design of a Δe23 BK channel splice variant- specific Taqman assay

The Δe23 BK channel alternative splice variant differs from the other splice variants investigated during this study as it results in exclusion of exon 23, normally encoding the channel downstream of splice site 2. The resulting 1bp frame- shift generates a stop codon close to the start of exon 24, causing this splice variant to encode a truncated channel. Design and optimisation of the Δe23 BK channel alternative splice variant assay was performed by Dr. Lie Chen.

In the case of Δe23, the Taqman probe was designed to span the splice junction at site C2, with the reverse primer annealing within exon 24. Three 25µl reactions were prepared, incorporating the Δe23- specific Taqman primer set in 1x Taqman Universal PCR master mix, using a logarithmic dilution of Δe23 cDNA over a starting concentration range of 2ng- 20fg as template, and a standard curve generated as before. Efficiency of this primer set was calculated, using the slope of the standard curve, to be 2.04, whilst there was a very high (> 0.99) correlation coefficient between the data and the trendline, indicating that this primer can be used to accurately determine the starting concentration of Δe23 in an unknown sample over a dynamic range of five orders of magnitude (fig. 4-10).

4-2-1-10 Design of a total BK channel Taqman assay

The recent rise in the use of quantitative real- time PCR in gene expression, mutation, genotyping and chimeric analyses has led to the development, by companies such as Applied Biosystems, of ready- made Taqman assays against a

Figure 4-10
Standard curve generated using Δe23- specific Taqman real time PCR primer and probe set

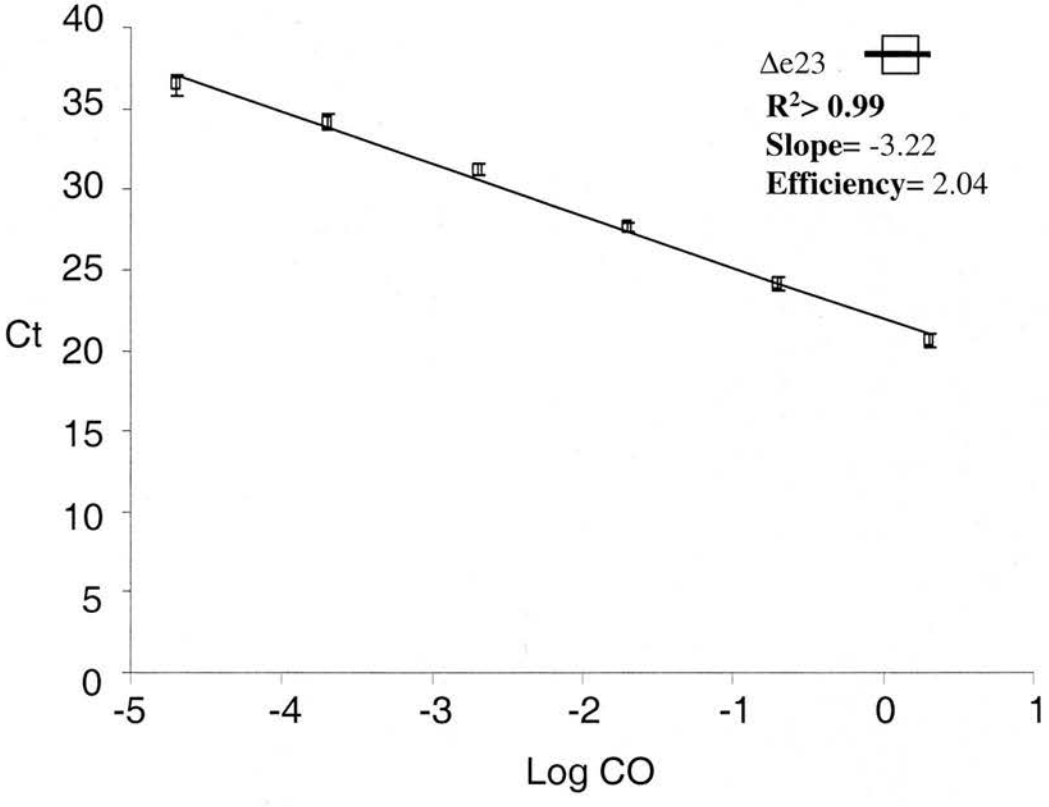

Figure 4-10 Standard curve generated using Δe23- specific Taqman real time PCR primer and probe set

Using a logarithmic dilution of Δe23 DNA, over seven orders of magnitude, with starting quantities of 2ng- 20fg as template, triplicate 25µl reactions were run using the Δe23 Taqman primer and probe set, in 1x Taqman Universal PCR mastermix (open squares, solid trendline). Data shown as triplicate Cts for each starting concentration (log scale) ± SEM. Correlation coefficient, slope and calculated efficiency are also shown. (Δe23- specific Taqman assay was designed by Dr. Lie Chen, who also generated the results shown in this figure).

vast number of targets, in human, mouse and rat, although these are mainly gene-specific, rather than splice variant- specific. Assay ID **Mm00516078_m1**, specific to mouse BK channel (fig. 4-4), was tested with the aim of using it as a normaliser against the other, splice variant- specific assays, and potentially establishing a protocol for relative quantitation of BK channel alternative splice variant expression using the comparative Ct method, eliminating the requirement for a standard curve in each run.

The target sequence of the mouse BK Assay on Demand primer set is located downstream of the C- terminal sites of alternative splicing, therefore ZERO, IYF, Exon22 and STREX splice variants should all be detected, regardless of splicing conformation. Triplicate 25 µl reactions were prepared in 1x Taqman Universal PCR master mix, with the mouse BK assay on demand primer set, using a logarithmic dilution of STREX cDNA as template over a starting concentration range of 2ng-20fg, and a standard curve was prepared. From this, the efficiency of the Assay on Demand mouse BK primer set was calculated to be 1.97, whilst the correlation coefficient was > 0.99. These results indicate that the mouse BK channel- specific Assay on Demand real time PCR may be used to accurately determine the starting concentration of mouse BK channel in an unknown sample when run in parallel conditions, by extrapolation of its Ct from the standard curve (fig. 4-11).

The Assay on Demand for mouse BK channel targets the sequence downstream of the C- terminal alternative splicing sites, which in theory should be present in all splice variants. However, in order to preclude the possibility of being unable to

Figure 4-11
Standard curve generated using Applied Biosystems' Assay on Demand mouse total BK primer set

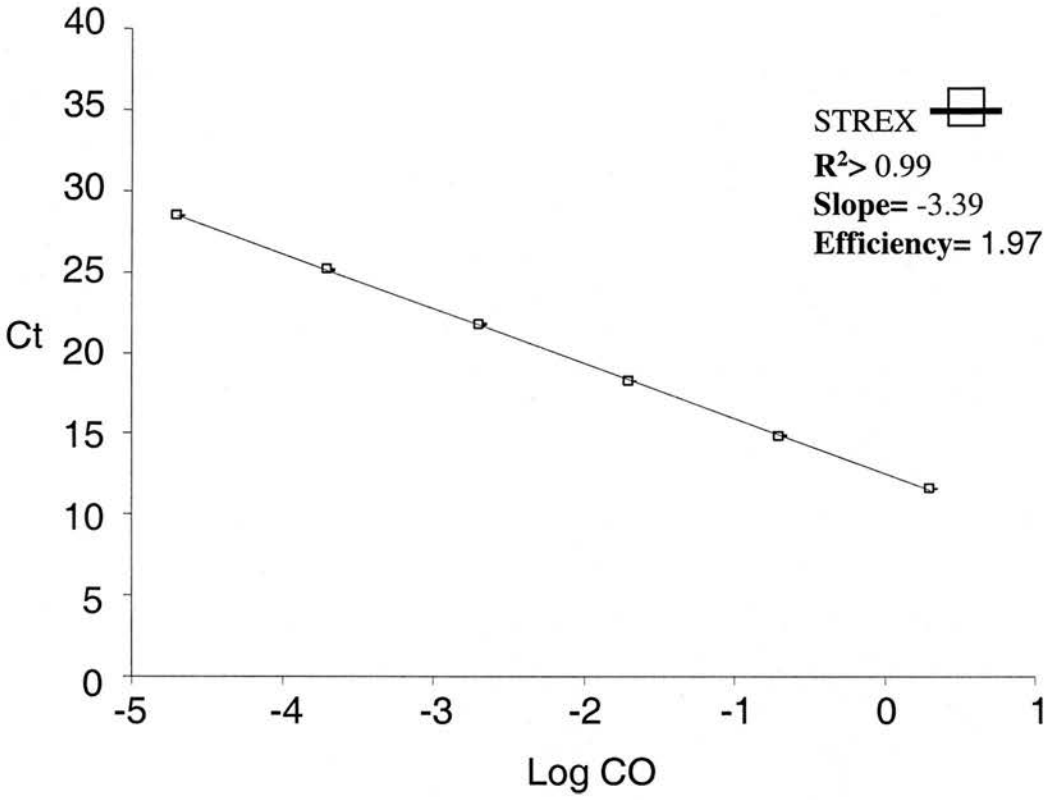

Figure 4-11 Standard curve generated using Applied Biosystems' Assay on Demand mouse total BK primer set

Using a logarithmic dilution of STREX (open squares, solid trendline) cDNA over seven orders of magnitude, with starting quantities of 2ng- 20fg, as template, triplicate 25µl reactions were run using Applied Biosystems' Assay on Demand for mouse BK channel, Assay ID Mm00516078_m1, primer and probe set, in 1x Taqman Universal PCR master mix. Data points shown as triplicate Cts for each starting concentration (log scale) ± SEM. Correlation coefficient (R^2), slope and calculated efficiency are also shown.

detect novel splice variants which give rise to a truncated channel, due to loss of the Assay on Demand target sequence, a Taqman primer and probe set was also designed upstream of the first C-terminal splice site (fig. 4-4). Triplicate 25µl reactions were set up using these primers, with a logarithmic dilution of either ZERO, STREX or IYF cDNA as template, over a starting concentration range of 2ng- 20fg, in 1x Taqman Universal PCR master mix, then standard curves were generated for each. Using the slope of the standard curves obtained, it was found that for ZERO, STREX or IYF template DNA, the efficiencies were almost identical- 1.95, 1.90 and 1.99 respectively. All three standard curves had very high correlation coefficients, all greater than 0.99. Taken together, these results indicate that this primer set can amplify the BK channel template with equal efficiency, regardless of the splice variant, and that data obtained can be reliably used to determine the concentration of BK channel sequence in a given sample using the relative standard curve assay (fig. 4-12). Table 4-1 summarises the sequences and amplicon length for all of the Taqman assays designed.

4-2-2 Validation of the comparative Ct method of quantitation using Taqman real time PCR assays

There has been shown to be no difference in accuracy of quantitation of samples when using either the relative standard curve, or comparative Ct method (Applied Biosystems, 2001, Dorak, 2005). However, it was of interest to try to establish a method for relative quantitation of BK channel alternative splice variant expression in unknown samples using comparative Ct analysis due to the high- throughput of this method, and lack of requirement for a standard curve in every run. To assess the

Figure 4-12
Standard curves generated using total BK Taqman real time PCR primer and probe set

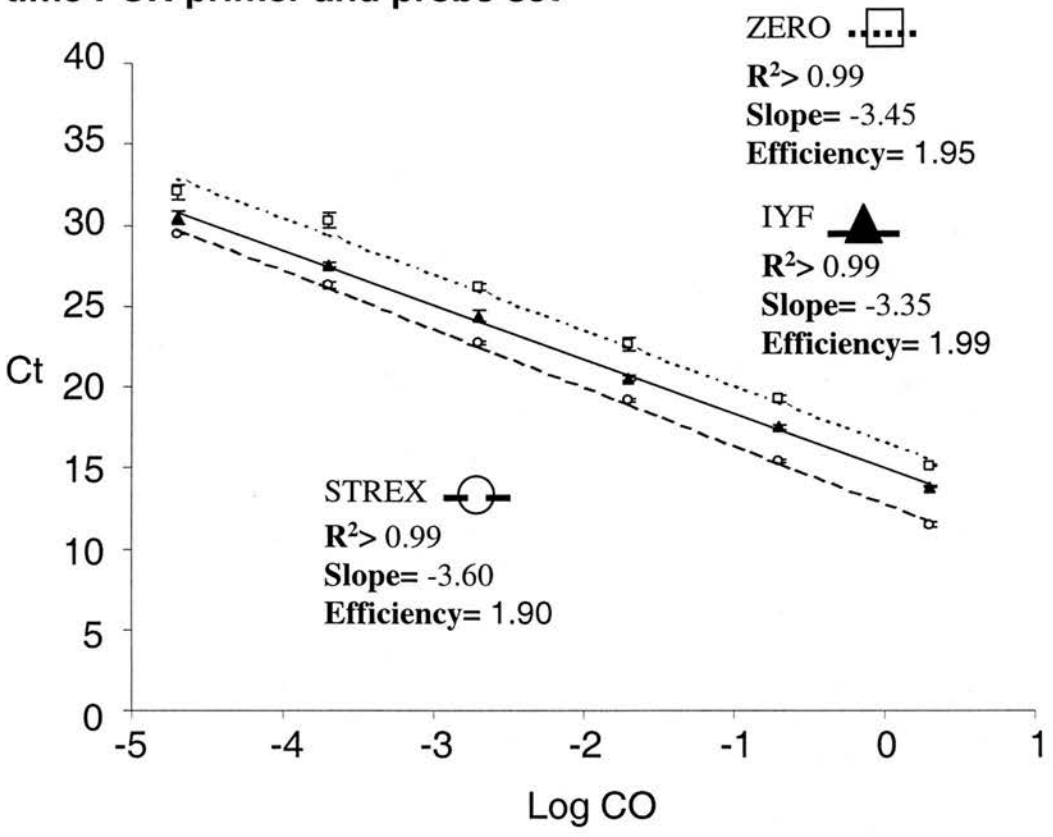

Figure 4-12 Standard curves generated using total BK Taqman real time PCR primer set

Using a logarithmic dilution of ZERO (open squares, dotted trendline), IYF (solid triangles, solid trendline) or STREX (open circles, dashed trendline) DNA over seven orders of magnitude, with starting quantities of 2ng- 20fg, as template, triplicate 25µl reactions were run using the total BK Taqman primer and probe set, in 1x Taqman Universal PCR master mix. Data points shown as triplicate Cts for each starting concentration (log scale) ± SEM. Correlation coefficient (R^2), slope and calculated efficiency are also shown.

Table 4-1
Primers used in optimisation of real time PCR protocols

Primer set		Sequence	Amplicon length
ZERO	F	GCCAAAGAAGTTAAAAGGGCATT	110bp
	R	CGGCTGCTCATCTTCAAGC	
	P	TGACGTCACAGATCCCAAAAGAATTAAAAAATGTG	
STREX	F	TTTGATTGCGGACGTTCTGA	77bp
	R	TCTCTCAAGGGTGTCCACGTTAC	
	P	CTGCTCGTGCATGTCAGGCCGT	
IYF	F	CTGCAGGCGGCTGATCTATTTT	75bp
	R	GCCCCCATTACGTTGTTTTTT	
	P	CAGCCGCCAACCCTGTCACCA	
Exon22	F	GCAGGCGGCTCAAGGTT	69bp
	R	GGAGTCGCATTCTTGTGCATAA	
	P	AAGCTAGAGCCCGCTATCACAAAGACCCA	
Total BK	F	CTCCAATGAAATGTACACAGAATATCTC	103bp
	R	CTATCATCAGGAGCTTAAGCTTCACA	
	P	CCTTCGTGGGTCTGTCCTTCCCTACTGTT	
Δe23	F	GACGTCACAGATCCCAAAAGAAT	78bp
	R	TGATCATTGCCAGGAATTAACAA	
	P	CTGCAGGCGGCGCATGACC	

Table 4-1 Primers used in optimisation of real-time PCR protocols

Forward (F), reverse (R) and Probe (P) sequences and amplicon length are shown for each primer set used. All Taqman probes were 5' labelled with FAM and 3' labelled with TAMRA.

suitability of the primer sets for use in such analysis, average Ct values, generated using ZERO, IYF and STREX as a template, for the total BK primer set were subtracted from those of each splice variant assay at each starting quantity, to give a difference in Ct values (dCt). These were then averaged for triplicate reactions, and plotted against log starting concentration to generate comparative efficiency plots. In all cases, the slope of the trendline was greater than 0.1 or less than –0.1, indicating that the efficiencies of amplification for the total BK primer set and the splice variant- specific assays were not close enough for them to be used for the comparative Ct method of quantitation (fig. 4-13).

4-2-3 BK channel alternative splice variant expression across mouse tissues

cDNA from a range of adult mouse tissues and selected embryonic stages (Mouse Rapidscan cDNA array (Origene)) was screened using previously generated Taqman PCR primer and probe sets specific to ZERO, IYF, Exon 22, STREX and Δe23 BK channel alternative splice variants, as well as Applied Biosystems "Assay on demand" for mouse BK channel, assay ID **Mm00516078_m1.** 25µl reactions were prepared containing 0.4µg total cDNA from each mouse tissue/ embryonic stage, with each primer/ probe set in 1x Applied Biosystems' Taqman Universal PCR master mix. For quantitation, a triplicate standard curve was run in parallel, over a starting concentration range from 2ng- 0.2fg of cDNA appropriate to the primer/ probe set used. Expression in each tissue was normalised to 19- day embryo, and expressed as a percentage of E19. For each splice variant assay, cDNA from several separate arrays was quantified and results averaged, therefore (n= X) represents

Figure 4-13
Relative efficiency plots of BK channel splice variant-specific Taqman assays compared with total BK primers

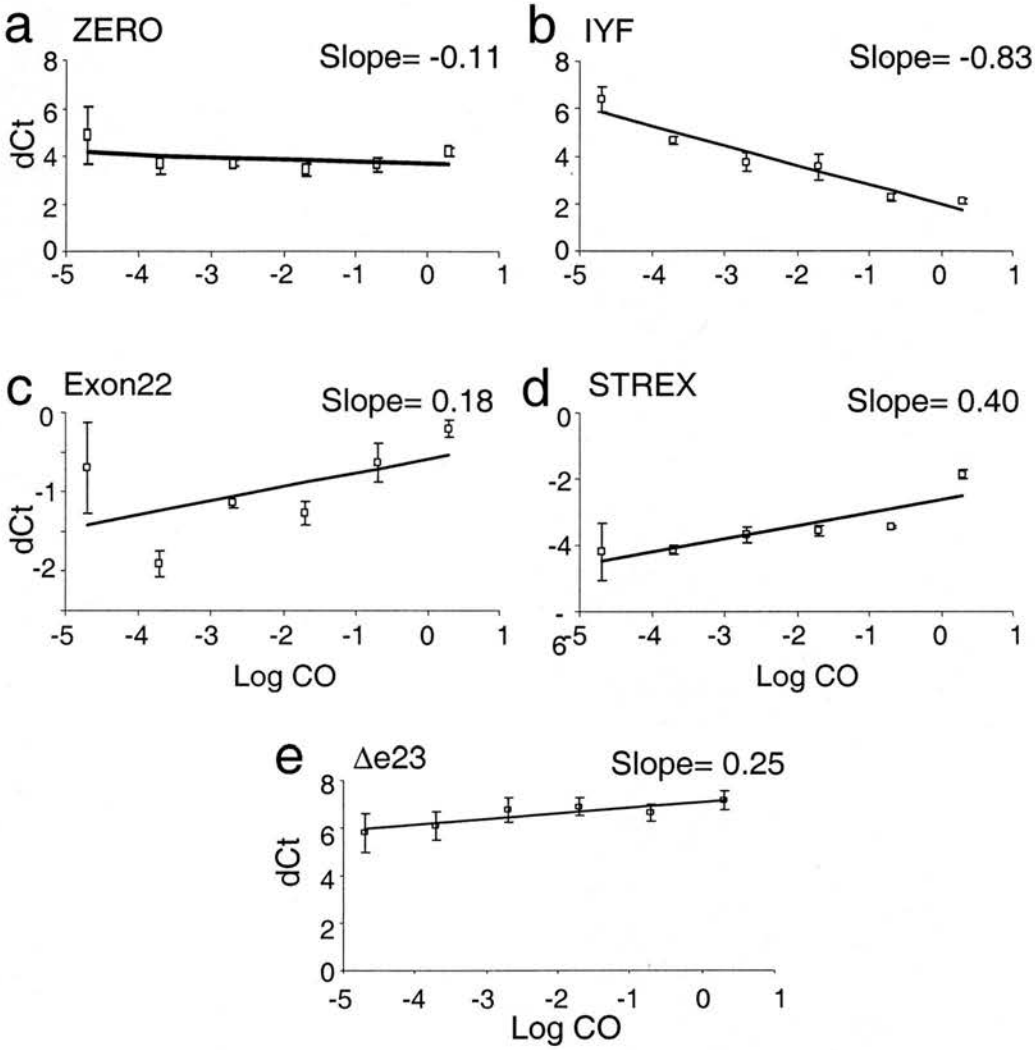

Figure 4-13 Relative efficiency plots of BK channel splice variant- specific Taqman assays compared with total BK primers

dCt values were calculated in triplicate by subtracting the mean Ct for the total BK Taqman primer set from the Ct at each starting concentration for **(a)** ZERO, **(b)** IYF, **(c)** Exon 22, **(d)** STREX and **e)** Δe23 real time PCR primer sets. The mean dCt values were then plotted against log input concentration, +/- SEM to give the relative efficiency plot for each splice variant- specific primer set, compared with the total BK primer set. A trendline slope between –0.1 and 0.1 indicates that the splice variant- specific primer set can be used with the total BK primer set for the comparative Ct assay.

the number of independent experiments performed. Although much of the previous work on BK channel alternative splicing has focused on the characterisation of individual splice variants from tissues (Saito *et al.*, 1997, Skinner *et al.*, 2003, Tian *et al.*, 2003), an approach using the Taqman assays created during this study will enable detailed profiling of the pattern of alternative splice variants across tissues of whole animals, or in combination with specific cell isolation protocols, amongst populations of cells from the same tissue. By generating a pool of readily deployable BK channel alternative splice variant- specific assays, high- throughput screening of tissues for expression of alternative splice variants, or changes thereof in response to experimental manipulations will be possible.

4-2-3-1 Total BK channel mRNA expression in mouse tissues

Mouse tissues were screened for BK channel mRNA expression, then for each tissue the level of total BK channel mRNA was expressed as a percentage of that in the 19 day embryo. In the mouse brain, average total BK channel mRNA expression was 178.4 ± 48.0% (n= 10) of E19. BK channel mRNA expression in the heart was 3.1 ± 1.0% (n= 10) of E19, whilst that in the kidney and spleen was 21.1 ± 6.0% (n= 10) and 9.8 ± 3.6% (n= 10) of E19 respectively. Average thymic BK channel mRNA expression was 39.0 ± 21.5% (n= 10) of E19. In the liver, BK channel mRNA expression was 3.0 ± 3.1% (n= 10) of E19, whilst that in the stomach was 64.1 ± 22.3% (n= 10) of E19. Small intestine total BK channel mRNA expression was 26.5 ± 5.1% (n=10) of that at E19. Skeletal muscle BK channel mRNA expression was 18.9 ± 3.9% (n= 10), whilst in lung, total BK mRNA expression was 8.8 ± 2.2% (n= 10) of that in the 19- day embryo. In the testis, the level of BK channel mRNA was

36.5 ± 8.2% (n= 10) of E19, whilst that of the skin was 17.8 ± 4.4% (n= 10) of E19. In the adrenal gland, average total BK mRNA expression was 69.7 ± 21.0% (n= 10) of E19. Pancreas expression was 10.3 ± 2.4% (n= 10), whilst that in the uterus was 27.4 ± 5.2% (n= 10) of E19. In the prostate, total BK mRNA expression was 121.9 ± 15.2% (n= 10) of E19. Pituitary BK channel expression was 78.0 ± 16.0% (n= 10) of E19 (fig. 4-14).

cDNA from mouse breast was also screened for BK channel expression, under various conditions. In the virgin breast, average total BK mRNA expression was 19.7 ± 3.9% (n= 10), whilst that in the breast of pregnant mice was 26.4 ± 6.9% (n= 10) of E19. During lactation, breast total BK channel mRNA expression was 24.6 ± 6.3% (n= 10) of E19, whilst in the involuting breast, total BK channel mRNA expression was 58.3 ± 34.3% (n= 10) of E19 (fig. 4-14).

Additionally, cDNA from whole mouse embryo at a range of developmental stages was assayed for total BK channel expression. At 8.5 days, the level of total BK channel mRNA expression in the mouse embryo was 16.3 ± 5.3% (n= 10) of E19. In the 9.5- day embryo, average total BK mRNA expression was 12.9 ± 3.9% (n= 10) of E19, whilst that in the 12.5- day embryo was 55.8 ± 9.2% (n= 10) of E19 (fig. 4-14). At 8.5 days, embryonic total BK channel mRNA expression was significantly ($p < 0.01$) lower than at E12.5 and E19. At E9.5, total BK mRNA expression was also significantly ($p < 0.01$) lower than at E12.5 and E19, whilst expression at E12.5 was also significantly lower ($p < 0.01$) than at E19.

Figure 4-14
Expression of total BK channel and ZERO BK channel alternative splice variant mRNA in mouse tissues relative to E19

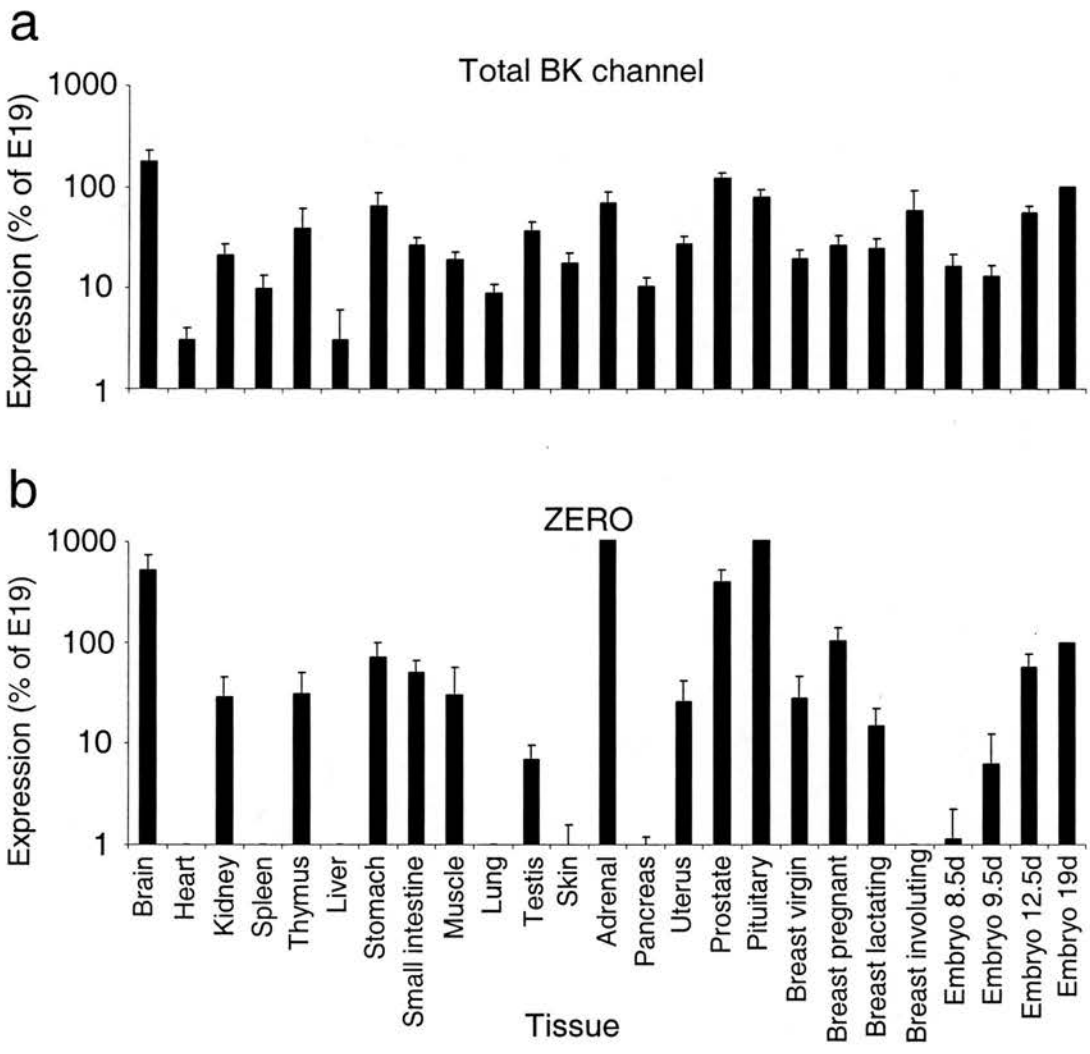

Figure 4-14 Expression of total BK channel and ZERO BK channel alternative splice variant mRNA in mouse tissue relative to E19

Showing expression of **a)** total BK channel (n= 10) and **b)** ZERO (n= 6) BK channel alternative splice variant mRNA as a percentage of expression in the 19-day mouse embryo for a range of mouse tissues on a logarithmic scale.

4-2-3-2 ZERO BK channel alternative splice variant mRNA expression in mouse tissues

The average level of mRNA expression of ZERO in mouse brain was 514.6 ± 218.5% (n= 6) of E19. No ZERO mRNA expression was detected in the heart. In the kidney, ZERO mRNA expression was 28.4 ± 16.8% (n= 6) of E19. In the spleen, no expression of ZERO mRNA was detected. Thymic ZERO mRNA expression was 30.5 ± 19.6% (n= 6) of that in E19, whilst no detectable ZERO mRNA expression was observed in the liver. In the stomach, ZERO mRNA expression was 71.9 ± 23.6% (n= 6) of that in the 19- day embryo, whilst that of the small intestine was 49.8 ± 15.5% (n= 6) of E19. In muscle, average ZERO mRNA expression was 30.2 ± 26.4% (n= 6) of E19. No ZERO mRNA expression was detected in the lung. In the testis, ZERO mRNA expression was 6.9 ± 2.7% (n= 6) of E19, whilst that in the skin was 0.8 ± 0.8% (n= 6) of E19. Adrenal gland expression of ZERO mRNA was 1289.4 ± 873.5% (n= 6) of E19. In the pancreas, ZERO mRNA expression was 0.6 ± 0.6% (n= 6) of E19. ZERO mRNA expression in the uterus was 25.8 ± 16.2% (n= 6), whilst that in the prostate was 405.7 ± 125.7% (n= 6) of E19. In the pituitary, ZERO mRNA expression was 1200.0 ± 238.0% (n= 6) of E19 (fig. 4-14).

In the virgin breast, average ZERO mRNA expression was 27.7 ± 18.3% (n= 6) of E19, whilst in pregnant mice, the level of expression of ZERO mRNA in the breast was 104.5 ± 36.9% (n= 6) of E19. ZERO mRNA expression in the lactating breast was 14.8 ± 7.4% of E19 (n= 6), whilst no expression of ZERO mRNA was detected in the involuting breast (fig. 4-14).

In the 8.5- day embryo, average ZERO mRNA expression was 1.1 ± 1.1% (n= 6) of E19. At 9.5 days, embryonic ZERO mRNA expression was 6.2 ± 6.1% (n= 6) of E19. In the 12.5-day embryo, the level of ZERO mRNA expression was 57.2 ± 19.7% (n= 6) of that at E19 (fig. 4-14). ZERO mRNA expression in the 8.5- day embryo was significantly ($p < 0.01$) lower than at either E12.5 or E19. At 9.5 days, ZERO mRNA expression was also significantly lower than that at 12.5 days ($p < 0.05$) and at 19 days ($p < 0.01$).

Mouse Rapidscan cDNA arrays were also screened for the IYF alternative splice variant of the BK channel, however in all tissues, mRNA expression of this splice variant was below the limit of detection for this assay.

4-2-3-3 STREX BK channel alternative splice variant mRNA expression mouse tissues

In mouse brain, expression of STREX mRNA was 35.4 ± 15.2% (n= 5) of that in the 19- day embryo. Average STREX mRNA expression in the heart was 1.75 ± 1.75% (n= 5) of E19. In the kidney, STREX mRNA expression was 14.3 ± 10.4% (n= 5), whilst that in the spleen was 1.9 ± 1.9% (n= 5) of E19. Thymic STREX mRNA expression was 1.6 ± 1.6% of E19 (n= 5). In the liver, no detectable STREX mRNA expression was observed. Stomach STREX mRNA expression was 28.4 ± 15.8% (n= 5) of E19, whilst that of the small intestine was 13.1 ± 10.1% (n= 5) of E19. Average STREX mRNA expression in muscle was 6.0 ± 5.3% (n= 5) of E19. In the lung, STREX mRNA expression was 6.3 ± 6.2% (n= 5) of E19. In the testis, STREX mRNA expression was 14.1 ± 14.1% (n= 5) of that in E19. Skin STREX mRNA

expression was 1.1 ± 1.1% (n= 5) of E19. In the adrenal gland STREX mRNA expression was 575.2 ± 81.9% (n= 5) of E19. In the pancreas, the level of STREX mRNA expression was 8.7 ± 8.3% (n= 5) of that at E19. Average STREX mRNA expression in the uterus was 26.6 ± 7.3% (n= 5) of E19, whilst that in the prostate was 407.0 ± 33.5% (n= 5) of E19. In the pituitary, average STREX mRNA expression was 549.0 ± 45.0% (n= 5) of that at E19 (fig. 4-15).

In the virgin breast, average STREX mRNA expression was 36.1 ± 17.0% (n= 5) of E19. In the breast during pregnancy, the level of STREX mRNA expression was 21.5 ± 8.4% (n= 5) of E19. STREX mRNA expression in the lactating breast was 16.6 ± 11.7% (n= 5) of E19. In the involuting breast, average STREX mRNA expression was 1.5 ± 1.5% (n= 5) of E19 (fig. 4-15).

STREX expression was also found to change during embryogenesis. In the 8.5- day embryo, average STREX mRNA expression was 8.1 ± 4.8% (n= 5) of E19, whilst that in the 9.5- day embryo was 3.3 ± 3.3% (n= 5) of E19. At 12.5 days, embryonic STREX mRNA expression was 78.6 ± 11.7% (n= 5) of E19 (fig. 4-15). At both 8.5 and 9.5 days, embryonic STREX mRNA expression was significantly ($p < 0.01$) lower than that in either the 12.5- or 19- day embryo.

4-2-3-4 Exon22 BK channel alternative splice variant mRNA expression in mouse tissues

Expression of the Exon22 BK channel alternative splice variant was also investigated in mouse tissues. No mRNA expression of Exon22 was detected in the brain, heart,

Figure 4-15
Expression of STREX and Exon22 BK channel alternative splice variant mRNA in mouse tissues relative to E19

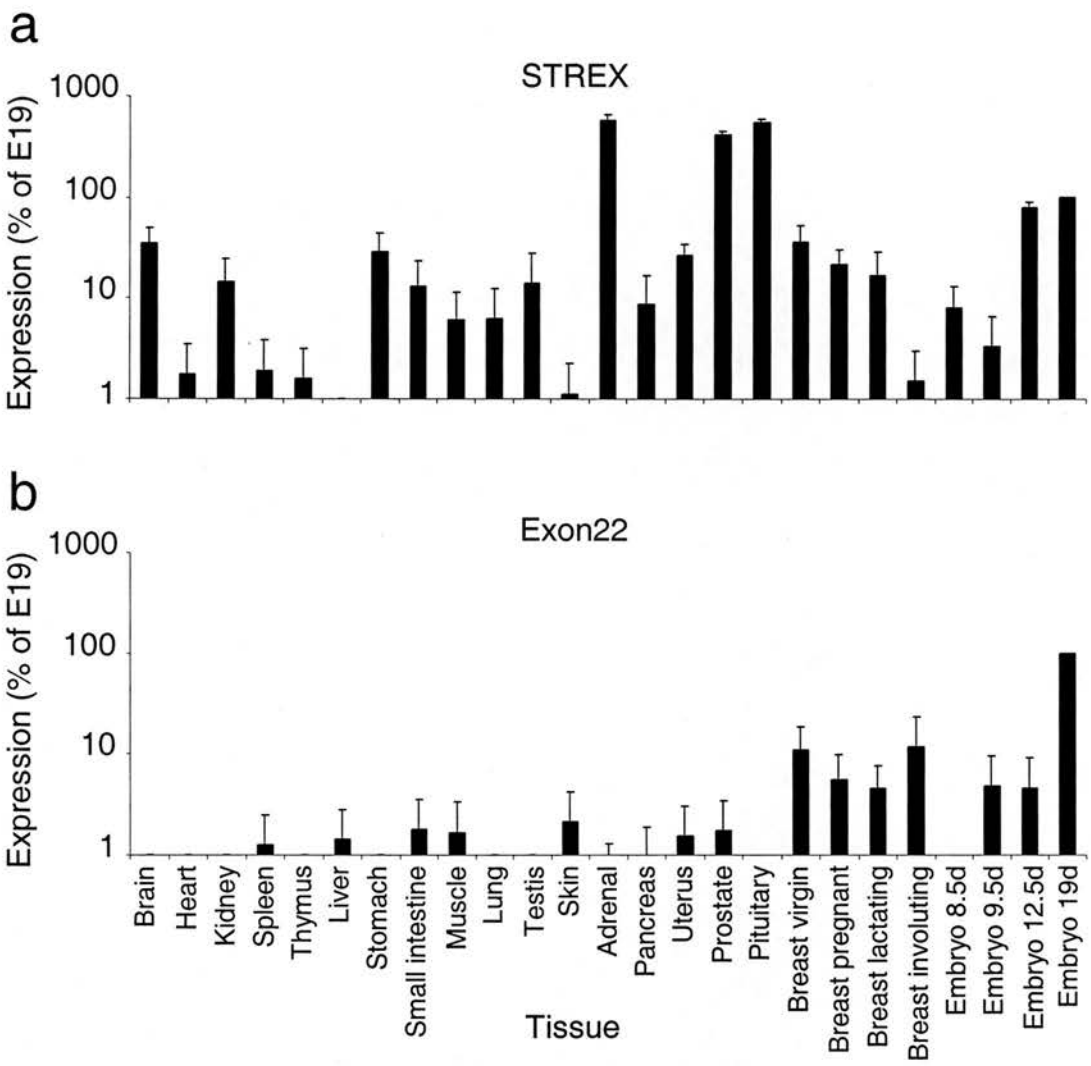

Figure 4-15 Expression of STREX and Exon22 BK channel alternative splice variant mRNA in mouse tissues relative to E19

Showing expression of **a)** STREX (n= 5) and **b)** Exon22 (n= 3) BK channel alternative splice variant mRNA as a percentage of expression in the 19- day mouse embryo for a range of mouse tissues on a logarithmic scale.

kidney, thymus, stomach, lung, testis, and pituitary. In the spleen, average Exon22 mRNA expression was 1.3 ± 1.2% (n= 3) of E19. Liver Exon22 mRNA expression was 1.4 ± 1.4% (n= 3) of E19. In the small intestine, average Exon22 mRNA expression was 1.8 ± 1.8% (n= 3), whilst that in muscle was 1.7 ± 1.7% (n= 3) of E19. Exon22 mRNA expression in skin was 2.1 ± 2.1% (n= 3) of E19. Adrenal gland Exon22 mRNA expression was 0.7 ± 0.6% (n= 3) of E19. Pancreas mRNA expression of Exon22 was 1.0 ± 0.9% (n= 3), whilst that in the uterus was 1.5 ± 1.5% (n= 3) of E19. In the prostate, average Exon22 mRNA expression was 1.7 ± 1.7% (n= 3) of E19 (fig. 4-15).

In the virgin mouse breast, average Exon22 mRNA expression was 10.7 ± 7.9% (n=3) of E19, whilst that in the breast during pregnancy was 5.6 ± 4.3% (n= 3) of E19. During lactation, average level of Exon22 mRNA expression in the breast was 4.6 ± 3.0% (n= 3) of E19, whilst that in the involuting breast was 11.6 ± 11.5% (n= 3) of E19 (fig. 4-15).

In the 8.5-day embryo, the average Exon22 mRNA expression was 0.5 ± 0.5% (n= 3) of that at E19. Exon22 mRNA expression in the 9.5- day embryo was 4.8 ± 4.7% (n= 3) of E19, whilst that in the 12.5- day embryo was 4.6 ± 4.5% (n= 3) of E19 (fig. 4-15). During embryogenesis, the level expression of Exon22 mRNA was significantly ($p< 0.01$) higher than at E8.5, E9.5 and E12.5.

4-2-3-5 Δe23 BK channel alternative splice variant mRNA expression in mouse tissues

Mouse tissues were also screened for expression of the truncated BK channel alternative splice variant, Δe23. In the brain, average Δe23 mRNA expression was 72.2 ± 17.0% (n= 3) of that in the 19-day embryo. Heart Δe23 mRNA expression was 56.0 ± 19.0% (n= 3) of E19. In the kidney, average Δe23 mRNA expression was 35.4 ± 20.0% (n= 3), whilst that in the spleen was 77.4 ± 15.0% (n= 3) of E19. Average thymic Δe23 mRNA expression was 50.1 ± 16.0% (n= 3) of E19. In the liver, the level of Δe23 mRNA expression was 69.2 ± 43.0% (n= 3) of that in the 19-day embryo. Average Δe23 mRNA expression in the stomach was 67.9 ± 25.0% (n= 3), whilst that in the small intestine was 71.8 ± 12.0% (n= 3) of E19. Δe23 mRNA expression in muscle was 59.2 ± 23.0% (n= 3) of that in E19. In the lung, average Δe23 mRNA expression was 99.8 ± 14.0% (n= 3) of E19. Testis Δe23 mRNA expression was 42.5 ± 9.0% (n= 3) of E19. Average Δe23 mRNA expression in skin was 44.0 ± 8.0% (n= 3) of E19, whilst that in the adrenal gland was 56.4 ± 5.6% (n= 3) of that in the 19-day embryo. The level of pancreas Δe23 mRNA expression was 33.2 ± 21.0% (n= 3) of E19. In the uterus, average Δe23 mRNA expression was 61.8 ± 16.0 (n= 3), whilst that of the prostate was 45.3 ± 5.0% (n= 3) of E19. Pituitary expression of Δe23 mRNA was 51.0 ± 26.0% (n= 3) of E19 (fig. 4-16).

Δe23 mRNA expression in the virgin breast was 61.0 ± 12.0% (n= 3) of E19, whilst that in the breast of pregnant mice was 137.7 ± 31.0% (n= 3) of E19. In the lactating breast, Δe23 mRNA expression was 62.9 ± 24.0% (n= 3) of E19, whilst in the

Figure 4-16
Expression of Δe23 BK channel alternative splice variant mRNA in mouse tissues relative to E19

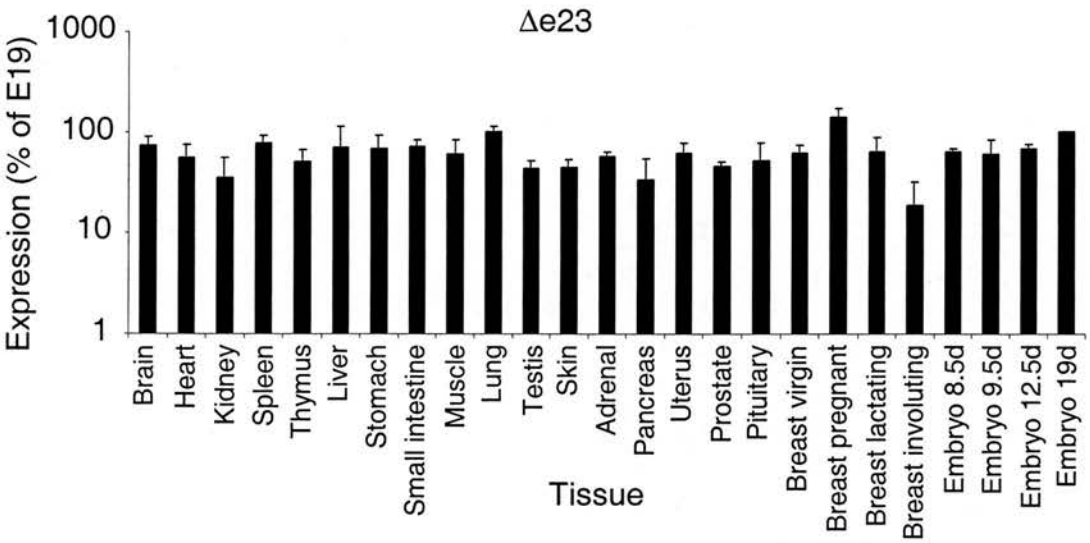

Figure 4-16 Expression of Δe23 BK channel alternative splice variant mRNA in mouse tissues relative to E19

Showing expression of Δe23 (n= 3) BK channel alternative splice variant mRNA as a percentage of expression in the 19- day mouse embryo for a range of mouse tissues on a logarithmic scale.

involuting breast the average level of Δe23 mRNA expression was 18.4 ± 13.0% (n= 3) of E19 (fig. 4-16).

During embryogenesis, the level of Δe23 mRNA expression in the whole embryo was investigated over the course of development. In the 8.5- day embryo, the average level of Δe23 mRNA expression was 63.3 ± 4.0% (n= 3) of E19, whilst that in the 9.5- day embryo was 60.3 ± 23.0% (n= 3) of E19. At 12.5 days, average expression of Δe23 mRNA was 68.6 ± 7.0% (n= 3) of E19 (fig. 4-16).

4-2-4 Relative expression of BK channel alternative splice variants in mouse tissues

In order to investigate the proportional representation of each BK channel alternative splice variant in mouse tissues, mRNA expression levels of ZERO, STREX, Exon22 and Δe23 were expressed as a percentage of total BK channel mRNA (fig. 4-17). The BK channel alternative splice variants were found to be differentially expressed across tissues. For example, in mouse brain, ZERO was the predominantly-expressed alternative splice variant, whilst in tissues such as the pancreas, ZERO comprised a smaller proportion of BK channel transcripts. Additionally, the mRNA expression of several BK channel alternative splice variants was found to vary relative to total BK channel mRNA expression both during different physiological states in the mouse breast, and also across development of the mouse embryo.

Figure 4-17
Relative expression of BK channel alternative splice variant mRNA in mouse tissues

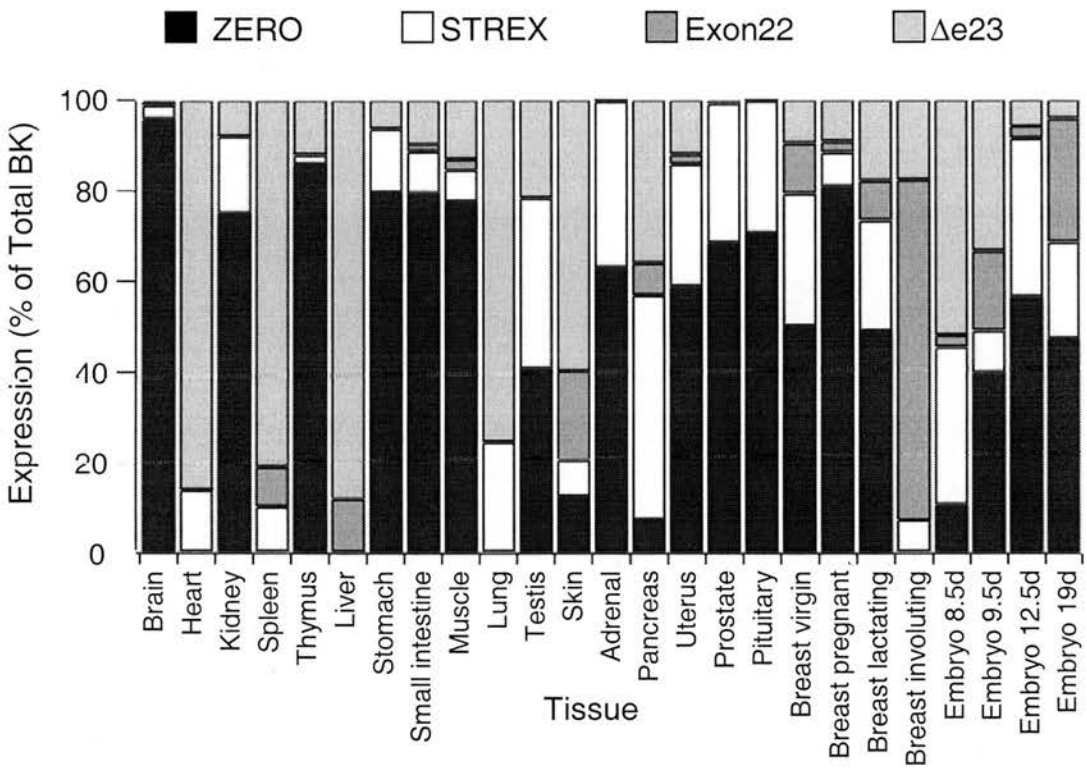

Figure 4-17 Relative expression of BK channel alternative splice variant mRNA in mouse tissues

Showing BK channel ZERO (black bars), STREX (white bars), Exon22 (dark grey bars) and Δe23 (light grey bars) alternative splice variant mRNA expression as a percentage of total BK channel mRNA for a range of mouse tissues and embryonic stages. Average mRNA expression for each splice variant was determined, then calculated as a percentage of total BK channel expression in each tissue. In this case, results were NOT normalised to 19-day embryo expression. Splice variant expression at less than 1% of total BK channel is not shown.

4-3 Summary

4-3-1 Design of BK channel alternative splice variant real time PCR assays

The BK channel alternative splice variant- specific Taqman real time PCR assays designed using the Primer Express program were shown to be sensitive over a starting concentration range of six orders of magnitude of starting template DNA, with high degree of correlation between the estimated values of the best fit line, and the actual data. The primer set that was initially designed against the IYF BK channel alternative splice variant was shown not to be specific to that splice variant alone. However, this did not preclude the use of the design strategy where a Taqman probe is generated with a 3' overhang across the splice junction, since this was used for the ZERO primer set, which was shown to specifically and accurately amplify only the ZERO BK channel alternative splice variant.

For all of the Taqman primer sets apart from the failed IYF set, the R^2 value was consistently close to 1, indicating that quantitation of unknown samples by extrapolation of their Ct value from the standard curves can be performed with a high degree of accuracy. Standard curves generated in the presence of a fixed amount of competing cDNA still showed positive correlation between trendline and data. Although the efficiency of the IYF- specific primer set was lower than for the other sets, it appeared to be specific, as neither the efficiency nor the R^2 value was altered greatly by the inclusion of an excess of competing template in the standard curve reactions.

All five sets of Taqman primers and probes generated using Primer Express appear to amplify their target sequence very specifically, as the amplification of the lowest concentrations (0.2fg for STREX and total BK, 20fg for Exon22, IYF and ZERO primer sets (table 4-2)) was unaffected by the presence of a competing template several orders of magnitude greater in concentration. This data indicates that quantitation of BK channel splice variants which are normally present in very low-abundance may be possible, even in cases where more common BK isoforms may be present in much greater concentration. There is also the potential to optimise these primer sets for use in multiplex real time PCR assays, where two primer sets are used in the same PCR reaction, with spectrally distinct reporter dyes, enabling the simultaneous quantitation of more than one splice variant in the same sample (Wittwer *et al.*, 2001).

Another method would have been to use one or more of the primer sets for relative quantitation using the comparative Ct method. However, although the primer and probe sets designed using Primer Express were specific and accurate enough to enable relative standard curve quantitation of samples, their efficiencies were not sufficiently similar to that of either of the total BK assays to justify the use of this type of analysis. Further optimisation via altering primer and Mg^{2+} concentrations etc. would be required in order to validate this method (Mason *et al.*, 2002). Therefore in this case, the absolute standard curve method is the preferred assay for the quantitation of BK channel alternative splice variant expression, and was used in all analyses in this thesis.

Table 4-2
Slope of standard curve and efficiencies for Taqman real time PCR primer sets

Primer Set	Template	Mean slope	Efficiency	Limit of detection
ZERO	ZERO	-3.64 ± 0.13	1.89 ± 0.05	20fg
IYF	IYF	-4.15 ± 0.03	1.74 ± 0.01	20fg
Exon 22	Exon 22	-3.19 ± 0.02	2.06 ± 0.01	20fg
STREX	STREX	-3.22 ± 0.03	2.04 ± 0.01	0.2fg
Δe23	Δe23	-3.22 ± 0.04	2.04 ± 0.04	20fg
AoD	STREX	-3.39 ± 0.00	1.97 ± 0.00	0.2fg
Total BK	ZERO	-3.45 ± 0.06	1.95 ± 0.02	0.2fg
Total BK	IYF	-3.46 ± 0.02	1.95 ± 0.01	0.2fg
Total BK	STREX	-3.56 ± 0.06	1.91 ± 0.02	0.2fg

Table 4-2 Slope of standard curve and efficiencies for Taqman real time PCR primer sets

For each Taqman primer and probe set, the template used in generating the standard curve from which the slope and efficiency were calculated is shown. Mean slope and efficiencies are calculated from 3 standard curves +/- SEM.

4-3-2 Differential expression of BK channel alternative splice variants in mouse tissues

Since it is known that BK channel expression may be delimited to certain tissues (Becker *et al.*, 1995) and subcellular regions (ZhuGe *et al.*, 2004, Bravo- Zehnder *et al.*, 2000, Knaus *et al.*, 1996) it is also intuitive to speculate that such distribution patterns are not ubiquitous to all BK channel splice variants, and expression in this defined manner may also be a direct result of alternative splicing of the channel, with certain splice variants influencing trafficking to specific regions (Zarei *et al.*, 2004). Results described in this chapter showed that, in addition to varying total BK channel expression across tissues, four of the known alternative splice variants of the BK channel, ZERO, Exon22, STREX and Δe23, were expressed at varying levels throughout the mouse, and further investigation is therefore required in order to determine the extent to which each splice variant contributes to the overall excitability of the cells in a particular tissue.

It may be the case that alternative splicing of the BK channel influences contractility of the smooth muscle in organs such as the stomach, small intestine and uterus, as it has been shown that the properties of native BK channels in smooth muscle from a range of sources are variable (McCobb *et al.*, 1995). Since expression of BK channel alternative splice variants can be dynamically regulated *in vivo* (Xie and McCobb, 1998), this suggests that the population of BK channels in a given tissue is not static, but can be altered to facilitate tuning of cell excitability to suit the current physiological requirements, or to enable subsets of channels to respond to specific signalling pathways (Tian *et al.*, 2001a, b).

It was found that expression of total BK channel relative to E19 was not significantly different in breast tissue of virgin mice compared to pregnant, lactating or involuting breast. However, a trend was observed of decreased expression of the ZERO, STREX and Δe23 alternative splice variants, although a large degree of variability was observed in the results, therefore only the ZERO alternative splice variant was found to be expressed at a significantly ($p< 0.05$) lower level in the involuting breast than in the pregnant breast. Further experiments are necessary to investigate the role of alternative splicing of the BK channel in the breast during and following pregnancy, and may reveal a possible role for the expression of specific splice variants under these conditions. For example, since the STREX alternative splice variant has been shown to confer glucocorticoid sensitivity on the BK channel, it may therefore be speculated that by expressing such a channel before and during pregnancy, tissues are 'primed' to respond rapidly to changes in hormone secretion during these physiological changes without the need for de novo channel synthesis. In the involuting breast, there may be a reduced requirement for rapid glucocorticoid-induced changes in cell excitability, therefore the expression of glucocorticoid-sensitive channels falls.

The multiple changes in the secretory paradigm that occur during and after pregnancy may influence BK channel splicing in several tissues. In the rat, it has been shown that late pregnancy is accompanied by changes in the electrophysiological properties of BK channels in the myometrium, and at the onset of parturition, the level of BK channel expression falls, possibly aiding uterine contractility (Song *et al.*, 1999). However, in late pregnancy in the mouse, the

opposite regulation occurs, with increased BK channel expression occurring, but also increased perinuclear accumulation of the channel protein, and diminished surface trafficking (Eghbali *et al.*, 2003), possibly achieving the same end. It may be the case that the mechanism responsible for this altered regulation is upregulated expression of the truncated, Δe23 BK channel alternative splice variant, which is not trafficked to the cell surface, but is instead localised in a perinuclear manner, and also prevents surface trafficking of other alternative splice variants (chapter 3), possibly by causing retention within the ER (Zarei *et al.*, 2004). Further investigation may therefore reveal whether expression of the Δe23 alternative splice variant in the mouse uterus is under hormonal control, and the extent to which it influences events of late pregnancy.

4-3-3 Regulated BK channel expression during mouse embryogenesis

During development of the mouse embryo, a trend of increasing total BK channel expression was observed. This is likely to be attributable to a requirement for increased expression during the patterning of systems where tight coupling of intracellular calcium with cell excitability is required. In addition to this, expression of several of the alternative splice variants of the BK channel was upregulated during development. Expression of ZERO and STREX were both found to be significantly higher at E12.5 and E19 than at E8.5 or E9.5, whilst expression of Exon22 was found to be significantly higher at E19 than E8.5, E9.5 or E12.5. The regulated expression of BK channel alternative splice variants may be of particular significance in development of specific systems within the embryo. For example, in *Xenopus,* expression of the xSlo59 BK channel alternative splice variant is delimited to

neurons, and only arises late in neuronal differentiation, whilst the other xSlo alternative splice variants are expressed in neurons and muscles, at several stages of development (Kukuljan *et al.*, 2003), and it may be the case that expression of splice variants such as Exon22 occurs in a similar, restricted manner.

Whilst the BK channel is implicated in control of smooth muscle contractility (Callera *et al.*, 2004, Archer *et al.*, 2003), as well as systems such as tonotopic organisation in the inner ear (Oberholtzer, 1999), the region with the highest total BK channel expression in this investigation was the brain. During mouse development, formation of the neural plate, from which the CNS develops, occurs at 7.5- 8 days (Downs and Davies, 1993), and since an upregulation of BK channel expression was observed shortly after this timepoint, it was speculated that this could be of significance for correct neuronal function in the developing CNS. Since BK channels are implicated in control of neurotransmitter release (Raffaelli *et al.*, 2004), and competitive elimination of synapses is required for normal CNS patterning (Ottersen, 2005), it might also be the case that the regulated expression of BK channel alternative splice variants in neurons of the developing CNS may contribute to regulation of signalling during such patterning, for example by conferring cell excitability phenotypes that are suited to more rapid, repetitive activity, thereby allowing increased rates of transmitter release.

Changing mRNA expression of BK channel alternative splice variants was observed during embryogenesis, and it was also found that splice variant mRNA expression changed as a proportion of total BK channel mRNA during development. Further

experiments are therefore required to investigate these developmentally- regulated changes in alternative splicing, in order to analyse the expression of BK channel alternative splice variants relative to total BK channel in specific tissues. Such an approach is taken in chapter 5, where the expression of the ZERO and STREX BK channel alternative splice variants is investigated in the tissues of the mouse CNS during development.

Chapter Five:

Regulation of BK channel alternative splicing during mouse CNS development

5-1 Introduction

5-1-1 Development of the central nervous system

Coordinated and selective gene expression enables central nervous system patterning (Rubenstein *et al.*, 1998, Carroll *et al.*, 2003). Many similarities exist among vertebrate species in the manner in which the tissues of the central nervous system are derived from the embryonic ectoderm (Rubenstein *et al.*, 1998). A critical point in embryogenesis is neurulation- the inward folding and closing of the neural plate to form the neural tube. Induction of the neural plate and formation of the neural tube is under the control of the organizer (reviewed in Lemaire and Kodjabachian 1996), a group of cells that arise in the endoderm, known as the node in the mouse (Beddington, 1994). Correct neurulation and neuronal proliferation is achieved via combinatorial control of differentiation and proliferation by multiple and complex interactions of signalling pathways. Significant regulators include retinoic acid (RA) (Wilson *et al.*, 2003), fibroblast growth factors (FGF) (Khot and Ghaskadbi, 2001), bone morphogenic proteins (BMP) (Selleck *et al.*, 1998), Wnts (Wu *et al.*, 2005) and Sonic Hedgehog proteins (Jarov *et al.*, 2003). Mechanisms modulating the activity of these secreted factors are themselves subject to multiple levels of control during development of the CNS. For example, retinoic acid is thought to be significant in the establishment of the neural tube; in quail chicks that have developed in the absence of RA, although neurulation occurs, significant abnormalities occur in both its morphology and cell proliferation (Wilson *et al.*, 2003). Disregulated expression of BMPs leads to defects in cell survival in developing tissues of the forebrain (Furuta *et al.*, 1997), and the coordinated secretion of BMP antagonists, noggin and

chordin prevents the severe, lethal deformities that arise following excess BMP activity (Anderson *et al.*, 2002).

The neural tube develops three enlargements in the anteroposterior direction: the prosencephalon (forebrain), mesencephalon (midbrain) and rhombencephalon (hindbrain). The prosencephalon expands laterally, at either side forming the telencephalon, which eventually gives rise to the cortex and other structures (Grove and Fukuchi-Shimogori, 2003), linked at the midline by the diencephalon, from which the thalamus, epithalamus, subthalamus and hypothalamus, amongst others, develop (Rubenstein *et al.*, 1998). The mesencephalon does not undergo morphological changes as extensive as those seen for the other CNS precursors, and develops into the midbrain (Liu and Joyner, 2001). The rhombencephalon expands to form two structures: the metencephalon - which gives rise to the cerebellum and pons - and the myelencephalon, from which the medulla develops (fig. 5-1).

5-1-2 BK channel in development

During chick development, an upregulation of BK channel expression is seen in spinal motoneurons around the time of neuromuscular innervation (Martin- Carballo and Dryer, 2002). Both retrograde signalling from the target tissue and also ongoing electrical activity were implicated as significant in developmental regulation of BK channel expression in this manner, and this type of regulation has been seen in other cell types from the central nervous system (Raucher and Dryer, 1995). Specific cell-cell interaction has also been shown to be critical for the correct expression of other potassium channel types during development (Dryer, 1998). Since numerous factors

Figure 5-1
Overview of developmental origins of mouse CNS regions examined during this chapter

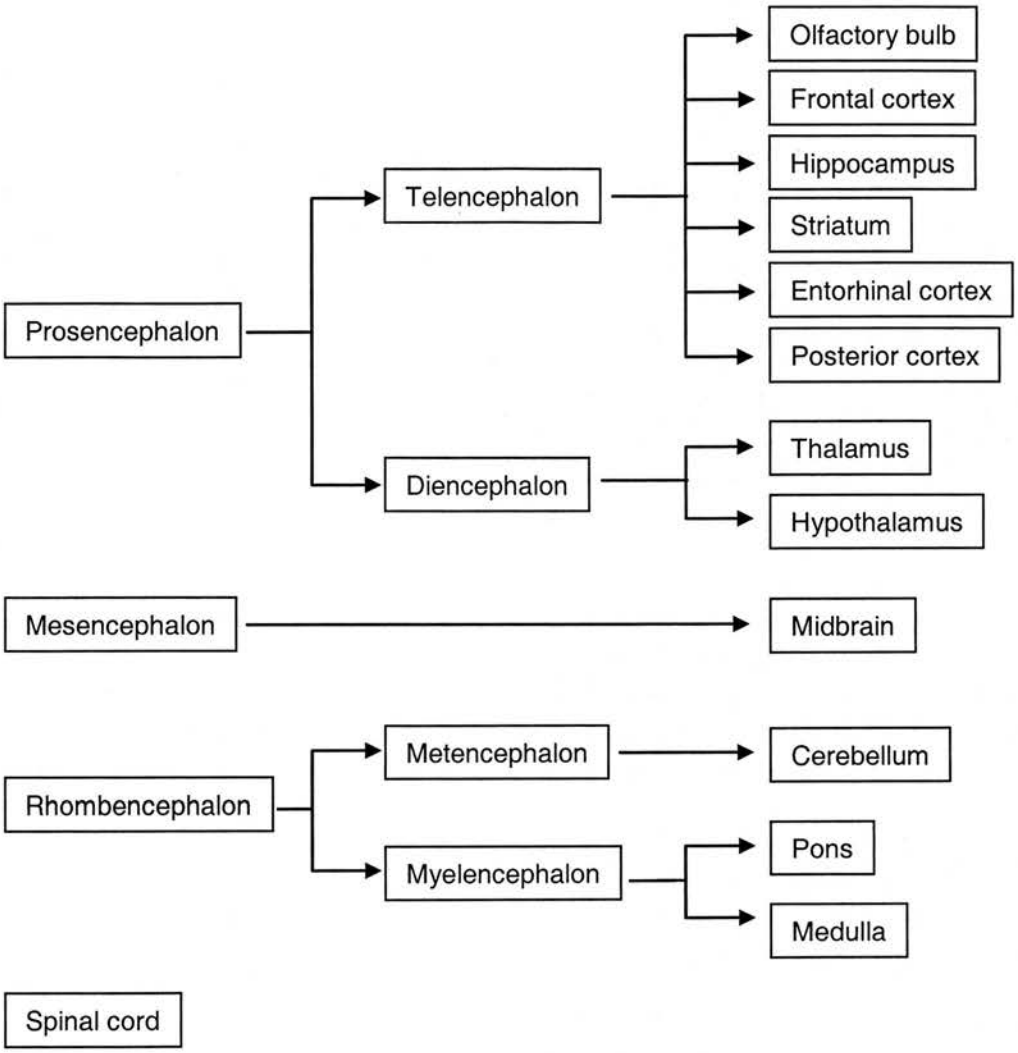

Figure 5-1 Overview of developmental origins of mouse CNS regions examined during this chapter

Showing the developmental origins of the CNS regions studied, illustrating tissues that develop from the three enlargements of the neural tube; the prosencephalon, mesencephalon and rhombencephalon.

released during neurogenesis modulate activity and patterning, and given the significant role of BK channels in determining cell excitability, it is possible that the presence of differentially- regulated BK channel alternative splice variants may provide a mechanism for generating diversity in cell responses to the complex and graded signalling that occurs during development. Since BK channels are implicated in the control of neurotransmitter release in the adult CNS (Raffaelli *et al.*, 2004), they may also influence signalling in this manner during development, for example by enabling control of trophic signalling gradients.

Considerable evidence supports the existence of regulated BK channel expression during development (Hafidi *et al.*, 2005, Kukuljan *et al.*, 2003). With particular reference to developmentally- regulated expression of alternative splicing, preliminary results shown in chapter 4 indicated that several of the known BK channel splice variants are upregulated over the course of embryogenesis. Switching of BK channel functional phenotypes may be of significance in development of the central nervous system, and it has been shown that a particular *Xenopus* splice variant is expressed solely during late neuronal differentiation, whilst the four other *Xenopus* splice variants are not delimited either by tissue or developmental stage (Kukuljan *et al.*, 2003). The neuronal development- specific splice variant is xSlo59, which contains a 59 amino acid insert that confers similar functional properties to STREX; inclusion of this insert results in channels with increased calcium and voltage sensitivity (Saito *et al.*, 1997, Kukuljan *et al.*, 2003). Additionally, it may also be the case that BK channel- specific retention/ retrieval mechanisms, similar to those initiated by the non- membrane trafficked splice variant, SV1 (Zarei *et al.*,

2004), are activated at certain stages of development, for example to cause downregulation of specific subsets of the channel population, and hence alter cell excitability to a level commensurate with functional requirements at that time, as occurs in other physiological conditions, such as pregnancy (Eghbali *et al.*, 2003). It is also known that correct BK channel expression in developing neurons is dependent on presence of specific target cells. For example, in neurons of the chick ciliary ganglion, transforming growth factor β1 (TGFβ1) released from the target tissue, in this case striated intraocular muscle cells, initiates signal transduction pathways involving MAP kinase activity, that result in translocation of BK channels to the plasma membrane (Lhuillier and Dryer, 2002).

5-1-3 Postnatal development

In addition to changes observed during embryonic patterning of the central nervous system, there is also evidence for the regulated expression of BK channels in the CNS during postnatal development (Kang *et al.*, 1996). In neocortical pyramidal neurons, the density of BK channels at the cell surface was found to increase significantly over the period of postnatal days P1 to P28, both on the somata and dendrites, although at P28, the density of dendritic BK channels was less than one half of that on the cell bodies. Alternative splicing may also be of significance in this clear developmental regulation of functional expression of the BK channel, and certain splice variants may be delimited to specific subcellular regions.

Developmental regulation of BK channel expression continues postnatally, with several systems reliant on correct expression of the channel to enable normal

physiological function and homeostasis. For example in the cortical collecting duct of the kidney in rabbits, development of flow- dependent potassium secretion is effected by a switch to increased BK channel expression at 5 weeks of age (Woda *et al.*, 2003). Changing BK channel expression during postnatal development has also been shown in the cochlea of the mouse, with significant upregulation of membrane BK channels coinciding with the stage at which the auditory system becomes functional at P12 (Hafidi *et al.*, 2005). Additionally, BK channels are implicated in the control of high- frequency synaptic transmission (Sausbier *et al.*, 2004), and this could also be influenced by modification of channel properties via alternative splicing. Since the BK channel may be a regulator of long- term changes in cell excitability (Nelson *et al.*, 2003) the changing of BK channel properties in this manner may assist critical processes in early learning (Edgerton and Reinhart 2003).

It can be seen that correctly timed and context- specific signalling is essential for CNS development both during embryogenesis and postnatally. Since BK channels are critical in coupling of membrane potential and intracellular calcium with cell excitability, channels targeted to nerve terminals (Knaus *et al.*, 1996) are able to limit calcium entry, and hence indirectly enable tight control of neurotransmitter release (Rafaelli *et al.*, 2004). As a result of this, the BK channel may be a modulator of synaptic efficacy, facilitating strengthening or weakening of synapses dependent on the number and electrophysiological properties of the channels expressed at the nerve terminal. The latter may be influenced by coassembly with β-subunits, protein kinase activity and alternative splicing of α-subunits. BK channel activity has been shown to influence synaptic transmission in the hippocampus of juvenile (4-7 day old) rats

(Raffaelli *et al.*, 2004) and since the hippocampus undergoes significant changes in synaptic activity during early postnatal development (Wasling *et al.*, 2004), it is intuitive to speculate that regulated activity in this manner also occurs in tissues of the embryonic CNS, and may be critical to refinement of synaptic connections. Several possibilities arise when considering alternative splicing of BK channel α-subunits in the developing CNS. Firstly, it is unclear whether a single paradigm exists for the expression of BK channel alternative splice variants in all neuronal tissues during embryogenesis and postnatal development, or whether each brain region bears a distinct mode of regulated channel expression, commensurate to requirements of cell excitability. It may be the case, however, that since axonal growth is dependent on competitive elimination of synapses based on strength of activity (Hua *et al.*, 2005), if BK channels modulate synaptic strength by determining transmitter release, a single high- activity phenotype such as STREX may be seen ubiquitously throughout all tissues, if only during the initial phases of establishment of synapses. Clear inverse regulation of alternative splice variants may be observed, whereby one splice variant is upregulated, whilst others are downregulated over the course of development. Since only the STREX and ZERO alternative splice variants were investigated during this study, it is unlikely that their expression fully reflects the contribution of BK channel pre-mRNA splicing to development of the CNS, since expression of other alternative splice variants was also seen to change during embryogenesis. However, it is also possible that not all of the BK splice variants are expressed in the CNS.

In order to determine whether expression of ZERO and STREX BK channel alternative splice variants were altered in the CNS during embryogenesis and early postnatal life, mRNA expression was investigated. By quantifying mRNA expression of total BK channel, as well as that of these two alternative splice variants, it was possible to generate a profile of the relative proportion of channel transcripts for STREX and ZERO at embryonic day 13 (E13), 15 (E15), 18 (E18) and postnatal day 7 (P7) and 35 (P35), to ensure that results reflected changing levels of splice variants within the BK channel population, rather than changing levels of overall BK channel expression.

5-2 Results

To investigate whether specific regulation of BK channel alternative splice variant mRNA occurs during embryonic and postnatal development, and also to determine whether such changes were ubiquitous throughout the tissues of the central nervous system, cDNA generated from the mouse CNS at stages of development from embryo day 13, 15, 18 and postnatal day 7 and 35, from the "mouse brain Rapidscan" cDNA array (Origene), was assayed using the Taqman real time PCR primer/ probe sets for total BK channel (Applied Biosystems "assay on demand" for mouse BK channel, assay ID Mm00516078_m1), and also the STREX and ZERO alternative splice variants. Samples were assayed in 25 µl reactions in 1x Applied Biosystems Taqman Universal PCR master mix, and quantified against a standard curve generated from a triplicate logarithmic dilution of STREX or ZERO cDNA, over a starting concentration range of 2ng- 0.2fg, as described previously (chapter 4).

To determine changes in the level of specific alternative splice variants across tissues and developmental stages, mRNA expression of each alternative splice variant was normalised to total BK channel to give the splice variant/ BK ratio. The ratios at each developmental stage were then expressed as a percentage of that in the 35- day old adult. This enabled the relative proportion of the STREX and ZERO alternative splice variants in the total BK channel population to be investigated, in order to reveal changes in splicing that occurred as development progressed. ZERO and STREX/ BK ratios from were generated from several separate Rapidscan cDNA arrays, then results were averaged, therefore in each case (n= X) represents the number of independent experiments carried out.

5-2-1 Regulated expression of total BK channel mRNA during mouse CNS development

Total BK channel mRNA expression in tissues of the mouse CNS from the 35 day-old juvenile was quantified, then normalised to frontal cortex. In the spinal cord, total BK channel mRNA expression was 51.5 ± 7.3% (n= 5) of that in the frontal cortex. Midbrain total BK mRNA expression was 57.2 ± 7.6% (n= 5), whilst that of the pons was 63.2 ± 8.6% (n= 5) of frontal cortex expression. In the medulla, expression of total BK channel mRNA was 45.0 ± 5.9% (n= 5) of frontal cortex. In the thalamus and hypothalamus, total BK channel mRNA expression was 63.9 ± 3.3% (n= 5) and 72.4 ± 12.4% (n= 5) of frontal cortex expression, respectively. In the posterior and entorhinal cortices, total BK channel mRNA expression was 45.3 ± 4.0% (n= 5) of frontal cortex expression, and 105.7 ± 12.0% (n= 5), respectively. Olfactory bulb total BK mRNA expression was 64.0 ± 3.8% (n= 5) of frontal cortex, whilst that of

the hippocampus was 79.9 ± 9.7% (n= 5). In the striatum, total BK channel mRNA expression was 58.5 ± 5.4% (n= 5), whilst that in the cerebellum was 40.8 ± 2.6% (n= 5) of expression in frontal cortex (fig. 5-2).

Total BK channel mRNA expression was shown to vary across the tissues of the mouse CNS at 35 days postnatally, possibly indicating differing levels of significance for BK channel regulation of cell excitability in each of those tissues. In order to investigate possible developmental changes in BK channel mRNA expression in the tissues of the CNS, BK channel mRNA expression was quantified at a number of stages- embryonic days 13, 15 and 18, and also postnatal days 7 and 35, then expressed as a percentage of P35. In the 13- day embryo, average spinal cord total BK channel mRNA expression was 59.4 ± 10.0% (n= 5) of that at postnatal day 35, and this was significantly ($p< 0.05$) lower than in the P35 juvenile. Average spinal cord total BK mRNA expression at E15 and E18 was 115.5 ± 38.0% (n= 5) and 118.2 ± 17.7% (n= 5) of P35, respectively, and neither of these was significantly different to that at P35, however E15 expression was significantly ($p< 0.01$) higher than that at P7. The average spinal cord total BK mRNA expression at P7 was 48.8 ± 10.0% (n= 5) of P35, and this was significantly ($p< 0.01$) lower than in the juvenile (fig. 5-3).

The embryonic mesencephalon develops into the adult midbrain (Liu and Joyner, 2001), therefore at E13 this tissue was used as a comparison for the developmental regulation of midbrain total BK channel mRNA expression. In the E13 mesencephalon, total BK channel mRNA expression was 23.4 ± 3.0% (n= 5) of that

Figure 5-2
Total BK channel mRNA expression in postnatal 35- day mouse CNS tissues

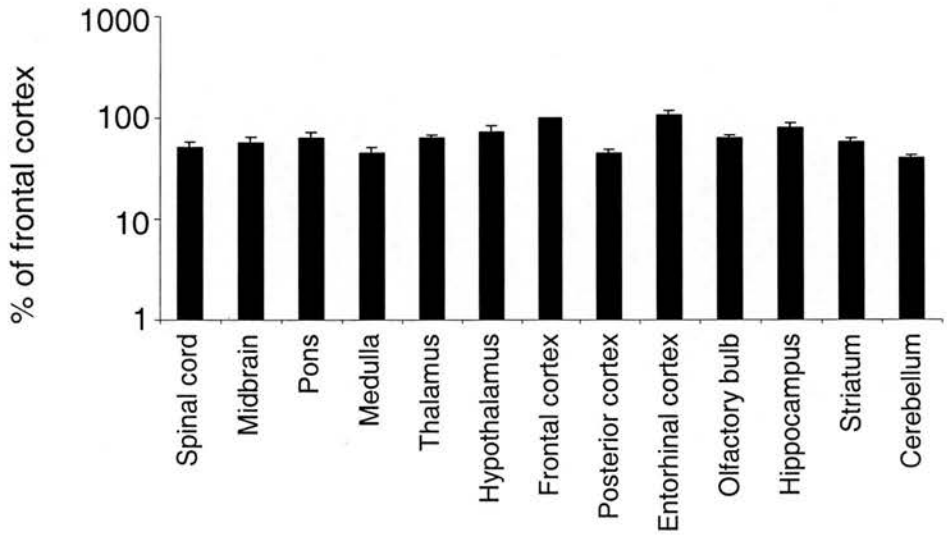

Figure 5-2 Total BK channel mRNA expression in postnatal 35- day mouse CNS tissues

Showing total BK channel mRNA expression in 35 day- old mouse CNS tissues, as a percentage of expression in frontal cortex ± SEM, on a logarithmic scale (n= 5).

Figure 5-3
Developmental regulation of total BK channel mRNA expression in mouse spinal cord, midbrain, pons and medulla

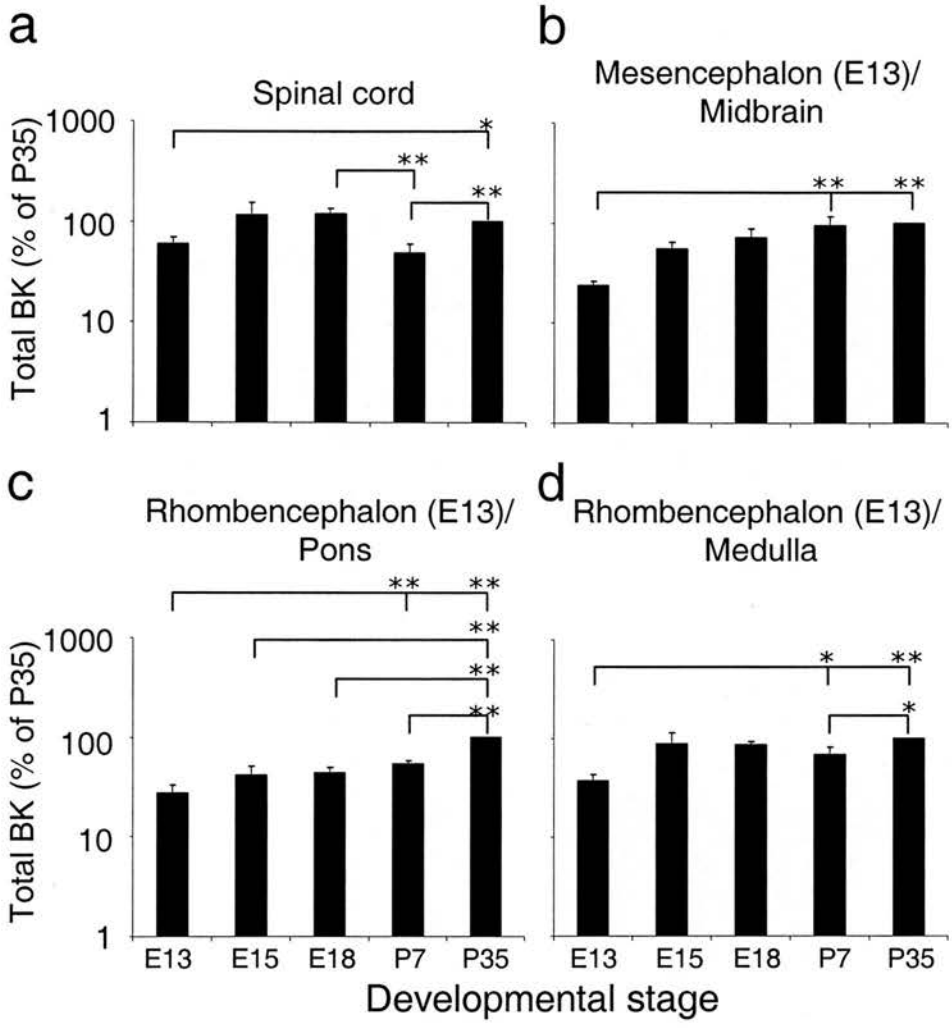

Figure 5-3 Developmental regulation of total BK channel mRNA expression in mouse spinal cord, midbrain, pons and medulla

Showing total BK channel mRNA expression as a percentage of postnatal day 35, in mouse **a)** spinal cord (n= 5), **b)** mesencephalon/ midbrain (n= 5), **c)** rhombencephalon/ pons (n= 5) and **d)** rhombencephalon/ medulla (n= 5) at embryonic day 13 (E13), 15 (E15), 18 (E18) and postnatal day 7 and 35 (P7 and 35 respectively) on a logarithmic scale. (*= $p < 0.05$, **= $p < 0.01$ ANOVA post hoc test Bonferroni/ Dunn.)

in the P35 midbrain, and was significantly ($p< 0.01$) lower than expression at either P7 or P35. Midbrain total BK mRNA expression was 54.8 ± 9.7% (n= 5) of P35 at E15, and 71.8 ± 14.3% (n= 5) of P35 at E18. At P7, midbrain total BK mRNA channel expression was 94.4 ± 22.2% (n= 5) of that in the P35 juvenile (fig. 5-3).

The rhombencephalon at E13 was used as a comparison for BK channel mRNA expression in the pons. At E13, rhombencephalon total BK channel mRNA expression was 27.4 ± 5.3% (n= 5) of that at P35, and this was significantly ($p< 0.01$) higher than at either P7 or P35. At E15 and E18, pons total BK channel mRNA expression was 41.3 ± 9.6% (n= 5) and 43.3 ± 6.3% (n= 5) of P35, respectively, and at both of these stages total BK mRNA expression was significantly ($p< 0.01$) lower than that in the P35 juvenile. At P7, total BK channel mRNA expression was 53.13 ± 4.9% (n= 5) of that in P35, and this was again significantly ($p< 0.01$) lower than in the P35 juvenile (fig. 5-3).

The medulla also arises from the rhombencephalon, therefore in early embryo this precursor tissue was used to investigate the developmental changes in medullary BK channel mRNA expression. At E13, rhombencephalon total BK channel mRNA expression was 37.3 ± 5.8% (n= 5) of that in the P35 medulla, and this was significantly lower than at P7 ($p< 0.05$) and P35 ($p< 0.01$). No significant differences were found between BK channel mRNA expression in the medulla at E15 and E18, compared to the postnatal stages- total BK mRNA expression in the medulla at these stages was 87.3 ± 27.6% (n= 5) and 86.2 ± 6.7% (n= 5) of P35 respectively. At P7,

total medulla BK channel mRNA expression was 68.5 ± 12.3% (n= 5) of P35, and was significantly ($p< 0.05$) lower than that in the P35 juvenile (fig. 5-3).

The thalamus arises from the diencephalon; therefore this precursor was used at E15 as a comparison for BK channel mRNA expression in the thalamus. In the E15 diencephalon, total BK mRNA expression was 40.0 ± 1.8% (n= 5) of that in the P35 thalamus, and was significantly lower than in either P7 ($p< 0.05$) or P35 ($p< 0.01$). Total BK channel mRNA expression in the E18 thalamus was 92.9 ± 11.5% (n= 5) of that at P35. At P7, total BK mRNA expression was 89.4 ± 19.5% (n= 5) of that in P35 (fig. 5-4).

The diencephalon is also the developmental precursor to the hypothalamus, therefore was used as the E15 comparison for this tissue. In the E15 diencephalon, total BK channel mRNA expression was 44.1 ± 13.8% (n= 5) of that in the P35 hypothalamus. Although average expression was lower, variability in results caused this difference to be not significant. At E18, hypothalamic BK channel mRNA expression was 112.7 ± 31.3% (n= 5) of that at P35. Total BK mRNA expression at P7 was 74.2 ± 24.3% (n= 5) of that at P35. Neither E18 nor P7 BK channel mRNA expression was significantly different to that in P35 (fig. 5-4).

Since the telencephalon is the embryonic precursor for the olfactory bulb, frontal, posterior and entorhinal cortices, hippocampus and striatum, this was used as a comparison at E13 and E15 for total BK channel mRNA expression in each of these CNS regions. In the telencephalon at E13, total BK channel mRNA expression was

Figure 5-4

Developmental regulation of total BK channel mRNA expression in mouse thalamus, hypothalamus, frontal and posterior cortex

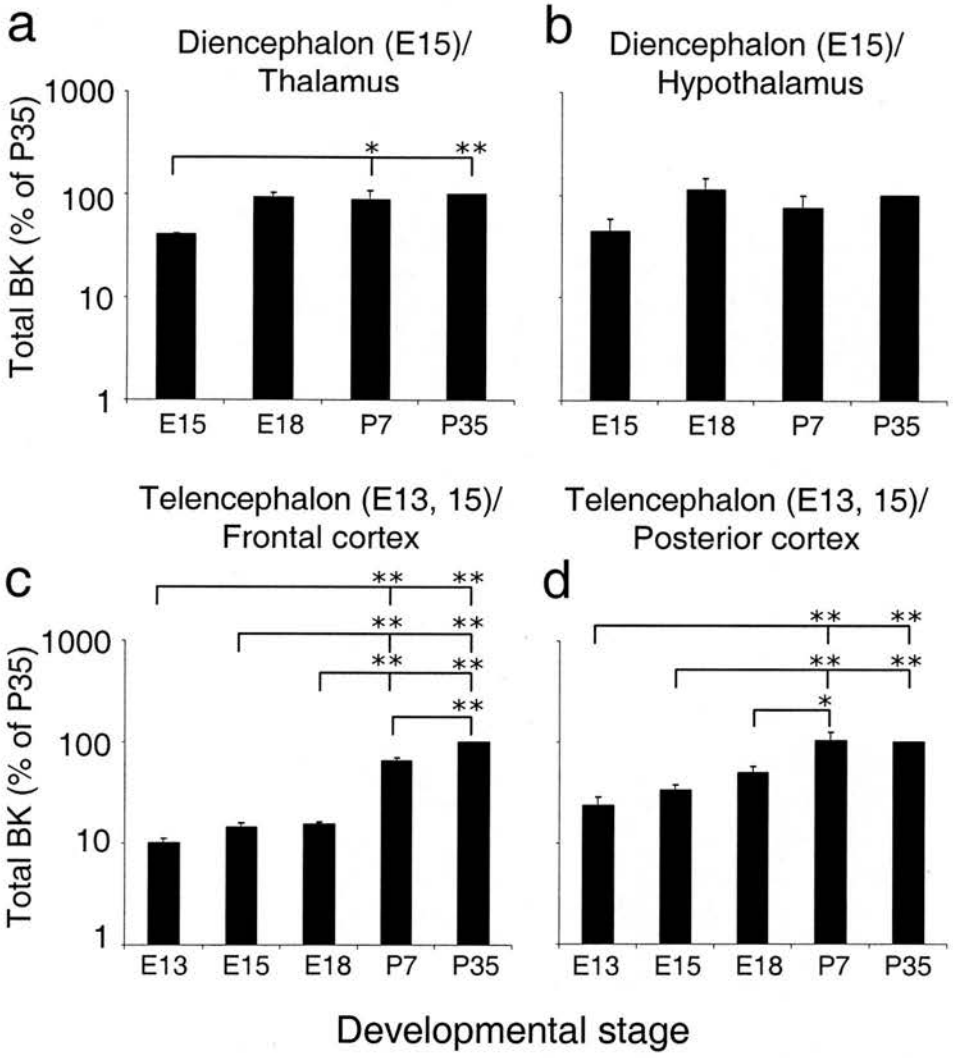

Figure 5-4 Developmental regulation of total BK channel mRNA expression in mouse thalamus, hypothalamus, frontal and posterior cortex

Showing total BK channel mRNA expression as a percentage of postnatal day 35, in mouse **a)** diencephalon/ thalamus (n= 5), **b)** diencephalon/ hypothalamus (n= 5) at embryonic day 15 (E15), 18 (E18) and postnatal day 7 and 35 (P7 and 35 respectively) and **c)** telencephalon/ frontal cortex (n= 5) and **d)** telencephalon/ posterior cortex (n= 5) at E13- P35 on a logarithmic scale. (*= $p < 0.05$, **= $p < 0.01$ ANOVA post hoc test Bonferroni/ Dunn.)

10.0 ± 1.2% (n= 5), whilst expression at E15 was 14.5 ± 1.4% (n= 5) of that in the frontal cortex at P35. At both of these stages, telencephalon total BK channel mRNA expression was significantly ($p< 0.01$) lower than that in the frontal cortex at either P7 or P35. In the frontal cortex, at E18 total BK channel mRNA expression was 15.5 ± 0.9% (n= 5) of P35, and was significantly ($p< 0.01$) lower than that at both P7 and P35. At P7, total BK channel mRNA expression was 65.1 ± 4.8% (n= 5) of that in the P35 juvenile, and this was significantly ($p< 0.01$) lower than in P35 (fig. 5-4).

At E13, telencephalon total BK channel mRNA expression was 23.6 ± 4.8% (n= 5), whilst expression in the E15 telencephalon was 33.0 ± 4.3% (n= 5) of that in the posterior cortex at P35. Telencephalon total BK channel mRNA expression at both E13 and E15 was significantly ($p< 0.01$) lower than that of the posterior cortex at either P7 or P35. At E18 in the posterior cortex, total BK channel mRNA expression was 49.1 ± 9.3% (n= 5) of that at P35, and was significantly ($p< 0.05$) lower than that at P7. In the P7 posterior cortex, total BK channel mRNA expression was not significantly different to that in the juvenile, at 103.1 ± 23.1% (n= 5) of P35 (fig. 5-4).

Significant upregulation of BK channel mRNA expression was seen in the entorhinal cortex during development. In the telencephalon at E13, total BK channel mRNA expression was 10.5 ± 2.6% (n= 5), whilst expression at E15 was 14.8 ± 2.7% (n= 5) of that in the entorhinal cortex at P35. Telencephalon total BK channel mRNA expression at both E13 and E15 was significantly ($p< 0.01$) lower than in the entorhinal cortex at either P7 or P35. At E18, total BK mRNA expression was 23.8 ±

0.8% (n= 4) of that at P35, and was significantly ($p < 0.01$) lower than at either P7 or P35. In the P7 entorhinal cortex, total BK mRNA expression was again significantly ($p < 0.01$) lower than in the juvenile, at 47.9 ± 3.7% (n= 5) of that at P35 (fig. 5-5).

In the olfactory bulb, upregulated total BK channel mRNA expression was also observed during development. In the telencephalon at E13, total BK channel mRNA expression was 16.2 ± 2.8% (n= 5), whilst expression in the E15 telencephalon was 22.9 ± 2.4% (n= 5) of that in the olfactory bulb at P35. In both cases, telencephalon total BK channel mRNA expression was significantly ($p < 0.01$) lower than in the olfactory bulb at either P7 or P35. At E18, total BK mRNA expression was 51.0 ± 2.8% (n= 5) of that in the P35 juvenile, and was significantly lower than at P7 ($p < 0.05$) and P35 ($p < 0.01$). At P7, total BK channel mRNA expression was not significantly lower than that in the juvenile, at 85.8 ± 14.2% (n= 5) of P35 mRNA expression (fig. 5-5).

Telencephalon total BK channel mRNA expression at E13 was 14.6 ± 4.3% (n= 5) of that in the P35 hippocampus. At E15, telencephalon total BK channel mRNA expression was 20.0 ± 4.2% (n= 5) of that in the hippocampus at P35. At both of these stages, total BK channel mRNA expression in the telencephalon was significantly ($p < 0.01$) lower than in the hippocampus at either P7 or P35. In the hippocampus, at E18, total BK channel mRNA expression was 14.9 ± 2.3% (n= 5) of that at P35, and this was significantly ($p < 0.01$) lower than at either P7 or P35. BK channel mRNA expression at P7 was also significantly ($p < 0.01$) lower than that in the juvenile, at 63.4 ± 5.4% (n= 5) of P35 mRNA expression (fig. 5-5).

Figure 5-5

Developmental regulation of total BK channel mRNA expression in mouse entorhinal cortex, olfactory bulb, hippocampus and striatum

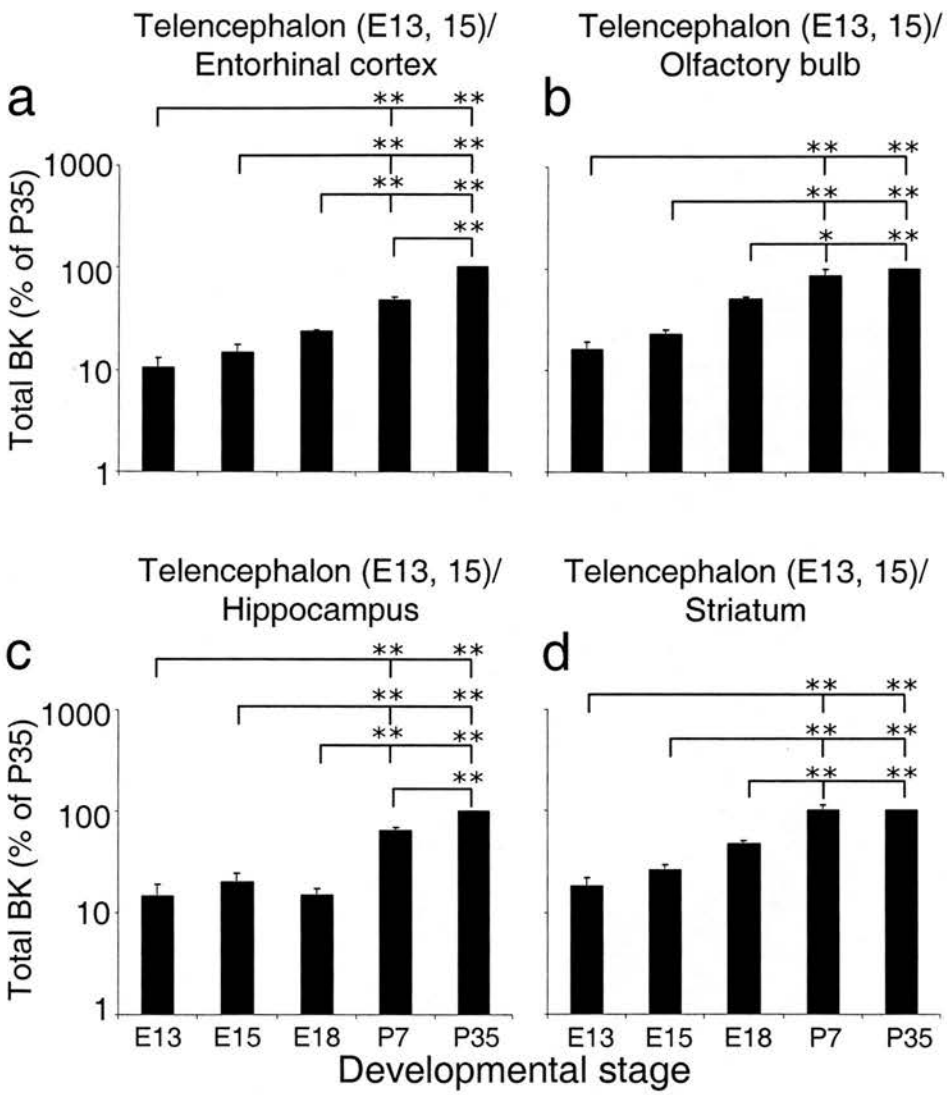

Figure 5-5 Developmental regulation of total BK channel mRNA expression in mouse entorhinal cortex, olfactory bulb, hippocampus and striatum

Showing total BK channel mRNA expression as a percentage of postnatal day 35, in mouse **a)** telencephalon/ entorhinal cortex (n= 5 (n=4 at E18)), **b)** telencephalon/ olfactory bulb (n= 5) **c)** telencephalon/ hippocampus (n= 5) and **d)** telencephalon/ striatum (n= 5) at embryonic day 13 (E13), 15 (E15) and 18 (E18), and postnatal day 7 and 35 (P7 and P35 respectively) on a logarithmic scale. (*= $p < 0.05$, **= $p < 0.01$ ANOVA post hoc test Bonferroni/ Dunn.)

Total BK channel mRNA expression in the telencephalon at E13 was 18.0 ± 3.6% (n= 5), whilst expression at E15 was 25.8 ± 3.7% (n= 5) of that in the striatum at P35. At both of these stages, telencephalon total BK channel mRNA expression was significantly ($p< 0.01$) lower than that in the striatum at either P7 or P35. In the striatum at E18, total BK channel mRNA expression was 47.1 ± 3.7% (n= 5) of that at P35, and was significantly ($p< 0.01$) lower than either P7 or P35. At P7, striatum total BK channel mRNA expression was not significantly different to that in the juvenile, at 99.8 ± 14.3% (n= 5) of P35 (fig. 5-5).

The rhombencephalon is the structure that gives rise to the cerebellum following differentiation through metencephalon/ myelencephalon formation and development of the pontine flexure. Unfortunately, cDNA was not available from the intermediary structures at E15 and E18 that go on to form the cerebellum, such as the rhombic lip of the metencephalic alar plate, therefore total BK channel mRNA expression in the E13 rhombencephalon was compared with that of the P7 and P35 cerebellum. In the E13 rhombencephalon, total BK channel mRNA expression was 40.4 ± 5.9% (n= 5) of that in the P35 cerebellum. This was significantly lower than at either P7 ($p< 0.05$) or P35 ($p< 0.01$). At P7, cerebellar total BK channel mRNA expression was significantly ($p< 0.01$) lower than that in the juvenile, at 66.2 ± 6.4% of P35 expression (fig. 5-6).

In order to investigate whether the mRNA expression of the STREX and ZERO BK channel alternative splice variants was variable across tissues of the mouse CNS, the average ratio of each splice variant to total BK channel in each tissue in the 35 day-

Figure 5-6
Developmental regulation of total BK channel mRNA expression in mouse cerebellum

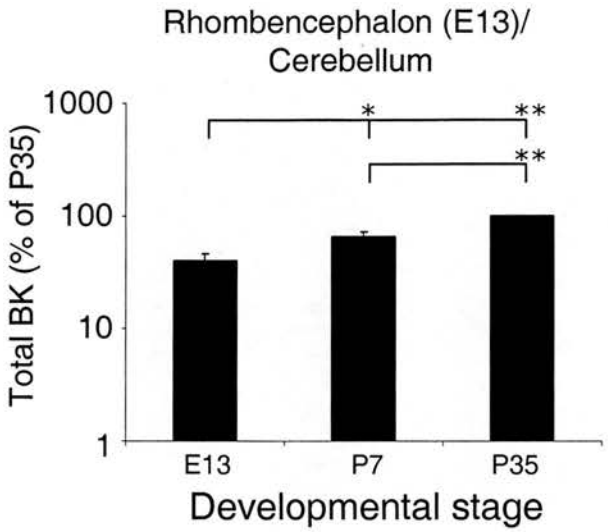

Figure 5-6 Developmental regulation of total BK channel mRNA expression in mouse cerebellum

Showing total BK channel mRNA expression as a percentage of postnatal day 35, in mouse rhombencephalon/ cerebellum (n= 5) at embryonic day 13 (E13) and postnatal day 7 and 35 (P7 and 35 respectively) on a logarithmic scale. (*= $p< 0.05$, **= $p< 0.01$ ANOVA post hoc test Bonferroni/ Dunn.)

old mouse was quantified, then expressed as a percentage of that in the frontal cortex. In the spinal cord at P35, the average STREX/ BK ratio was 64.3 ± 3.0 (n= 3) of that in the frontal cortex. Midbrain STREX/ BK ratio was 69.1 ± 6.7% (n= 3) of that in frontal cortex, whilst pons STREX/ BK ratio was 60.9 ± 5.4% (n= 3). In the medulla, average STREX/ BK ratio was 72.3 ± 24.3% (n= 3) of that in the frontal cortex. In the thalamus and hypothalamus, the STREX/ BK ratio was 102.5 ± 13.3 (n= 3) and 80.9 ± 15.6% (n= 3) of frontal cortex, respectively. In the posterior and entorhinal cortices, the average STREX/ BK ratio was 71.4 ± 6.5% (n= 3) and 103.2 ± 18.8% (n= 3) of frontal cortex, respectively. STREX/ BK ratio in the olfactory bulb was 64.3 ± 20.8% (n= 3) of frontal cortex, whilst that in the hippocampus was 75.2 ± 22.1% (n= 3). In the striatum, average STREX/ BK ratio was 84.5 ± 9.0% (n= 3) of that in the frontal cortex. Average cerebellar STREX/ BK ratio was 39.1 ± 7.4% (n= 3) of frontal cortex (fig. 5-7).

In the P35 spinal cord, the average ZERO/ BK ratio was 126.5 ± 23.3% (n= 3) of that in the frontal cortex. In midbrain, the ZERO/ BK ratio was 112.7 ± 40.3% (n= 3) of frontal cortex. Average ZERO/ BK ratios in the pons and medulla were 39.9 ± 11.7% (n= 3) and 66.4 ± 34.9% (n= 3), respectively, of that in the frontal cortex. In the thalamus, the average ZERO/ BK ratio was 69.0 ± 16.3% (n= 3), whilst that in the hypothalamus was 128.0 ± 50.1% (n= 3) of that in the frontal cortex. In the posterior and entorhinal cortices, the average ZERO/ BK ratio was 126.5 ± 91.6% (n= 3) and 244.7 ± 97.0% (n= 3) of frontal cortex, respectively. Olfactory bulb ZERO/ BK ratio was 128.2 ± 23.2% (n= 3) of frontal cortex. Average ZERO/ BK ratio in the hippocampus was 120.7 ± 55.2% (n= 3), whilst that in the striatum was 81.8 ± 47.4%

Figure 5-7
STREX/BK and ZERO/BK ratios in postnatal 35- day mouse CNS tissues

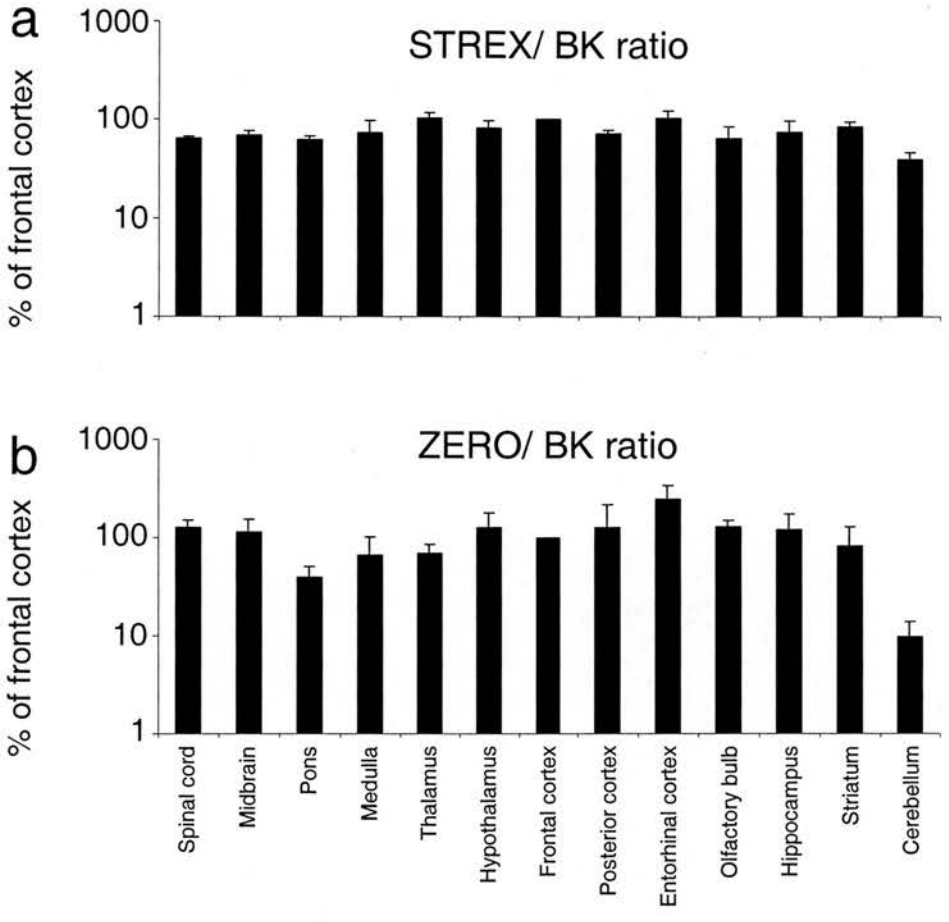

Figure 5-7 STREX/BK and ZERO/BK ratios in postnatal 35- day mouse CNS tissues

Showing **a)** STREX/BK ratio (n= 3) and **b)** ZERO/BK ratio (n= 3) in 35 day-old mouse CNS tissues, as a percentage of expression in frontal cortex ± SEM, on a logarithmic scale.

(n= 3) of frontal cortex. In the cerebellum, the average ZERO/ BK ratio was 9.8 ± 4.4% (n= 3) of that in the frontal cortex (fig. 5-7).

Total BK channel mRNA expression was found to vary across CNS tissues in the P35 mouse, and was also significantly upregulated in several of these regions during development. In addition to this, the ratio of the STREX and ZERO BK channel alternative splice variant mRNA to total BK channel mRNA was also found to vary across CNS tissues in the P35 mouse. Since these two alternative splice variants form channels with distinct modes of regulation (Tian *et al.*, 2004, Saito *et al.*, 1997), this suggests that expression of these differentially- regulated channels may ie altered according to the requirements of specific tissues. It may also be the case that alternative splicing in this manner is dynamic, and the expression of specific splice variants in the CNS can be regulated according to context, as has previously been shown for the BK channel in tissues involved in secretory responses to stress (McCobb *et al.*, 2003).

Preliminary results in chapter 4 suggested that several of the BK channel alternative splice variants were also differentially expressed in the whole embryo as development progressed. In order to preclude the possibility that observed changes in splice variant mRNA expression were simply due to changing levels of total BK channel mRNA, the ratio of splice variant to total BK channel was investigated in the developing CNS. If the observed changes were a genuine effect of regulated channel alternative splicing, the ratio of splice variant to total BK channel would be found to vary across developmental stages.

5-2-2 Developmental regulation of BK channel alternative splice variant mRNA expression in mouse spinal cord

In *Xenopus*, the BK channel alternative splice variant xSlo59, which has similar activation properties to STREX (Kukuljan *et al.*, 2003), as well as a shorter variant, xSlo56, have been shown to be upregulated in the late stages of development of spinal neurons, suggesting a requirement for the increased calcium and voltage sensitivity of the former as the organism matures. In the mouse spinal cord, however, a decrease in STREX mRNA as a proportion of total BK channel mRNA was observed over the course of development, with the most striking differences observed in the early embryo compared with postnatal stages. At embryonic day 13, STREX/ BK ratio was 1016.2 ± 193.9% (n= 3) of that in P35 spinal cord. This was significantly ($P< 0.01$) higher than at postnatal day 7 and 35. At embryo day 15, STREX/ BK ratio was 777.4 ± 125.7 (n= 3) of P35, again significantly ($p< 0.01$) higher than both postnatal stages assayed. In embryonic day 18, although the STREX/ BK ratio was higher than the postnatal stages, at 834.0 ± 334.8 (n= 3) of P35, this difference was not significant. Postnatally, 7 days after birth, average spinal cord STREX/ BK ratio was 184.3 ± 40.7% (n= 3) of that in the 35- day old juvenile (fig. 5-8). These results followed a trend of decreasing STREX/ BK ratio as embryogenesis and postnatal development progressed, indicating that in the spinal cord, STREX mRNA expression is developmentally- regulated. Since this downregulation of STREX mRNA occurred, the same embryonic and postnatal stages were investigated for the expression of ZERO BK channel mRNA, in order to observe whether changing mRNA expression of one splice variant was accompanied by similar, or inverse changes in the other.

Figure 5-8
Developmental regulation of BK channel alternative splice variant mRNA expression in mouse spinal cord

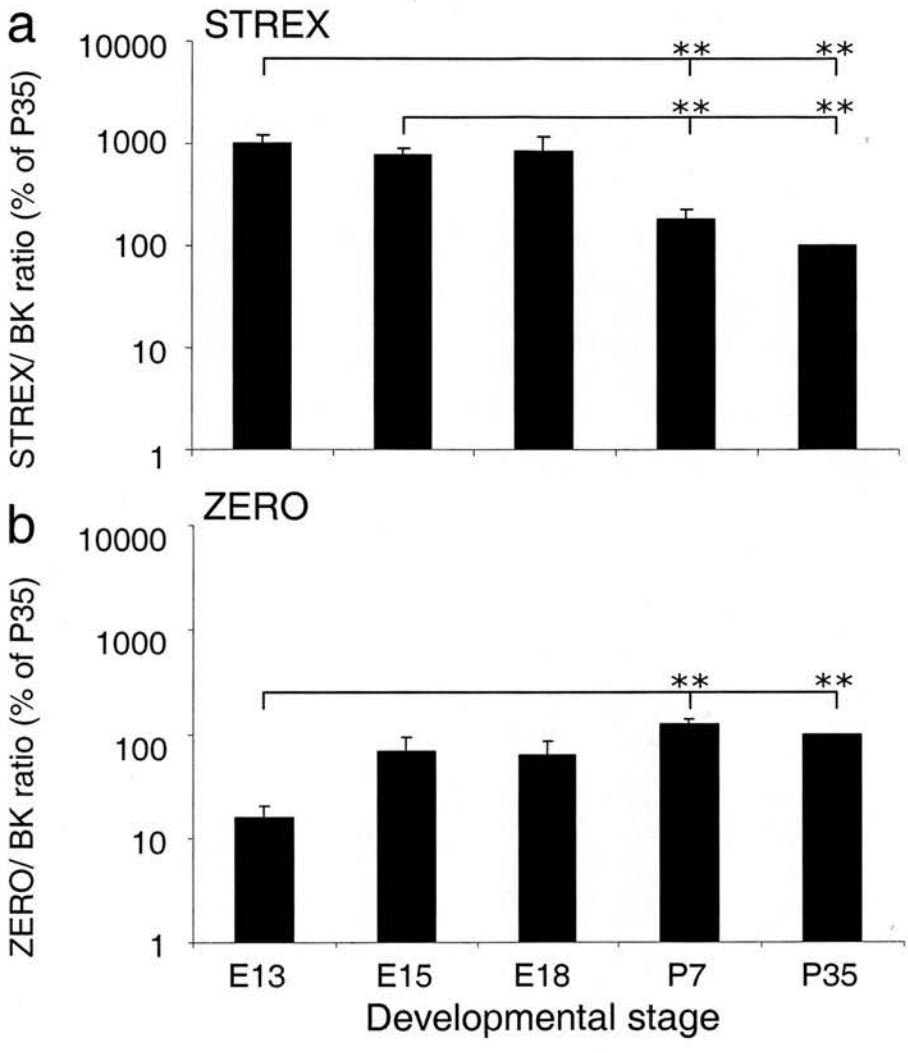

Figure 5-8 Developmental regulation of BK channel alternative splice variant mRNA expression in mouse spinal cord

Showing **a)** STREX/ BK ratio (n= 3) and **b)** ZERO/ BK ratio (n= 3) expressed as a percentage of postnatal day 35, in mouse spinal cord at embryonic day 13, 15, 18 (E13, E15, E18 respectively) and postnatal day 7 and 35 (P7 and 35 respectively) on a logarithmic scale. (**= $p < 0.01$ ANOVA post hoc test Bonferroni/ Dunn.)

In contrast with the decreasing STREX mRNA expression, ZERO mRNA was found to increase as a proportion of that of total BK channel over the course of spinal cord development. ZERO/ BK ratio was significantly ($p< 0.01$) lower than either P7 or P35 in embryo day 13, at 15.7 ± 4.4% (n= 3) of that in P35. ZERO/ BK ratio was 67.0 ± 26.7% (n= 3) of P35 in embryo day 15 spinal cord, and 61.6 ± 23.6% (n= 3) in embryo day 18. Although ZERO mRNA expression was slightly lower in both of these embryonic stages than in the postnatal spinal cord, this difference was not large enough to be significant. Postnatally, at 7 days, the spinal cord ZERO/ BK ratio was 125.0 ± 13.2% of that in the 35- day old juvenile (fig. 5-8). These results indicate that developmental regulation of ZERO BK channel mRNA expression also occurs, and specific alternative splice variants, or a combination thereof, may be necessary for correct signalling during development.

5-2-3 Developmentally- regulated BK channel alternative splice variant mRNA expression in mouse mesencephalon/ midbrain

Decreasing STREX mRNA expression was also seen in the mesencephalon/ midbrain during the course of development. At embryo day 13, the STREX/ BK ratio in the mesencephalon was 1441.7 ± 337.6% (n= 3) of that in the P35 midbrain. This was significantly higher than both P7 ($p< 0.05$) and P35 ($p< 0.01$). By embryonic day 15, midbrain STREX/ BK ratio had fallen, but not significantly, to 858.0 ± 201.0% (n= 3). Again, the STREX/ BK ratio was significantly ($p< 0.05$) higher at P15 than either postnatal stage investigated. At embryo day 18, midbrain STREX/ BK ratio was 721.7 ± 246.0% (n= 3), although this was not significantly higher than in the postnatal stages. At postnatal day 7 the STREX/ BK ratio was 190.4 ± 16.2%

(n= 3) of that in P35 (fig. 5-9). These findings are similar to observations made for the spinal cord, where STREX mRNA expression fell during development.

ZERO splicing of the BK channel in the midbrain was, as in spinal cord, upregulated during development, again the opposite effect to that seen for the STREX alternative splice variant. At embryonic day 13, ZERO/ BK ratio was 16.0 ± 6.0% (n= 3) of that in P35, and was significantly ($p< 0.05$) lower than that of the P7 mouse. In the day 15 and day 18 embryonic stages, ZERO/ BK ratio was 68.9 ± 30.9% (n= 3) and 42.5 ± 10.1% (n= 3) of the P35 juvenile respectively, and in both cases this was not significantly lower than in either of the postnatal stages. At postnatal day 7, ZERO/ BK ratio in the midbrain increased, but not significantly, to 135.7 ± 39.0% (n= 3) of the level in P35 (fig. 5-9).

5-2-4 Developmentally- regulated BK channel alternative splice variant mRNA expression in mouse rhombencephalon/ pons

In the developmental precursor to the pons, the rhombencephalon at E13, the average ratio of STREX mRNA to total BK channel mRNA was 1629.8 ± 369.1% (n= 3) of that in the 35- day juvenile pons. This was significantly ($p< 0.01$) higher than in both postnatal stages that were investigated. At embryo day 15, pons STREX/ BK ratio was 1265.7 ± 325.3% (n= 3), and this was again significantly ($p< 0.05$) higher than in the postnatal stages. At embryonic day 18, the average STREX/ BK ratio was 1014.2 ± 381.7% of the P35 juvenile. At postnatal day 7, average STREX/ BK ratio in the pons was 186.2 ± 51.3% (n= 3) of that in the 35 day- old (fig. 5-10).

Figure 5-9
Developmental regulation of BK channel alternative splice variant mRNA expression in mouse mesencephalon/ midbrain

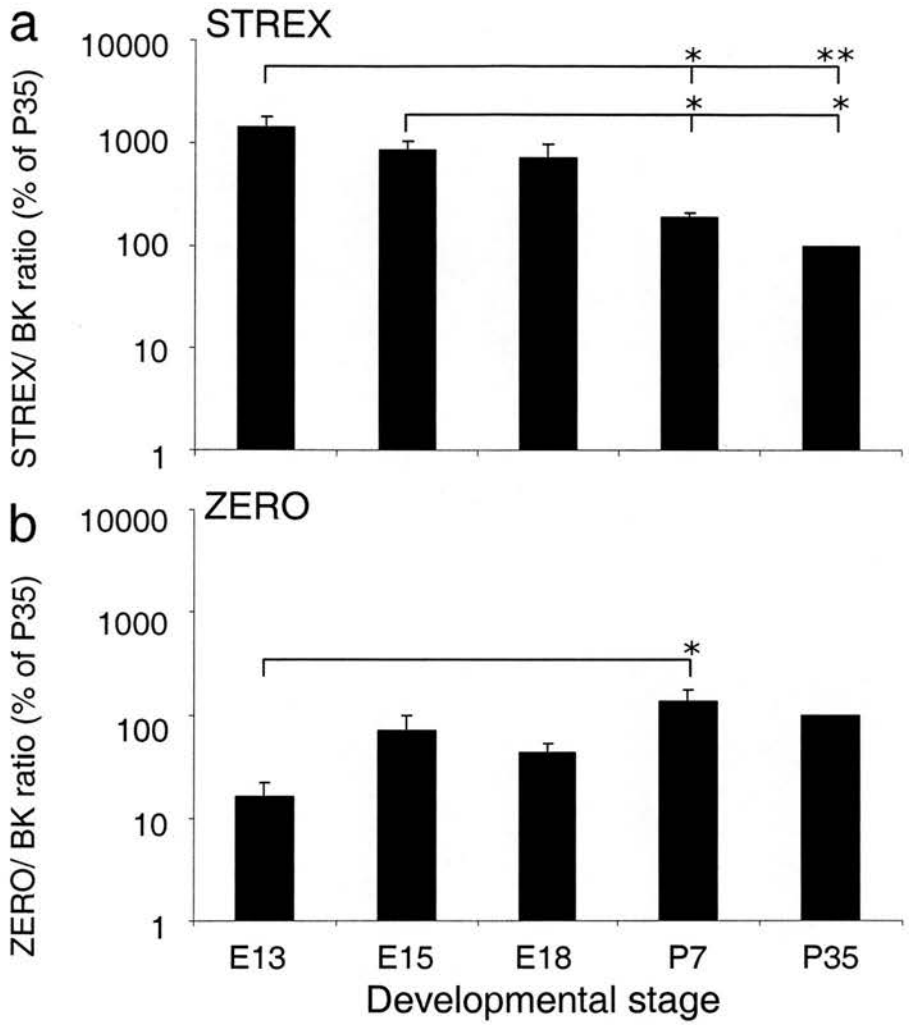

Figure 5-9 Developmental regulation of BK channel alternative splice variant mRNA expression in mouse mesencephalon/ midbrain

Showing **a)** STREX/ BK ratio (n= 3) and **b)** ZERO/ BK ratio (n= 3) expressed as a percentage of postnatal day 35, in mouse mesencephalon (E13)/ midbrain at embryonic day 13, 15, 18 (E13, E15, E18 respectively) and postnatal day 7 and 35 (P7 and 35 respectively) on a logarithmic scale. (*= $p < 0.05$, **= $p < 0.01$ ANOVA post hoc test Bonferroni/ Dunn.)

Figure 5-10
Developmental regulation of BK channel alternative splice variant mRNA expression in mouse rhombencephalon/ pons

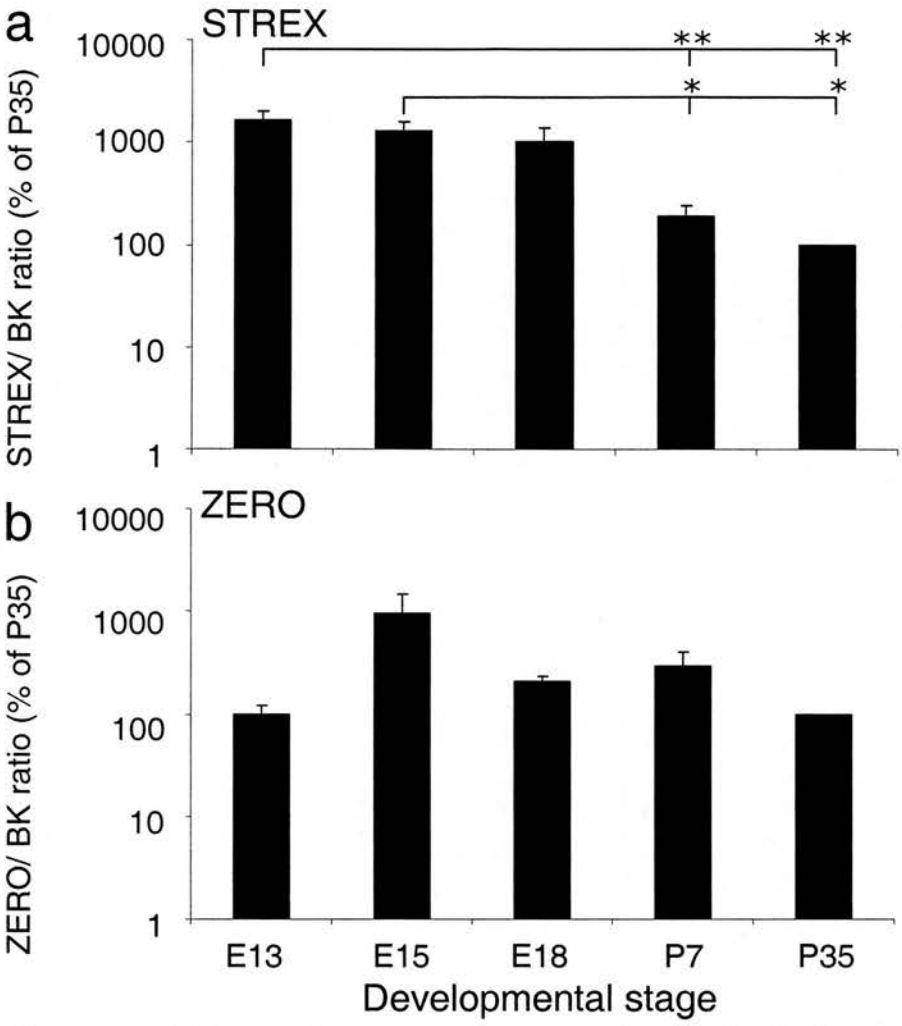

Figure 5-10 Developmental regulation of BK channel alternative splice variant mRNA expression in mouse rhombencephalon/ pons

Showing **a)** STREX/ BK ratio (n= 3) and **b)** ZERO/ BK ratio (n= 3) expressed as a percentage of postnatal day 35, in mouse rhombencephalon (E13)/ pons at embryonic day 13, 15, 18 (E13, E15, E18 respectively) and postnatal day 7 and 35 (P7 and 35 respectively) on a logarithmic scale. (*= $p< 0.05$, **= $p< 0.01$ ANOVA post hoc test Bonferroni/ Dunn.)

ZERO/ BK ratio in the E13 rhombencephalon was 99.6 ± 22.7% (n= 3) of that in the P35 juvenile pons. At E15, this had increased to 958.3 ± 506.3% (n= 3), although this was not significantly higher due to high variability in the results, and subsequently no significant differences were observed between ZERO/ BK ratio in this and the postnatal stages. In the pons at postnatal day 18, ZERO/ BK ratio was 205.0 ± 30.1% (n= 3) of that in P35, and this was not significantly different to either of the postnatal stages investigated. At postnatal day 7, ZERO/ BK ratio was 296.3 ± 110.2% (n= 3) of that at P35 (fig. 5-10).

5-2-5 Developmental regulation of BK channel alternative splice variant mRNA expression in mouse rhombencephalon/ medulla

At E13, the rhombencephalon STREX/ BK ratio was 1473.3 ± 273.0% (n= 3) of that in the P35 medulla, and this was significantly ($p < 0.01$) higher than at either of the postnatal stages investigated. In the E15 medulla, average STREX/ BK ratio was 1145.0 ± 324.1% (n= 3) of P35, and this was again significantly ($p < 0.01$) higher than at either postnatal stage. At E18, medulla STREX/ BK ratio was 749.2 ± 160.1% (n= 3) of P35, and was significantly ($p < 0.01$) higher than in both postnatal stages investigated. STREX/ BK ratio in the P7 medulla was 114.3 ± 41.7% (n= 3) of P35 (fig. 5-11).

ZERO/ BK ratio in the E13 rhombencephalon was 99.6 ± 22.7% (n= 3) of that in P35 medulla. At E15, the medulla ZERO/ BK ratio was 225.2 ± 142.8% (n= 3) of P35; although higher, this was not significantly different to that in either of the postnatal stages. In the E18 medulla, ZERO/ BK ratio was 94.2 ± 57.1% (n= 3) of that in P35,

Figure 5-11
Developmental regulation of BK channel alternative splice variant mRNA expression in mouse rhombencephalon/ medulla

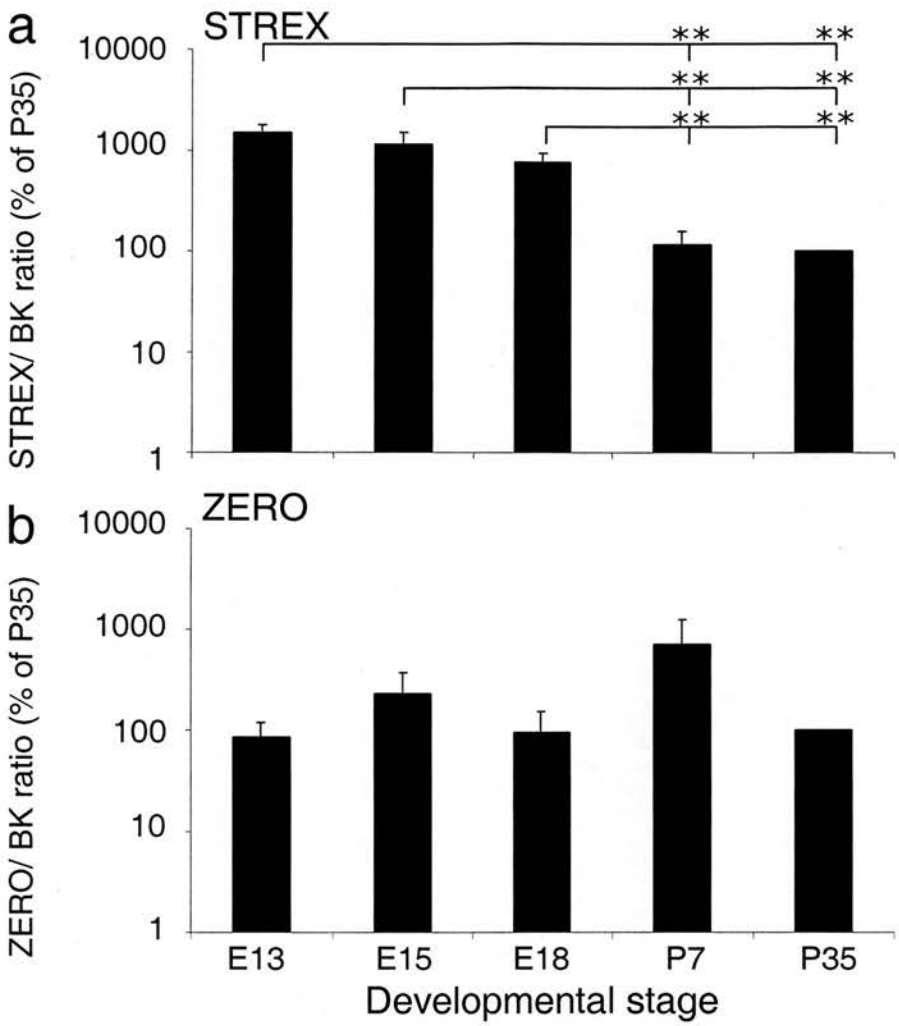

Figure 5-11 Developmental regulation of BK channel alternative splice variant mRNA expression in mouse rhombencephalon/ medulla

Showing **a)** STREX/ BK ratio (n= 3) and **b)** ZERO/ BK ratio (n= 3) expressed as a percentage of postnatal day 35, in mouse rhombencephalon (E13)/ medulla at embryonic day 13, 15, 18 (E13, E15 and E18 respectively) and postnatal day 7 and 35 (P7 and 35 respectively) on a logarithmic scale. (**= $p < 0.01$ ANOVA post hoc test Bonferroni/ Dunn.)

and again this was not significantly different to ratios observed in the two postnatal stages. At P7, ZERO/ BK ratio was 709.0 ± 544.6% (n= 3) of P35 (fig. 5-11). Although this was very high, a large variability in the results accounted for this, and as a result, the P7 ZERO/ BK ratio was not significantly different to that in other stages.

5-2-6 Developmental regulation of BK channel alternative splice variant mRNA expression in mouse diencephalon/ thalamus

The diencephalon at embryo day 15 is the precursor to the thalamus, therefore at this stage it was used to investigate the developmental changes in STREX and ZERO mRNA expression in this tissue. At E15, diencephalon STREX/ BK ratio was 428.9 ± 70.0% (n= 3) of that in the P35 thalamus. This was significantly ($p < 0.05$) higher than at postnatal day 7 and also P35 ($p < 0.01$). At E18, thalamus STREX/ BK ratio was 494.1 ± 123.8% (n= 3) of that in P35. This was significantly ($p < 0.05$) higher than in postnatal day 35. At postnatal day 7, STREX/ BK ratio was 181.6 ± 30.8% (n= 3) of P35 (fig. 5-12).

At E15, ZERO/ BK channel ratio in the diencephalon was 159.0 ± 38.0% (n= 3) of that in the P35 thalamus- this was not significantly different to mRNA expression observed at either postnatal stage investigated. At E18, ZERO/ BK ratio was 64.6 ± 17.7% (n= 3) of P35, and again this was not significantly different to mRNA expression in P7 and P35. ZERO/ BK ratio at P7 was 169.2 ± 66.6% (n= 3) of that at P35, and was not significantly different to the latter (fig. 5-12).

Figure 5-12
Developmental regulation of BK channel alternative splice variant mRNA expression in mouse diencephalon/ thalamus

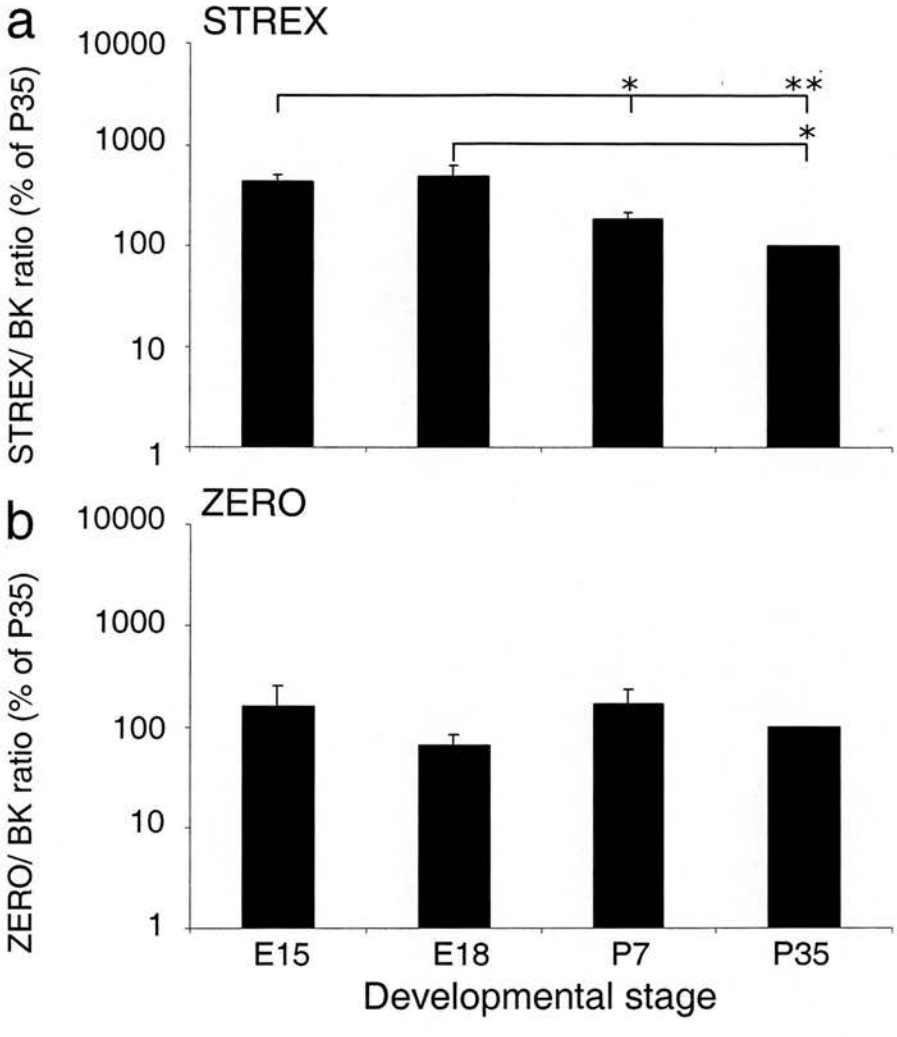

Figure 5-12 Developmental regulation of BK channel alternative splice variant mRNA expression in mouse diencephalon/ thalamus

Showing **a)** STREX/ BK ratio (n= 3) and **b)** ZERO/ BK ratio (n= 3) expressed as a percentage of postnatal day 35, in mouse diencephalon (E15)/ thalamus at embryonic day 15, 18 (E15 and E18 respectively) and postnatal day 7 and 35 (P7 and 35 respectively) on a logarithmic scale. (*= $p< 0.05$, **= $p< 0.01$ ANOVA post hoc test Bonferroni/ Dunn.)

5-2-7 Developmental regulation of BK channel alternative splice variant mRNA expression in mouse diencephalon/ hypothalamus

The hypothalamus is also derived from the diencephalon, therefore this tissue was used as a comparison to investigate the developmental changes in STREX and ZERO BK channel mRNA expression that occur in the hypothalamus during development. At E15, STREX/ BK ratio in the diencephalon was 574.4 ± 136.2% (n= 3) of that in the P35 hypothalamus, and was significantly ($p < 0.05$) higher than at P35. At E18, STREX/ BK ratio in the hypothalamus was 634.0 ± 79.9% (n= 3) of that in P35. This was significantly ($p < 0.01$) higher than at either postnatal day 7 or 35. STREX/ BK ratio in the P7 hypothalamus was 248.6 ± 39.3% (n= 3) of that in P35 (fig. 5-13).

In the E15 diencephalon, ZERO/ BK ratio was 132.2 ± 44.1% (n= 3) of that in the P35 hypothalamus, and was not significantly different to that in either of the postnatal stages investigated. At E18, ZERO/ BK ratio was 87.6 ± 45.2 (n= 3) of P35. Again, this was not significantly different to expression in the postnatal stages. At P7, hypothalamic ZERO/ BK ratio was 43.6 ± 10.2% of that in P35 (fig. 5-13).

5-2-8 Developmental regulation of BK channel alternative splice variant mRNA expression in mouse telencephalon/ frontal cortex

Since the frontal cortex is derived from the telencephalon, this was used as a comparison for BK channel splice variant mRNA expression at E13 and E15. In the telencephalon at E13, average STREX/ BK ratio was 739.8 ± 194.1% (n= 3), whilst average STREX/ BK ratio at E15 was 739.8 ± 194.1% (n= 3) of that in the frontal cortex at P35. At both of these stages, the STREX/ BK ratio was significantly ($p <$

Figure 5-13
Developmental regulation of BK channel alternative splice variant mRNA expression in mouse diencephalon/ hypothalamus

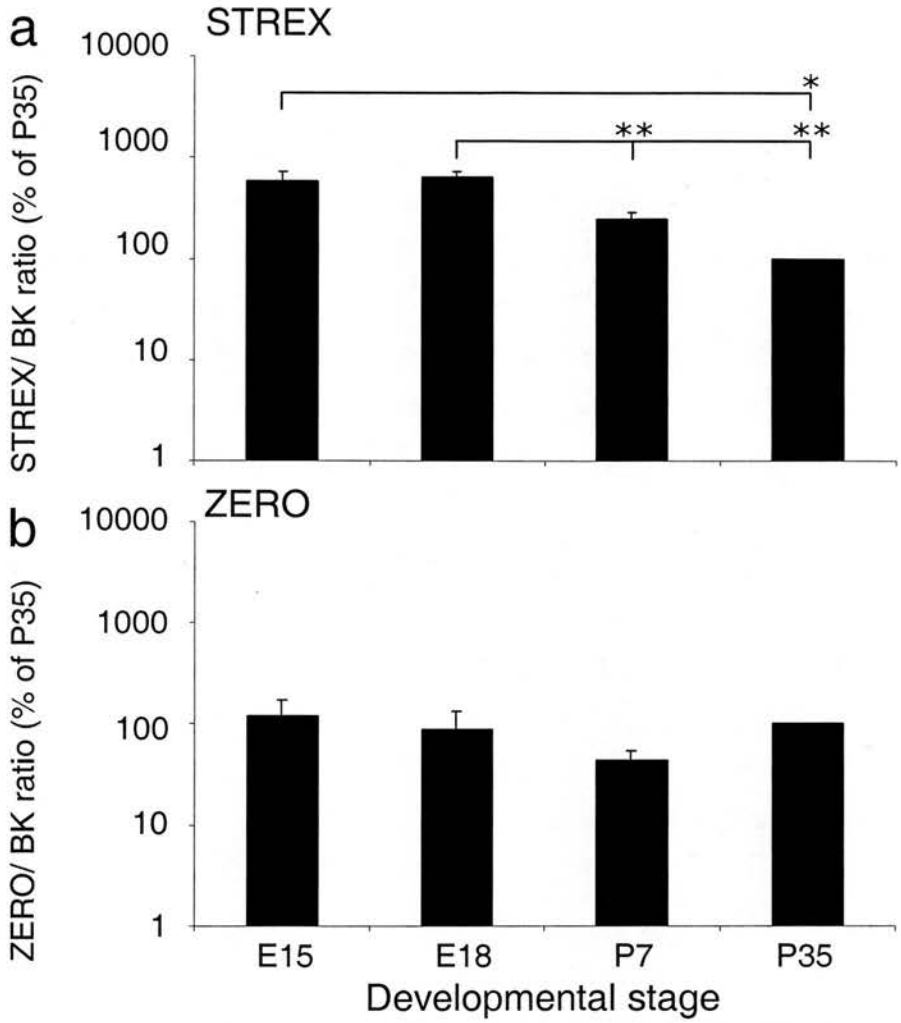

Figure 5-13 Developmental regulation of BK channel alternative splice variant mRNA expression in mouse diencephalon/ hypothalamus

Showing **a)** STREX/ BK ratio (n= 3) and **b)** ZERO/ BK ratio (n= 3) expressed as a percentage of postnatal day 35, in mouse diencephalon (E15)/ hypothalamus at embryonic day 15, 18 (E15 and E18 respectively) and postnatal day 7 and 35 (P7 and 35 respectively) on a logarithmic scale. (*= $p < 0.05$, **= $p < 0.01$ ANOVA post hoc test Bonferroni/ Dunn.)

0.05) higher than that in the frontal cortex at either P7 or P35. In the frontal cortex at E18, STREX/ BK ratio was 386.3 ± 73.1% (n= 3) of P35, significantly ($p < 0.05$) higher than that in postnatal day 7 or 35. At P7, the average STREX/ BK ratio was 145.5 ± 23.8% of P35 (fig. 5-14).

No significant differences were observed in ZERO/ BK channel ratio during development of the frontal cortex. In the telencephalon at E13 and E15, average ZERO/ BK ratios were 12.7 ± 8.2% (n= 3) and 50.8 ± 8.1% (n= 3), respectively, of that in the frontal cortex at P35. At E18, ZERO/ BK ratio was 54.3 ± 33.8% (n= 3) of that in P35. At P7, ZERO/ BK ratio was 98.9 ± 39.0% (n= 3) of P35 (fig. 5-14).

5-2-9 Developmental regulation of BK channel alternative splice variant mRNA expression in mouse telencephalon/ posterior cortex

Since the posterior cortex is also derived from the telencephalon, this was used as a comparison at E13 and E15. In the telencephalon at E13, average STREX/ BK ratio was 1006.4 ± 216.6% (n= 3) of that in the posterior cortex at P35. This was significantly ($p < 0.05$) higher than in the posterior cortex at P7, and also significantly ($p < 0.01$) higher than at P35. At E15, average STREX/ BK ratio in the telencephalon was 989.8 ± 147.5 (n= 3) of that in the posterior cortex at P35, and was significantly ($p < 0.01$) higher than the average STREX/ BK ratio in the posterior cortex at either P7 or P35. In the posterior cortex, STREX/ BK ratio at E18 was 535.5 ± 132.5% (n= 3) of P35, significantly ($p < 0.05$) higher than that in the P35 juvenile, although not significantly different to that in postnatal day 7, where STREX/ BK ratio was 186.8 ± 46.4% (n= 3) of P35 (fig. 5-15).

Figure 5-14
Developmental regulation of BK channel alternative splice variant mRNA expression in mouse telencephalon/ frontal cortex

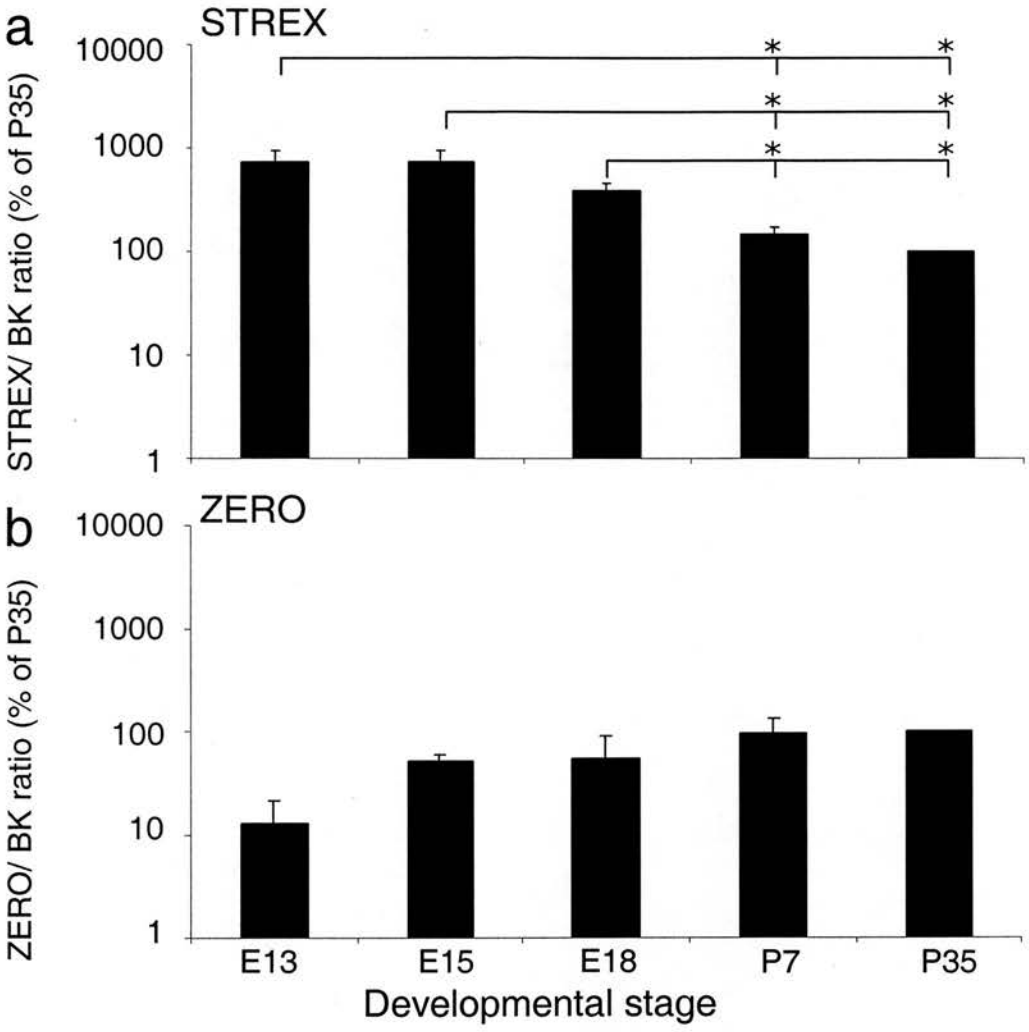

Figure 5-14 Developmental regulation of BK channel alternative splice variant mRNA expression in mouse telencephalon/ frontal cortex

Showing **a)** STREX/ BK ratio (n= 3) and **b)** ZERO/ BK ratio (n= 3) expressed as a percentage of postnatal day 35, in mouse telencephalon at embryonic day 13 (E13) and 15 (E15), and frontal cortex at embryonic day 18 (E18) and postnatal day 7 and 35 (P7 and 35 respectively) on a logarithmic scale. (*= $p < 0.05$ ANOVA post hoc test Bonferroni/ Dunn.)

Figure 5-15
Developmental regulation of BK channel alternative splice variant mRNA expression in mouse telencephalon/ posterior cortex

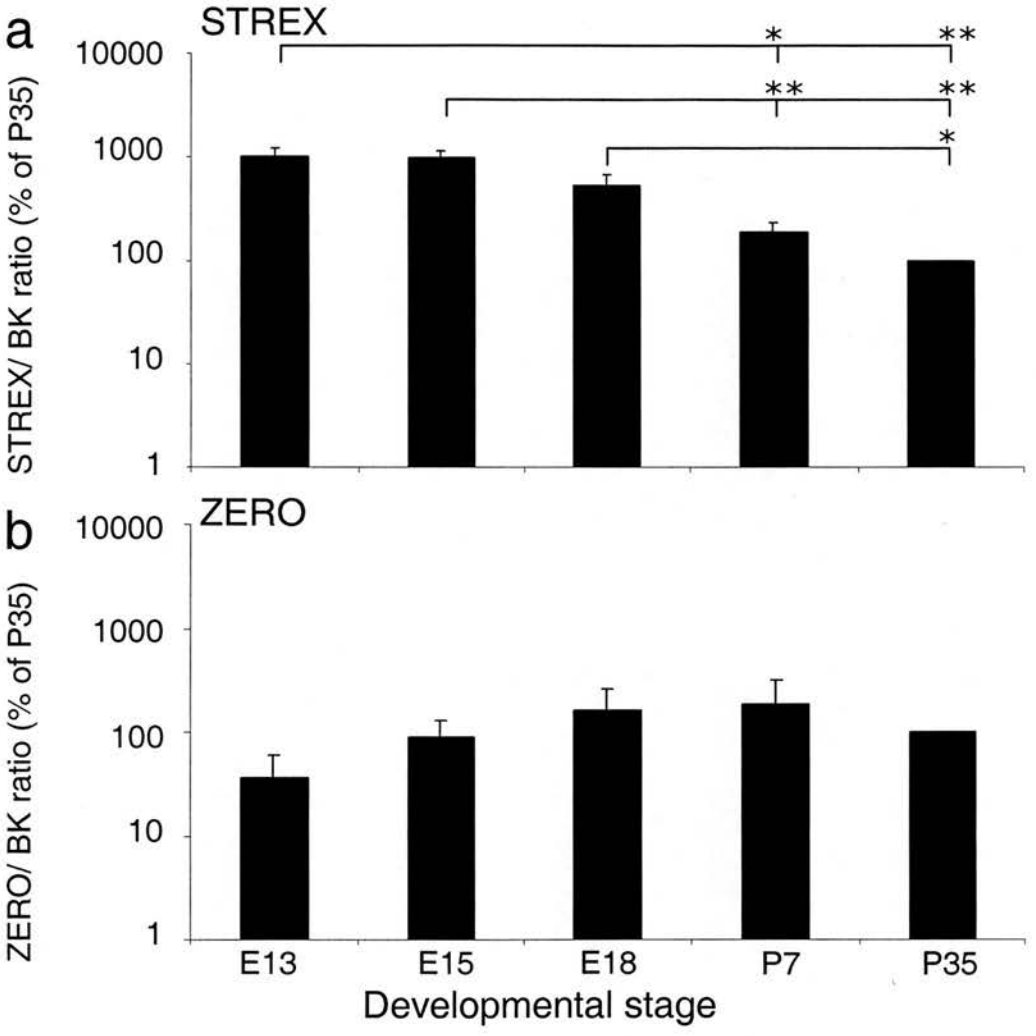

Figure 5-15 Developmental regulation of BK channel alternative splice variant mRNA expression in mouse telencephalon/ posterior cortex

Showing **a)** STREX/ BK ratio (n= 3) and **b)** ZERO/ BK ratio (n= 3) expressed as a percentage of postnatal day 35, in mouse telencephalon at embryonic day 13 (E13) and 15 (E15), and posterior cortex at embryonic day 18 (E18) and postnatal day 7 and 35 (P7 and 35 respectively) on a logarithmic scale. (*= $p < 0.05$, **= $p < 0.01$ ANOVA post hoc test Bonferroni/ Dunn.)

ZERO mRNA expression was not significantly altered during the period from E13 to P35 in the telencephalon/ posterior cortex. In the E13 telencephalon, average ZERO/ BK ratio was 36.4 ± 23.7% (n= 3), whilst at E15, average ZERO/ BK ratio in the telencephalon was 90.6 ± 36.9% (n= 3) of that in the posterior cortex at P35. At E18, the average ZERO/ BK ratio was 160.4 ± 98.8% (n= 3) of that in P35. At P7, average ZERO/ BK ratio was 187.3 ± 131.1% (n= 3) of P35 (fig. 5-15).

5-2-10 Developmental regulation of BK channel alternative splice variant mRNA expression in mouse telencephalon/ entorhinal cortex

The entorhinal cortex is derived from the telencephalon, therefore this was used as a comparison for BK channel splice variant expression at E13 and E15. Significant regulation of STREX mRNA expression was observed in the entorhinal cortex during development. In the telencephalon at E13, average STREX/ BK ratio was 765.1 ± 265.0% (n= 3) of that in the entorhinal cortex at P35. Due to variability in the results, this difference was not considered significant. At E15, average STREX/ BK ratio in the telencephalon was 743.5 ± 217.5% (n= 3) of that in the entorhinal cortex at P35, and this was significantly ($p< 0.05$) higher than the average STREX/ BK ratio in the entorhinal cortex at either P7 or P35. At E18, average STREX/ BK ratio in the entorhinal cortex was 302.2 ± 72.4% (n= 3) of that at P35, and was significantly ($p< 0.05$) higher than the average STREX/ BK ratio at that timepoint. STREX/ BK ratio at P7 was not significantly different to that in the P35 juvenile, at 124.9 ± 14.8% (n= 3) of P35 (fig. 5-16).

Figure 5-16
Developmental regulation of BK channel alternative splice variant mRNA expression in mouse telencephalon/ entorhinal cortex

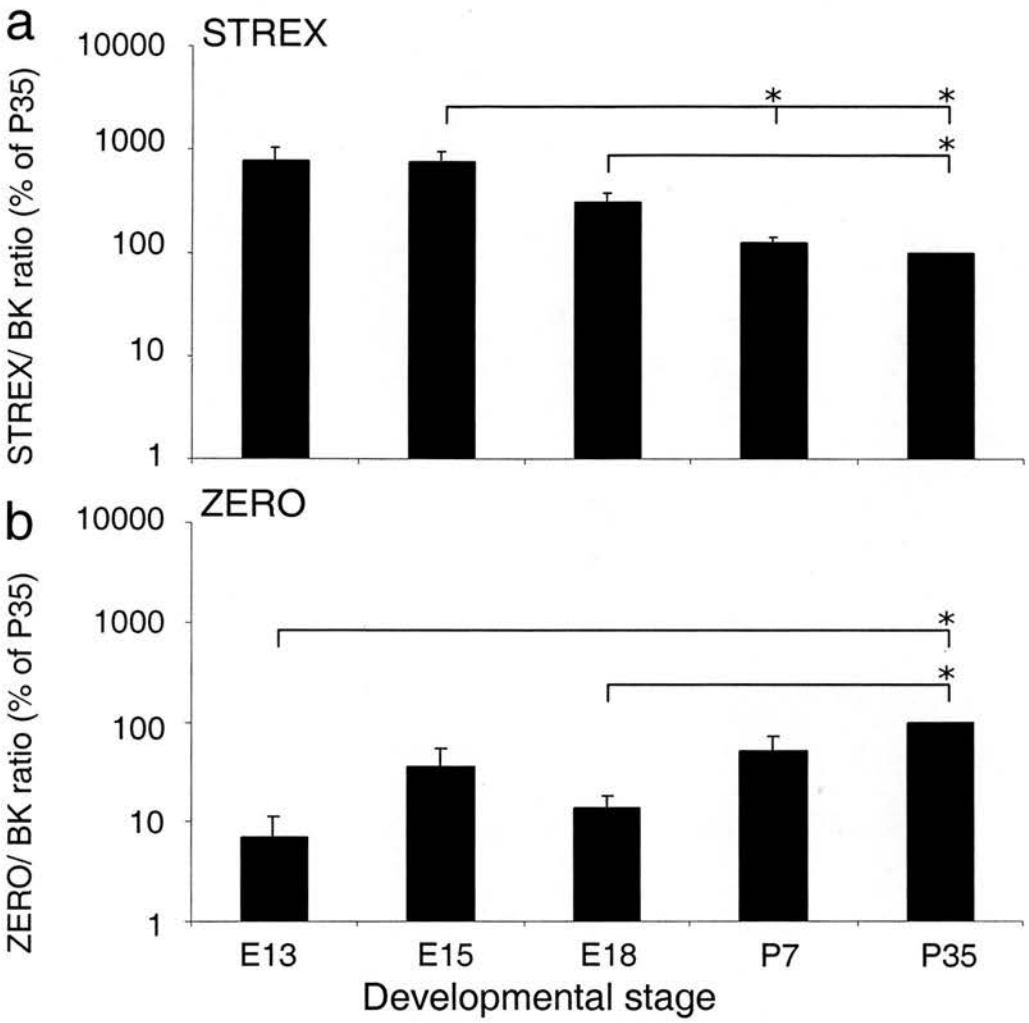

Figure 5-16 Developmental regulation of BK channel alternative splice variant mRNA expression in mouse telencephalon/ entorhinal cortex

Showing **a)** STREX/ BK ratio (n= 3) and **b)** ZERO/ BK ratio (n= 3) expressed as a percentage of postnatal day 35, in mouse telencephalon at embryonic day 13 (E13) and 15 (E15), and entorhinal cortex at embryonic day 18 (E18) and postnatal day 7 and 35 (P7 and 35 respectively) on a logarithmic scale. (*= $p < 0.05$ ANOVA post hoc test Bonferroni/ Dunn.)

An upregulation of ZERO mRNA expression was observed in the telencephalon/ entorhinal cortex over the course of development. At E13, average ZERO/ BK ratio in the telencephalon was 7.1 ± 4.1% (n= 3) of that in the entorhinal cortex at P35, and was significantly ($p < 0.05$) lower than at that timepoint. At E15, average ZERO/ BK ratio in the telencephalon was 35.8 ± 19.4% of that in the entorhinal cortex at P35, however this difference was not significant. At E18, average ZERO/ BK ratio was significantly ($p < 0.05$) lower than in the P35 juvenile, at 13.8 ± 4.3% (n= 3) of P35. At P7, ZERO/ BK ratio was elevated slightly, but not significantly so, to 51.7 ± 20.7% (n= 3) of P35 (fig. 5-16).

5-2-11 Developmental regulation of BK channel alternative splice variant mRNA expression in mouse telencephalon/ olfactory bulb

Since the olfactory bulb is derived from the telencephalon, this was used as a comparison for BK channel alternative splice variant expression at E13 and E15. Downregulation of STREX mRNA expression was found to occur in the telencephalon/ olfactory bulb during development. In the telencephalon at E13, average STREX/ BK ratio was 1202.0 ± 168.7% (n= 3), whilst the average STREX/ BK ratio at E15 was 1227 ± 185.2% (n= 3) of that in the olfactory bulb at P35. At both E13 and E15, telencephalon STREX/ BK ratio was significantly ($p < 0.01$) higher than in the olfactory bulb at either P7 or P35. At E18, average STREX/ BK ratio was 800.2 ± 155.6% (n= 3) of that in P35- significantly ($p < 0.05$) higher than in either postnatal day 7 or 35. At P7, average STREX/ BK ratio was 285.3 ± 96.4% (n= 3) of P35, although this difference was not significant (fig. 5-17).

Figure 5-17
Developmental regulation of BK channel alternative splice variant mRNA expression in mouse telencephalon/ olfactory bulb

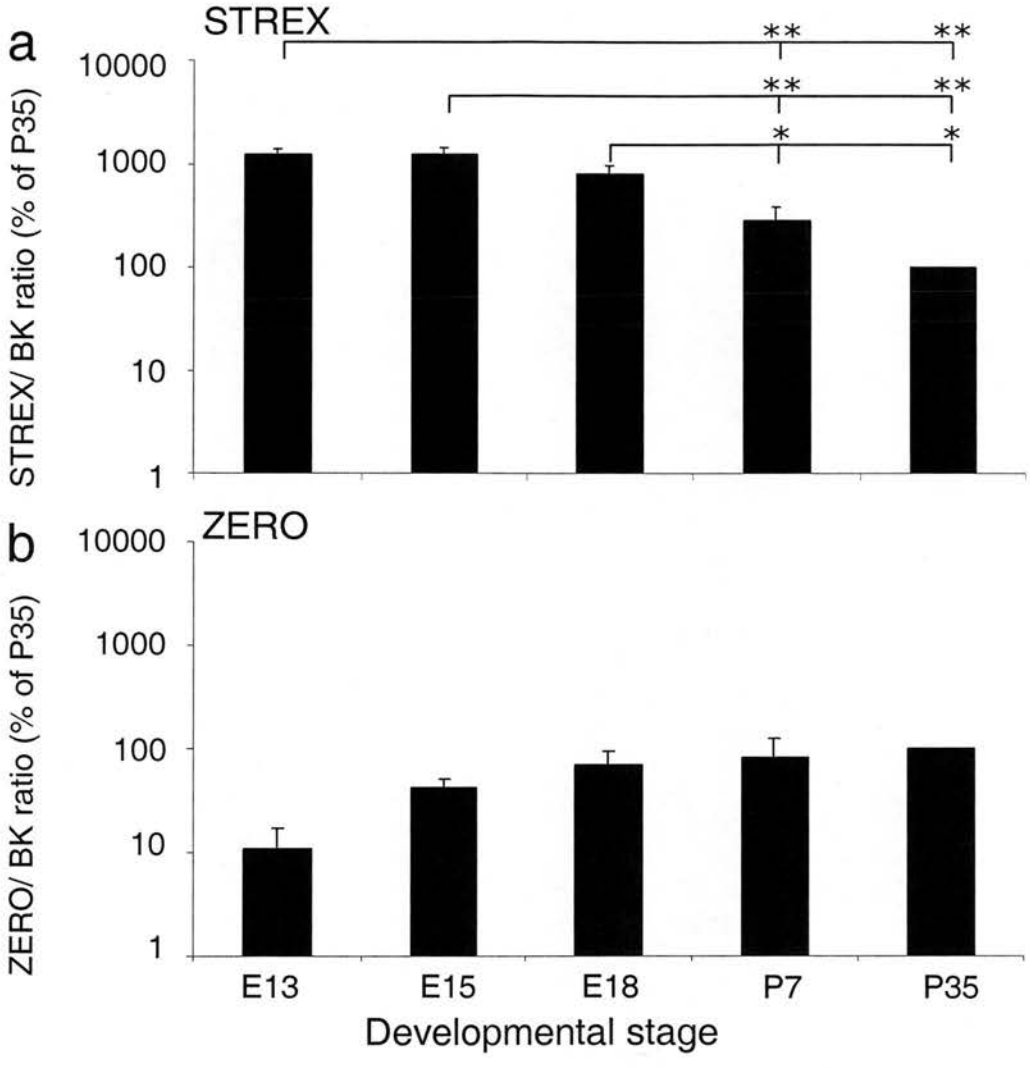

Figure 5-17 Developmental regulation of BK channel alternative splice variant mRNA expression in mouse telencephalon/ olfactory bulb

Showing **a)** STREX/ BK ratio (n= 3) and **b)** ZERO/ BK ratio (n= 3) expressed as a percentage of postnatal day 35, in mouse telencephalon at embryonic day 13 (E13) and 15 (E15), and olfactory bulb at embryonic day 18 (E18) and postnatal day 7 and 35 (P7 and 35 respectively) on a logarithmic scale. (*= $p < 0.05$, **= $p < 0.01$ ANOVA post hoc test Bonferroni/ Dunn.)

No significant differences were observed in the mRNA expression of the ZERO BK channel alternative splice variant across development of the telencephalon/ olfactory bulb. In the telencephalon at E13, average ZERO/ BK ratio was 11.0 ± 6.1% (n= 3), whilst at E15, average ZERO/ BK ratio was 42.0 ± 9.5% (n= 3) of that in the P35 olfactory bulb. At E18, average ZERO/ BK ratio was 69.6 ± 23.7% (n= 3) of that in P35. At P7, the average ZERO/ BK ratio was 81.8 ± 42.9% (n= 3) of P35 (fig. 5-17).

5-2-12 Developmental regulation of BK channel alternative splice variant mRNA expression in mouse telencephalon/ hippocampus

The hippocampus also arises from the telencephalon, therefore this was used as a comparison for BK channel splice variant expression at E13 and E15. In the telencephalon at E13, average STREX/ BK ratio was 1050.9 ± 312.0% (n= 3) of that in the hippocampus at P35, and was significantly ($p < 0.05$) higher than at that timepoint. At E15, average STREX/ BK ratio in the telencephalon was 1039.7 ± 253.1% (n= 3) of that in the P35 hippocampus, and was significantly ($p < 0.05$) higher than at either P7 or P35. At E18, average STREX/ BK ratio was 1425.4 ± 528.7% (n= 3) of that in P35. Due to large variability in results this was not significantly higher than STREX/ BK ratio in the postnatal stages. At P7, average STREX/ BK ratio was 209.1 ± 59.2% (n= 3) of P35. Again, this was not significantly different to that in the P35 juvenile (fig. 5-18).

No significant differences were observed in the expression of ZERO during telencephalon/ hippocampus development. In the telencephalon at E13, average

Figure 5-18
Developmental regulation of BK channel alternative splice variant mRNA expression in mouse telencephalon/ hippocampus

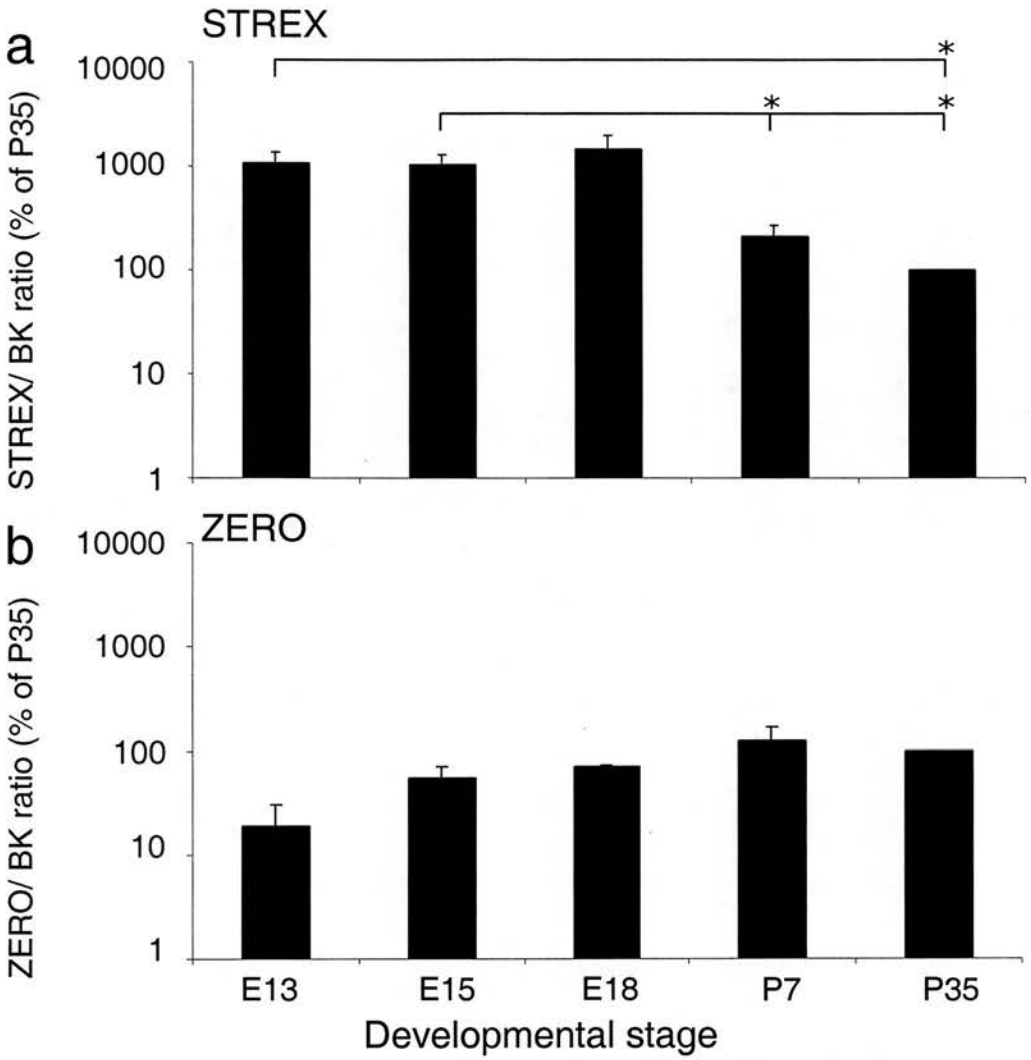

Figure 5-18 Developmental regulation of BK channel alternative splice variant mRNA expression in mouse telencephalon/ hippocampus

Showing **a)** STREX/ BK ratio (n= 3) and **b)** ZERO/ BK ratio (n= 3) expressed as a percentage of postnatal day 35, in mouse telencephalon at embryonic day 13 (E13) and 15 (E15), and hippocampus at embryonic day 18 (E18) and postnatal day 7 and 35 (P7 and 35 respectively) on a logarithmic scale. (*= $p < 0.05$ ANOVA post hoc test Bonferroni/ Dunn.)

ZERO/ BK channel ratio was 18.8 ± 11.6% (n= 3), whilst average ZERO/ BK ratio at E15 was 54.9 ± 16.6% (n= 3) of that in the hippocampus at P35. At E18, average ZERO/ BK ratio was 70.7 ± 2.7% (n= 3) of that in P35. At postnatal day 7, the average ZERO/ BK ratio was 123.0 ± 42.6% (n= 3) of that in P35 (fig. 5-18).

5-2-13 Developmental regulation of BK channel alternative splice variant mRNA expression in mouse telencephalon/ striatum

The striatum is derived from the telencephalon, therefore this was used as a comparison at E13 and E15 to examine BK channel alternative splice variant expression. STREX mRNA expression was found to be downregulated during development of the striatum. In the telencephalon at E13, average STREX/ BK ratio was 849.9 ± 177.4% (n= 3), whilst STREX/ BK ratio at E15 was 837.9 ± 123.3% of (n= 3) that in the striatum at P35. At both of these stages, average STREX/ BK ratio was significantly ($p< 0.01$) higher than in the striatum at either P7 or P35. At E18, average STREX/ BK ratio was 488.1 ± 60.1% (n= 3) of that in the P35 striatum, and was significantly ($p< 0.01$) higher than in either of the postnatal stages investigated. At P7, average STREX/ BK ratio was 144.4 ± 16.5% (n= 3) of that in the P35 juvenile, although this difference was not significant (fig. 5-19).

Additionally, no significant differences in expression of ZERO mRNA were observed in the telencephalon/ striatum across development. In the telencephalon at E13 and E15, average ZERO/ BK ratios were 39.7 ± 28.0% (n= 3) and 96.6 ± 30.2% (n= 3), respectively, of that in the striatum at P35. At E18, average ZERO/ BK ratio

Figure 5-19
Developmental regulation of BK channel alternative splice variant mRNA expression in mouse telencephalon/ striatum

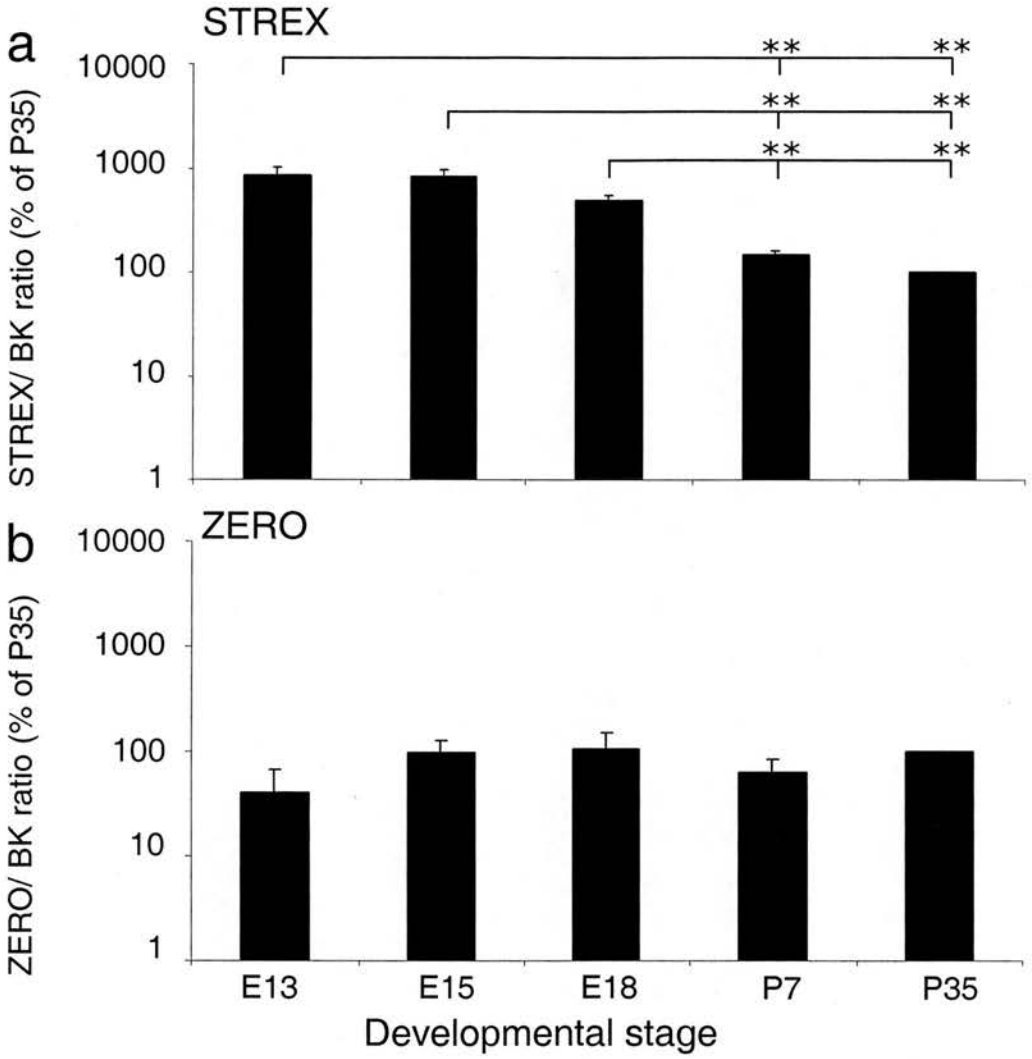

Figure 5-19 Developmental regulation of BK channel alternative splice variant mRNA expression in mouse telencephalon/ striatum

Showing **a)** STREX/ BK ratio (n= 3) and **b)** ZERO/ BK ratio (n= 3) expressed as a percentage of postnatal day 35, in mouse telencephalon at embryonic day 13 (E13) and 15 (E15), and striatum at embryonic day 18 (E18) and postnatal day 7 and 35 (P7 and 35 respectively) on a logarithmic scale. (**= $p < 0.01$ ANOVA post hoc test Bonferroni/ Dunn.)

was 105.1 ± 44.1% (n= 3) of that in P35 striatum. At P7, the average ZERO/ BK ratio was 63.9 ± 19.8% (n=3) of that in P35 (fig. 5-19).

5-2-14 Developmental regulation of BK channel alternative splice variant mRNA expression in mouse rhombencephalon/ cerebellum

Since the cerebellum is ultimately derived from the rhombencephalon, but cDNA from the intermediary developmental structures was not available for analysis, STREX and ZERO/ BK ratios were compared from the E13 rhombencephalon with the P35 cerebellum. At E13, the average STREX/ BK ratio in the rhombencephalon was 2479.5 ± 190.9% (n= 3) of that in the P35 cerebellum. This was significantly ($p < 0.01$) higher than in either P7 or the P35 juvenile. At P7, STREX/ BK ratio in the cerebellum was 263.0 ± 34.9% (n= 3) of that at P35, and again this was significantly ($p < 0.01$) higher. No significant differences were observed in ZERO mRNA expression in the developing cerebellum. In the E13 rhombencephalon, the average ZERO/ BK ratio was 486.2 ± 162.5% (n= 3) of that in the P35 cerebellum. At P7, average ZERO/ BK ratio in the cerebellum was 1060.6 ± 377.1% (n= 3) of that at P35 (fig. 5-20).

5-3 Summary

5-3-1 Developmental changes in total BK channel mRNA expression in mouse CNS

To investigate whether expression of BK channel mRNA changed in the mouse CNS during embryogenesis and early postnatal life, mouse CNS tissues were screened at several stages of development, showing that in many cases, the expression of total

Figure 5-20
Developmental regulation of BK channel alternative splice variant mRNA expression in mouse rhombencephalon/ cerebellum

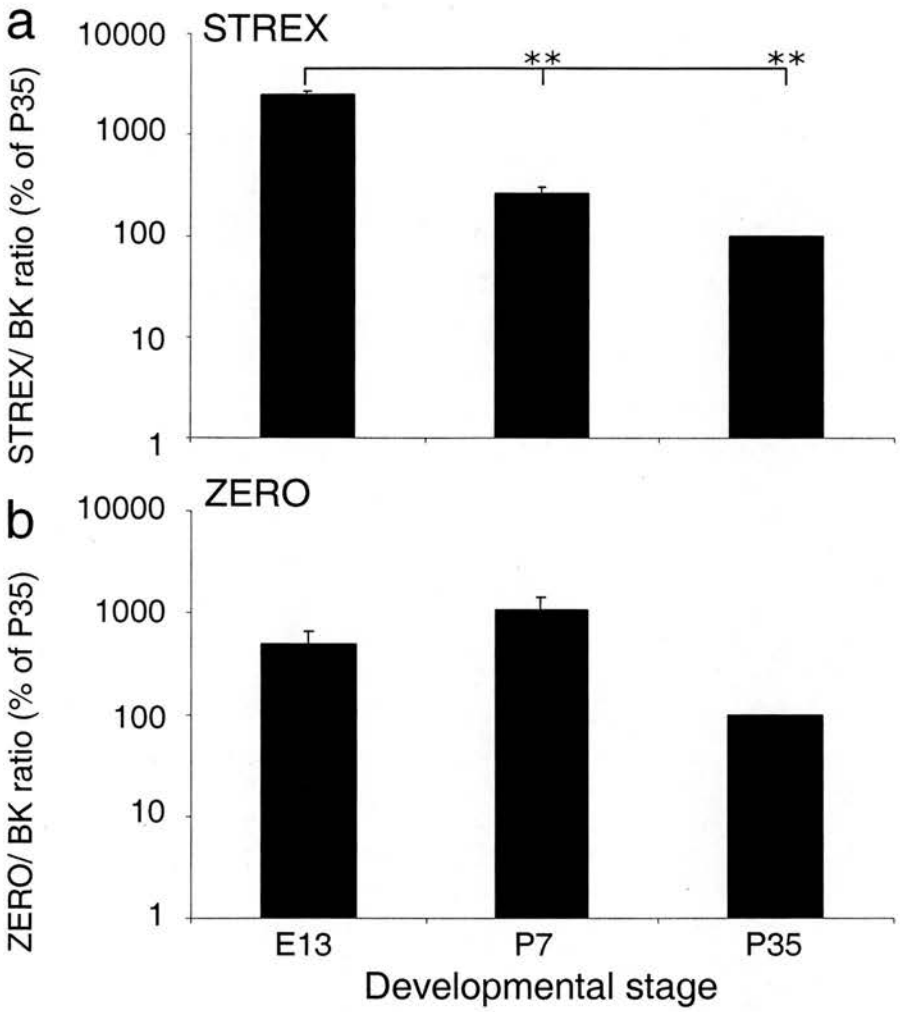

Figure 5-20 Developmental regulation of BK channel alternative splice variant mRNA expression in mouse rhombencephalon/ cerebellum

Showing **a)** STREX/ BK ratio (n= 3) and **b)** ZERO/ BK ratio (n= 3) expressed as a percentage of postnatal day 35, in mouse rhombencephalon (E13)/ cerebellum at embryonic day 13 (E13) and postnatal day 7 and 35 (P7 and 35 respectively) on a logarithmic scale. (**= $p < 0.01$ ANOVA post hoc test Bonferroni/ Dunn.)

BK channel mRNA increased significantly, relative to the postnatal stages. Activity dependent regulation of dendritic growth and synaptogenesis is a key factor in the development of the CNS (Wong and Ghosh, 2002, Aamodt and Constantine- Paton, 1999). By influencing vital processes such as neurotransmitter release, it is possible that BK channels are critical to establishment and refinement of synaptic connections. Additionally, since BK channels are often colocalised with voltage-dependent calcium channels, this coupling of intracellular calcium to cell excitability may be of significance in the calcium signalling events that determine early central nervous system differentiation (Moreau and Leclerc, 2004).

In the hypothalamus, no significant change in BK channel mRNA expression was observed during development. However, since a significant developmental upregulation of BK channel mRNA expression was observed in the thalamus, which arises from the same precursor tissue, it may be the case that for the hypothalamus, variability in the results was sufficient to render comparisons between the embryonic and postnatal stages not significant, therefore further experiments may be required to confirm whether or not developmental regulation of BK channel mRNA expression can occur in this tissue.

5-3-2 Developmental changes in STREX mRNA expression in mouse CNS

Expression of differentially- regulated BK channel alternative splice variants may facilitate an increased range of responses by cells to the many signalling events that occur during CNS development. In several of the mouse CNS regions that were

investigated, total BK channel mRNA expression was found to be upregulated as development progressed. This therefore raised the possibility that previously observed developmental changes in BK channel alternative splice variant mRNA expression might be attributable solely to differences in the overall BK channel population, as opposed to changes in the relative amount of each alternative splice variant. To address this, cDNA from a number of mouse CNS tissues was assayed for the presence of the STREX and ZERO BK channel alternative splice variants, which were expressed as a ratio of total BK channel. This was then normalised to P35, to investigate changes that occurred in the mRNA expression of each splice variant within the BK channel population across development. In all of the mouse CNS tissues investigated, the expression of STREX mRNA, as a percentage of total BK channel mRNA, was found to decrease significantly over the course of development relative to that in the 35- day old juvenile.

Since the STREX BK channel has an altered activation phenotype (Shipston *et al.*, 1999, Hanaoka *et al.*, 1999, Saito *et al.*, 1997) compared to the ZERO splice variant, the high level of mRNA expression of such channels in the early embryonic stages suggests that during this period, distinct modes of regulation alter cell responsiveness and signalling, which are not utilised, or are less significant once embryonic neuronal differentiation and patterning are completed. The 'rapid activation' phenotype, attributable to increased calcium and voltage sensitivity conferred by the STREX insert (Xie and McCobb, 1998), as well as increased rates of activation, and decreased rate of deactivation (Saito *et al.*, 1997) may facilitate synapse formation by favouring increased rates of neurotransmitter release. Since competitive elimination

of synapses is a prerequisite for regulated axonal growth and connectivity (Ottersen, 2005), it is possible that the activity phenotype engendered by STREX may facilitate fast synaptic transmission, thus ensuring persistence of synaptic connections. Once patterning of the CNS tissues is completed, the regulatory effect on neurotransmitter release by STREX BK channels might only be required in specific subsets of cells, or regions of the brain, for example the hippocampus or the cerebellum, thereby accounting for the decreased expression observed in the postnatal stages. Additionally, inclusion of the STREX exon causes BK channels to be inhibited by PKA, whilst channels lacking STREX are activated (Tian *et al.*, 2001b). This may therefore be of significance during the embryonic patterning of the CNS, where Sonic Hedgehog signalling is critical to neural differentiation, as functional crosstalk has been demonstrated between the Shh pathway and PKA activation (Epstein *et al.*, 1996). Since the STREX insert confers glucocorticoid sensitivity on the BK channel (Shipston *et al.*, 1996), it may also be the case that the maternal glucocorticoids may influence some aspects of CNS development via BK channel modulation.

In rats, low birth weight and developmental organ defects result from disregulated in utero glucocorticoid exposure (Seckl and Meaney 2004). Sex steroids can also have an effect on CNS structural development and plasticity (Simerly, 2002). Since BK channel gating can be regulated by steroids (Duncan, 2005), and given the high levels of STREX- containing channels in the embryonic CNS, it is possible that some of the effects mediated by BK channel activity during embryonic CNS development are subject to steroid regulation.

Another paradigm of developmentally- regulated BK channel activity has been demonstrated in ovine foetal arterial smooth muscle cells, where phosphorylation by channel associated protein phosphatases and kinases (CAPAKs), and the rates of CAPAK activity change substantially across the developmental period (Lin *et al.*, 2005). In this case, the embryonic BK channels have increased sensitivity to intracellular calcium, and this is diminished in adults. The modulation of channel activity by developmentally changing phosphorylation in this manner may therefore also be of significance in the regulation of CNS development, and it is likely that the existence of multiple BK channel α-subunit alternative splice variant and β-subunit combinations precludes the existence of a single factor that regulates activity in this context.

5-3-3 Developmental changes in ZERO mRNA expression in mouse CNS

Whilst STREX mRNA expression was seen to fall over the course of development from E13 to P35, the opposite regulation was recorded for the insertless, ZERO BK channel alternative splice variant. However, in this case, a significant upregulation of ZERO mRNA expression was only observed in the spinal cord, midbrain and entorhinal cortex, with ZERO mRNA expression in the other tissues investigated remaining constant throughout development This suggests that during maturation of BK channel populations into the adult phenotype, regulated expression of STREX may be more significant. However, since many other alternative splice variants of the BK channel exist, potentially combining to give rise to a very large number of proteins, it is highly likely that interplay of ZERO and STREX splice variants is not the only mechanism that exists to effect changes in cell excitability of embryonic

neurons. Also, the high variability in many of the results may have masked genuine differences in ZERO expression during development. For example, in several cases, such as the pons, medulla and cerebellum, although variability was sufficiently high to render differences insignificant, it appeared that the ZERO/ BK ratio was varied across developmental stages, increasing at certain points, then falling again, in contrast to the situations where significant ZERO regulation was actually seen, where the mRNA expression level was low at early embryonic stages, then increased up to the P35 level.

Additionally, the presence of alternative splice inserts at the other sites of splicing in the intracellular C-terminus (Clark *et al.*, 1999), or in the N-terminal region of the BK channel may exert a regulatory influence on neuronal activity that profoundly influences CNS development, for example by altering cell excitability to adjust neurotransmitter release, or changing channel surface trafficking (Zarei *et al.*, 2001). Possibly, other splice variants may introduce sites of regulation that are targets for components of the multiple signalling pathways activated during stages of CNS development. Furthermore, the presence of heterotetramers of alternatively spliced BK channel α-subunits may also contribute to regulated signalling, as it has been shown that activation and inhibition of such channels is dependent on their subunit composition (Tian *et al.*, 2004).

During this study, changes were detected in mRNA expression of total BK channel, as well as that of the STREX and ZERO splice variants, suggesting that BK channel splicing is regulated during development. However, further methods to measure such

expression should also be considered. To reinforce the results from this study, future experiments may use techniques such as quantitative western blotting, to facilitate measurement of BK channel protein expression. Furthermore, other regulatory mechanisms, such as differential subcellular localisation of BK channel alternative splice variants, may also be of significance in determining changes in cell excitability that may be critical for development, therefore the development of BK channel splice variant-specific antibodies may in the future prove to be a useful tool for this type of investigation.

The assembly of channel α-subunit tetramers with accessory β-subunits may also be of significance, and it has been shown that distinct modes of regulation exist for channels assembled in this manner (Lingle *et al.*, 2001). However, since a lack of BK channels does not appear to significantly affect the gross morphological development of the tissues of the CNS, although producing ataxia and severe learning difficulties (Sausbier *et al.*, 2004), it may be the case that the study of the effects of the many BK channel alternative splice variants is dependent on the specific analysis of establishment and refinement of synapses, and that BK channels serve to modulate the kinetics of synaptic transmission, with presence of certain firing phenotypes able to significantly affect the establishment of the neural network in order to permit normal postnatal learning and development.

Chapter Six:

Effect of HPA axis manipulation on BK channel alternative splicing

6-1 Introduction

6-1-1 Effects of stress on the mammalian central nervous system

During situations of novelty, perceived threat or distress, activity of the hypothalamic- pituitary- adrenocortical (HPA) axis becomes upregulated (fig. 6-1). Cells in the paraventricular nucleus (PVN) of the hypothalamus secrete corticotrophin- releasing hormone (CRH), which acts synergistically with arginine vasopressin (AVP) on the anterior pituitary, causing release of adrenocorticotropic hormone (ACTH). The adrenal gland is stimulated by ACTH to release glucocorticoids- most significantly cortisol in humans, and corticosterone (CORT) in rodents. Increased circulating CORT then has a negative feedback effect on the hippocampus, hypothalamus and pituitary, enabling control of hormone release, and return of HPA axis activity to a resting level. Factors such as crosstalk between the HPA and HPG (hypothalamic- pituitary- gonadal) axes (Viau, 2002), resulting in sex differences (Coleman *et al.*, 1998) and genetic predisposition towards adaptive or aggressive responses to stress (Veenema *et al.*, 2004) contribute to the large variability in HPA axis regulation seen across individuals. In addition to this, stressful experiences during early life, such as prolonged maternal separation, can have profound effects on responses to stress during adulthood (Mirescu *et al.*, 2004). Activation of the HPA axis during stress enables efficient crisis responses, leading to more immediate proactive behaviours, or longer- term adaptive coping.

Since the BK channel has previously been shown to be an important regulator of cell excitability in the adrenal cortex and anterior pituitary, and can be influenced by signalling from the pituitary (Lovell and McCobb, 2001), investigation of differential

Figure 6-1
Overview of the Hypothalamic- pituitary-adrenocortical (HPA) axis

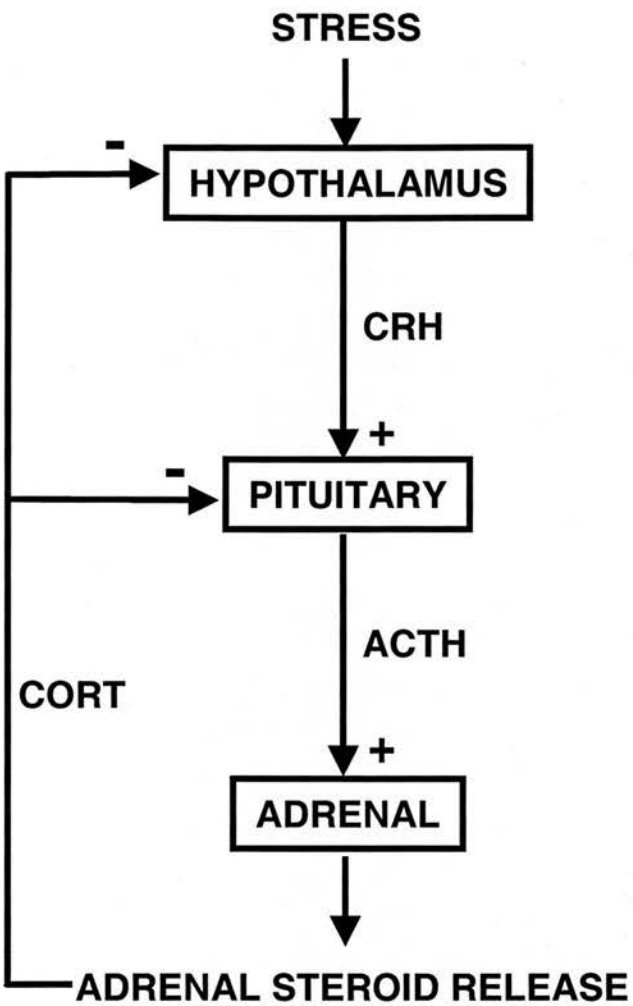

Figure 6-1 Overview of the Hypothalamic- pituitary-adrenocortical (HPA) axis

During stressful experiences, HPA axis activity is upregulated. Corticotrophin-releasing hormone (CRH) is released by cells of the paraventricular nucleus in the hypothalamus. CRH stimulates the anterior pituitary, causing release of adrenocorticotropic hormone (ACTH). This then stimulates release of glucocorticoids from the adrenal- most significantly cortisol in humans and corticosterone in rodents (CORT). Increased serum CORT acts as negative feedback to enable correct control of hormone release

alternative splicing of this channel in the tissues of the HPA axis may increase understanding of the mechanisms involved in control of the hormone cascade that facilitates stress responses. Additionally, the alternatively spliced exon, STREX, confers glucocorticoid sensitivity upon BK channel α-subunits in which it is included (Tian *et al.*, 2001a). It may therefore be speculated that differential splicing of the STREX insert may occur in a regulated manner in tissues that are targets for glucocorticoid action, with significant consequences for cell excitability, enabling a dynamic tuning of activity to appropriately respond to glucocorticoid stimulation.

The hippocampus is implicated in the formation of spatial, declarative and contextual memory, as well as nociception, and has a significant role in regulation of behavioural and physiological stress responses. Biphasic regulation of cell excitability in the hippocampus has been shown in response to adrenal steroids (reviewed in McEwen, 2001) and high levels of glucocorticoid receptors have been reported in this region (Sousa *et al.*, 1989). Steroid hormones have been shown to significantly influence excitability of hippocampal neurons, with activation of corticosterone receptors modulating long- term potentiation (LTP) and long- term depression (LTD) (Coussens *et al.*, 1997, Pavlides *et al.*, 1996) and influencing hippocampus- mediated learning. Modulation of hippocampal excitability by specific types of stress can occur in a manner that can be either dependent or independent of adrenal steroids (de Kloet *et al.*, 1998, Shors *et al.*, 1990). Use of distinct modes of inducing stress, as well as experimental manipulations of the HPA axis may lead to increased understanding of modulation of BK channel alternative splicing in the hippocampus during stress responses. For example, distinct physiological outcomes

may arise as a result of acute, painful stress, as opposed to chronic, non- painful stress (Herman and Cullinan, 1997, Andersen *et al.*, 2004), and it is likely that changes in excitability resulting from modulation of BK channel alternative splice variants within tissues of the HPA axis and related systems are dependent upon the duration and type of stress applied.

The cerebellum is a target for adrenal steroids, and cerebellar purkinje neurons are also a major site for neurosteroidogenesis (Tsutsui *et al.*, 2004). High levels of glucocorticoid receptors are expressed in the cerebellum (Sousa *et al.*, 1989), therefore responses to adrenal and neural- derived steroids are likely to be important for regulation of cell excitability. Acceleration of myelination in the cerebellum under the influence of progesterone is thought to be significant during postnatal development and dendritic outgrowth (Ghoumari *et al.*, 2003, Sakamoto *et al.*, 2001), and this process is strongly linked with neuronal activity (Pareek *et al.*, 1997). Since the BK channel has been implicated as a major regulator of purkinje cell excitability (Womack and Khodakhah, 2002), it may be the case that differential expression of BK channel alternative splice variants enables enhanced responsiveness during increased steroid- induced activity in the cerebellum. Disregulation of circulating glucocorticoid levels arising from potent, long- term stress might be speculated to affect changes in cerebellar function in a manner similar to that seen in the hippocampus where considerable remodelling takes place during stress responses.

6-1-2 Stress as a modifier of cellular excitability

Although whole- animal behavioural responses are a result of the integration of many neurochemical processes, the underlying mechanisms governing response and adaptation to stimuli can be linked to variability in responses of cells within relevant systems. An example of a model system where an external stimulus causes robust changes in behaviour as a result of multiple functional and anatomical changes in the CNS is chronic stress (McEwen, 2001, Xie and McCobb 1998). Many behavioural and neurochemical changes that occur in response to chronic psychosocial stress in animal models parallel those in human depression (Fuchs *et al.*, 2001). Experimental manipulation of this model may therefore enable dissection of the molecular mechanisms governing such responses. Ablation of the HPA hormone cascade by removal of the pituitary (hypophysectomy) in rats causes a dramatic reduction in serum corticosterone levels, as well as reduced adrenal transcription of phenylethanolamine- *N*- methyltransferase (PNMT) and concomitant changes in the expression of STREX BK channel relative to the ZERO alternative splice variant in rat adrenal chromaffin cells. This regulation of STREX expression could be prevented by administration of ACTH (Xie and McCobb, 1998). BK channels are significant modulators of chromaffin cell function (Lingle *et al.*, 1996, Lovell *et al.*, 2000) therefore this regulation of alternative splicing represents a possible mechanism for tuning chromaffin cell excitability, enabling context- dependent control of epinephrine secretion during responses to acute or chronic stress.

Since experimental ablation of HPA axis function caused a reduction in STREX expression in rat adrenal chromaffin cells, it would be intuitive to speculate that

behavioural stresses, which cause an upregulation of HPA axis function, would therefore cause the opposite regulation of STREX expression in adrenal chromaffin cells, indicating a bidirectional modulation. However, the application of 4-6 weeks of chronic subordination stress in adult male tree shrews was found also to reduce the proportion of transcripts containing the STREX exon in the adrenal gland (McCobb *et al.*, 2003). Nevertheless, this was consistent with the observation of depression-like symptoms in animals exposed to this type of stress, since a reduction in STREX-BK channel expression would favour lower maximal rates of chromaffin cell firing, and subsequent passive coping behaviours. It is therefore clear that tuning of the excitability of cells in this manner is the end- result of a complex, multifactorial process whose response, although likely to be dynamic and bidirectional, has yet to be examined fully.

In order to investigate the effects of repeated stresses on alternative splicing of the BK channel in the tissues of the HPA axis, as well as other steroid- responsive neuronal tissues, mice were exposed to two different modes of chronic stress: rat exposure and restraint; the former model would test responses during chronic perceived threat, whilst the latter contained no inherent threat *per se*, therefore these two models might lead to physiological changes reflecting different coping strategies under such varying conditions. For example, chronic exposure to the threat of attack by a larger animal might cause upregulation of STREX expression in the adrenal chromaffin cells, to facilitate more rapid, repetitive firing, and increased secretion of adrenal steroids to enable proactive 'fight or flight' responses, whereas in the same tissue during restraint stress, an opposite reaction might be observed, as the animal

becomes accustomed to confinement in this manner, therefore an adaptive coping response would result from reduced excitability in the tissues of the HPA axis. However, in the investigation of dynamic regulation of alternative splicing of the BK channel in response to stress, it is likely that the end- results of chronic stress are not fully descriptive of this paradigm- acute responses to situations of threat or novelty may involve a short- term increase in excitability, followed by a long- term decrease to dampen responses to the same, repeated stimulus.

To investigate the effect of manipulation of the glucocorticoid response on BK channel α-subunit alternative splicing in the aforementioned tissues, removal of the adrenal gland and administration of dexamethasone were also investigated. The removal of adrenal endocrine activity, and significantly, the removal of the negative feedback influence of CORT on tissues upstream in the HPA axis will allow investigation of the possibility that regulation of hypothalamic and pituitary activity by adrenal glucocorticoids involves selective tuning of the responses of cells in these tissues by specific expression of BK channel populations containing alternatively-spliced exons which impart distinct electrophysiological phenotypes.

In addition to this, STREX splicing was investigated in the hippocampus, anterior pituitary, adrenal gland, hippocampus and cerebellum of unstressed female mice, in order to identify any possible sex differences in the alternative splicing of BK channel α-subunits in these tissues. There is a high degree of functional crosstalk between the HPA and HPG axes (Viau, 2002), and differences in gonadal secretion are not only implicated in variable activation of the HPA axis in response to stress

across sexes (Kudielka and Kirschbaum, 2005), but are also likely to be a contributing factor to the inter- individual variability in stress responses and adaptation.

6-2 Results

cDNA was generated from total RNA harvested from mouse adrenal gland, anterior pituitary, cerebellum, hippocampus and hypothalamus following the different treatments. Each sample was assayed using the Taqman real time PCR primer/ probe set specific to the STREX BK channel alternative splice variant, and also the Applied Biosystems "assay on demand ID **Mm00516078_m1**" primer/ probe set for total BK channel, in 25µl reactions in 1x Applied Biosystems Taqman Universal PCR master mix, and quantified using a triplicate logarithmic dilution of STREX cDNA, over a starting concentration range of 2ng- 0.2fg to generate a standard curve for quantitation purposes, as demonstrated in chapter 4. For each sample, the STREX BK channel alternative splice variant was normalised to total BK channel, then results calculated to express STREX as a mean percentage of total BK channel, where (n= X) represents the number of individual animals assayed. In some samples, STREX was detected at up to almost twice the amount of total BK channel in the sample, even though both primer sets used in this assay were previously shown to amplify the respective targets with similarly high efficiencies (fig. 4-9, 4-10). The total BK channel "assay on demand" primer set is specific to a region conserved across splice variants, located towards the C-terminus of the channel, between splice sites 4 and 5, whilst the STREX exon inserts at splice site C2. Although the concept of one splice variant outnumbering the total channel at first appears counter-

intuitive, the excess of STREX observed herein may represent partial transcripts. The retrospective design of a total BK primer set specific to a conserved region of the channel upstream of the sites of alternative splicing may therefore allow more accurate normalisation.

6-2-1 STREX splicing in response to stress in mouse tissues

6-2-1-1 STREX splicing in response to stress in mouse adrenal gland

In the adrenal glands of control male subjects, STREX- containing transcripts were found to comprise 90.4 ± 23.2% (n= 7) of total BK channel cDNA. In animals exposed to rat stress, this representation was reduced to 64.7 ± 20.0% (n= 7), although this was not a significant difference. In dexamethasone- treated animals, STREX accounted for 54.4 ± 8.0% (n= 6) of total BK channel, however this was again not significantly lower when compared to the control male STREX/ BK ratio. In animals subjected to restraint stress, STREX comprised 69.5 ± 13.2% (n= 8); again this was not significantly different to the controls. Finally, in untreated female mice, 98.1 ± 19.3% (n= 7) of total detected BK channel was found to contain STREX (fig. 6-2).

6-2-1-2 STREX splicing in response to stress in mouse anterior pituitary

In the anterior pituitary glands of control male mice, STREX was found to account for 53.22 ± 18.0% (n=8) of total BK channel. In animals exposed to chronic rat stress, this was not significantly altered, with STREX- containing transcripts comprising 51.23 ± 7.59% (n= 8) of total BK channel. Dexamethasone was also found not to have a significant effect on STREX expression in the anterior pituitary,

Figure 6-2
STREX/ BK ratio in mouse tissues

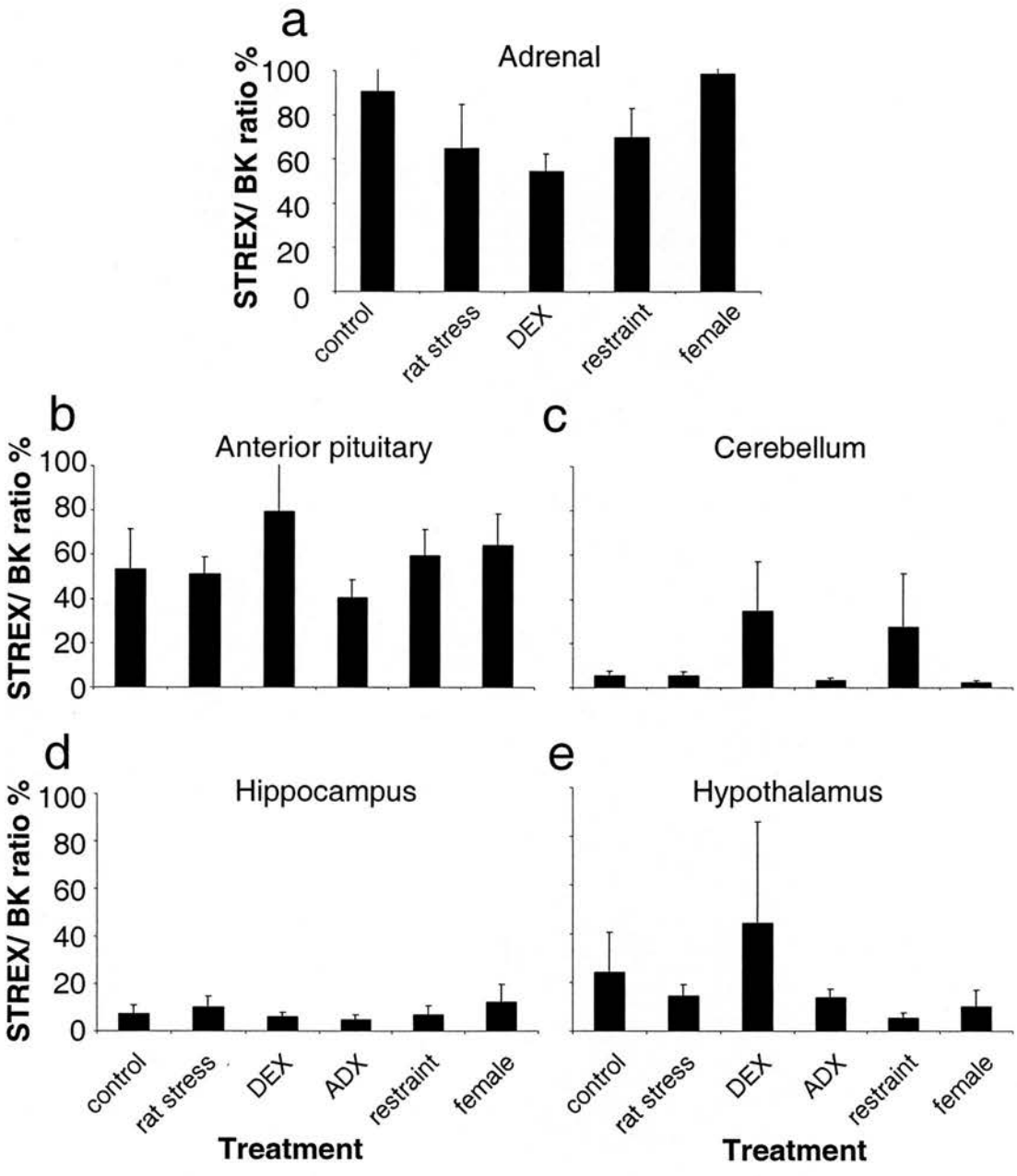

Figure 6-2 STREX/ BK ratio in mouse tissues

Data shown as an average ratio (± SEM) of STREX as a percentage of total BK channel mRNA expression in **a)** adrenal gland, **b)** anterior pituitary, **c)** cerebellum, **d)** hippocampus and **e)** hypothalamus of mice under different conditions as described in chapter 2; control (n= 7, 8, 9, 7 and 6 respectively), rat stress (n= 7, 8, 7, 5 and 3), dexamethasone (DEX) (n= 6, 8, 6, 6 and 3), adrenalectomy (ADX) (n= 5, 6, 5 and 4), restraint (n= 8, 7, 7, 7 and 7) and female (n= 7, 7, 8, 5 and 5).

where STREX comprised 79.5 ± 22.2% (n= 8) of total BK. Removal of the adrenal gland, resulting in abolished feedback regulation of the HPA axis was also found not to have an effect on STREX expression in the anterior pituitary. In adrenalectomised animals, STREX accounted for 40.42 ± 8.2% (n= 5) of total BK. Restraint stress also had no significant effect on STREX expression compared to control, with STREX comprising 59.6 ± 11.7% (n= 7) of total BK. Finally, no difference in STREX expression in the anterior pituitary was found in female animals (64.1 ± 14.4% (n= 7) compared to control male (fig. 6-2).

6-2-1-3 STREX splicing in response to stress in mouse cerebellum

STREX expression in the mouse cerebellum was found to be lower than that in the adrenal or anterior pituitary, however a spectrum of splice variant expression across tissues is expected, since the BK channel alternative splice variants expressed would be regulated commensurate to the function of that tissue. In control male mice, STREX was found to comprise 5.3 ± 2.1% (n= 9) of total BK channels. The STREX/ BK ratio in the cerebellum of animals subjected to rat stress was not significantly different to that of controls, at 5.2 ± 1.9% (n= 7). Administration of dexamethasone also had no significant effect on STREX expression; in animals treated with DEX, the average STREX/ BK ratio was 34.7 ± 22.3% (n=6). Average cerebellar STREX/ BK ratio in adrenalectomised animals was 3.2 ± 1.1% (n= 6), which was again not significantly different from the controls. In animals subjected to restraint stress, the cerebellar STREX/ BK ratio, 27.5 ± 24.2% (n= 7), was not significantly altered compared to controls. Finally, no significant differences were found in the cerebellar

STREX/ BK ratio of female animals (2.2 ± 0.9% (n= 8)) compared to the control males (fig. 6-2).

6-2-1-4 STREX splicing in response to stress in mouse hippocampus

In the control male hippocampus, the average STREX/ BK ratio was 7.3 ± 3.8% (n= 7). STREX/ BK ratio in hippocampi of rat stressed animals was 9.8 ± 4.7% (n= 5). Dexamethasone also did not significantly alter STREX/ BK ratio in the hippocampus- following treatment, STREX comprised 5.8 ± 1.9% (n= 6) of total BK channel. STREX/ BK ratio was also not significantly changed in the hippocampi of adrenalectomised animals, at 4.7 ± 2.3% (n= 5). In animals subjected to restraint stress, hippocampal STREX/ BK was not significantly different to that of controls, at 6.9 ± 3.6% (n= 7). Additionally, no significant difference was observed across sexes- average STREX/ BK ratio in unstressed females was 12.3 ± 7.5% (n= 5) (fig. 6-2).

6-2-1-5 STREX splicing in response to stress in mouse hypothalamus

Average STREX/ BK ratio in control male hypothalamus was 24.0 ± 16.7% (n= 6). In rat stressed animals, hypothalamic STREX/ BK ratio was 14.5 ± 4.6% (n= 3), which was not significantly different to that of controls. In the hypothalamus of animals systemically administered with dexamethasone, STREX/ BK ratio was 44.2 ± 41.9% (n= 3) and this was not significantly different to controls. In adrenalectomised animals, hypothalamic STREX/ BK ratio was 13.8 ± 3.3% (n= 4), and again this was not significantly altered relative to control animals. Restraint stress also had no effect on hypothalamic STREX/ BK ratio which, although the mean was reduced to 5.3 ± 2.1% (n= 7), was again not significantly different to that

of controls, due to the large error in control samples. No significant difference was observed between control males and unstressed females where the average STREX/ BK ratio was 9.9 ± 6.9% (n= 5) (fig. 6-2).

6-2-2 Correlation of STREX/ BK ratio with serum corticosterone and ACTH

6-2-2-1 Corticosterone and ACTH responses to experimental manipulations

Chronic stress- induced activation of the HPA axis leads to increased serum corticosterone levels in rodents. Adult mice were treated using conditions described in chapter 2, to investigate the possibility that chronic stress, surgical manipulation of the HPA axis, glucocorticoid stimulation and gender may affect BK channel splicing in the hypothalamus, anterior pituitary, adrenal gland, hippocampus and cerebellum. Average serum corticosterone concentration was measured in animals subjected to each of the treatments described previously. In control male mice, the average serum corticosterone concentration was 117.9 ± 28.6 pmol/ ml (n= 12). Females had significantly higher ($p< 0.01$) serum CORT levels, at 297.0 ± 74.2 pmol/ ml (n= 8). In male animals subjected to the two different chronic stress models, average serum corticosterone was 112.2 ± 23.5 pmol/ ml (n= 10) for rat stress and 204.1 ± 28.0 pmol (n= 8) following restraint stress. Significant changes in serum corticosterone were not observed under either of the chronic stress paradigms. In animals subjected to bilateral adrenalectomy, which would be expected to cause ablation of HPA axis feedback, average serum CORT concentration was 69.0 ± 16.5 pmol/ ml (n= 6), which was not significantly different to that of control, 14 days following removal of

the adrenal. In animals that received chronic dexamethasone, average serum CORT concentration was also not significantly different to that of the control animal, at 79.1 ± 4.4 pmol/ ml (n= 8) (fig. 6-3).

In certain cases, blood collected after sacrificing animals was insufficient to provide serum for both CORT and ACTH measurement, therefore average serum ACTH concentrations are only available for control, rat stress, adrenalectomised and dexamethasone- treated animals. In untreated control male mice, average serum ACTH concentration was 60.2 ± 16.7 fmol/ ml (n= 4). Following 14 days of chronic rat stress, no significant difference was observed in average serum [ACTH], which was measured at 55.0 ± 14.0 fmol/ ml (n= 10). In animals treated with chronic administration of dexamethasone, average serum [ACTH] was 117.0 ± 16.1 fmol/ ml (n= 8). Again, this was not significantly altered compared to control animals. In adrenalectomised animals, average serum [ACTH] was 96.4 ± 21.5 fmol/ ml (n= 6), and this was again not significantly different to that of control animals (fig. 6-3).

6-2-2-2 Correlation of serum corticosterone and ACTH with adrenal STREX BK channel alternative splicing

Elevated serum corticosterone and ACTH have been shown to occur following stress in animal models. However, this is not singularly descriptive of the secretory paradigm during the stress response, since variability in secretion has been shown not only in response to stress, but also to vary across sexes, and is influenced by previous exposure to stress (Knuth *et al.*, 2005), therefore genuine changes in secretion may be obscured by these factors, leading to misreporting of results. During this study,

Figure 6-3
Serum corticosterone and adrenocorticotropin hormone levels in mice following treatment

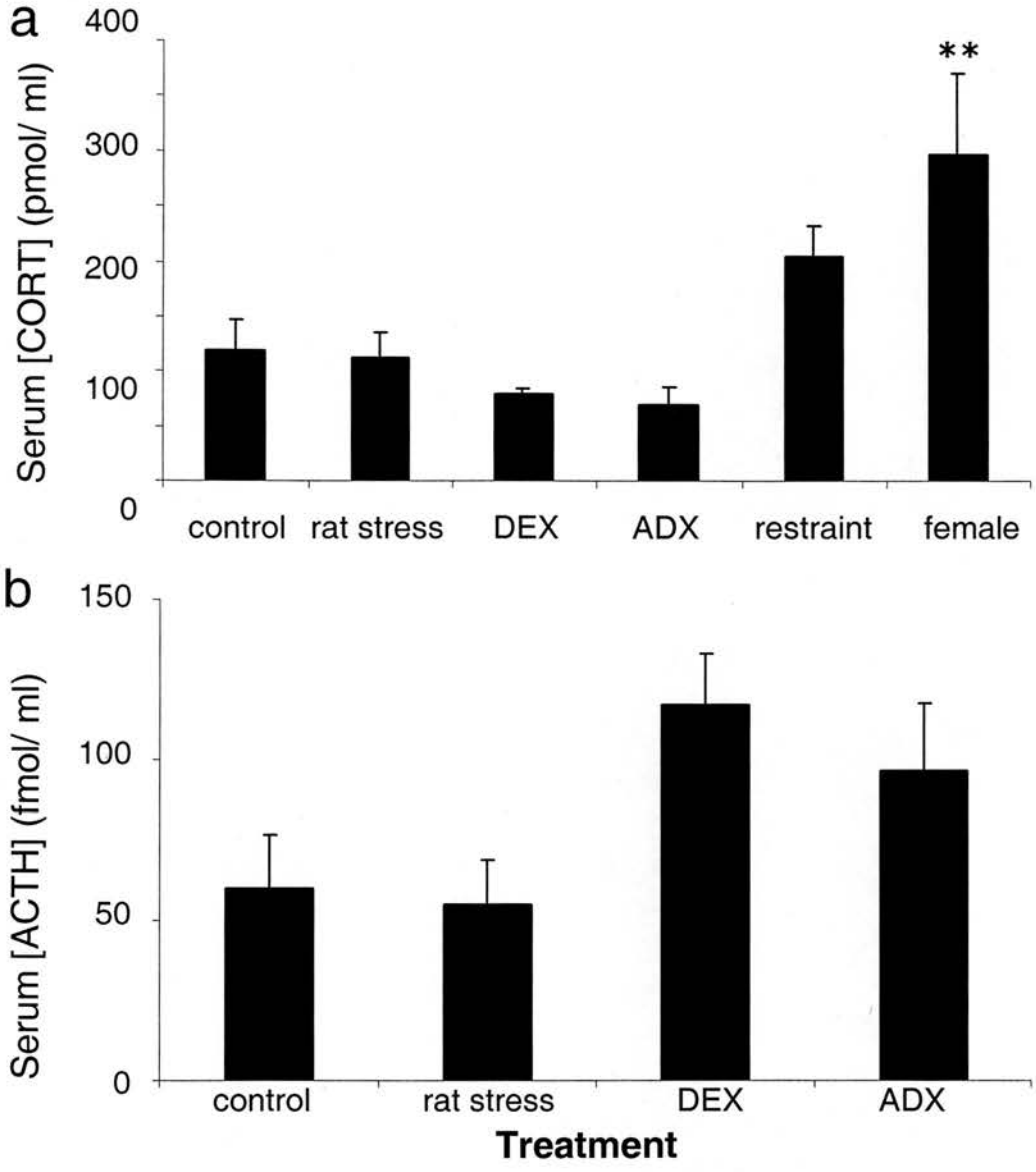

Figure 6-3 Serum corticosterone and adrenocorticotropin hormone levels in mice following treatment.

Data shown as **a)** average serum corticosterone (CORT) concentration (pmol/ ml) ± SEM in adult mice for: untreated male (control, n= 12), male subjected to rat stress (rat stress, n= 10), male treated with dexamethasone (DEX, n= 8), adrenalectomised male (ADX, n= 6), male subjected to restraint stress (restraint, n= 8) and untreated female (female, n= 8). **b)** shows average serum adrenocorticotropin hormone (ACTH) concentration (fmol/ ml) ± SEM in adult mice for: untreated male (control, n= 4), male subjected to rat stress (rat stress, n= 10), male treated with dexamethasone (DEX, n= 8) and untreated female (female, n= 6). (**= $p < 0.01$ ANOVA post hoc test Student-Newman-Keuls).

different stress models as well as manipulation of HPA axis responses were used in order to investigate whether changes in corticosterone and ACTH concentration could be correlated with variable alternative splicing of BK channel α-subunits. STREX/ BK ratios in each tissue were plotted against serum corticosterone or ACTH concentration ([CORT], pmol/ ml and [ACTH], fmol/ml respectively) for individual mice tested in this study. Spearman's rank test was used to assess correlation between STREX/ BK ratio and serum [CORT] or [ACTH] in mouse adrenal gland, anterior pituitary, cerebellum, hippocampus and hypothalamus following each of the treatments described in chapter 2.

In the adrenal glands of control male mice, poor correlation was observed between STREX/ BK ratio and serum [CORT], with R_s= -0.360 (n= 7). In animals subjected to rat stress, there was also poor correlation, R_s= 0.429 (n= 7). In mice subjected to chronic restraint stress, increasing serum [CORT] was correlated with increasing STREX/ BK ratio in the adrenal, indicated by R_s of 0.833 (n= 8). Correlation between diminishing STREX/ BK ratio and increasing serum [CORT] was higher in the adrenal gland in mice treated chronically with dexamethasone, where the R_s was -0.829 (n= 6). In female mice, no correlation was observed between STREX/ BK ratio in the adrenal gland and serum corticosterone concentration, as indicated by an R_s of 0.571 (n= 7) (fig. 6-4).

STREX/ BK ratio was also examined for correlation with circulating ACTH level in mice exposed to the behavioural and pharmacological manipulations described previously, although in several cases there was insufficient serum obtained to assay

Figure 6-4
Correlation of STREX/ BK ratio with serum corticosterone concentration in mouse adrenal gland

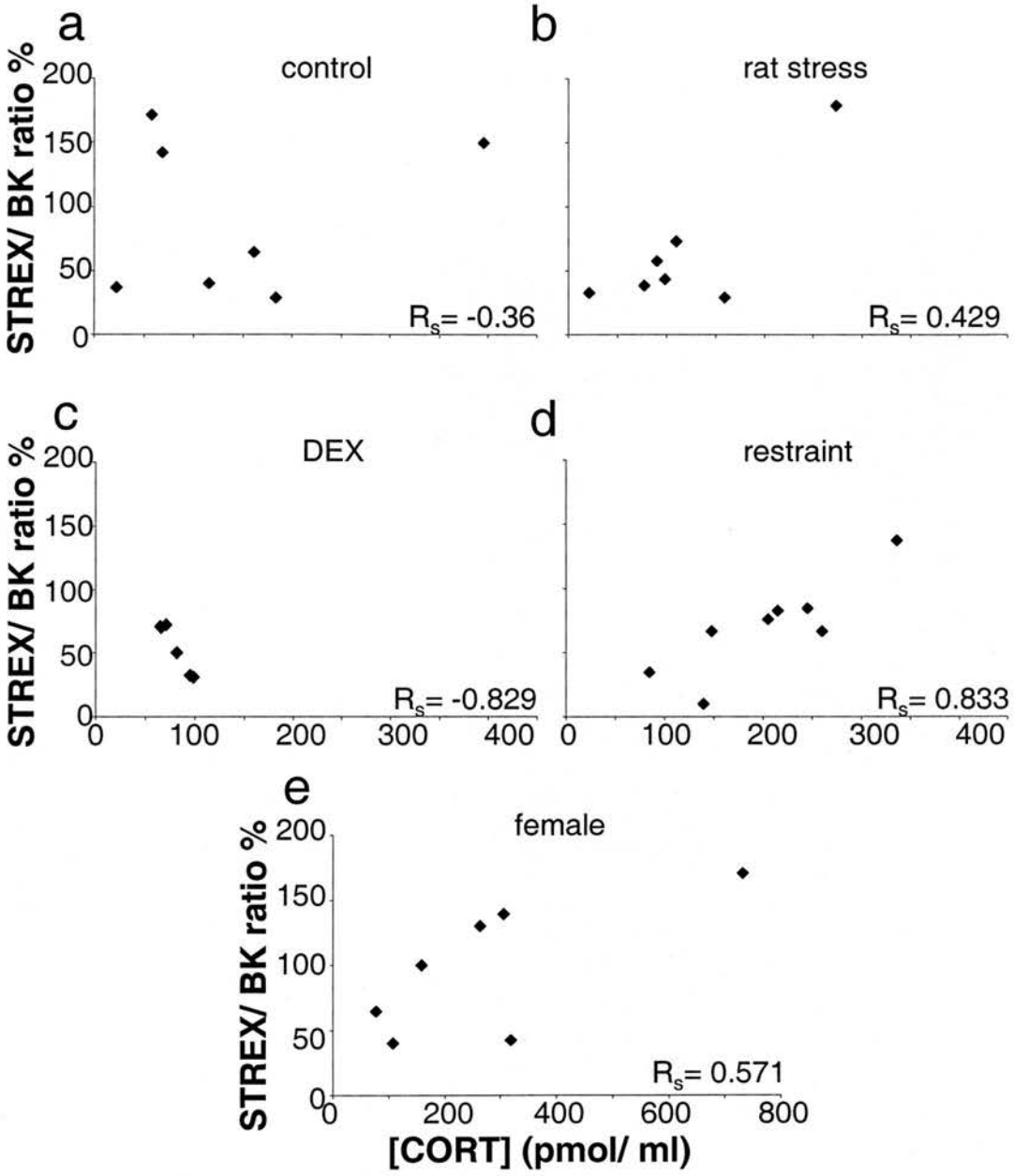

Figure 6-4 Correlation of STREX/ BK ratio with serum corticosterone concentration in mouse adrenal gland

Data plotted using STREX as a percentage of total BK channel in the adrenal gland against serum corticosterone concentration (pmol/ ml) for individual mice under different conditions as described in chapter 2; **a)** control (n= 7), **b)** rat stress (n= 7), **c)** dexamethasone (DEX) (n= 6), **d)** restraint (n= 8) and **e)** female (n= 7). Spearman rank correlation coefficient (R_s) is shown in each case.

both [CORT] and [ACTH], therefore data was only obtained for mice under control, rat stress, dexamethasone and adrenalectomised animals. In the adrenal glands of control, rat stress and DEX- treated mice, no correlation was observed between changing STREX/ BK ratio and circulating ACTH concentration, as indicated by R_s of 0.600 (n= 4), 0.179 (n= 7) and 0.314 (n= 6) respectively (fig. 6-5).

6-2-2-3 Correlation of serum corticosterone and ACTH with anterior pituitary STREX BK channel alternative splicing

In the anterior pituitary, STREX/ BK ratio was not significantly affected by increasing serum [CORT] in control mice, indicated by R_s of –0.750 (n= 7). When mice were exposed to 14 days of repeated, randomised- timing rat stress, low correlation was again observed between STREX/ BK ratio and serum [CORT], indicated by Rs of –0.524 (n= 8). Restraint also had no effect on correlation of STREX splicing in the anterior pituitary with changing serum [CORT], again demonstrated by a low R_s of 0.393 (n= 7). Correlation of STREX splicing to serum [CORT] was also not influenced by the chronic administration of dexamethasone, as shown by a low R_s of 0.048 (n= 8). Following adrenalectomy, increasing serum corticosterone concentration could be correlated with diminishing STREX splicing in the anterior pituitary, as indicated by an R_s of –0.900 (n= 5). In unstressed female animals, there was no observable correlation between serum [CORT] and pituitary STREX splicing, shown by a low R_s of –0.143 (n= 7) (fig. 6-6).

In the anterior pituitaries of control, rat stressed, DEX- treated and adrenalectomised mice, no correlation between serum [ACTH] and STREX splicing was found, with

Figure 6-5
Correlation of STREX/ BK ratio with serum ACTH concentration in mouse adrenal gland

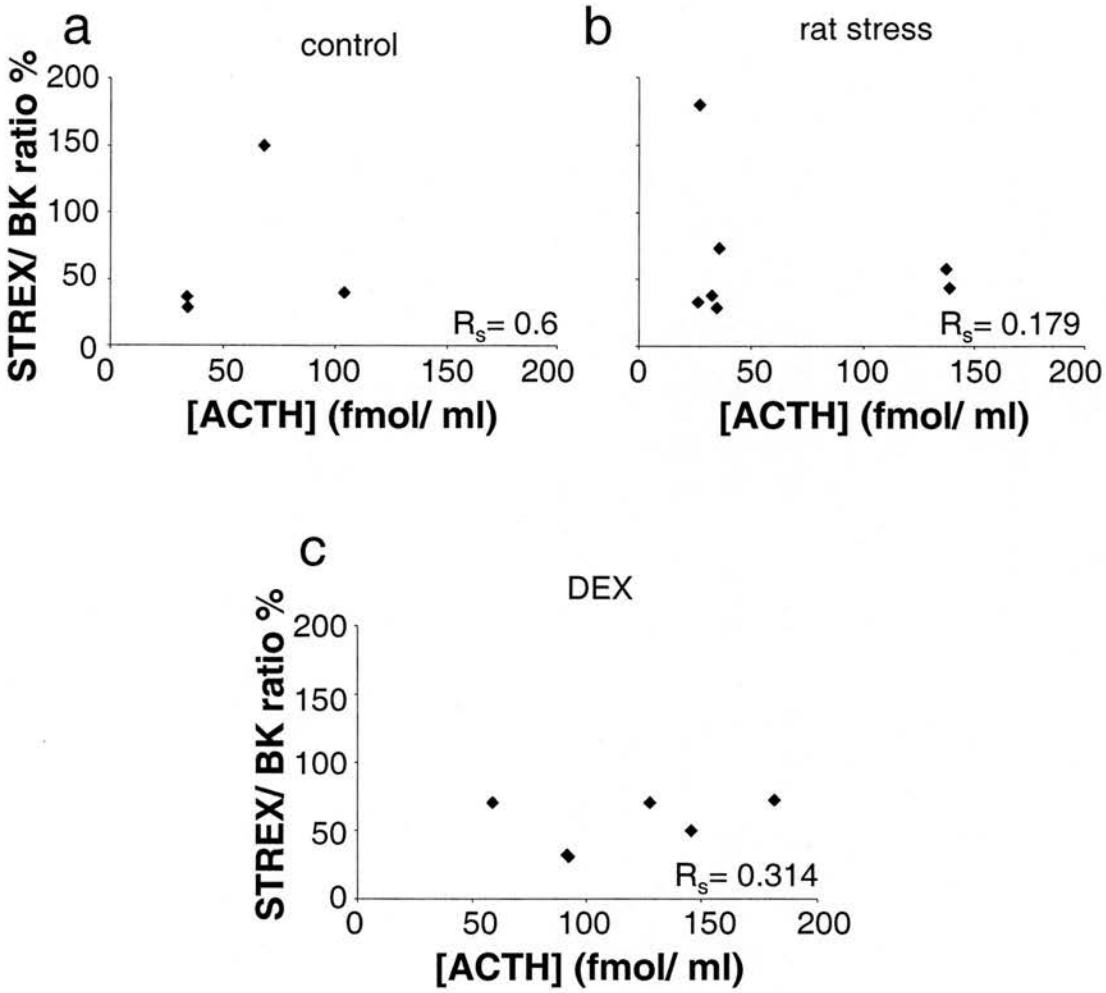

Figure 6-5 Correlation of STREX/ BK ratio with serum ACTH concentration in mouse adrenal gland

Data plotted using STREX as a percentage of total BK channel in the adrenal gland against serum ACTH concentration (fmol/ ml) for individual mice under different conditions as described in chapter 2; **a)** control (n= 4), **b)** rat stress (n= 7) and **c)** dexamethasone (DEX) (n= 6). Spearman rank correlation coefficient (Rs) is shown in each case.

Figure 6-6
Correlation of STREX/ BK ratio with serum corticosterone concentration in mouse anterior pituitary

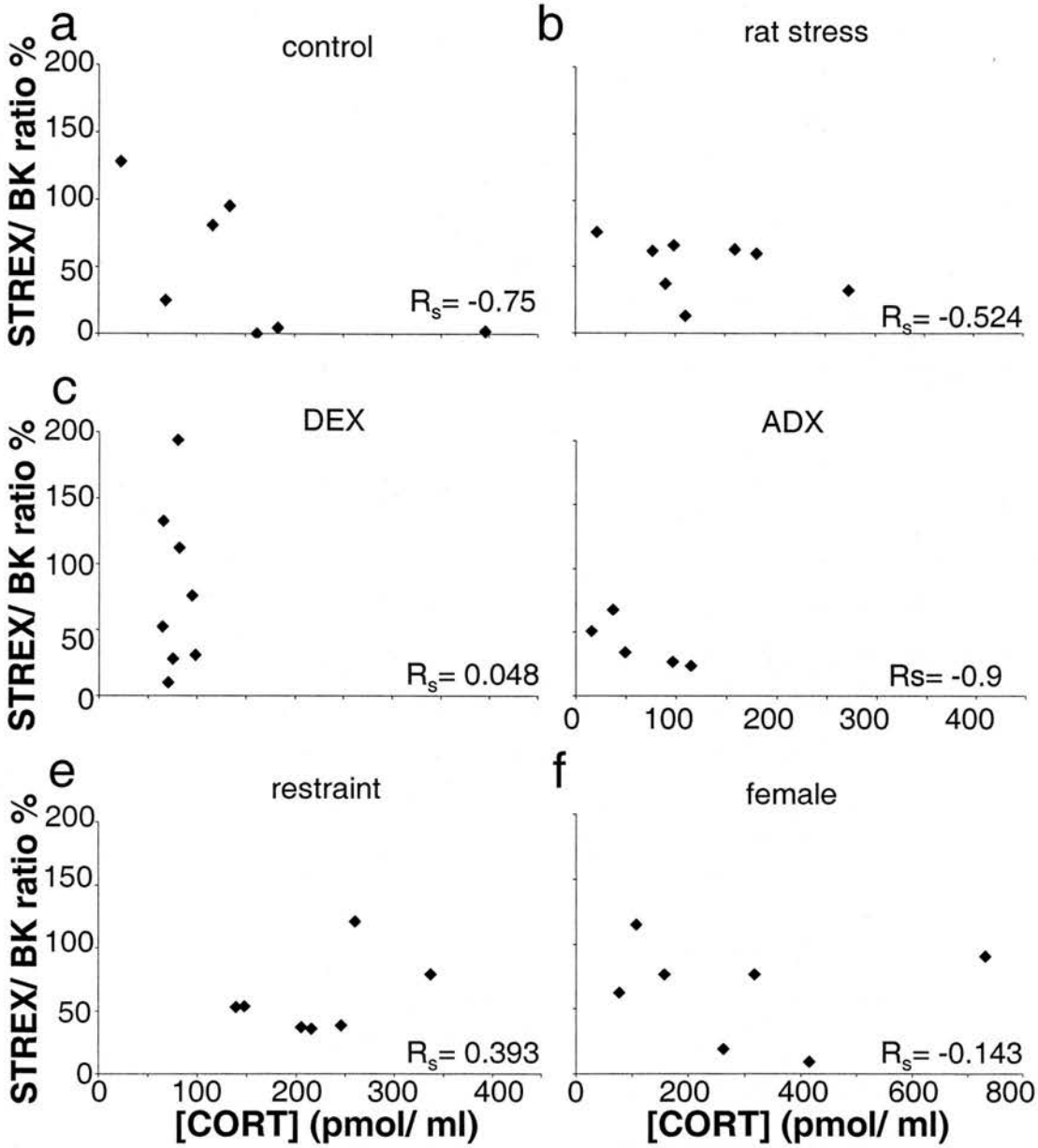

Figure 6-6 Correlation of STREX/ BK ratio with serum corticosterone concentration in mouse anterior pituitary

Data plotted using STREX as a percentage of total BK channel in the anterior pituitary against serum corticosterone concentration (pmol/ ml) for individual mice under different conditions as described in chapter 2; **a)** control (n= 7), **b)** rat stress (n= 8), **c)** dexamethasone (DEX) (n= 8), **d)** adrenalectomy (ADX) (n= 5), **e)** restraint (n= 7), and **f)** female (n= 7). Spearman rank correlation coefficient (Rs) is shown in each case.

low Spearman rank correlation coefficients in all cases- R_s= -0.400 (n= 4), -0.071 (n= 8), 0.190 (n= 8) and 0.300 (n= 5) respectively (fig. 6-7).

6-2-2-4 Correlation of serum corticosterone and ACTH with cerebellar STREX BK channel alternative splicing

In the cerebellum, STREX/ BK ratio was not correlated with changes in serum corticosterone concentration in control mice. R_s in this case was –0.150 (n= 9). Following both of the chronic stress models used in this study, STREX splicing in the cerebellum was not correlated with changing corticosterone concentration, as indicated by R_s of 0.286 (n= 7) and –0.036 (n= 7) for rat stress and restraint respectively. Following chronic administration of dexamethasone, no correlation was observed between STREX/ BK ratio and serum [CORT], indicated by an R_s of –0.143 (n= 6). Bilateral adrenalectomy also did not influence correlation of STREX/ BK ratio with serum [CORT] in the cerebellum, as shown by an R_s of –0.671 (n= 6). In the female cerebellum, there was again no correlation between STREX splicing and serum [CORT], indicated by the low R_s of –0.494 (n= 8) (fig. 6-8).

Alternative splicing of STREX in the cerebellum was also not correlated with circulating adrenocorticotropic hormone. In control animals, as well as those subjected to rat stress, chronic treatment with dexamethasone or adrenalectomised, R_s was not sufficiently high to indicate correlation; -0.400 (n= 4), -0.107 (n= 7), -0.086 (n= 6) and 0.329 (n= 6) respectively (fig. 6-9).

Figure 6-7
Correlation of STREX/ BK ratio with serum ACTH concentration in mouse anterior pituitary

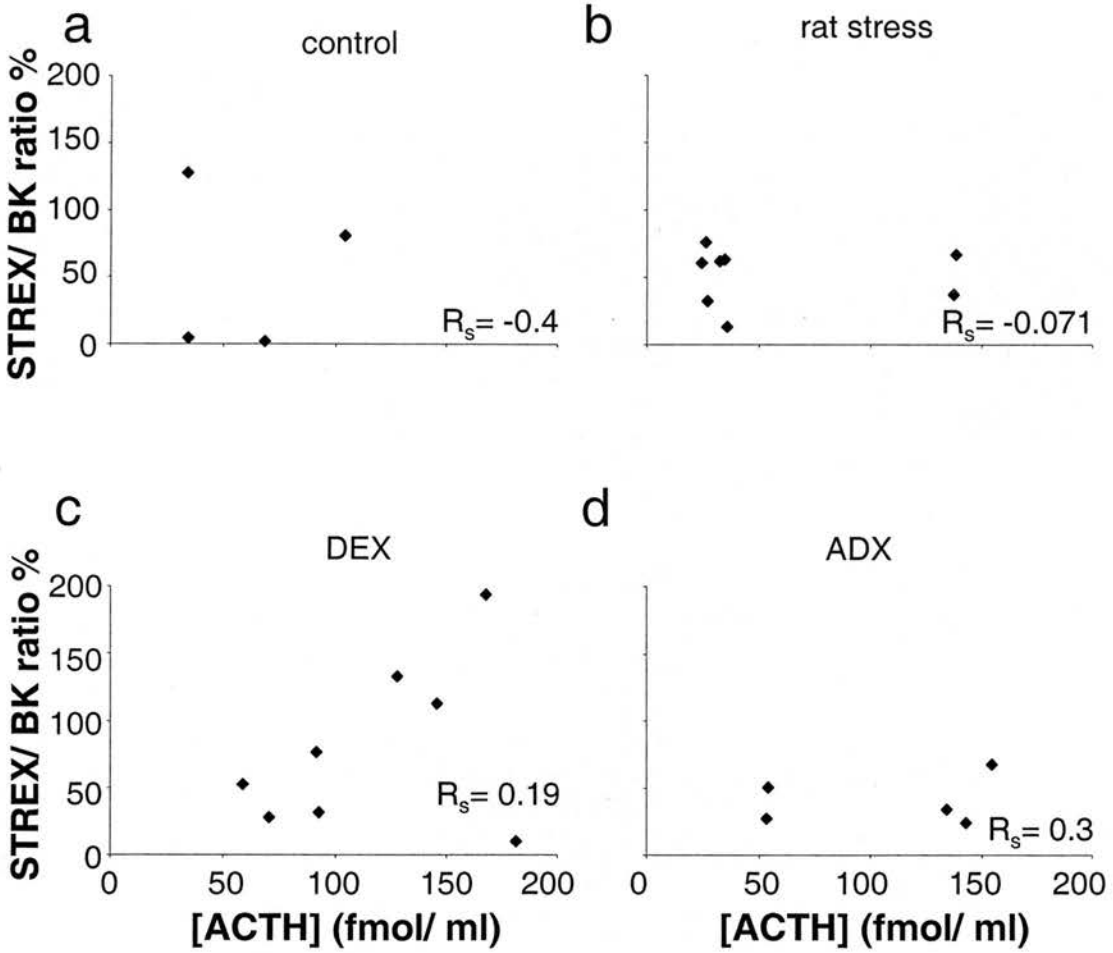

Figure 6-7 Correlation of STREX/ BK ratio with serum ACTH concentration in mouse anterior pituitary

Data plotted using STREX as a percentage of total BK channel in the anterior pituitary against serum ACTH concentration (fmol/ ml) for individual mice under different conditions as described in chapter 2; **a)** control (n= 4), **b)** rat stress (n= 8), **c)** dexamethasone (DEX) (n= 8) and **d)** adrenalectomy (ADX) (n= 5). Spearman rank correlation coefficient (Rs) is shown in each case.

Figure 6-8
Correlation of STREX/ BK ratio with serum corticosterone concentration in mouse cerebellum

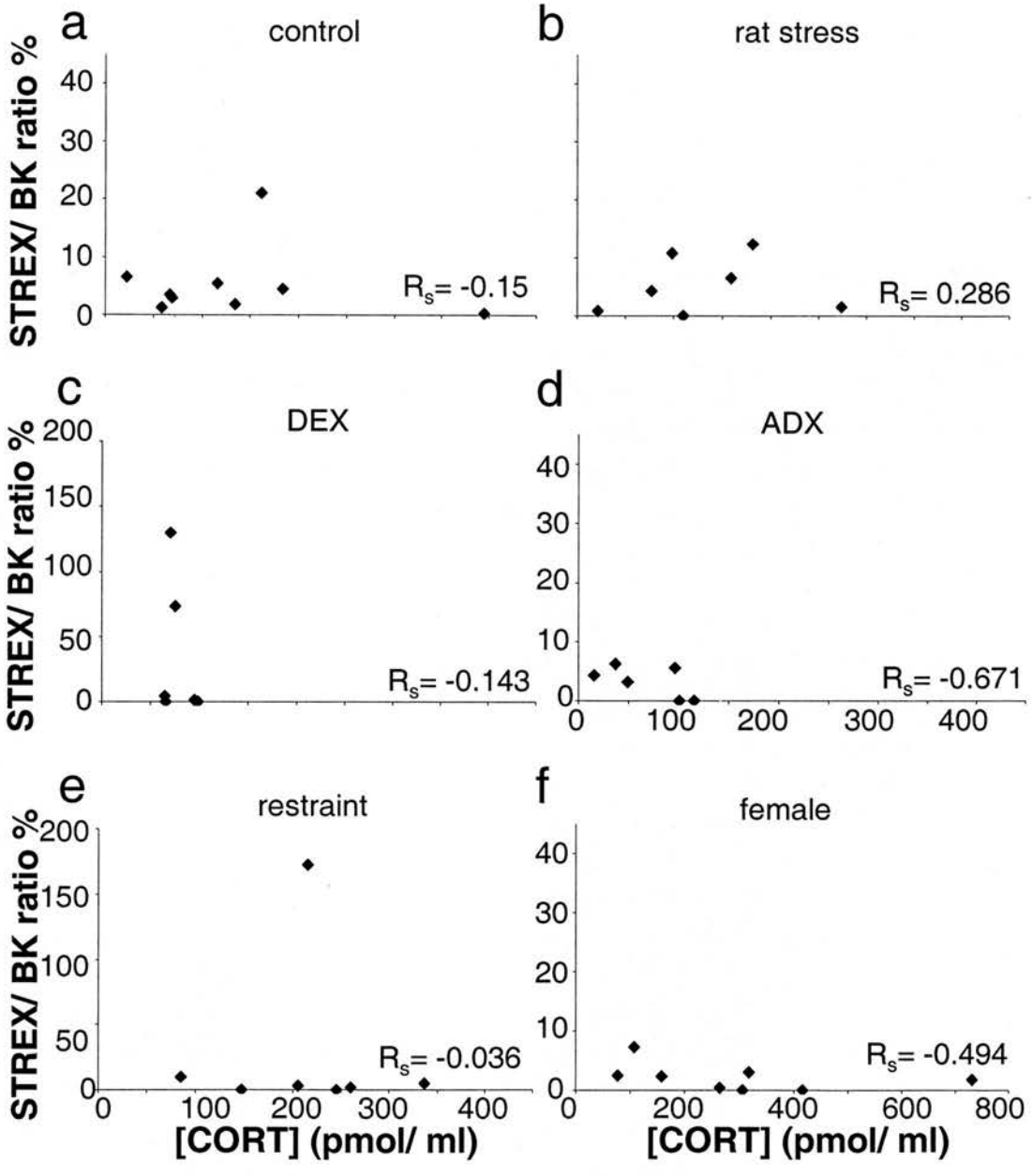

Figure 6-8 Correlation of STREX/ BK ratio with serum corticosterone concentration in mouse cerebellum

Data plotted using STREX as a percentage of total BK channel in the cerebellum against serum corticosterone concentration (pmol/ ml) for individual mice under different conditions as described in chapter 2; **a)** control (n= 9), **b)** rat stress (n= 7), **c)** dexamethasone (DEX) (n= 6), **d)** adrenalectomy (ADX) (n= 6), **e)** restraint (n= 7), and **f)** female (n= 8). Spearman rank correlation coefficient (Rs) is shown in each case.

Figure 6-9
Correlation of STREX/ BK ratio with serum ACTH concentration in mouse cerebellum

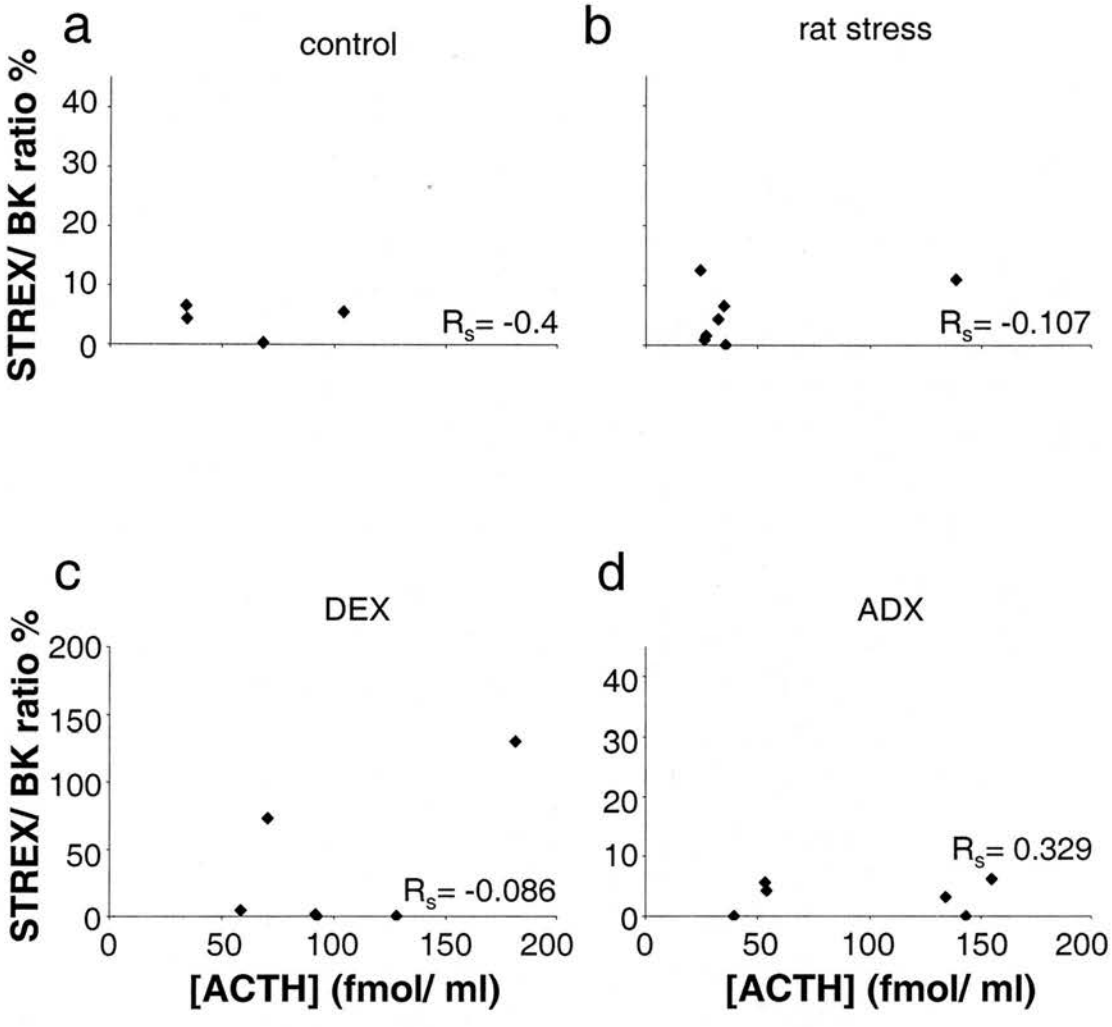

Figure 6-9 Correlation of STREX/ BK ratio with serum ACTH concentration in mouse cerebellum

Data plotted using STREX as a percentage of total BK channel in the cerebellum against serum ACTH concentration (fmol/ ml) for individual mice under different conditions as described in chapter 2; **a)** control (n= 4), **b)** rat stress (n= 7), **c)** dexamethasone (DEX) (n= 6) and **d)** adrenalectomy (ADX) (n= 6). Spearman rank correlation coefficient (Rs) is shown in each case.

6-2-2-5 Correlation of serum corticosterone and ACTH with hippocampal STREX BK channel alternative splicing

In the hippocampus of control mice, STREX/ BK ratio was not correlated with serum [CORT], as indicated by an R_s of –0.371 (n= 6). Neither of the chronic stress models caused a change in STREX splicing in the hippocampus that could be correlated with increasing serum [CORT], as shown by R_s values of –0.300 (n= 5) and –0.071 (n= 7) for rat stress and restraint stress respectively. Chronic administration of dexamethasone also did not cause changes in hippocampal STREX splicing that could be correlated with changing serum [CORT] levels, indicated by an R_s of 0.486 (n= 6). Following adrenalectomy, a high inverse correlation was observed between hippocampal STREX splicing and serum [CORT], indicated by an R_s of –0.925 (n= 5). In the female hippocampus, very low correlation of STREX splicing with serum [CORT] was observed, indicated by an R_s of 0.100 (n= 5) (fig. 6-10).

In the hippocampus of control animals, there appeared to be a strong correlation between increasing circulating ACTH concentration and decreasing STREX/ BK ratio, indicated by a Spearman rank correlation coefficient of –1. However, since sufficient serum to measure ACTH was only collected from 3 subjects, this has to be interpreted with caution, and more experiments are required to confirm such correlation. Chronic rat stress, dexamethasone and adrenalectomy all showed low correlation between STREX splicing in the hippocampus and changing serum ACTH, indicated by R_s values of 0.500 (n= 5), 0.257 (n= 6) and 0.675 (n= 5) respectively (fig. 6-11).

Figure 6-10
Correlation of STREX/ BK ratio with serum corticosterone concentration in mouse hippocampus

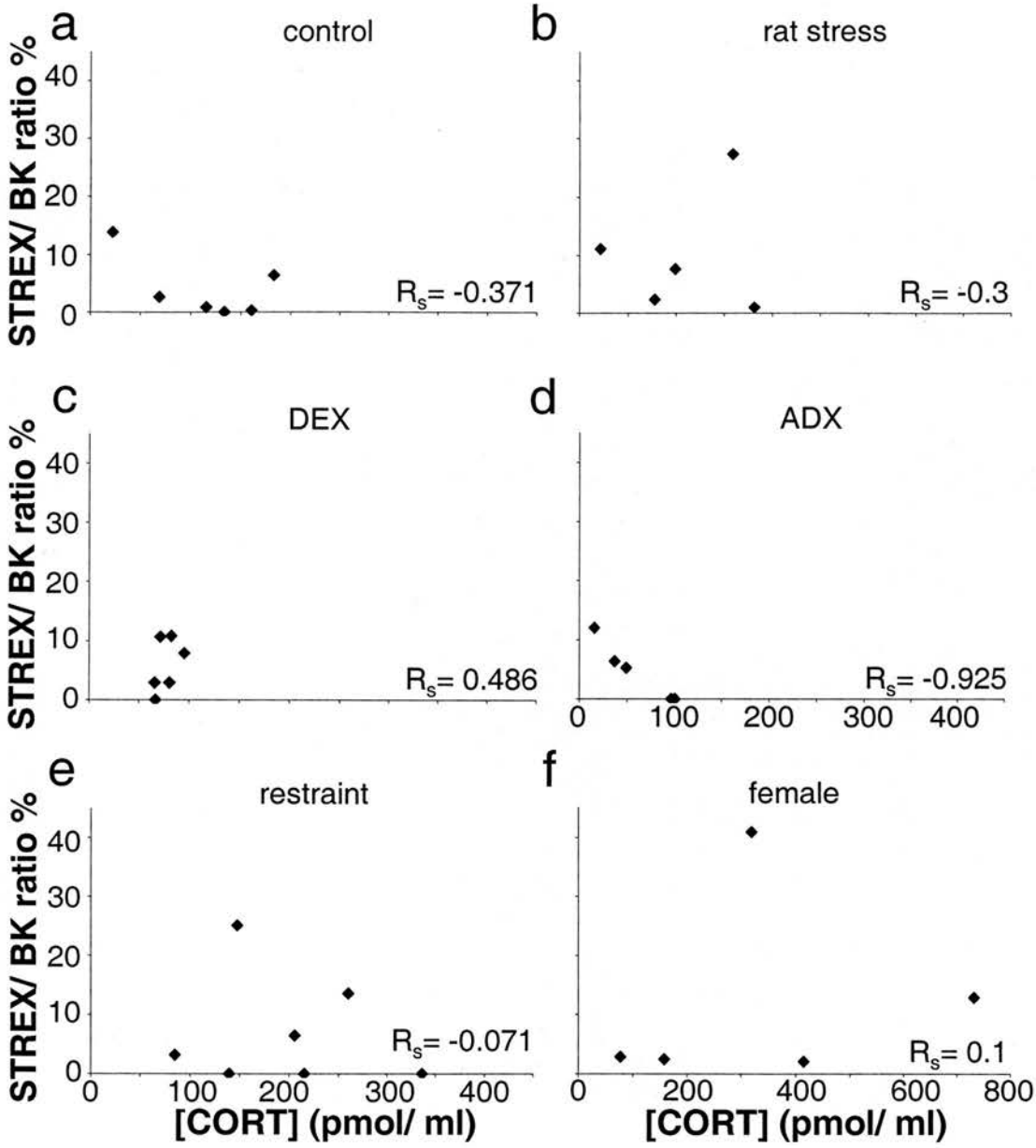

Figure 6-10 Correlation of STREX/ BK ratio with serum corticosterone concentration in mouse hippocampus

Data plotted using STREX as a percentage of total BK channel in the hippocampus against serum corticosterone concentration (pmol/ ml) for individual mice under different conditions as described in chapter 2; **a)** control (n= 6), **b)** rat stress (n= 5), **c)** dexamethasone (DEX) (n= 6), **d)** adrenalectomy (ADX) (n= 5), **e)** restraint (n= 7), and **f)** female (n= 5). Spearman rank correlation coefficient (Rs) is shown in each case.

Figure 6-11
Correlation of STREX/ BK ratio with serum ACTH concentration in mouse hippocampus

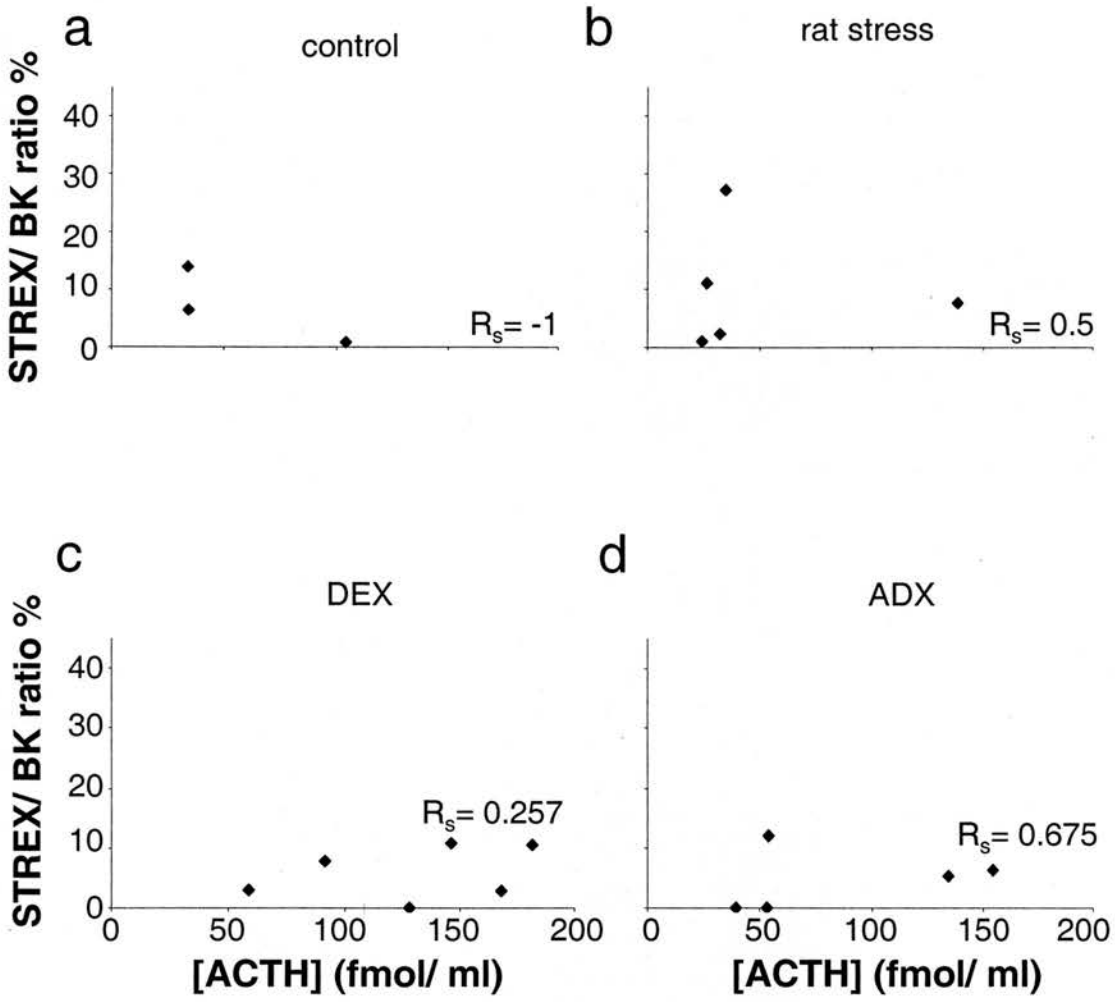

Figure 6-11 Correlation of STREX/ BK ratio with serum ACTH concentration in mouse hippocampus

Data plotted using STREX as a percentage of total BK channel in the hippocampus against serum ACTH concentration (fmol/ ml) for individual mice under different conditions as described in chapter 2; **a)** control (n= 3), **b)** rat stress (n= 5), **c)** dexamethasone (DEX) (n= 6) and **d)** adrenalectomy (ADX) (n= 5). Spearman rank correlation coefficient (Rs) is shown in each case.

6-2-2-6 Correlation of serum corticosterone and ACTH with hypothalamic STREX BK channel alternative splicing

Differential splicing of STREX in the hypothalamus was not correlated with changing serum [CORT], as indicated by an R_s value of –0.500 (n= 3). Whilst the chronic rat stress model appeared to induce changes in hypothalamic STREX splicing that were strongly correlated with increasing serum corticosterone, R_s= 1, only 3 subjects were assayed, therefore whether such a trend is descriptive of results obtained from a larger group of samples remains to be determined. Chronic restraint stress did not induce any changes in STREX/ BK ratio in the hypothalamus that could be strongly correlated with changes in serum [CORT], indicated by an R_s of 0.036 (n= 7). Neither chronic administration of dexamethasone nor adrenalectomy were found to influence STREX splicing in the hypothalamus in a manner that strongly correlated with changing serum [CORT], as indicated by R_s of –0.500 (n= 3) and –0.600 (n= 4) respectively. Finally, in the female hippocampus, changing STREX splicing could not be correlated with changing serum corticosterone, as indicated by an R_s of –0.525 (n= 5) (fig. 6-12).

Due to insufficient serum, an ACTH measurement was only obtained for one of the mice assayed for hypothalamic STREX splicing; therefore it was not possible to examine the correlation of STREX/ BK ratio with serum [ACTH]. Following chronic rat stress, decreasing hypothalamic STREX splicing appeared to be strongly correlated with increasing [ACTH], indicated by an R_s of 1. However, since the number of samples was low (n= 3) this correlation must be examined using a larger number of animals. STREX splicing in the hypothalamus was not strongly correlated

Figure 6-12
Correlation of STREX/ BK ratio with serum corticosterone concentration in mouse hypothalamus

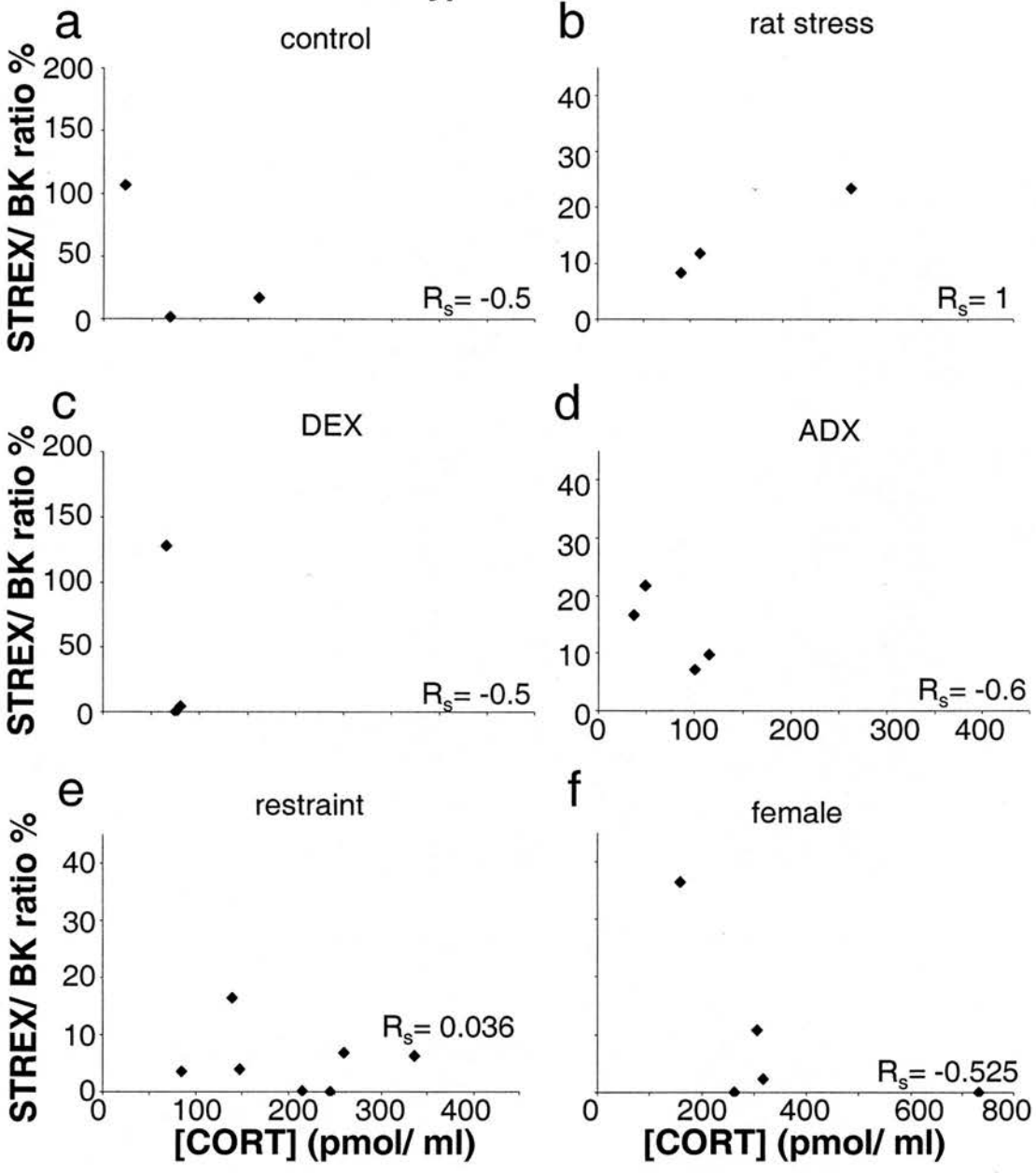

Figure 6-12 Correlation of STREX/ BK ratio with serum corticosterone concentration in mouse hypothalamus

Data plotted using STREX as a percentage of total BK channel in the hypothalamus against serum corticosterone concentration (pmol/ ml) for individual mice under different conditions as described in chapter 2; **a)** control (n= 3), **b)** rat stress (n= 3), **c)** dexamethasone (DEX) (n= 3), **d)** adrenalectomy (ADX) (n= 4), **e)** restraint (n= 7), and **f)** female (n= 5). Spearman rank correlation coefficient (Rs) is shown in each case.

with serum [ACTH] following chronic administration of dexamethasone or adrenalectomy, as indicated by R_s of –0.500 (n= 3) and 0.400 (n= 4) respectively (fig. 6-13).

6-3 Summary

6-3-1 Differential splicing of STREX BK channel alternative splice variant across tissues

During this study, the tissues of the hypothalamic- pituitary- adrenal axis, and also the hippocampus and cerebellum were assayed for presence of the STREX alternative splice insert of the BK channel, then this was normalised to total BK channel, in order to estimate the percentage of STREX- containing channels within the BK population in each tissue.

In control animals, the percentage of BK channels containing the STREX insert was found to vary across the tissues investigated. Such variability is unsurprising, since the expression of heterogeneous populations of alternatively- spliced BK channels has been shown to be required for correct function in a tissue- specific manner (Fettiplace and Fuchs, 1999). In addition to this, it is also important to note that a large variability was observed in STREX/ BK ratios across individuals from the same experimental group. It is therefore possible that such inter- individual variations are sufficient to increase experimental error such that genuine differences between experimental groups are obscured. However, it may also be the case that different paradigms of control are required, with experimental animals being matched in terms of basal secretion and pre- experiment stressor exposure. Under

Figure 6-13
Correlation of STREX/ BK ratio with serum ACTH concentration in mouse hypothalamus

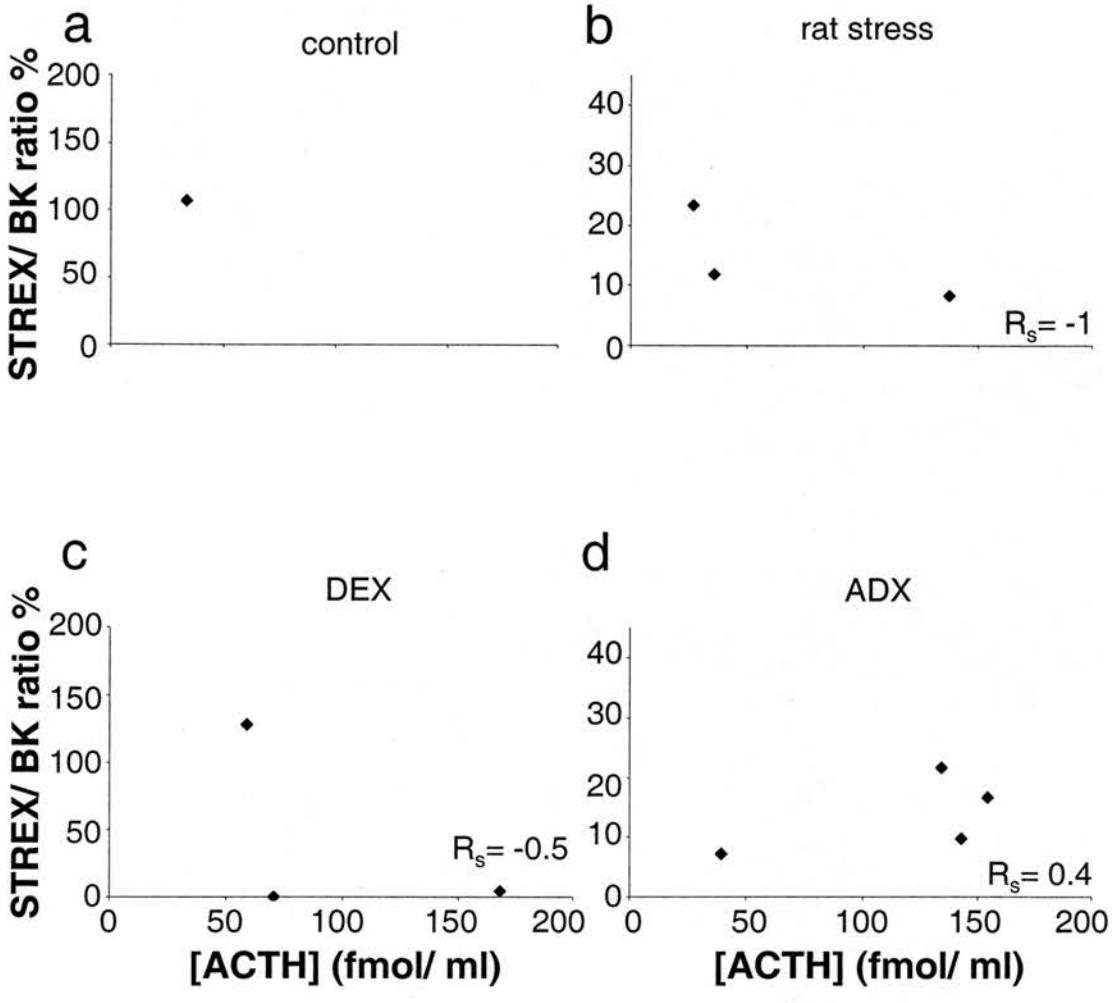

Figure 6-13 Correlation of STREX/ BK ratio with serum ACTH concentration in mouse hypothalamus

Data plotted using STREX as a percentage of total BK channel in the hypothalamus against serum ACTH concentration (fmol/ ml) for individual mice under different conditions as described in chapter 2; **a)** control (n= 1), **b)** rat stress (n= 3), **c)** dexamethasone (DEX) (n= 3) and **d)** adrenalectomy (ADX) (n= 4). Spearman rank correlation coefficient (Rs) is shown in each case.

'normal' conditions, in unstressed animals, the adrenal gland was found to have the highest expression of STREX as a percentage of total BK channel, with a slightly lower percentage of STREX as a proportion of total BK channel observed in the anterior pituitary, then lower expression in the hypothalamus, and lowest expression in the hippocampus and cerebellum. The BK channel is a significant modifier of adrenal chromaffin cell function, and in rats, glucocorticoids have been shown to modulate BK channel activity in an acute manner, with a direct effect on action potential firing (Lovell *et al.*, 2004). Adrenal chromaffin cells are exposed to high transient concentrations of adrenal steroids at times of acutely elevated adrenal secretion (Betito *et al.*, 1994), therefore a rapid change in BK channel activity, and subsequent effects on fell firing, may be a significant and immediate means of regulating adrenal secretion. Since the STREX exon confers glucocorticoid responsiveness on BK channels, it is possible that the observed high level of STREX expression represents an important means of modifying adrenal excitability in the mouse.

CRH- stimulated pituitary ACTH secretory responses require BK channel function (Shipston *et al.*, 1996), and it may be the case that variable expression of STREX in this tissue enables modulation of responses in a dynamic manner. Additionally, the existence of several differentially- regulated alternative splice variants of the BK channel in the pituitary may allow tight control of ACTH secretion during crisis responses by enabling regulation of a subset of channels independently of those responsible for maintenance of normal stimulatory secretory levels (Tian *et al.*, 2001a).

Since the hypothalamic paraventricular nucleus is the initiator for the HPA axis hormonal cascade, tuning of cell excitability in this region by alternative splicing of BK channel α subunits may be critical for regulated responses not only during stress, but also could enable independent control of secretion above basal levels by expression of a subset of channels with increased responses to enable more rapid activation during stressful situations, which are differentially regulated from those involved in control of normal homeostatic function.

Whilst expression of STREX in both the hippocampus and cerebellum was low in control animals, it may be the case that during 'normal' activity, these tissues do require the functional phenotype that is conferred by STREX. Alternatively, the presence of a small number of STREX channels may not necessarily be descriptive of their role in the tissue as a whole, since they may be delimited to specific small groups of neurons, where they significantly influence cell excitability, with vital consequences on regulation of the tissue as a whole.

6-3-2 Effect of stress on alternative splicing of the BK channel α-subunit

In order to determine the effect of chronic stress on STREX splicing in the mouse, two models of chronic stress were applied: rat stress and restraint. It has been previously shown that both such stresses cause an upregulation of HPA axis activity in mice after exposure (Linthorst *et al.*, 2000, Vallès *et al.*, 2003). Although it was speculated that increases in cell excitability during stress might necessitate an upregulation of BK channel alternative splice variant expression in the tissues of the

HPA axis, as well as other steroid responsive tissues such as the hippocampus and cerebellum, in fact altered levels of expression of the STREX BK channel α-subunit were not seen in any of these.

Several possibilities arise when considering this result: firstly, expression of the STREX BK alternative splice variant may be constant, and this pool of STREX channels is sufficient to alter activation in response to varying glucocorticoid levels (Tian *et al.*, 2001a) during normal physiological conditions, such as the diurnal rhythm. This subset of BK channels can then also be independently regulated to facilitate rapid activation in response to acute stresses. In the event of chronic stress, it may be the case that the control levels of STREX channels are sufficient to mediate increased cell responses. At longer timepoints than the 14 days used during this study, or during extreme crisis responses, such as actual attack by predators, heightened expression of the STREX channel might be observed, above the 'basal' levels seen previously. Whilst other studies demonstrated a downregulation of STREX splicing (McCobb *et al.*, 2003), this appeared to mark the onset of passive coping behaviours, in response to social subordination stress therefore it is likely that the type of stress applied influences BK channel splicing decisions.

Additionally, since STREX expression was found to be already very high in adrenal glands of control mice, it might be the case that only small shifts in expression are required to induce functional changes, and tailoring of cell responsiveness by alternative splicing could occur in a very subtle manner. Alternatively, it is possible that although a high level of STREX expression was observed in the adrenal as a

whole, functional regulation of cell responsiveness may be effected by changing expression in subpopulations of cells, which would again be masked by a high total adrenal STREX expression.

6-3-3 Effect of manipulation of glucocorticoid responses on BK channel alternative splicing

Administration of dexamethasone was found not to alter the expression of STREX as a percentage of total BK channel in the tissues assayed during this study. This synthetic glucocorticoid analogue has previously been shown to exert non- genomic effects on cell excitability by influencing BK channel gating (Lovell *et al.*, 2004) as well as genomic effects that determine regulation of the channel by other pathways (Tian *et al.*, 2001a, b, Tian *et al.*, 1998, Shipston *et al.*, 1996), and chronic elevation of circulating glucocorticoids may cause upregulation of activity of BK channels. However, it may be the case that such application does not necessitate de novo expression if the glucocorticoid- sensitive STREX channels are already present in sufficient numbers to elicit an appropriate response commensurate with such stimulation. It is also evident that the effects of glucocorticoids exerted locally may differ from those resulting from changing circulating levels, since concentration of corticosterone can be as much as 100- fold higher in the adrenal than in the serum (Xie and McCobb, 1998). Additionally, *in vivo*- administered dexamethasone has been shown to poorly penetrate the blood- brain barrier (Meijer *et al.*, 1998), therefore it is difficult to replicate the local effects of endogenous glucocorticoids using systemically administered synthetic analogues.

The removal of glucocorticoid feedback, and subsequent disruption of HPA axis activity, by bilateral adrenalectomy was initially thought not to have affected splicing of STREX in the other tissues in the HPA axis, nor in the hippocampus and cerebellum. Disruption of HPA axis function has been shown to influence STREX splicing in the rat adrenal (Lovell and McCobb, 2001) where hypophysectomy resulted in a significant decrease in serum corticosterone, however in this case, removal of the source of adrenal glucocorticoids did not cause a statistically significant reduction in population mean serum [CORT], suggesting that surgery was not effective, therefore it is not possible to conclude that the absence of glucocorticoid feedback does not influence alternative splicing of BK channel α subunits in other tissues.

6-3-4 Effect of circulating corticosterone and ACTH on BK channel alternative splicing

None of the treatments used during this study caused significant up- or downregulation of serum corticosterone levels in male mice, compared to controls, also serum ACTH levels were not significantly different following rat stress, dexamethasone treatment or adrenalectomy, compared to control males. Although no significant differences were observed under these different paradigms, it may be the case that responses of some animals to stress was altered as a result of preconditioning during development (Bhatnagar *et al.*, 2005) or neonatal experience (Kalinichev *et al.*, 2002). Additionally, a large degree of variability was observed in the serum concentrations of CORT and ACTH between the experimental animals, therefore it may be the case that this masked subtle shifts in secretion in response to

stress. Further experiments where animals were grouped prior to stress exposure, according to their basal levels of secretion, may therefore provide a means of observing small, but physiologically significant changes in CORT and ACTH release under these conditions. Female circulating corticosterone was significantly higher than control male, however no significant differences were observed compared to male in STREX/ BK channel ratio in any of the tissues investigated. Gonadal factors have been shown to alter HPA axis function in response to stress (Seale *et al.*, 2004). Testosterone can modulate STREX splicing in rats (Mahmoud and McCobb, 2004), and oestrogen can modulate BK channel activation (Dimitropoulou *et al.*, 2005). It may be the case that inter- individual differences in basal gonadal secretion, as well as HPA axis function, cause sufficient variability to mask genuine differences in regulation in response to stress when a small group of animals is sampled, as in this study.

Alternative splicing of the STREX BK channel α-subunit alternative splice variant was investigated for correlation with increasing corticosterone and ACTH concentration. In control animals, no such correlation was observed the adrenal, anterior pituitary, hypothalamus or cerebellum. Although in the hippocampus a Spearman rank correlation coefficient of –1 was recorded for STREX/ BK ratio and increasing serum ACTH, only 3 data points were available for this, therefore this result may not be descriptive of splicing changes accompanying changing corticosterone levels. These data suggest that alternative splicing of the STREX exon in BK channel α-subunits is not significantly regulated in response to changing serum corticosterone concentration within the limits of normal 'basal' secretion. In

female mice, although the average serum corticosterone concentration was significantly higher than that of control males, similarly no correlation between increasing serum [CORT] and increased/ decreased STREX splicing was observed in any of the tissues investigated.

No strong correlation was observed between STREX splicing and corticosterone concentration following rat stress in any of the tissues that were investigated, suggesting that either changes in cell excitability, particularly in the adrenal gland given the nature of the threatening stressor applied in this case, that would be conferred by STREX are not required, or an increase in adrenal responsiveness can readily be effected without newly- synthesised STREX channels. Since STREX already comprised a high percentage of total BK channel in the adrenal gland, the latter possibility may be the case.

In adrenal glands of animals subjected to restraint stress, a positive correlation was observed, with increasing serum corticosterone accompanied by increased STREX splicing. One possible model to explain this is that adrenal cell excitability is increased by alternative splicing of BK channel α-subunits during stress, to enable more rapid activation, but since the STREX channel is glucocorticoid- sensitive, this acts as a feedback mechanism to prevent feed- forward amplification of the adrenal response.

In the adrenal gland of dexamethasone- treated animals, STREX/ BK ratio was seen to fall as serum corticosterone rose, suggesting that endogenous corticosterone, in the

presence of systemically administered dexamethasone, may have an additive effect on negative feedback regulation of the HPA axis, with the resultant effect that adrenal cell excitability is downregulated by reducing expression of STREX channels. No other correlations were seen in the other tissues examined for STREX splicing in relation to corticosterone concentration, and whilst BK channel splicing in other tissues may not be regulated in this manner, other factors such as CRH, given its role in changing synaptic efficacy (Wang *et al.*, 1998) may be significant in modulating such genomic effects on cell excitability.

In adrenalectomised animals, a negative correlation between STREX/ BK ratio and serum [CORT] in the anterior pituitary and hippocampus was observed. BK channel alternative splicing may be a means to fine- tune secretory responsiveness in the anterior pituitary (Van Goor *et al.*, 2001) and a reduction in the expression of the 'rapid activation' phenotype STREX channel α-subunits may represent the end-result of corticosterone- driven negative feedback on tissues upstream of the adrenal in the HPA axis. Furthermore, the regulatory role of BK channels may differ between cell types in certain tissues, since evidence suggests that BK activation in pituitary somatotrophs prolongs action potential depolarisations (Van Goor *et al.*, 2001), whilst pituitary GH3 cells, their primary role appears to be in ending the action potential (Miranda *et al.*, 2003). This cell- type specific regulation of function by BK channels is also likely to occur in other tissues, where the expression of the channel may vary in certain cell types, or the expression of particular splice variants may be delimited to specific cell populations. In addition to being a target for adrenal glucocorticoids, the hippocampus is also a regulator of HPA axis function (Buchanan

et al., 2004). Whilst acute stress is associated with increased excitability in the CA1 pyramidal neurons and increased circulating [CORT] (Weiss *et al.*, 2005), the end result of chronic stress, leading to adaptation, may be to decrease cell responsiveness, possibly by selective expression of functionally distinct BK channel splice variants.

No correlations were made between serum ACTH concentration and alternative splicing of the BK channel in any of the tissues studied. However, since there is already considerable inter- individual variation in HPA axis responses, and multifactorial regulation of ACTH secretion in response to different stress modalities exists, it is possible that correlation between cell responsiveness and ACTH secretion does exist, but in a manner that varies in both timing and magnitude. For example, transient increases in ACTH secretion may lead to sustained corticosterone responses (Lenczowski *et al.*, 1998) therefore it may be the case that during the timecourse of this experiment, sampling of ACTH at the 14- day endpoint may not be accurately descriptive of dynamic regulation of ACTH in response to stress. Consequently, this might lead to difficulty in determining whether ACTH alters cell responsiveness via BK channel- regulated changes in excitability.

Chapter Seven:

Summary and conclusions

7-1 Imaging of BK channel alternative splice variant expression using fluorescent protein labelled constructs

The mouse BK channel was used as a model to investigate whether alternative splice variants, at site C2 of the BK channel C-terminus, were differentially localised at the cell surface. The subcellular localisation of ZERO and STREX BK channel alternative splice variants was investigated using –EGFP labelled BK channel fusion proteins. No significant differences were observed in the subcellular localisation of either STREX-EGFP or ZERO-EGFP in HEK293, PC12 or MDCK cells, therefore it is likely that the STREX exon does not modify cell surface trafficking of the BK channel, in either the presence or absence of endogenous BK channels. By subcloning novel splice inserts, as well as combinations of known inserts, into the existing BK channel fluorescent constructs, it will be possible to generate a library of expression vectors, enabling the detailed study of the effects of alternative splicing on assembly and trafficking of the BK channel.

It is becoming increasingly clear that regulated surface trafficking of the BK channel is physiologically relevant in processes such as pregnancy (Eghbali *et al.*, 2003, Song *et al.*, 1999) and aging of cerebral arteries (Nishimaru *et al.*, 2004). The finding that mouse myometrial BK channel expression increases in late pregnancy, whilst surface trafficking falls, suggests a mechanism where multimerisation with alternatively-spliced α-subunits which are not trafficked to the plasma membrane, may be used to prevent the surface expression of other alternative splice variants, for example by causing retention in, or retrieval to, the endoplasmic reticulum. Regulation in this manner is suggested by the data of Zarei and co-workers (Zarei *et al.*, 2001, 2004).

To examine whether a site C2 BK channel alternative splice variant may affect cell membrane expression, by acting as a dominant-negative suppressor of trafficking of other BK channel α-subunits, the truncated Δe23 splice variant was investigated. The predominantly perinuclear expression of the Δe23 BK channel alternative splice variant was reminiscent of ER localisation, and Δe23 also caused the retention of coexpressed STREX α-subunits in a perinuclear compartment. Since Δe23 is truncated, it lacks the ER export signal, DLIFCL, at residues 1105-1110 at the C-terminus of the channel (Kwon and Guggino, 2004). It is therefore likely that the observed perinuclear accumulation of this splice variant occurs in the endoplasmic reticulum, and whilst the distribution of Δe23 is also morphologically similar to the ER retention of the SV1 splice variant (Zarei *et al.*, 2004), further studies using compartment- specific markers, will enable confirmation of whether the retention of Δe23 is delimited to the ER.

In chapter 3, constructs were generated encoding –HcRed labelled ZERO and STREX BK channel α-subunits, which were found to be incorrectly trafficked, and were trapped in intracellular puncta, rather than expressing at the cell surface, in a manner independent of endogenous trafficking mechanisms. Whilst the reason for this altered trafficking is unclear, analysis of solubility of the –HcRed labelled BK channel α-subunits in non-ionic detergent may be used to indicate any gross abnormalities in the folding of these proteins, which would prevent them from being processed and trafficked correctly (Marquardt and Helenius, 1992). However, since the –HcRed labelled α-subunits were able to exert a BK channel- specific dominant negative effect on the surface expression on –EGFP labelled α-subunits, this suggests

that the domains responsible for channel multimerisation (Quirk and Reinhart, 2001) at least remain accessible. In order to confirm this, association between ZERO or STREX-EGFP could be assessed using a co-immunoprecipitation strategy.

It may be the case that a hierarchy of dominance exists between splice variants that influence surface trafficking. Modes of regulated expression may exist that are similar to those seen for BK channel regulation by phosphorylation where, although heteromeric channels form, regulation of the channel is essentially digital (Tian *et al.*, 2004). The dominant-negative effect of the –HcRed labelled BK channel α-subunits on surface expression of the –EGFP labelled α-subunits suggests that assembly of channels containing a single ZERO or STREX-HcRed α-subunit may be sufficient to prevent surface trafficking. Therefore, although it was not possible during this study to generate constructs that would allow simultaneous imaging of two BK channel alternative splice variants at the plasma membrane, the lack of interaction of ZERO-HcRed and STREX-HcRed with syntaxin-1A, which normally binds to, and modulates BK channels, suggests that these fluorescent protein-labelled α-subunits represent a novel tool for specific knockdown of surface BK channel expression. If further experiments determine that ZERO-HcRed and STREX-HcRed expression do not have any deleterious effects on cell viability, these fusion proteins may be useful in studies to determine the lifetime of the channel at the cell surface.

7-2 Real time PCR assays for BK channel alternative splice variants

In chapter 4, highly- specific real time PCR assays were designed, enabling high-throughput, high-sensitivity screening for several BK channel alternative splice

variants. This method allows investigation of relative expression of splice variants that may be of insufficient size to be detected by traditional end-point PCR, or are expressed in low abundance, without requiring the specialised primer- specific protocols that have been used in previous studies of relative BK channel splice variant expression (Mahmoud *et al.*, 2002, Lai and McCobb, 2002). Real time PCR investigation of changes in splice variant expression relative to total BK channel will enable the analysis of changes in expression of splice variants that accompanies physiological states such as pregnancy (Benkusky *et al.*, 2000), stress (McCobb et al, 2003) and development (Zhang *et al.*, 2004). This approach will also allow investigation of altered BK channel expression in pathological states, in a more rapid and reproducible manner than end- point PCR, since reactions and quantitation are carried out in a closed-tube format, thus reducing the possibility of contamination, or inconsistencies in gel electrophoresis. Since upregulation of certain BK channel alternative splice variants may be a marker for specific diseases (Weaver *et al.* 2004), screening of tissue samples by real-time PCR may enable rapid diagnosis of such conditions, and increased understanding of the regulatory changes in BK channel expression might facilitate development of novel therapies.

7-3 BK channel alternative splice variant mRNA expression in mouse tissues

Screening using real time PCR revealed mRNA expression of certain BK channel splice variants to be clearly delimited to specific tissues. Furthermore, the mRNA expression of each splice variant was found to vary across tissues, as a proportion of total BK channel. Since the real time PCR method is used to quantitate mRNA

expression, further techniques such as quantitative western blotting will be required to confirm that this represents expression of the BK channel protein. Additionally, electrophysiological analysis of tissues where differential alternative splicing occurred would then allow the characterisation of changes in cell excitability that arose from such regulated splicing. Investigation of the tissue distribution and subcellular localisation of BK channel alternative splice variant proteins would be facilitated by development of splice variant- specific antibodies for use in immunohistochemical analyses.

It may be the case that expression of BK channel alternative splice variants in a tissue- specific manner facilitates the tuning of cell excitability for correct physiological function, and distinct modes of regulation by splice variant expression may exist. For example, rapid glucocorticoid- mediated changes in adrenal chromaffin cell excitability may be achieved by expression of glucocorticoid-sensitive STREX channels as a proportion of the BK channel population, precluding the requirement for newly- synthesised channels at each stimulus. Conversely, the observed reduction in surface BK channel expression in the mouse myometrium during late pregnancy (Eghbali et al., 2003), facilitating increased uterine contractility, may be achieved by expression of a differentially- trafficked BK channel alternative splice variant, similar to SV1 (Zarei et al., 2004) or Δe23, that can multimerise with other BK channel α-subunits, causing retention in intracellular compartments, thereby preventing newly- synthesised channels from reaching the cell membrane.

Expression of several BK channel alternative splice variants was found to change in the breast, under varying physiological conditions. Whilst this was not investigated further during this study, it is likely that such changes may correlate with hormonal secretion, and altered BK channel expression in breast tissue may be of significance in process such as the controlled vascular expansion during pregnancy and lactation, and regression during involution (Djonov *et al.*, 2001), or hormonally- controlled proliferation of cells of the mammary epithelium (Frech *et al.*, 2005, Clarke, 2003).

7-4 BK channel alternative splicing in the developing mouse CNS

Following the observation that total BK channel expression, as well as that of several alternative splice variants, was upregulated during embryogenesis, shortly after the stage at which the neural plate forms, led to the hypothesis that BK channel splicing might be regulated during mouse CNS development. Using the real time PCR approach to quantify both total BK channel, as well as STREX and ZERO expression in tissues of the developing mouse CNS in chapter 5 showed that although total BK channel was upregulated over the course of development from embryo day 13 to postnatal day 35, expression of both of the splice variants investigated was also altered. STREX expression was seen to fall as a proportion of total BK channel, whilst ZERO was found to increase over this developmental period, suggesting significant roles for regulated BK channel splicing in determining the electrophysiological phenotype of cells in the developing central nervous system. Further investigation will determine whether the other known splice variants are regulated in a similar manner. Since BK channels contribute to control of neurotransmitter release (Raffaelli *et al.*, 2004), it may be the case that regulated

expression of BK channel alternative splice variants in the neurons of the developing CNS facilitates regulated signalling that is critical for establishment and maintenance of synaptic connections during embryogenesis and postnatal development.

7-5 Stress-induced changes in BK channel alternative splicing

Whilst previous studies indicated that chronic psychosocial stress and surgical manipulations of hypothalamic- pituitary- adrenal (HPA) axis activity (McCobb *et al.*, 2003, Xie and McCobb, 1998) can cause changes in the expression of STREX in the adrenal glands of tree shrews and rats respectively, during this study two different stress paradigms – restraint and rat stress – were not found to significantly influence STREX splicing in the tissues of the mouse HPA axis, nor other steroid-responsive brain regions. Pharmacological manipulation by systemic administration of dexamethasone, and surgical removal of the adrenal gland were also not found to have significant effects on STREX splicing in the tissues investigated. The subordination stress paradigm used by McCobb and coworkers in tree shrews exploited a 28- day period of stress, as well as a 10- day recovery period following stress, therefore it may be the case that induction of stress- related changes in the STREX splicing paradigm may require a longer period of stimulation than the 14-day model used during this investigation. Additionally, the recovery period may also be of significance- since the animals assayed during this study were sacrificed immediately following the final stress treatment, it may be the case that changes in splicing were not observed since insufficient time was given between the end of stress stimulation and harvesting of tissues. Whilst sex differences were observed in STREX splicing in tree shrew adrenals (McCobb *et al.*, 2003), similar differences

were not seen in mice used during this study, however this may be attributable to a high degree of variability between samples. Furthermore, during the study by McCobb and co-workers, average STREX expression in control male tree shrew adrenals was 12.4 ± 0.98 (n= 14), whilst that in control females was 6.13 ± 5.14% (n= 9) of total BK channel, whereas in the mice used during this study, control male adrenal STREX expression was 90.40 ± 23.2% (n=7), and that in unstressed female mice was 98.1 ± 19.3% (n= 7) of total BK channel, clearly indicating inter- species differences in splicing of STREX in the adrenal gland. It may therefore be the case that in the mouse, the paradigm of feedback regulation of HPA axis activity, and dynamic regulation of cell excitability in the adrenal gland by context- specific expression of BK channel alternative splice variants with distinct activation properties, is dissimilar to that in other species.

There was no correlation between HPA axis output and STREX splicing, however it should be noted that a large degree of variability was observed in serum CORT and ACTH levels in the experimental animals. Therefore, future experimental protocols will require more stringent controls for this- for example, animals might be grouped according to basal secretion levels, then a relationship might be observed between STREX splicing and change in secretory activity following stress. Furthermore, it is also necessary to determine the other splice variants contributing to cell excitability in the tissues of the HPA axis, and other steroid- responsive tissues in the mouse. For example, during this study, in the cerebellum, STREX was found to comprise only 5.3 ± 2.1% (n= 9) of the total BK channel population, therefore it is likely that during periods of heightened glucocorticoid stimulation, such as during stress, if changes

occur in cerebellar excitability, these might be mediated by expression of other BK channel alternative splice variants. Additionally, expression may be confined to a small subpopulation of cells, such as the Purkinje cells. Spatial analysis of the distribution and expression of BK channel alternative splice variants, for example using an in-situ hybridisation approach, will allow this to be investigated.

Whilst the role of BK channel expression in many physiological processes remains unclear, it is evident that expression of BK channel alternative splice variants facilitates regulation of channel activity in a wide variety of contexts. During this study, it has been possible to establish a system for the investigation of BK channel subcellular localisation *in vitro*, which may in the future be used in living cells, and the generation of potentially useful tools to knock down BK channel surface expression will facilitate the investigation of issues such as the lifetime of the BK channel at the cell membrane. In addition, the development of highly sensitive BK channel splice variant- specific assays represents a powerful technique to facilitate investigation of the contribution of differentially- spliced BK channel populations to the function of many tissues, and regulation of dynamic changes in BK channel splicing during physiological and pathological processes.

Bibliography

Aamodt, S. M. and Constantine-Paton, M. (1999). The Role of Neural Activity in Synaptic Development and its Implications for Adult Brain Function. *Advances in Neurology* **79**: 133-144.

Ahluwalia, J., Tinker, A., Clapp, L. H., Duchen, M. R., Abramov, A. Y., Pope, S., Nobles, M. and Segal, A. W. (2004). The Large-Conductance Ca^{2+}-Activated K^+ Channel is Essential for Innate Immunity. *Nature* **427**: 853-858.

al'Absi, M. and Arnett, D. K. (2000). Adrenocortical Responses to Psychological Stress and Risk for Hypertension. *Biomedicine and Pharmacotherapy* **54**: 234-244.

Amberg, G. C., Bonev, A. D., Rossow, C. F., Nelson, M. T. and Santana, L. F. (2003). Modulation of the Molecular Composition of Large Conductance, Ca^{2+} Activated K^+ Channels in Vascular Smooth Muscle During Hypertension. *Journal of Clinical Investigation* **112**: 717-724.

Andersen, M. L., Bignotto, M., Machado, R. B. and Tufik, S. (2004). Different Stress Modalities Result in Distinct Steroid Hormone Responses by Male Rats. *Brazilian Journal of Medical and Biological Research* **37**: 791-797.

Anderson, R. M., Lawrence, A. R., Stottmann, R. W., Bachiller, D. and Klingensmith, J. (2002). Chordin and Noggin Promote Organizing Centers of Forebrain Development in the Mouse. *Development* **129**: 4975-4987.

Applied Biosystems (2001). Relative Quantitation of Gene Expression. *ABI Prism 7700 Sequence Detection System, User Bulletin #2.*

Archer, S. L., Gragasin, F. S., Wu, X., Wang, S., McMurtry, S., Kim, D. H., Platonov, M., Koshal, A., Hashimoto, K., Campbell, W. B., Falck, J. R. and Michelakis, E. D. (2003). Endothelium-Derived Hyperpolarizing Factor in Human Internal Mammary Artery is 11,12-Epoxyeicosatrienoic Acid and Causes Relaxation by Activating Smooth Muscle BKca Channels. *Circulation* **107**: 769-776.

Arien, H., Wiser, O., Arkin, I. T., Leonov, H. and Atlas, D. (2003). Syntaxin 1A Modulates the Voltage-Gated L-Type Calcium Channel (Ca(v)1.2) in a Cooperative Manner. *Journal of Biological Chemistry* **278**: 29231-29239.

Babot, Z., Cristofol, R. and Sunol, C. (2005). Excitotoxic Death Induced by Released Glutamate in Depolarized Primary Cultures of Mouse Cerebellar Granule Cells is Dependent on $GABA_A$ Receptors and Niflumic Acid-Sensitive Chloride Channels. *European Journal of Neuroscience* **21**: 103-112.

Bahring, R., Dannenberg, J., Peters, H. C., Leicher, T., Pongs, O. and Isbrandt, D. (2001). Conserved Kv4 N-Terminal Domain Critical for Effects of Kv Channel-Interacting Protein 2.2 on Channel Expression and Gating. *Journal of Biological Chemistry* **276**: 23888-23894.

Barman, S. A., Zhu, S., Han, G. and White, R. E. (2003). cAMP Activates BK_{Ca} Channels in Pulmonary Arterial Smooth Muscle Via cGMP-Dependent Protein Kinase. *American Journal of Physiology. Lung Cellular and Molecular Physiology* **284**: L1004-1011.

Barman, S. A., Zhu, S. and White, R. E. (2004). PKC Activates BK_{Ca} Channels in Rat Pulmonary Arterial Smooth Muscle Via cGMP-Dependent Protein Kinase. *American Journal of Physiology. Lung Cellular and Molecular Physiology* **286**: L1275-1281.

Becker, M. N., Brenner, R. and Atkinson, N. S. (1995). Tissue-Specific Expression of a Drosophila Calcium-Activated Potassium Channel. *Journal of Neuroscience* **15**: 6250-6259.

Beddington, R. S. (1994). Induction of a Second Neural Axis by the Mouse Node. *Development* **120**: 613-620.

Benkusky, N. A., Fergus, D. J., Zucchero, T. M. and England, S. K. (2000). Regulation of the Ca^{2+}-Sensitive Domains of the Maxi-K Channel in the Mouse Myometrium During Gestation. *Journal of Biological Chemistry* **275**: 27712-27719.

Betito, K., Mitchell, J. B., Bhatnagar, S., Boksa, P. and Meaney, M. J. (1994). Regulation of the Adrenomedullary Catecholaminergic System after Mild, Acute Stress. *American Journal of Physiology. Regulatory, Integrative and Comparative Physiology* **267**: R212-220.

Bhatnagar, S., Lee, T. M. and Vining, C. (2005). Prenatal Stress Differentially Affects Habituation of Corticosterone Responses to Repeated Stress in Adult Male and Female Rats. *Hormones and Behavior* **47**: 430-438.

Bolivar, J. J. and Cereijido, M. (1987). Voltage and Ca^{2+}-Activated K^+ Channel in Cultured Epithelial Cells (MDCK). *Journal of Membrane Biology* **97**: 43-51.

Bordey, A., Sontheimer, H. and Trouslard, J. (2000). Muscarinic Activation of BK Channels Induces Membrane Oscillations in Glioma Cells and Leads to Inhibition of Cell Migration. *Journal of Membrane Biology* **176**: 31-40.

Boris-Moller, F. and Wieloch, T. (1998). Changes in the Extracellular Levels of Glutamate and Aspartate During Ischemia and Hypoglycemia. *Experimental Brain Research* **121**: 277-284.

Bravo-Zehnder, M., Orio, P., Norambuena, A., Wallner, M., Meera, P., Toro, L., Latorre, R. and Gonzalez, A. (2000). Apical Sorting of a Voltage- and Ca^{2+}-Activated K^+ Channel A -Subunit in Madin-Darby Canine Kidney Cells is Independent of N-Glycosylation. *Proceedings of the National Academy of Sciences USA* **97**: 13114-13119.

Brelidze, T. I., Niu, X. and Magleby, K. L. (2003). A Ring of Eight Conserved Negatively Charged Amino Acids Doubles the Conductance of BK Channels and Prevents Inward Rectification. *Proceedings of the National Academy of Sciences USA* **100**: 9017-9022.

Buchanan, T. W., Kern, S., Allen, J. S., Tranel, D. and Kirschbaum, C. (2004). Circadian Regulation of Cortisol after Hippocampal Damage in Humans. *Biological Psychiatry* **56**: 651-656.

Burckhardt, B. C. and Gogelein, H. (1992). Small and Maxi K^+ Channels in the Basolateral Membrane of Isolated Crypts from Rat Distal Colon: Single-Channel and Slow Whole-Cell Recordings. *Pflugers Archiv. European Journal of Physiology* **420**: 54-60.

Bustin, S. A. (2000). Absolute Quantification of mRNA Using Real-Time Reverse Transcription Polymerase Chain Reaction Assays. *Journal of Molecular Endocrinology* **25**: 169–193.

Butterfield, I., Warhurst, G., Jones, M. N. and Sandle, G. I. (1997). Characterization of Apical Potassium Channels Induced in Rat Distal Colon During Potassium Adaptation. *Journal of Physiology (London)* **501**(3): 537-547.

Callera, G. E., Yogi, A., Tostes, R. C., Rossoni, L. V. and Bendhack, L. M. (2004). Ca^{2+}-Activated K^+ Channels Underlying the Impaired Acetylcholine-Induced Vasodilation in 2k-1c Hypertensive Rats. *Journal of Pharmacology and Experimental Therapeutics* **309**: 1036-1042.

Carroll, E. A., Gerrelli, D., Gasca, S., Berg, E., Beier, D. R., Copp, A. J. and Klingensmith, J. (2003). Cordon-Bleu is a Conserved Gene Involved in Neural Tube Formation. *Developmental Biology* **262**: 16-31.

Chanrachakul, B., Pipkin, F. B. and Khan, R. N. (2004). Contribution of Coupling between Human Myometrial β2-Adrenoreceptor and the BK_{Ca} Channel to Uterine Quiescence. *American Journal of Physiology. Cell Physiology* **287**: C1747-1752.

Christianson, J. C. and Green, W. N. (2004). Regulation of Nicotinic Receptor Expression by the Ubiquitin-Proteasome System. *EMBO Journal* **23**: 4156-4165.

Cibulsky, S. M., Fei, H. and Levitan, I. B. (2005). Syntaxin-1A Binds to and Modulates the *Slo* Calcium-Activated Potassium Channel Via an Interaction That Excludes Syntaxin Binding to Calcium Channels. *Journal of Neurophysiology* **93**: 1393-1405.

Clark, A. G., Hall, S. K. and Shipston, M. J. (1999). ATP Inhibition of a Mouse Brain Large-Conductance K^+ (*mSlo*) Channel Variant by a Mechanism Independent of Protein Phosphorylation. *Journal of Physiology (London)* **516**: 45-53.

Clarke, R. B. (2003). Steroid Receptors and Proliferation in the Human Breast. *Steroids* **68**: 789-794.

Cohen, D. and Musch, A. (2003). Apical Surface Formation in MDCK Cells: Regulation by the Serine/Threonine Kinase Emk1. *Methods* **30**: 269-276.

Coleman, M. A., Garland, T., Marler, C. A., Newton, S. S., Swallow, J. G. and Carter, P. A. (1998). Glucocorticoid Response to Forced Exercise in Laboratory House Mice (*Mus Domesticus*). *Physiology and Behaviour* **63**: 279-285.

Coussens, C. M., Kerr, D. S. and Abraham, W. C. (1997). Glucocorticoid Receptor Activation Lowers the Threshold for NMDA-Receptor-Dependent Homosynaptic Long-Term Depression in the Hippocampus through Activation of Voltage-Dependent Calcium Channels. *Journal of Neurophysiology* **78**: 1-9.

Cox, D. H. (2005). The BK_{Ca} Channel's Ca^{2+}-Binding Sites, Multiple Sites, Multiple Ions. *Journal of General Physiology* **125**: 253-255.

Cui, J. and Aldrich, R. W. (2000). Allosteric Linkage between Voltage and Ca^{2+}-Dependent Activation of BK-Type *mSlo*1 K^+ Channels. *Biochemistry* **39**: 15612-15619.

De Kloet, E. R., Vreugdenhil, E., Oitzl, M. S. and Joels, M. (1998). Brain Corticosteroid Receptor Balance in Health and Disease. *Endocrine Reviews* **19**: 269-301.

Diaz, L., Meera, P., Amigo, J., Stefani, E., Alvarez, O., Toro, L. and Latorre, R. (1998). Role of the S4 Segment in a Voltage-Dependent Calcium-Sensitive Potassium (*hSlo*) Channel. *Journal of Biological Chemistry* **273**: 32430-32436.

Dimitropoulou, C., White, R. E., Ownby, D. R. and Catravas, J. D. (2005). Estrogen Reduces Carbachol-Induced Constriction of Asthmatic Airways by Stimulating Large-Conductance Voltage and Calcium-Dependent Potassium Channels. *American Journal of Respiratory Cell and Molecular Biology* **32**: 239-247.

Djonov, V., Andres, A.-C. and Ziemiecki, A. (2001). Vascular Remodelling During the Normal and Malignant Life Cycle of the Mammary Gland. *Microscopy Research and Technique* **52**: 182-189.

Dopico, A. M., Widmer, H., Wang, G., Lemos, J. R. and Treistman, S. N. (1999). Rat Supraoptic Magnocellular Neurones Show Distinct Large Conductance, Ca^{2+}-Activated K^+ Channel Subtypes in Cell Bodies Versus Nerve Endings. *Journal of Physiology (London)* **519**: 101-114.

Dorak, M. T. (2005). Real-Time PCR. *http://dorakmt.tripod.com/genetics/realtime.html*

Downs, K. M. and Davies, T. (1993). Staging of Gastrulating Mouse Embryos by Morphological Landmarks in the Dissecting Microscope. *Development* **118**: 1255-1266.

Dryer, S. E. (1998). Role of Cell-Cell Interactions in the Developmental Regulation of Ca^{2+}-Activated K^+ Currents in Vertebrate Neurons. *Journal of Neurobiology* **37**: 23-36.

Du, W., Bautista, J. F., Yang, H., Diez-Sampedro, A., You, S.-A., Wang, L., Kotagal, P., Luders, H. O., Shi, J., Cui, J., Richerson, G. B. and Wang, Q. K. (2005). Calcium-Sensitive Potassium Channelopathy in Human Epilepsy and Paroxysmal Movement Disorder. *Nature Genetics* **37**: 733-738.

Duncan, R. K. (2005). Tamoxifen Alters Gating of the BK α Subunit and Mediates Enhanced Interactions with the Avian β Subunit. *Biochemical Pharmacology* **70**: 47-58.

Duncan, R. K. and Fuchs, P. A. (2003). Variation in Large-Conductance, Calcium-Activated Potassium Channels from Hair Cells Along the Chicken Basilar Papilla. *Journal of Physiology* **547**: 357-371.

Edgerton, J. R. and Reinhart, P. H. (2003). Distinct Contributions of Small and Large Conductance Ca^{2+}-Activated K^+ Channels to Rat Purkinje Neuron Function. *Journal of Physiology (London)* **548**: 53-69.

Eghbali, M., Toro, L. and Stefani, E. (2003). Diminished Surface Clustering and Increased Perinuclear Accumulation of Large Conductance Ca^{2+}-Activated K^+ Channel in Mouse Myometrium with Pregnancy. *Journal of Biological Chemistry* **278**: 45311-45317.

Epstein, D. J., Marti, E., Scott, M. P. and McMahon, A. P. (1996). Antagonizing cAMP-Dependent Protein Kinase A in the Dorsal CNS Activates a Conserved Sonic Hedgehog Signalling Pathway. *Development* **122**: 2885-2894.

Erxleben, C., Everhart, A. L., Romeo, C., Florance, H., Bauer, M. B., Alcorta, D. A., Rossie, S., Shipston, M. J. and Armstrong, D. L. (2002). Interacting Effects of N-Terminal Variation and STREX Exon Splicing on *Slo* Potassium Channel Regulation by Calcium, Phosphorylation, and Oxidation. *Journal of Biological Chemistry* **227**: 27045–27052.

Fernández-Fernández, J. M., Tomás, M., Vázquez, E., Orio, P., Latorre, R., Sentí, M., Marrugat, J. and Valverde, M. A. (2004). Gain-of-Function Mutation in the KCNMB1 Potassium Channel Subunit is Associated with Low Prevalence of Diastolic Hypertension. *Journal of Clinical Investigation* **113**: 1032-1039.

Fettiplace, R. and Fuchs, P. A. (1999). Mechanisms of Hair Cell Tuning. *Annual Review of Physiology* **61**: 809-834.

Fong, N., Bird, G., Vigneron, M. and Bentley, D. L. (2003). A 10 Residue Motif at the C-Terminus of the RNA Pol II CTD is Required for Transcription, Splicing and 3' End Processing. *EMBO Journal* **22**: 4274-4282.

Forster, T. (1948). Zwischemolekulare Energiewanderung Und Fluoreszenz. *Annalen der Physik* **2**: 55-67.

Frech, M. S., Halama, E. D., Tilli, M. T., Singh, B., Gunther, E. J., Chodosh, L. A., Flaws, J. A. and Furth, P. A. (2005). Deregulated Estrogen Receptor α Expression in Mammary Epithelial Cells of Transgenic Mice Results in the Development of Ductal Carcinoma in Situ. *Cancer Research* **65**: 681-685.

Fuchs, E., Flugge, G., Ohl, F., Lucassen, P., Vollmann-Honsdorf, G. K. and Michaelis, T. (2001). Psychosocial Stress, Glucocorticoids, and Structural Alterations in the Tree Shrew Hippocampus. *Physiology & Behavior* **73**: 285-291.

Furuta, Y., Piston, D. W. and Hogan, B. L. (1997). Bone Morphogenetic Proteins (Bmps) as Regulators of Dorsal Forebrain Development. *Development* **124**: 2203-2212.

Gavin, P., Devenish, R. J. and Prescott, M. (2002). An Approach for Reducing Unwanted Oligomerisation of DsRed Fusion Proteins. *Biochemical and Biophysical Research Communications* **298**: 707-713.

Ghoumari, A. M., Ibanez, C., El-Etr, M., Leclerc, P., Eychenne, B., O'Malley, B. W., Baulieu, E. E. and Schumacher, M. (2003). Progesterone and its Metabolites Increase Myelin Basic Protein Expression in Organotypic Slice Cultures of Rat Cerebellum. *Journal of Neurochemistry* **86**: 848-859.

Giulietti, A., Overbergh, L., Valckx, D., Decallonne, B., Bouillon, R. and Mathieu, C. (2001). An Overview of Real-Time Quantitative PCR: Applications to Quantify Cytokine Gene Expression. *Elsevier Science Methods* **25**: 386-401.

Gong, L.-W., Gao, T.-M., Huang, H. and Tong, Z. (2001). Properties of Large Conductance Calcium-Activated Potassium Channels in Pyramidal Neurons from the Hippocampal CA1 Region of Adult Rats. *Japanese Journal of Physiology* **51**: 725-731.

Gong, X. D., Li, J. C. H., Leung, G. P. H., Cheung, K. H. and Wong, P. Y. D. (2002). A BK_{Ca} to Kv Switch During Spermatogenesis in the Rat Seminiferous Tubules. *Biology of Reproduction* **67**: 46-54.

Gribkoff, V. K., Starrett, J. E., Jr. and Dworetzky, S. I. (2001). Maxi-K Potassium Channels: Form, Function, and Modulation of a Class of Endogenous Regulators of Intracellular Calcium. *Neuroscientist* **7**: 166-177.

Grove, E. A. and Fukuchi-Shimogori, T. (2003). Generating the Cerebral Cortical Area Map. *Annual Review of Neuroscience* **26**: 355-380.

Grumolato, L., Louiset, E., Alexandre, D., Ait-Ali, D., Turquier, V., Fournier, A., Fasolo, A., Vaudry, H. and Anouar, Y. (2003). PACAP and NGF Regulate Common and Distinct Traits of the Sympathoadrenal Lineage: Effects on Electrical Properties, Gene Markers and Transcription Factors in Differentiating PC12 Cells. *European Journal of Neuroscience* **17**: 71-82.

Grunnet, M. and Kaufmann, W. A. (2004). Coassembly of Big Conductance Ca^{2+}-Activated K^+ Channels and L-Type Voltage-Gated Ca^{2+} Channels in Rat Brain. *Journal of Biological Chemistry* **279**: 36445-36453.

Hafidi, A., Beurg, M., and Dulon, D. (2005). Localization and developmental expression of BK channels in mammalian cochlear hair cells. *Neuroscience* **130**: 475-484.

Hanaoka, K., Wright, J. M., Cheglakov, I. B., Morita, T. and Guggino, W. B. (1999). A 59 Amino Acid Insertion Increases Ca^{2+} Sensitivity of *RbSlo1*, a Ca^{2+}-Activated K^+ Channel in Renal Epithelia. *Journal of Membrane Biology* **172**: 193-201.

Herman, J. P. and Cullinan, W. E. (1997). Neurocircuitry of Stress: Central Control of the Hypothalamo-Pituitary- Adrenocortical Axis. *Trends in Neurosciences* **20**: 78-84.

Herrera, G. M., Etherton, B., Nausch, B. and Nelson, M. T. (2005). Negative Feedback Regulation of Nerve-Mediated Contractions by K_{Ca} Channels in Mouse Urinary Bladder Smooth Muscle. *American Journal of Physiology. Regulatory, Integrative and Comparative Physiology* **289**: R402-409.

Hu, H., Shao, L.-R., Chavoshy, S., Gu, N., Trieb, M., Behrens, R., Laake, P., Pongs, O., Knaus, H. G., Ottersen, O. P. and Storm, J. F. (2001). Presynaptic Ca^{2+}-Activated K^+ Channels in Glutamatergic Hippocampal Terminals and Their Role in Spike Repolarization and Regulation of Transmitter Release. *Journal of Neuroscience* **21**: 9585-9597.

Hu, S., Labuda, M. Z., Pandolfo, M., Goss, G. G., Mcdermid, H. E. and Ali, D. W. (2003). Variants of the KCNMB3 Regulatory Subunit of Maxi BK Channels Affect Channel Inactivation. *Physiological Genomics* **15**: 191-198.

Hua, J. Y., Smear, M. C., Baier, H. and Smith, S. J. (2005). Regulation of Axon Growth in Vivo by Activity-Based Competition. *Nature* **434**: 1022-1026.

Hulme, J. T., Ahn, M., Hauschka, S. D., Scheuer, T. and Catterall, W. A. (2002). A Novel Leucine Zipper Targets AKAP15 and Cyclic AMP-Dependent Protein Kinase to the C Terminus of the Skeletal Muscle Ca^{2+} Channel and Modulates its Function. *Journal of Biological Chemistry* **277**: 4079-4087.

James, A. F. and Okada, Y. (1994). Maxi K^+ Channels from the Apical Membranes of Rabbit Oviduct Epithelial Cells. *Journal of Membrane Biology* **137**: 109-118.

Jarov, A., Williams, K. P., Ling, L. E., Koteliansky, V. E., Duband, J. L. and Fournier-Thibault, C. (2003). A Dual Role for Sonic Hedgehog in Regulating Adhesion and Differentiation of Neuroepithelial Cells. *Developmental Biology* **261**: 520-536.

Jiang, Y., Pico, A., Cadene, M., Chait, B. T. and Mackinnon, R. (2001). Structure of the RCK Domain from the E. Coli K^+ Channel and Demonstration of its Presence in the Human BK Channel. *Neuron* **29**: 593-601.

Jiang, Z., Wallner, M., Meera, P. and Toro, L. (1999). Human and Rodent MaxiK Channel β-Subunit Genes: Cloning and Characterization. *Genomics* **55**: 57-67.

Jimenez-Gonzalez, C., Mclaren, G. J. and Dale, N. (2003). Development of Ca^{2+}-Channel and BK-Channel Expression in Embryos and Larvae of Xenopus Laevis. *European Journal of Neuroscience* **18**: 2175-2187.

Joiner, W. J., Basavappa, S., Vidyasagar, S., Nehrke, K., Krishnan, S., Binder, H. J., Boulpaep, E. L. and Rajendran, V. M. (2003). Active K^+ Secretion through Multiple K_{Ca}-Type Channels and Regulation by IK_{Ca} Channels in Rat Proximal Colon. *American Journal of Physiology. Gastrointestinal and Liver Physiology* **285**: G185-196.

Jones, H. M., Hamilton, K. L., Papworth, G. D., Syme, C. A., Watkins, S. C., Bradbury, N. A. and Devor, D. C. (2004). Role of the NH2 Terminus in the Assembly and Trafficking of the Intermediate Conductance Ca^{2+}-Activated K^+ Channel hIK1. *Journal of Biological Chemistry* **279**: 15531-15540.

Jovanovic, S., Crawford, R. M., Ranki, H. J. and Jovanovic, A. (2003). Large Conductance Ca^{2+}-Activated K^+ Channels Sense Acute Changes in Oxygen Tension in Alveolar Epithelial Cells. *American Journal of Respiratory Cell and Molecular Biology* **28**: 363-372.

Jurica, M. S. and Moore, M. J. (2003). Pre-mRNA Splicing: Awash in a Sea of Proteins. *Molecular cell* **12**: 5-14.

Kalantaridou, S. N., Makrigiannakis, A., Zoumakis, E. and Chrousos, G. P. (2004). Stress and the Female Reproductive System. *Journal of Reproductive Immunology* **62**: 61-68.

Kalinichev, M., Easterling, K. W., Plotsky, P. M. and Holtzman, S. G. (2002). Long-Lasting Changes in Stress-Induced Corticosterone Response and Anxiety-Like Behaviors as a Consequence of Neonatal Maternal Separation in Long-Evans Rats. *Pharmacology, Biochemistry, and Behaviour* **73**: 131-140.

Kang, J., Huguenard, J. R. and Prince, D. A. (1996). Development of BK Channels in Neocortical Pyramidal Neurons. *Journal of Neurophysiology* **76**: 188-198.

Katsuki, H., Shinohara, A., Fujimoto, S., Kume, T. and Akaike, A. (2005). Tetraethylammonium Exacerbates Ischemic Neuronal Injury in Rat Cerebrocortical Slice Cultures. *European Journal of Pharmacology* **508**: 85-91.

Khot, S. and Ghaskadbi, S. (2001). FGF Signalling is Essential for the Early Events in the Development of the Chick Nervous System and Mesoderm. *International Journal of Developmental Biology* **45**: 877-885.

Kidd, I. M., Clark, D. A. and Emery, V. C. (2000). A Non-Radioisotopic Quantitative Competitive Polymerase Chain Reaction Method: Application in Measurement of Human Herpesvirus 7 Load. *Journal of Virological Methods* **87**: 177-181.

Knaus, H. G., Folander, K., Garcia-Calvo, M., Garcia, M. L., Kaczorowski, G. J., Smith, M. and Swanson, R. (1994). Primary Sequence and Immunological Characterization of Beta-Subunit of High Conductance Ca^{2+}-Activated K^+ Channel from Smooth Muscle. *Journal of Biological Chemistry* **269**: 17274-17278.

Knaus, H. G., Schwarzer, C., Koch, R. O., Eberhart, A., Kaczorowski, G. J., Glossmann, H., Wunder, F., Pongs, O., Garcia, M. L. and Sperk, G. (1996). Distribution of High-Conductance Ca^{2+}-Activated K^+ Channels in Rat Brain: Targeting to Axons and Nerve Terminals. *Journal of Neuroscience* **16**: 955-963.

Knuth, E. D., and Etgen, A. M. (2005) Corticosterone secretion induced by chronic isolation in neonatal rats is sexually dimorphic and accompanied by elevated ACTH. *Hormones and Behaviour* **47**: 65-75

Komuro, H. and Rakic, P. (1996). Intracellular Ca^{2+} Fluctuations Modulate the Rate of Neuronal Migration. *Neuron* **17**: 275-285.

Kornblihtt, A. R., Mata, M. D. L., Fededa, J. P., Muñoz, M. J. and Nogués, G. (2004). Multiple Links between Transcription and Splicing. *RNA* **10**: 1489–1498.

Kraft, R., Krause, P., Jung, S., Basrai, D., Liebmann, L., Bolz, J. R. and Patt, S. (2003). BK Channel Openers Inhibit Migration of Human Glioma Cells. *Pflugers Archiv. European Journal of Physiology* **446**: 248-255.

Kristian, T. and Siesjo, B. K. (1998). Calcium in Ischemic Cell Death. *Stroke* **29**: 705-718.

Kudielka, B. M. and Kirschbaum, C. (2005). Sex Differences in HPA Axis Responses to Stress: A Review. *Biological Psychology* **69**: 113-132.

Kukuljan, M., Taylor, A., Chouinard, H., Olguin, P., Rojas, C. V. and Ribera, A. B. (2003). Selective Regulation of *xSlo* Splice Variants During *Xenopus* Embryogenesis. *Journal of Neurophysiology* **90**: 3352-3360.

Kumada, T. and Komuro, H. (2004). Completion of Neuronal Migration Regulated by Loss of Ca^{2+} Transients. *Proceedings of the National Academy of Sciences USA* **101**: 8479-8484.

Kunz, L., Thalhammer, A., Berg, F. D., Berg, U., Duffy, D. M., Stouffer, R. L., Dissen, G. A., Ojeda, S. R. and Mayerhofer, A. (2002). Ca^{2+}-Activated, Large Conductance K^+ Channel in the Ovary: Identification, Characterization, and Functional Involvement in Steroidogenesis. *Journal of Clinical Endocrinology and Metabolism* **87**: 5566-5574.

Kwok, S., Kellogg, D. E., Mckinney, N., Spasic, D., Godal, L., Levenson, C. and Sninsky, J. J. (1990). Effects of Primer - Template Mismatches on the Polymerase Chain Reaction: Human Immunodeficiency Virus Type 1 Model Studies. *Nucleic Acids Research* **18**: 999-1005.

Kwon, S.-H. and Guggino, W. B. (2004). Multiple Sequences in the C Terminus of MaxiK Channels Are Involved in Expression, Movement to the Cell Surface, and Apical Localization. *Proceedings of the National Academy of Sciences USA* **101**: 15237-15242.

Lai, G.-J. and McCobb, D. P. (2002). Opposing Actions of Adrenal Androgens and Glucocorticoids on Alternative Splicing of *Slo* Potassium Channels in Bovine Chromaffin Cells. *Proceedings of the National Academy of Sciences USA* **99**: 7722-7727.

Lam, R. S., Shaw, A. R. and Duszyk, M. (2004). Membrane Cholesterol Content Modulates Activation of BK Channels in Colonic Epithelia. *Biochimica et Biophysica acta* **1667**: 241-248.

Langer, P. Grunder, S. and Rüsch, A. (2003). Expression of Ca^{2+}-Activated BK Channel mRNA and its Splice Variants in the Rat Cochlea. *The Journal of Comparative Neurology* **455**: 198-209.

Lauf, U., Lopez, P. and Falk, M. M. (2001). Expression of Fluorescently Tagged Connexins: A Novel Approach to Rescue Function of Oligomeric DsRed-Tagged Proteins. *FEBS Letters* **498**: 11-15.

Lemaire, P. and Kodjabachian, L. (1996). The Vertebrate Organizer: Structure and Molecules. *Trends in Genetics* **12**: 525-531.

Lenczowski, M. J. P., Schmidt, E. D., Van Dam, A. M., Gaykema, R. P. A. and Tilders, F. J. H. (1998). Individual Variation in Hypothalamus-Pituitary-Adrenal Responsiveness of Rats to Endotoxin and Interleukin-1β. *Annals of the New York Academy of Sciences* **856**: 139-147.

Lhuillier, L. and Dryer, S. E. (2002). Developmental Regulation of Neuronal K_{Ca} Channels by TGFbeta 1: An Essential Role for PI3 Kinase Signalling and Membrane Insertion. *Journal of Neurophysiology* **88**: 954-964.

Li, W. and Aldrich, R. W. (2004). Unique Inner Pore Properties of BK Channels Revealed by Quaternary Ammonium Block. *Journal of General Physiology* **124**: 43-57.

Lim, M. C., Shipston, M. J. and Antoni, F. A. (1998). Depolarization Counteracts Glucocorticoid Inhibition of Adenohypophysical Corticotroph Cells. *British Journal of Pharmacology* **124**: 1735-1743.

Lin, M. T., Longo, L. D., Pearce, W. J. and Hessinger, D. A. (2005). Ca^{2+}-Activated K^+ Channel-Associated Phosphatase and Kinase Activities During Development. *American Journal of Physiology. Heart and Circulatory Physiology* **289**: H414-425.

Lingle, C. J., Solaro, C. R., Prakriya, M., Ding, J. P (1996). Calcium-Activated Potassium Channels in Adrenal Chromaffin Cells. *Ion Channels* **4**:261-301

Lingle, C. J., Zeng, X.-H., Ding, J. P. and Xia, X.-M. (2001). Inactivation of BK Channels Mediated by the NH2 Terminus of the β3b Auxiliary Subunit Involves a Two-Step Mechanism: Possible Separation of Binding and Blockade. *Journal of General Physiology* **117**: 583-606.

Linthorst, A. C. E., Flachskamm, C., Barden, N., Holsboer, F. and Reul, J. M. H. M. (2000). Glucocorticoid Receptor Impairment Alters CNS Responses to a Psychological Stressor: An in Vivo Microdialysis Study in Transgenic Mice. *European Journal of Neuroscience* **12**: 283-291.

Liu, A. and Joyner, A. L. (2001). Early Anterior/Posterior Patterning of the Midbrain and Cerebellum. *Annual Review of Neuroscience* **24**: 869-896.

Liu, G., Shi, J., Yang, L., Cao, L., Park, S. M., Cui, J. and Marx, S. O. (2004). Assembly of a Ca^{2+}-Dependent BK Channel Signalling Complex by Binding to Beta 2 Adrenergic Receptor. *EMBO Journal* **23**: 2196-2205.

Liu, X., Chang, Y., Reinhart, P. H. and Sontheimer, H. (2002). Cloning and Characterization of Glioma BK, a Novel BK Channel Isoform Highly Expressed in Human Glioma Cells. *Journal of Neuroscience* **22**: 1840-1849.

Livak, K. J. (1999). Allelic Discrimination Using Fluorogenic Probes and the 5' Nuclease Assay. *Genetic Analysis: Biomolecular Engineering* **14**: 143-149.

Livak, K. J., Flood, S. J., Marmaro, J., Giusti, W. and Deetz, K. (1995). Oligonucleotides with Fluorescent Dyes at Opposite Ends Provide a Quenched Probe System Useful for Detecting PCR Product and Nucleic Acid Hybridization. *PCR Methods and Applications* **4**: 357-362.

Lovell, P. V., James, D. G. and McCobb, D. P. (2000). Bovine Versus Rat Adrenal Chromaffin Cells: Big Differences in BK Potassium Channel Properties. *Journal of Neurophysiology* **83**: 3277-3286.

Lovell, P. V., King, J. T. and McCobb, D. P. (2004). Acute Modulation of Adrenal Chromaffin Cell BK Channel Gating and Cell Excitability by Glucocorticoids. *Journal of Neurophysiology* **91**: 561-570.

Lovell, P. V. and McCobb, D. P. (2001). Pituitary Control of BK Potassium Channel Function and Intrinsic Firing Properties of Adrenal Chromaffin Cells. *Journal of Neuroscience* **21**: 3429-3442.

Ma, D., Zerangue, N., Raab-Graham, K., Fried, S. R., Jan, Y. N. and Jan, L. Y. (2002). Diverse Trafficking Patterns Due to Multiple Traffic Motifs in G Protein-Activated Inwardly Rectifying Potassium Channels from Brain and Heart. *Neuron* **33**: 715-729.

Mackinnon, R. (2003). Potassium Channels. *FEBS Letters* **555**: 62-65.

Mahmoud, S. F., Bezzerides, A. L., Riba, R., Lai, G.-J., Lovell, P. V., Hara, Y. and McCobb, D. P. (2002). Accurate Quantitative RT-PCR for Relative Expression of *Slo* Splice Variants. *Journal of Neuroscience Methods* **115**: 189-198.

Mahmoud, S. F. and McCobb, D. P. (2004). Regulation of *Slo* Potassium Channel Alternative Splicing in the Pituitary by Gonadal Testosterone. *Journal of Neuroendocrinology* **16**: 237-243.

Marquardt, T. and Helenius, A. (1992). Misfolding and Aggregation of Newly Synthesized Proteins in the Endoplasmic Reticulum. *Journal of Cell Biology* **117**: 505-513.

Marrion, N. V. and Tavalin, S. J. (1998). Selective Activation of Ca^{2+}-Activated K^+ Channels by Co-Localized Ca^{2+} Channels in Hippocampal Neurons. *Nature* **395**: 900-905.

Martin-Caraballo, M. and Dryer, S. E. (2002). Activity- and Target-Dependent Regulation of Large-Conductance Ca^{2+}-Activated K^+ Channels in Developing Chick Lumbar Motoneurons. *Journal of Neuroscience* **22**: 73-81.

Marty, A. (1981). Ca-Dependent K Channels with Large Unitary Conductance in Chromaffin Cell Membranes. *Nature* **291**: 497-500.

Mason, G., Provero, P., Vaira, A. M. and Accotto, G. P. (2002). Estimating the Number of Integrations in Transformed Plants by Quantitative Real-Time PCR. *Biomed Central Biotechnology* **2**: 20.

Mathialahan, T., Maclennan, K. A., Sandle, L. N., Verbeke, C. and Sandle, G. I. (2005). Enhanced Large Intestinal Potassium Permeability in End-Stage Renal Disease. *Journal of Pathology* **206**: 46-51.

McCobb, D. P., Fowler, N. L., Featherstone, T., Lingle, C. J., Saito, M., Krause, J. E. and Salkoff, L. (1995). A Human Calcium-Activated Potassium Channel Gene Expressed in Vascular Smooth Muscle. *American Journal of Physiology. Heart and Circulatory Physiology* **269**: H767-777.

McCobb, D. P., Hara, Y., Lai, G.-J., Mahmoud, S. F. and Flugge, G. (2003). Subordination Stress Alters Alternative Splicing of the *Slo* Gene in Tree Shrew Adrenals. *Hormones and Behaviour* **43**: 180-186.

McEwen, B. S. (2001). Plasticity of the Hippocampus: Adaptation to Chronic Stress and Allostatic Load. *Annals of the New York Academy of Sciences* **933**: 265-277.

McManus, O. B. (1991). Calcium-Activated Potassium Channels: Regulation by Calcium. *Journal of Bioenergetics and Biomembranes* **23**: 537-560.

Meera, P., Wallner, M., Song, M. and Toro, L. (1997). Large Conductance Voltage- and Calcium-Dependent K^+ Channel, a Distinct Member of Voltage-Dependent Ion Channels with Seven N-Terminal Transmembrane Segments (S0-S6), an Extracellular N Terminus, and an Intracellular (S9-S10) C terminus. *Proceedings of the National Academy of Sciences USA* **94**: 14066-14071.

Meera, P., Wallner, M. and Toro, L. (2000). A Neuronal Beta Subunit (KCNMB4) Makes the Large Conductance, Voltage- and Ca^{2+}-Activated K^+ Channel Resistant to Charybdotoxin and Iberiotoxin. *Proceedings of the National Academy of Sciences USA* **97**: 5562-5567.

Meijer, O. C., De Lange, E. C. M., Breimer, D. D., De Boer, A. G., Workel, J. O. and De Kloet, E. R. (1998). Penetration of Dexamethasone into Brain Glucocorticoid Targets is Enhanced in Mdr1a P-Glycoprotein Knockout Mice. *Endocrinology* **139**: 1789-1793.

Meredith, A. L., Thorneloe, K. S., Werner, M. E., Nelson, M. T. and Aldrich, R. W. (2004). Overactive Bladder and Incontinence in the Absence of the BK Large Conductance Ca^{2+}-Activated K^+ Channel. *Journal of Biological Chemistry* **279**: 36746-36752.

Meyer, E. and Fromherz, P. (1999). Ca^{2+} Activation of *hSlo* K^+ Channel is Suppressed by N-Terminal GFP Tag. *European Journal of Neuroscience* **11**: 1105-1108.

Miranda, P., de la Peña, P., Gomez-Varela, D. and Barros, F. (2003). Role of BK Potassium Channels Shaping Action Potentials and the Associated $[Ca^{2+}]_i$ Oscillations in GH3 Rat Anterior Pituitary Cells. *Neuroendocrinology* 77: 162-176.

Mirescu, C., Peters, J. D. and Gould, E. (2004). Early Life Experience Alters Response of Adult Neurogenesis to Stress. *Nature* 7: 841-846.

Mirshahi, T. and Logothetis, D. E. (2002). GIRK Channel Trafficking: Different Paths for Different Family Members. *Molecular Interventions* **2**: 289-291.

Moreau, M. and Leclerc, C. (2004). The Choice between Epidermal and Neural Fate: A Matter of Calcium. *International Journal of Developmental Biology* **48**: 75-84.

Moreira, R. F. and Noren, C. J. (1995). Minimum Duplex Requirements for Restriction Enzyme Cleavage near the Termini of Linear DNA Fragments. *Biotechniques* **19**: 58-59.

Myers, M. P., Yang, J. and Stampe, P. (1999). Visualization and Functional Analysis of a Maxi-K Channel (*mSlo*) Fused to Green Fluorescent Protein (GFP). *Electronic Journal of Biotechnology* **2**: 140-151.

Nagayama, T., Yoshida, M., Suzuki-Kusaba, M., Hisa, H., Kimura, T. and Satoh, S. (1998). The Role of BK(Ca) Channels in the Nitric Oxide-Mediated Regulation of Adrenal Catecholamine Secretion. *European Journal of Pharmacology* **353**: 169-176.

Nelson, A. B., Krispel, C. M., Sekirnjak, C. and Du Lac, S. (2003). Long-Lasting Increases in Intrinsic Excitability Triggered by Inhibition. *Neuron* **40**: 609-620.

Nelson, M. T. and Bonev, A. D. (2004). The β1 Subunit of the Ca^{2+}-Sensitive K^+ Channel Protects against Hypertension. *Journal of Clinical Investigation* **113**: 955-957.

Nishimaru, K., Eghbali, M., Stefani, E. and Toro, L. (2004). Function and Clustered Expression of MaxiK Channels in Cerebral Myocytes Remain Intact with Aging. *Experimental Gerontology* **39**: 831-839.

Oberholtzer, J. C. (1999). Frequency Tuning of Cochlear Hair Cells by Differential Splicing of BK Channel Transcripts. *Journal of Physiology (London)* **518**: 629.

Orio, P., Rojas, P., Ferreira, G., Latorre, R. (2002). New Disguises for an Old Channel: MaxiK Channel β Subunits. *News in Physiological Sciences* **17**: 151-161.

Ortega, B., Millar, I. D., Beesley, A. H., Robson, L. and White, S. J. (2000). Stable, Polarised, Functional Expression of Kir1.1b Channel Protein in Madin-Darby Canine Kidney Cell Line. *Journal of Physiology (London)* **528**: 5-13.

Ottersen, O. P. (2005). Neurobiology: Sculpted by Competition. *Nature* **434**: 969.

Ottschytsch, N., Raes, A., Van Hoorick, D. and Snyders, D. J. (2002). Obligatory Heterotetramerization of Three Previously Uncharacterized Kv Channel Alpha-Subunits Identified in the Human Genome. *Proceedings of the National Academy of Sciences USA* **99**: 7986-7991.

Pareek, S., Notterpek, L., Snipes, G. J., Naef, R., Sossin, W., Laliberte, J., Iacampo, S., Suter, U., Shooter, E. M. and Murphy, R. A. (1997). Neurons Promote the Translocation of Peripheral Myelin Protein 22 into Myelin. *Journal of Neuroscience* **17**: 7754-7762.

Pavlides, C., Ogawa, S., Kimura, A. and McEwen, B. S. (1996). Role of Adrenal Steroid Mineralocorticoid and Glucocorticoid Receptors in Long-Term Potentiation in the CA1 Field of Hippocampal Slices. *Brain Research* **738**: 229-235.

Pedarzani, P., Kulik, A., Muller, M., Ballanyi, K. and Stocker, M. (2000). Molecular Determinants of Ca^{2+}-Dependent K^+ Channel Function in Rat Dorsal Vagal Neurones. *Journal of Physiology (London)* **527**: 283-290.

Piskorowski, R. and Aldrich, R. W. (2002). Calcium Activation of BK_{Ca} Potassium Channels Lacking the Calcium Bowl and RCK Domains. *Nature* **420**: 499-502.

Potter, B. A., Ihrke, G., Bruns, J. R., Weixel, K. M. and Weisz, O. A. (2004). Specific N-Glycans Direct Apical Delivery of Transmembrane, but Not Soluble or Glycosylphosphatidylinositol-Anchored Forms of Endolyn in Madin-Darby Canine Kidney Cells. *Molecular Biology of the Cell* **15**: 1407-1416.

Quirk, J. C. and Reinhart, P. H. (2001). Identification of a Novel Tetramerization Domain in Large Conductance K_{Ca} Channels. *Neuron* **32**: 13-23.

Raffaelli, G., Saviane, C., Mohajerani, M. H., Pedarzani, P. and Cherubini, E. (2004). BK Potassium Channels Control Transmitter Release at CA3-CA3 Synapses in the Rat Hippocampus. *Journal of Physiology (London)* **557**: 147-157.

Raucher, S. and Dryer, S. E. (1995). Target-Derived Factors Regulate the Expression of Ca^{2+}-Activated K^+ Currents in Developing Chick Sympathetic Neurones. *Journal of Physiology* **486**: 605-614.

Reeves, E. P., Lu, H., Jacobs, H. L., Messina, C. G. M., Bolsover, S., Gabella, G., Potma, E. O., Warley, A., Roes, J. and Segal, A. W. (2002). Killing Activity of Neutrophils is Mediated through Activation of Proteases by K^+ Flux. *Nature* **416**: 291-297.

Robitaille, R., Garcia, M. L., Kaczorowski, G. J. and Charlton, M. P. (1993). Functional Colocalization of Calcium and Calcium-Gated Potassium Channels in Control of Transmitter Release. *Neuron* **11**: 645-655.

Rosenbrock, H., Koros, E., Bloching, A., Podhorna, J. and Borsini, F. (2005). Effect of Chronic Intermittent Restraint Stress on Hippocampal Expression of Marker Proteins for Synaptic Plasticity and Progenitor Cell Proliferation in Rats. *Brain Research* **1040**: 55-63.

Rubenstein, J. L. R., Shimamura, K., Martinez, S. and Puelles, L. (1998). Regionalization of the Prosencephalic Neural Plate. *Annual Review of Neuroscience* **21**: 445-477.

Runden-Pran, E., Haug, F. M., Storm, J. F. and Ottersen, O. P. (2002). BK Channel Activity Determines the Extent of Cell Degeneration after Oxygen and Glucose Deprivation: A Study in Organotypical Hippocampal Slice Cultures. *Neuroscience* **112**: 277-288.

Safronov, B. V. and Vogel, W. (1998). Large Conductance Ca^{2+}-Activated K^+ Channels in the Soma of Rat Motoneurones. *Journal of Membrane Biology* **162**: 9-15.

Sah, P. (1996). Ca^{2+}-Activated K^+ Currents in Neurones: Types, Physiological Roles and Modulation. *Trends in Neurosciences* **19**: 150-154.

Saito, M., Nelson, C., Salkoff, L. and Lingle, C. J. (1997). A Cysteine-Rich Domain Defined by a Novel Exon in a *Slo* Variant in Rat Adrenal Chromaffin Cells and PC12 Cells. *Journal of Biological Chemistry* **272**: 11710-11717.

Sakamoto, H., Ukena, K. and Tsutsui, K. (2001). Effects of Progesterone Synthesized De Novo in the Developing Purkinje Cell on its Dendritic Growth and Synaptogenesis. *Journal of Neuroscience* **21**: 6221-6232.

Sausbier, M., Hu, H., Arntz, C., Feil, S., Kamm, S., Adelsberger, H., Sausbier, U., Sailer, C. A., Feil, R., Hofmann, F., Korth, M., Shipston, M. J., Knaus, H. G., Wolfer, D. P., Pedroarena, C. M., Storm, J. F. and Ruth, P. (2004). Cerebellar Ataxia and Purkinje Cell Dysfunction Caused by Ca^{2+}-Activated K^+ Channel Deficiency. *Proceedings of the National Academy of Sciences USA* **101**: 9474-9478.

Schams, D. and Berisha, B. (2002). Steroids as Local Regulators of Ovarian Activity in Domestic Animals. *Domestic Animal Endocrinology* **23**: 53-65.

Schreiber, M. and Salkoff, L. (1997). A Novel Calcium-Sensing Domain in the BK Channel. *Biophysical Journal* **73**: 1355-1363.

Schreiber, M., Yuan, A. and Salkoff, L. (1999). Transplantable Sites Confer Calcium Sensitivity to BK Channels. *Nature Neuroscience* **2**: 416-421.

Schubert, R. and Nelson, M. T. (2001). Protein Kinases: Tuners of the BK_{Ca} Channel in Smooth Muscle. *Trends in Pharmacological Sciences* **22**: 505-512.

Schwab, A., Reinhardt, J., Schneider, S. W., Gassner, B. and Schuricht, B. (1999). K^+ Channel-Dependent Migration of Fibroblasts and Human Melanoma Cells. *Cellular Physiology and Biochemistry* **9**: 126-132.

Seale, J. V., Wood, S. A., Atkinson, H. C., Bate, E., Lightman, S. L., Ingram,C. D., Jessop, D. S. and Harbuz, M. S. (2004). Gonadectomy Reverses the Sexually Diergic Patterns of Circadian and Stress-Induced Hypothalamic-Pituitary-Adrenal Axis Activity in Male and Female Rats. *Journal of Neuroendocrinology* **16**: 516-524

Seckl, J. R. and Meaney, M. J. (2004). Glucocorticoid Programming. *Annals of the New York Academy of Sciences* **1032**: 63-84.

Selleck, M. A., Garcia-Castro, M. I., Artinger, K. B. and Bronner-Fraser, M. (1998). Effects of Shh and Noggin on Neural Crest Formation Demonstrate That BMP is Required in the Neural Tube but Not Ectoderm. *Development* **125**: 4919-4930.

Sheu, S.-J., Wu, S.-N., Hu, D.-N. and Chen, J.-F. (2004). The Influence of Hypotonicity on Large-Conductance Calcium-Activated Potassium Channels in Human Retinal Pigment Epithelial Cells. *Journal of Ocular Pharmacology and Therapeutics* **20**: 563-575.

Shipston, M. J. (2001). Alternative Splicing of Potassium Channels: A Dynamic Switch of Cellular Excitability. *Trends in Cell Biology* **11**: 353-358.

Shipston, M. J., Duncan, R. R., Clark, A. G., Antoni, F. A. and Tian, L. (1999). Molecular Components of Large Conductance Calcium-Activated Potassium (BK) Channels in Mouse Pituitary Corticotropes. *Molecular Endocrinology* **13**: 1728-1737.

Shipston, M. J., Kelly, J. S. and Antoni, F. A. (1996). Glucocorticoids Block Protein Kinase A Inhibition of Calcium-Activated Potassium Channels. *Journal of Biological Chemistry* **271**: 9197-9200.

Shors, T. J., Levine, S. and Thompson, R. F. (1990). Effect of Adrenalectomy and Demedullation on the Stress-Induced Impairment of Long-Term Potentiation. *Neuroendocrinology* **51**: 70-75.

Simerly, R. B. (2002). Wired for Reproduction: Organization and Development of Sexually Dimorphic Circuits in the Mammalian Forebrain. *Annual Review of Neuroscience* **25**: 507-536.

Skinner, L. J., Enee, V., Beurg, M., Jung, H. H., Ryan, A. F., Hafidi, A., Aran, J.-M. and Dulon, D. (2003). Contribution of BK Ca^{2+}-Activated K^+ Channels to Auditory Neurotransmission in the Guinea Pig Cochlea. *Journal of Neurophysiology* **90**: 320-332.

Sohma, Y., Harris, A., Wardle, C. J., Gray, M. A. and Argent, B. E. (1994). Maxi K^+ Channels on Human Vas Deferens Epithelial Cells. *Journal of Membrane Biology* **141**: 69-82.

Song, M., Zhu, N., Olcese, R., Barila, B., Toro, L. and Stefani, E. (1999). Hormonal Control of Protein Expression and mRNA Levels of the MaxiK Channel α-Subunit in Myometrium. *FEBS Letters* **460**: 427-432.

Sousa, R. J., Tannery, N. H. and Lafer, E. M. (1989). In Situ Hybridization Mapping of Glucocorticoid Receptor Messenger Ribonucleic Acid in Rat Brain. *Molecular Endocrinology* **3**: 481-494.

Spitzer, N. C. and Ribera, A. B. (1998). Development of Electrical Excitability in Embryonic Neurons: Mechanisms and Roles. *Journal of Neurobiology* **37**: 190-197.

Standen, N. B. and Quayle, J. M. (1998). K^+ Channel Modulation in Arterial Smooth Muscle. *Acta Physiologica Scandinavica* **164**: 549-557.

Strang, C., Cushman, S. J., Derubeis, D., Peterson, D. and Pfaffinger, P. J. (2001). A Central Role for the T1 Domain in Voltage-Gated Potassium Channel Formation and Function. *Journal of Biological Chemistry* **276**: 28493-28502.

Sun, Q. Q. and Dale, N. (1998). Rapid Report: Developmental Changes in Expression of Ion Currents Accompany Maturation of Locomotor Pattern in Frog Tadpoles. *Journal of Physiology (London)* **507**: 257-264.

Swan, D. C., Tucker, R. A., Holloway, B. P. and Icenogle, J. P. (1997). A Sensitive, Type-Specific, Fluorogenic Probe Assay for Detection of Human Papillomavirus DNA. *Journal of Clinical Microbiology* **35**: 886-891.

Takeuchi, S., Marcus, D. C. and Wangemann, P. (1992). Ca^{2+}-Activated Nonselective Cation, Maxi K^+ and Cl^- Channels in Apical Membrane of Marginal Cells of Stria Vascularis. *Hearing Research* **61**: 86-96.

Tang, X. D., Daggett, H., Hanner, M., Garcia, M. L., McManus, O. B., Brot, N., Weissbach, H., Heinemann, S. H. and Hoshi, T. (2001). Oxidative Regulation of Large Conductance Calcium-Activated Potassium Channels. *Journal of General Physiology*. **117**: 253-274.

Tian, L., Coghill, L. S., Macdonald, S. H. F., Armstrong, D. L. and Shipston, M. J. (2003). Leucine Zipper Domain Targets cAMP-Dependent Protein Kinase to Mammalian BK Channels. *Journal of Biological Chemistry* **278**: 8669-8677.

Tian, L., Coghill, L. S., McClafferty, H., Macdonald, S. H. F., Antoni, F. A., Ruth, P., Knaus, H.-G. and Shipston, M. J. (2004). Distinct Stoichiometry of BK_{Ca} Channel Tetramer Phosphorylation Specifies Channel Activation and Inhibition by cAMP-Dependent Protein Kinase. *Proceedings of the National Academy of Sciences USA* **101**: 11897-11902.

Tian, L., Hammond, M. S. L., Florance, H., Antoni, F. A. and Shipston, M. J. (2001a). Alternative Splicing Determines Sensitivity of Murine Calcium-Activated Potassium Channels to Glucocorticoids. *Journal of Physiology (London)* **537**: 57-68.

Tian, L., Duncan, R. R., Hammond, M. S. L., Coghill, L. S., Wen, H., Rusinova, R., Clark, A. G., Levitan, I. B. and Shipston, M. J. (2001b). Alternative Splicing Switches Potassium Channel Sensitivity to Protein Phosphorylation. *Journal of Biological Chemistry* **276**: 7717-7720.

Tian, L., Knaus, H.-G. and Shipston, M. J. (1998). Glucocorticoid Regulation of Calcium-Activated Potassium Channels Mediated by Serine/Threonine Protein Phosphatase. *Journal of Biological Chemistry* **273**: 13531-13536.

Toro, L., Wallner, M., Meera, P. and Tanaka, Y. (1998). Maxi-K_{Ca}, a Unique Member of the Voltage-Gated K Channel Superfamily. *News in Physiological Sciences* **13**: 112-117.

Tsutsui, K., Sakamoto, H., Shikimi, H. and Ukena, K. (2004). Organizing Actions of Neurosteroids in the Purkinje Neuron. *Neuroscience Research* **49**: 273-279.

Vagin, O., Turdikulova, S. and Sachs, G. (2004). The H,K-ATPase β Subunit as a Model to Study the Role of N-Glycosylation in Membrane Trafficking and Apical Sorting. *Journal of Biological Chemistry* **279**: 39026-39034.

Valles, A., Marti, O. and Armario, A. (2003). Long-Term Effects of a Single Exposure to Immobilization Stress on the Hypothalamic-Pituitary-Adrenal Axis: Transcriptional Evidence for a Progressive Desensitization Process. *European Journal of Neuroscience* **18**: 1353-1361.

Van Goor, F., Li, Y.-X. and Stojilkovic, S. S. (2001). Paradoxical Role of Large-Conductance Calcium-Activated K^+ (BK) Channels in Controlling Action Potential-Driven Ca^{2+} Entry in Anterior Pituitary Cells. *Journal of Neuroscience* **21**: 5902-5915.

Vaudry, D., Stork, P. J. S., Lazarovici, P. and Eiden, L. E. (2002). Signalling Pathways for PC12 Cell Differentiation: Making the Right Connections. *Science* **296**: 1648-1649.

Veenema, A. H., Koolhaas, J. M. and De Kloet, E. R. (2004). Basal and Stress-Induced Differences in HPA Axis, 5-HT Responsiveness, and Hippocampal Cell Proliferation in Two Mouse Lines. *Annals of the New York Academy of Sciences* **1018**: 255-265.

Vega-Salas, D. E., Salas, P. J., Gundersen, D. and Rodriguez-Boulan, E. (1987). Formation of the Apical Pole of Epithelial (Madin-Darby Canine Kidney) Cells: Polarity of an Apical Protein is Independent of Tight Junctions While Segregation of a Basolateral Marker Requires Cell-Cell Interactions. *Journal of Cell Biology* **104**: 905-916.

Vergara, C., Latorre, R., Marrion, N. V. and Adelman, J. P. (1998). Calcium-Activated Potassium Channels. *Current Opinion in Neurobiology* **8**: 321-329.

Viau, V. (2002). Functional Cross-Talk between the Hypothalamic-Pituitary-Gonadal and -Adrenal Axes. *Journal of Neuroendocrinology* **14**: 506-513.

Wallner, M., Meera, P. and Toro, L. (1996). Determinant for Beta -Subunit Regulation in High-Conductance Voltage-Activated and Ca^{2+}-Sensitive K^+ Channels: An Additional Transmembrane Region at The N terminus. *Proceedings of the National Academy of Sciences USA* **93**: 14922-14927.

Wang, S.-X., Ikeda, M. and Guggino, W. B. (2003). The Cytoplasmic Tail of Large Conductance, Voltage- and Ca^{2+}-Activated K^+ (MaxiK) Channel is Necessary for its Cell Surface Expression. *Journal of Biological Chemistry* **278**: 2713-2722.

Wang, S. Y., Yoshino, M., Sui, J. L., Wakui, M., Kao, P. N. and Kao, C. Y. (1998). Potassium Currents in Freshly Dissociated Uterine Myocytes from Nonpregnant and Late-Pregnant Rats. *Journal of General Physiology* **112**: 737-756.

Wang, T. and Brown, M. J. (1999). mRNA Quantification by Real Time Taqman Polymerase Chain Reaction: Validation and Comparison with RNAse Protection. *Analytical Biochemistry* **269**: 198-201.

Wang, Y.-W., Ding, J. P., Xia, X.-M. and Lingle, C. J. (2002). Consequences of the Stoichiometry of *Slo1*α and Auxiliary Beta Subunits on Functional Properties of Large-Conductance Ca^{2+}-Activated K^{+} Channels. *Journal of Neuroscience* **22**: 1550-1561.

Wanner, S. G., Koch, R. O., Koschak, A., Trieb, M., Garcia, M. L., Kaczorowski, G. J. and Knaus, H.-G. (1999). High-Conductance Calcium-Activated Potassium Channels in Rat Brain: Pharmacology, Distribution, and Subunit Composition. *Biochemistry* **38**: 5392-5400.

Ward, C. L. and Kopito, R. R. (1994). Intracellular Turnover of Cystic Fibrosis Transmembrane Conductance Regulator. Inefficient Processing and Rapid Degradation of Wild-Type and Mutant Proteins. *Journal of Biological Chemistry* **269**: 25710-25718.

Wasling, P., Hanse, E. and Gustafsson, B. (2004). Developmental Changes in Release Properties of the CA3-CA1 Glutamate Synapse in Rat Hippocampus. *Journal of Neurophysiology* **92**: 2714-2724.

Weaver, A. K., Liu, X. and Sontheimer, H. (2004). Role for Calcium-Activated Potassium Channels (BK) in Growth Control of Human Malignant Glioma Cells. *Journal of Neuroscience Research* **78**: 224-234.

Weiss, C., Sametsky, E., Sasse, A., Spiess, J. and Disterhoft, J. F. (2005). Acute Stress Facilitates Trace Eyeblink Conditioning in C57BL/6 Male Mice and Increases the Excitability of Their CA1 Pyramidal Neurons. *Learning and Memory* **12**: 138-143.

Wellman, G. C. and Nelson, M. T. (2003). Signalling between SR and Plasmalemma in Smooth Muscle: Sparks and the Activation of Ca^{2+}-Sensitive Ion Channels. *Cell Calcium* **34**: 211-229.

Widmer, H. A., Rowe, I. C. M. and Shipston, M. J. (2003). Conditional Protein Phosphorylation Regulates BK Channel Activity in Rat Cerebellar Purkinje Neurons. *Journal of Physiology (London)* **552**: 379-391.

Wilhelm, J. and Pingoud, A. (2003). Real-Time Polymerase Chain Reaction. *ChemBioChem* **4**: 1120-1128.

Williams, S. E. J., Wootton, P., Mason, H. S., Bould, J., Iles, D. E., Riccardi, D., Peers, C. and Kemp, P. J. (2004). Hemoxygenase-2 is an Oxygen Sensor for a Calcium-Sensitive Potassium Channel. *Science* **306**: 2093-2097.

Wilson, L., Gale, E. and Maden, M. (2003). The Role of Retinoic Acid in the Morphogenesis of the Neural Tube. *Journal of Anatomy* **203**: 357-368.

Wittwer, C. T., Herrmann, M. G., Gundry, C. N. and Elenitoba-Johnson, K. S. J. (2001). Real-Time Multiplex PCR Assays. *Elsevier Science Methods* **25**: 430-442.

Woda, C. B., Bragin, A., Kleyman, T. R. and Satlin, L. M. (2001). Flow-Dependent K^+ Secretion in the Cortical Collecting Duct is Mediated by a Maxi-K Channel. *American Journal of Physiology. Renal Physiology* **280**: F786-793.

Woda, C. B., Miyawaki, N., Ramalakshmi, S., Ramkumar, M., Rojas, R., Zavilowitz, B., Kleyman, T. R. and Satlin, L. M. (2003). Ontogeny of Flow-Stimulated Potassium Secretion in Rabbit Cortical Collecting Duct: Functional and Molecular Aspects. *American Journal of Physiology. Renal Physiology* **285**: F629-639.

Womack, M. D. and Khodakhah, K. (2002). Characterization of Large Conductance Ca^{2+} Activated K^+ Channels in Cerebellar Purkinje Neurons. *European Journal of Neuroscience* **16**: 1214-1222.

Wong, R. O. L. and Ghosh, A. (2002). Activity- Dependent Regulation of Dendritic Growth and Patterning. *Nature Reviews Neuroscience* **3**: 803-812.

Wu, J., Yang, J. and Klein, P. S. (2005). Neural Crest Induction by the Canonical Wnt Pathway Can Be Dissociated from Anterior-Posterior Neural Patterning in Xenopus. *Developmental Biology* **279**: 220-232.

Wu, S. N. (2003). Large-Conductance Ca^{2+}- Activated K^+ Channels: Physiological Role and Pharmacology. *Current Medical Chemistry* **10**: 649-661.

Xia, X.-M., Zeng, X. and Lingle, C. J. (2002). Multiple Regulatory Sites in Large-Conductance Calcium-Activated Potassium Channels. *Nature* **418**: 880-884.

Xie, J. and Black, D. L. (2001). A CaMK IV Responsive RNA Element Mediates Depolarization-Induced Alternative Splicing of Ion Channels. *Nature* **410**: 936-939.

Xie, J. and McCobb, D. P. (1998). Control of Alternative Splicing of Potassium Channels by Stress Hormones. *Science* **280**: 443-446.

Zarei, M. M., Eghbali, M., Alioua, A., Song, M., Knaus, H.-G., Stefani, E. and Toro, L. (2004). An Endoplasmic Reticulum Trafficking Signal Prevents Surface Expression of a Voltage- and Ca^{2+}-Activated K^+ Channel Splice Variant. *Proceedings of the National Academy of Sciences USA* **101**: 10072-10077.

Zarei, M. M., Zhu, N., Alioua, A., Eghbali, M., Stefani, E. and Toro, L. (2001). A Novel MaxiK Splice Variant Exhibits Dominant-Negative Properties for Surface Expression. *Journal of Biological Chemistry* **276**: 16232–16239.

Zhang, Y., Joiner, W. J., Bhattacharjee, A., Rassendren, F., Magoski, N. S. and Kaczmarek, L. K. (2004). The Appearance of a Protein Kinase A-Regulated Splice Isoform of *Slo* is Associated with the Maturation of Neurons That Control Reproductive Behavior. *Journal of Biological Chemistry* **279**: 52324-52330.

Zhong, H., Lai, J. and Yau, K.-W. (2003). Selective Heteromeric Assembly of Cyclic Nucleotide-Gated Channels. *Proceedings of the National Academy of Sciences USA* **100**: 5509-5513.

Zhorov, B. S. and Tikhonov, B, D. (2004). Potassium, Sodium, Calcium and Glutamate-Gated Channels: Pore Architecture and Ligand Action. *Journal of Neurochemistry* **88**: 782-799.

ZhuGe, R., Fogarty, K. E., Baker, S. P., Mccarron, J. G., Tuft, R. A., Lifshitz, L. M. and Walsh, J. V., Jr. (2004). Ca^{2+} Spark Sites in Smooth Muscle Cells Are Numerous and Differ in Number of Ryanodine Receptors, Large-Conductance K^{+} Channels, and Coupling Ratio between Them. *American Journal of Physiology. Cell Physiology* **287**: C1577-1588.

Publications

Publications

Tian, L., Coghill, L. S., Macdonald, S. H. F., Armstrong, D. L. and Shipston, M. J. (2003). Leucine Zipper Domain Targets cAMP-Dependent Protein Kinase to Mammalian BK Channels. *Journal of Biological Chemistry* **278**: 8669-8677.

Tian, L., Coghill, L. S., McClafferty, H., Macdonald, S. H. F., Antoni, F. A., Ruth, P., Knaus, H.-G. and Shipston, M. J. (2004). Distinct Stoichiometry of BK_{Ca} Channel Tetramer Phosphorylation Specifies Channel Activation and Inhibition by cAMP-Dependent Protein Kinase. *Proceedings of the National Academy of Sciences USA* **101**: 11897-11902.

Abstract

Detection and quantitation of murine large conductance calcium- and voltage- activated potassium (BK) channel alternative splice variants.

Stephen H-F MacDonald, Lie Chen & Michael J Shipston. Centre for Integrative Physiology, University of Edinburgh Medical School, Edinburgh, Scotland, UK. EH8 9XD.

BK channels regulate membrane potential in a variety of tissues, and are activated by voltage and intracellular calcium. They control the duration and frequency of action potentials, as well as release of neurotransmitters and hormones in neurons and endocrine cells, and are also important regulators of vascular tone. BK channels are also implicated in a wide range of processes in non-excitable cells, such as proliferation and cell migration. Although encoded by a single gene, they undergo extensive alternative pre- mRNA splicing in order to generate a diverse range of functional phenotypes, providing a dynamic means of regulating cell function and excitability in response to physiological signals such as depolarisation or stress hormones. In particular, alternative splicing at site C2 in the intracellular C-terminal tail of mammalian BK channels results in splice variants with distinct properties and regulation. Changes in BK channel expression have been implicated in a variety of disease states including certain cancers and blood pressure regulation however little is known regarding BK channel splice variant distribution in different tissues. To address the tissue distribution of distinct splice variants resulting from splicing at site C2 we have generated and optimised a range of real- time PCR primer/probe sets using the Taqman fluorogenic 5- 3' exonuclease assay. Primer/probe sets with high efficiency (>0.99), sensitivity (< 2fg) and discrimination between splice variants (individual variants reproducibly quantified in the presence of at least a 1000 fold excess of other variants) were generated for five distinct variants. Analysis of site C2 splice variant distribution in a range of murine tissues revealed both overlapping and distinct patterns of splice variant expression. For example, the Stress regulated exon (STREX) was highly expressed in a range of adult endocrine tissues including, anterior pituitary, adrenal gland and pancreas with very low /undetectable expression in kidney and lung. In contrast, expression of the e22 variant was largely confined to defined windows of developmental expression with maximal expression at embryonic day 19. The robust quantification of splice variant expression provides a platform for screening splice variant expression in health and disease.

(2005) XXXIII congress of the Spanish Society of Physiological Sciences. *Journal of Physiology and Biochemistry* **61:** 111 (Abs)